National Library of Canada
Bibliothèque nationale du Canada

Acquisitions and Bibliographic Services Branch
Direction des acquisitions et des services bibliographiques

395 Wellington Street
Ottawa, Ontario
K1A 0N4

395, rue Wellington
Ottawa (Ontario)
K1A 0N4

NOTICE

The quality of this microform is heavily dependent upon the quality of the original thesis submitted for microfilming. Every effort has been made to ensure the highest quality of reproduction possible.

If pages are missing, contact the university which granted the degree.

Some pages may have indistinct print especially if the original pages were typed with a poor typewriter ribbon or if the university sent us an inferior photocopy.

Reproduction in full or in part of this microform is governed by the Canadian Copyright Act, R.S.C. 1970, c. C-30, and subsequent amendments.

AVIS

La qualité de cette microforme dépend grandement de la qualité de la thèse soumise au microfilmage. Nous avons tout fait pour assurer une qualité supérieure de reproduction.

S'il manque des pages, veuillez communiquer avec l'université qui a conféré le grade.

La qualité d'impression de certaines pages peut laisser à désirer, surtout si les pages originales ont été dactylographiées à l'aide d'un ruban usé ou si l'université nous a fait parvenir une photocopie de qualité inférieure.

La reproduction, même partielle, de cette microforme est soumise à la Loi canadienne sur le droit d'auteur, SRC 1970, c. C-30, et ses amendements subséquents.

Canada

University of Alberta

Binuclear Alkyl and Hydrido Complexes of Rhodium and Iridium

by

Frederick Hansen Antwi-Nsiah

A thesis
submitted to the Faculty of Graduate Studies and Research
in partial fulfillment of the requirements
for the degree of Doctor of Philosophy

Department of Chemistry

Edmonton, Alberta
Spring, 1994

National Library of Canada
Acquisitions and Bibliographic Services Branch
395 Wellington Street
Ottawa, Ontario
K1A 0N4

Bibliothèque nationale du Canada
Direction des acquisitions et des services bibliographiques
395, rue Wellington
Ottawa (Ontario)
K1A 0N4

Your file Votre référence

Our file Notre référence

The author has granted an irrevocable non-exclusive licence allowing the National Library of Canada to reproduce, loan, distribute or sell copies of his/her thesis by any means and in any form or format, making this thesis available to interested persons.

L'auteur a accordé une licence irrévocable et non exclusive permettant à la Bibliothèque nationale du Canada de reproduire, prêter, distribuer ou vendre des copies de sa thèse de quelque manière et sous quelque forme que ce soit pour mettre des exemplaires de cette thèse à la disposition des personnes intéressées.

The author retains ownership of the copyright in his/her thesis. Neither the thesis nor substantial extracts from it may be printed or otherwise reproduced without his/her permission.

L'auteur conserve la propriété du droit d'auteur qui protège sa thèse. Ni la thèse ni des extraits substantiels de celle-ci ne doivent être imprimés ou autrement reproduits sans son autorisation.

ISBN 0-612-11145-8

Canada

University of Alberta

Release Form

Name of Author:	Frederick Hansen Antwi-Nsiah
Title of Thesis:	**Binuclear Alkyl and Hydrido Complexes of Rhodium and Iridium**
Degree:	Doctor of Philosophy
Year this Degree Granted:	1994

Permission is hereby granted to the University of Alberta Library to reproduce single copies of this thesis and to lend or sell such copies for private, scholarly or scientific research purposes only.

The author reserves all other publication rights, and neither the thesis nor extensive extracts from it may be printed or otherwise reproduced without the author's prior written permission.

(Signed) 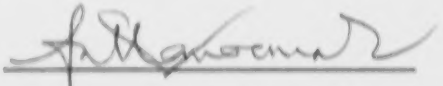

Frederick Hansen Antwi-Nsiah

Permanent Address: c/o Mr. W. L. Hansen
P. O. Box 3546
Accra, Ghana.

Date 27TH January, 1994

University of Alberta

Faculty of Graduate Studies and Research

The undersigned certify that they have read, and recommend to the Faculty of Graduate Studies and Research for acceptance, a thesis entitled **Binuclear Alkyl and Hydrido Complexes of Rhodium and Iridium** submitted by Frederick Hansen Antwi-Nsiah in partial fulfillment of the requirements for the degree of Doctor of Philosophy.

M. Cowie (Supervisor)

C. P. Kubiak
(External Examiner)

J. Takats

H. J. Liu

R. Cavell

D. T. Lynch

Date 27th January, 1994

To Mom and Christina

Abstract

Binuclear 'RhIr' and 'Ir_2' alkyl complexes bridged by $((C_6H_5)_2P)_2CH_2$ (dppm) have been synthesized. The reactions of $[MIr(CO)_3(dppm)_2]$ (M = Rh (**1**), Ir (**2**)) with $CF_3SO_3CH_3$ yield $[RhIr(CH_3)(CO)_3(dppm)_2][CF_3SO_3]$ (**3**), and the unusual product of C-H activation of a CH_3 group, $[Ir_2(H)(CO)_3(\mu\text{-}CH_2)(dppm)_2][CF_3SO_3]$ (**4**), respectively.

Compound **3** differs from several related Rh-containing, hetero-binuclear alkyl complexes, in having its CH_3 group bound to the saturated metal (Ir). The reactions of **3** with H_2, CF_3SO_3H, CO, ^{t}BuNC, and PMe_3 yield $[RhIr(H)(CO)_2(\mu\text{-}H)_2(dppm)_2]^+$ (**5**), $[RhIr(H)(CH_3)(CO)_2(\mu\text{-}CO)\text{-}(dppm)_2]^+$ (**6**), $[RhIr(CO)_3(COCH_3)(dppm)_2]^+$ (**7**), the iminoacyl species, $[RhIr(CO)_2(\mu\text{-}C(CH_3)\text{=}N^tBu)(dppm)_2]^+$ (**8**), and $[RhIr(CH_3)(CO)_2(PMe_3)\text{-}(dppm)_2]^+$ (**9**), respectively, while its reactions with C_2H_4 and SO_2, result in the migration of the CH_3 group from Ir to Rh to yield $[RhIr(CH_3)(C_2H_4)\text{-}(CO)_2(dppm)_2]^+$ (**10**), and $[RhIr(COCH_3)(CO)_2(\mu\text{-}SO_2)(dppm)_2]^+$ (**11**), respectively.

^{1}H NMR spin saturation transfer experiments indicate that in **4**, the hydride and the protons of the CH_2 group bridging the metals are exchanging, presumably via the intermediate complex $[Ir_2(CH_3)(CO)_3\text{-}(dppm)_2]^+$ (**12**) ($\Delta H^{\ddagger}$ = 10.3 kcal/mol and $\Delta S^{\ddagger}$ = -11.2 eu have been calculated for this process from the results of ^{1}H NMR selective inversion recovery experiments). The reactions of **4** with C_2H_4, CO, and SO_2 result in the reversal of the C-H activation to yield $[Ir_2(CH_3)(C_2H_4)(CO)_2(dppm)_2]^+$ (**13**), $[Ir_2(CH_3)(CO)_4(dppm)_2]^+$ (**14**) (and $[Ir_2(CO)_4(COCH_3)(dppm)_2]^+$ (**15**)) and $[Ir_2\text{-}(CH_3)(CO)_3(\mu\text{-}SO_2)(dppm)_2]^+$ (**16**), respectively, while those with ^{t}BuNC and phosphines yield $[Ir_2(H)(CO)_2(\mu\text{-}CH_2)(L)(dppm)_2]^+$ (L = ^{t}BuNC (**17**),

phosphine (**18**), respectively), and those with H_2, CF_3SO_3H and Me_3NO yield, $[Ir_2(H)(CO)_2(\mu\text{-}H)_2(dppm)_2]^+$ (**19**), $[Ir_2(CO)_3(OSO_2CF_3)(dppm)_2]^+$ (**20**), and $[Ir_2(CO)_2(\mu\text{-}CH_3)(dppm)_2]^+$ (**21**), respectively. In **21** the CH_3 group symmetrically bridges the two Ir centers. The reactions of **21** with ^{t}BuNC, phosphines and C_2H_4 yield **17**, **18**, and **13**, respectively, while its reaction with SO_2 yields $[Ir_2(CO)_2(\mu\text{-}CH_3)(\mu\text{-}SO_2)(dppm)_2]^+$ (**22**), in which the CH_3 group unsymmetrically bridges the Ir centers, being σ-bound to one center while engaging in an agostic C-H-Ir interaction with the other.

The reactions of **3** and **4** with C_2H_2, PhC≡CH and $(MeCO_2)_2C_2$ (DMAD) yield a variety of products including, $[MIr(CH_3)(CO)_3(\mu\text{-}C{=}C(H)R)(dppm)_2]^+$ (M = Rh, R = Ph (**23**); M= Ir, R = H (**24**), Ph(**25**)), $[MIr(CH_3)(CO)_3(\mu\text{-}C_2R_2)(dppm)_2]^+$ (M = Rh, R = H (**26**); M =Ir, R = H (**27**), Ph(**28**)), $[MIr(H)(CH_3)(CO)_3(\mu\text{-}\eta^1{:}\eta^2\text{-}C{\equiv}CR)(dppm)_2]^+$ (M = Rh, R = Ph (**29**); M = Ir, R = H (**30**)), $[RhIr(CH_3)(CO)_3(dppm)(HC{=}C(H)P(Ph_2)CH_2PPh_2)]^+$ (**31**) (the result of a formal insertion of C_2H_2 into a Rh-P bond in **3**), $[RhIr(\mu\text{-}\eta^1{:}\eta^2\text{-}C{\equiv}CPh)(CO)_3(dppm)_2]^+$ (**33**), $[RhIr(C{\equiv}CPh)_2(CO)_2(\mu\text{-}H)(dppm)_2]^+$ (**34**) and $[MIr(RC{=}C(CH_3)R)(CO)_3(dppm)_2]^+$ (R = CO_2Me; M = Rh (**35**), Ir (**36**)).

The compound $[Ir_2(H)(CO)_2(\mu\text{-}H)_2(dppm)_2][BF_4]$ (**37**), reacts with C_2F_4, DMAD, $(CF_3)_2C_2$, C_2H_2, C_2H_4, and Ph_2C_2 to yield the compounds, $[Ir_2(H)_2(CO)_2(\mu\text{-}H)(\mu\text{-}C_2R_2)(dppm)_2]^+$ (R = F_2 (**38**), CO_2Me (**39**), CF_3 (**40**) and H (**41**)), $[Ir_2(C_2H_4)(CO)_2(\mu\text{-}H)(dppm)_2]^+$ (**42**) (and ethane), and $[Ir_2(CO)_2(\mu\text{-}H)(\mu\text{-}C_2Ph_2)(dppm)_2]^+$ (**43**) (and *cis*-stilbene), respectively, while with PhC≡CH, it yields styrene and several uncharacterized species.

X-ray crystallographic methods have been employed in the characterization of **8** and **34** and in confirming the structures assigned to **3** and **42** on the basis of their NMR spectra.

Acknowledgements

I wish to express my gratitude to my supervisor, Professor Martin Cowie for his direction and encouragement during the course of this work. The immense help he has offered me, especially in matters related to X-ray crystallography, have been greatly appreciated.

I thank Dr. R. E. D. McClung and Mrs. G. Aarts for their assistance, especially in carrying out and in interpreting the results of the selective inversion recovery experiments. I acknowledge Dr. R. McDonald for his expert advice on matters related to X-ray structure determination. I wish to express my appreciation for his enthusiasm in helping me out with my numerous questions in this area. I also thank Dr. Bernie Santarsiero for his help in the area of X-ray crystallography, as well as Dr. S. Fraga and Dr. R. B. Jordan for their help in many ways.

I thank my fellow research group members, Li-Sheng Wang, Brian Sterenberg, Darren George, Todd Graham, Oke Okemona and Jeff Thorkelson for their friendship and encouragement. I also wish to express my gratitude to Dr. George Richter-Addo and Dr. Rob Hilts for their help in the initial stages of my research work. I am grateful to Kingsley Donkor, who was of immense help to me when I first arrived in Edmonton, and who has been a special friend since then. I thank Ebenezer Antwi, Kwasi Egyir, Joe and Thereas Bervell, Dr. and Mrs Charles Ahene, Dr. Giovanni Moro, John Langat, Clara Hernandez and Kweku Graham for their friendship and encouragement.

I am also indebted to the staff of the NMR Lab, Spectral Services, Elemental Analysis Lab, the Machine Shop, the Electronics Shop, the Store Room, the General Office, the Purchasing Section and the Mail Room for

their assistance in many different ways. I also thank Mr. Ron Gardner for his help with the laser printer.

Special thanks go to my mother, my brother Ebenezer and my sisters Gloria, Cherub and Pat, for their prayers, support and encouragement. I especially thank my mother for the sacrifices she made to support me in school. I also acknowledge my father and my uncle, Mr. W. Hansen. I thank Dr. Gordon Fletcher, his wife Betty and their children, Sara, Jon-Rae, and Laurisse, as well as Pastor David Hazzard and the church family at Evangel Pentecostal Assembly for their prayers and for playing the role of my family in Edmonton.

Very special thanks go to my wife Christina for her prayers, encouragement and help, as well as the nights she spent alone when I had to carry out NMR experiments overnight.

Finally, I give thanks to God, for bringing me this far. To him be all the glory.

Table of Contents

Chapter 1

Introduction 1

References and Footnotes 21

Chapter 2

Alkyl Complexes Involving the "RhIr(dppm)$_2$" Framework 26

Introduction 26

Experimental Section 27

Preparation of Compounds 28

X-ray Data Collection 38

(a) [RhIr(CH$_3$)(CO)$_3$(dppm)$_2$][CF$_3$SO$_3$]·CH$_2$Cl$_2$ (**2**) 38

(b) [RhIr(CO)$_2$(μ-C(CH$_3$)=N^{t}Bu)(dppm)$_2$][CF$_3$SO$_3$] (**8**) 38

Structure Solution and Refinement 41

(a) [RhIr(CH$_3$)(CO)$_3$(dppm)$_2$][CF$_3$SO$_3$]·CH$_2$Cl$_2$ (**2**) 41

(b) [RhIr(CO)$_2$(μ-C(CH$_3$)=N^{t}Bu)(dppm)$_2$][CF$_3$SO$_3$] (**8**) 45

Results and Discussion 49

(a) Preparation and Characterization of

[RhIr(CH$_3$)(CO)$_3$(dppm)$_2$][CF$_3$SO$_3$] (**1**) 49

(b) Reactivity Studies 60

Conclusions 78

References and Footnotes 82

Chapter 3

Alkyl Complexes Involving the "$Ir_2(dppm)_2$" Framework 87

Introduction 87

Experimental Section 88

Preparation of Compounds 88

^1H NMR Magnetization Transfer Experiments on $[Ir_2(H)(CO)_3(\mu\text{-}CH_2)(dppm)_2][CF_3SO_3]$ (**2**) 101

Results and Discussion 102

(a) Preparation and Characterization of Compound **2** 102

(b) Reactivity studies 115

(c) Bridging Methyl Complexes 126

(d) Hydrides and Reductive Elimination of Methane 134

Conclusions 141

References and Footnotes 145

Chapter 4

The Reactions of $[Ir_2(H)(CO)_3(\mu\text{-}CH_2)(dppm)_2][CF_3SO_3]$ and $[RhIr(CH_3)(CO)_3(dppm)_2][CF_3SO_3]$ with Alkynes 149

Introduction 149

Experimental Section 150

Preparation of Compounds 150

X-ray Data Collection 163

Structure Solution and Refinement 166

Results 166

Discussion 196

References and Footnotes 203

Chapter 5

The Reactions of $[Ir_2(H)(CO)_2(\mu\text{-}H)_2(dppm)_2][BF_4]$ and Related Compounds with Alkynes and Alkenes 207

Introduction 207

Experimental Section 208

Preparation of Compounds 208

X-ray Data Collection 214

Structure Solution and Refinement 215

Results and Discussion 219

Summary 243

References and Footnotes 245

Chapter 6

Conclusions 248

References and Footnotes 261

Appendix

Solvents and Drying Agents 262

List of Tables

Chapter 2

Table 2.1. $^{31}P\{^1H\}$ and ^1H NMR Spectroscopic Data 29

Table 2.2. $^{13}C\{^1H\}$ NMR and Infrared Spectroscopic Data 32

Table 2.3. Crystallographic Data for $[RhIr(CH_3)(CO)_3(dppm)_2][CF_3SO_3]\cdot CH_2Cl_2$ (**2**) 39

Table 2.4. Crystallographic Data for $[RhIr(CO)_2(\mu\text{-}C(CH_3)=N^tBu)(dppm)_2][CF_3SO_3]$ (**8**) 42

Table 2.5. Positional and Thermal Parameters for the Atoms of Compound **2** 46

Table 2.6. Positional and Thermal Parameters for the Atoms of Compound **8** 50

Table 2.7. Selected Distances (Å) in Compound **2** 56

Table 2.8. Selected Angles (deg) in Compound **2** 57

Table 2.9. Selected Distances (Å) in Compound **8** 68

Table 2.10. Selected Angles (deg) in Compound **8** 69

Chapter 3

Table 3.1. $^{31}P\{^1H\}$ and ^1H NMR Spectroscopic Data 89

Table 3.2. $^{13}C\{^1H\}$ NMR and Infrared Spectroscopic Data 93

Table 3.3. Values used for the Eyring Plot in Figure 3.5 112

Chapter 4

Table 4.1. $^{31}P\{^1H\}$ and ^1H NMR Spectroscopic Data.....151

Table 4.2. $^{13}C\{^1H\}$ NMR and Infrared Spectroscopic Data.....155

Table 4.3. Crystallographic Data for
$[RhIr(C{\equiv}CPh)_2(CO)_2(\mu\text{-}H)(dppm)_2][CF_3SO_3]\cdot 2CH_2Cl_2$ (**12**)...164

Table 4.4. Positional and Thermal Parameters for the Atoms of Compound **12**.....167

Table 4.5. Selected Distances (Å) in Compound **12**.....187

Table 4.6 Selected Angles (deg) in Compound **12**.....188

Chapter 5

Table 5.1 $^{31}P\{^1H\}$ and ^1H NMR Spectroscopic Data.....209

Table 5.2 $^{13}C\{^1H\}$ NMR and Infrared Spectroscopic Data.....211

Table 5.3 Crystallographic Data for
$[Ir_2(C_2H_4)(CO)_2(\mu\text{-}H)(dppm)_2][BF_4]$ (**9**).....216

Table 5.4 Positional and Thermal Parameters for the Atoms of Compound **9**.....220

Table 5.5 Selected Distances (Å) in Compound **9** 238

Table 5.6 Selected Angles (deg) in Compound **9**.....239

List of Figures

Chapter 2

Figure 2.1. A perspective view of the $[RhIr(CH_3)(CO)_3(dppm)_2]^+$ cation, showing the numbering scheme.....55

Figure 2.2. A perspective view of the $[RhIr(CO)_2(\mu\text{-}C(CH_3)\text{=}N^tBu)\text{-}(dppm)_2]^+$ cation, showing the numbering scheme.....67

Chapter 3

Figure 3.1. ^1H and $^1H\{^{31}P\}$ NMR spectra of compound **2** at -40 °C.....104

Figure 3.2. Carbonyl region of the $^{13}C\{^1H\}$ NMR spectra of compound **2** at temperatures between -60°C and 0 °C.....109

Figure 3.3. (+,-) Magnetizations, $M_i(t)$ (arbitrary units) at the CH_2 (1) and hydride (2) sites of compound **2**, following a selective inversion of site 2 magnetization for (a) $k = 10.28\ s^{-1}$ (-29.7 °C), (b) $k = 5.86\ s^{-1}$ (-40.6 °C) (c) $k = 2.17\ s^{-1}$ (-46.9 °C), (d) $k = 1.23\ s^{-1}$ (-50.6 °C) and (e) $k = 0.81\ s^{-1}$ (-56.4 °C).....110

Figure 3.4. Eyring plot for the methylene-hydride exchange process in compound **2** 112

Figure 3.5. ^1H NMR spectrum of compound **13**, at 20 °C, showing the methyl and dppm methylene resonances 127

Figure 3.7. Hydride region of the ^1H NMR spectra of compound **21** at temperatures between -80 °C and 25 °C.....137

Chapter 4

Figure 4.1. A perspective view of the $[RhIr(C{\equiv}CPh)_2(CO)_2(\mu\text{-}H)\text{-}(dppm)_2]^+$ cation, showing the numbering scheme.....186

Chapter 5

Figure 5.1. $^{31}P\{^1H\}$ NMR spectra of compound **9** at -40 °C and -80 °C.....235

Figure 5.2. A perspective view of the $[Ir_2(C_2H_4)(CO)_2(\mu\text{-}H)(dppm)_2]^+$ cation, showing the numbering scheme.....237

List of Schemes

Chapter 1

Scheme 1.1. 7

Scheme 1.2. 17

Scheme 1.3. 19

Chapter 2

Scheme 2.1. 53

Scheme 2.2. 63

Scheme 2.3. 65

Scheme 2.4. 75

Chapter 3

Scheme 3.1. 103

Scheme 3.2. 107

Scheme 3.3. 117

Scheme 3.4. 121

Scheme 3.5. 132

Scheme 3.6. 136

Scheme 3.7. 139

Chapter 4

Scheme 4.1. 172

Scheme 4.2. 176

Scheme 4.3. 179
Scheme 4.4. 184
Scheme 4.5. 193
Scheme 4.6. 194

Chapter 5

Scheme 5.1. 224
Scheme 5.2. 228
Scheme 5.3. 232
Scheme 5.4. 234

List of Abbreviations and Symbols

anal.	analyses
Bu	butyl, C_4H_9-
ca.	circa (approximately)
dB	decibels
DANTE	Delays Alternating with Nutations for Tailored Excitation
DMAD	dimethyl acetylenedicarboxylate, $CH_3O_2CC{\equiv}CCO_2CH_3$
dmpm	bis(dimethylphosphino)methane, $((CH_3)_2P)_2CH_2$
dppm	bis(diphenylphosphino)methane, $((C_6H_5)_2P)_2CH_2$
Et	ethyl, C_2H_5-
FID	free induction decay
h	hour(s)
HFB	hexafluoro-2-butyne
IR	infrared
L	ligand
M	molar
Me	methyl, CH_3-
mg	milligrams
min	minute(s)
mL	milliliters
mmol	millimoles
NMR	nuclear magnetic resonance
NOE	Nuclear Overhauser Effect

Ph	phenyl, C_6H_5-
ppm	parts per million
s	seconds
t	tertiary
THF	tetrahydrofuran
μL	microliters
μs	microseconds

Crystallographic Abbreviations and Symbols

a, b, c	lengths of the x, y, and z axes, respectively, of the unit cell
B	isotropic thermal parameter
deg (or °)	degrees
F_c	calculated structure factor
F_o	observed structure factor
h, k, l	Miller indices defining lattice planes, where the plane intersects the unit cell axes at $1/h$, $1/k$, $1/l$ of the respective lengths of a, b and c
p	experimental instability factor (used in calculation of $\sigma(I)$ to downweight intense reflections)
R	residual index (conventional R factor)
R_w	weighted residual index
V	unit cell volume
w	weighting factor applied to structure factor
Å	angstrom(s) (1 Å = 10^{-10} meters)
α, β, γ	angles between b and c, a and c, and a and b axes, respectively, of unit cell
β_{ij}	anisotropic displacement parameters
λ	wavelength
ρ	density
σ	standard deviation

Chapter 1

Introduction

Transition metal alkyl complexes are of unusual importance; apart from the significance and role in nature of the cobalt-carbon bonds in the vitamin B_{12} system,[1a,2a] transition metal alkyl derivatives are important intermediates in most catalytic processes involving syntheses or transformations of a wide variety of organic compounds.[1b,2b,3a,4] These processes include the carbonylation of methanol, hydrogenation of carbon monoxide, and olefin hydrogenation, hydroformylation and hydrosilation.[1b,2b,3a,4,5]

Although $[Me_3PtI]_4$ was synthesized in 1907 by Pope and Peachy,[6] earlier attempts to prepare compounds such as $(C_2H_5)_3Fe$, by reactions of Grignard reagents with metal halides failed. Even though there was evidence of unstable species in solution at low temperatures, no alkyl compounds could be isolated.[3b] Originally it was thought that the instability of transition metal alkyl compounds was an intrinsic thermodynamic property, by which the transition metal-carbon bond was inherently weaker than main group M-C bonds. Furthermore, the realization in the 1950s and 1960s that thermally stable alkyls could be prepared if ligands such as η^5-C_5H_5, CO and PMe_3 were present (eg. $[(\eta^5\text{-}C_5H_5)Mo(CH_3)(CO)_3]$, $[(CH_3)Mn(CO)_5]$ and *cis*-$[(C_2H_5)_2Pt(PMe_3)_2]$), led to the suggestion by Chatt and Shaw[7] that such ligands were needed to stabilize the M-C bond. However the available evidence today shows that M-C bonds can be of comparable strength for transition metals and main group elements,[2b,3b,4,8] and that the apparent

instability of transition metal alkyl complexes is kinetic rather than thermodynamic, by virtue of the low activation energy pathways available for their decomposition.

One very important and well documented pathway by which these complexes can decompose is β-elimination, wherein a hydrogen atom is transferred from the second or β-carbon of the alkyl chain to the metal as shown below. The intermediate hydrido-alkene complex can then lose the alkene to give a metal hydride complex, as shown below.

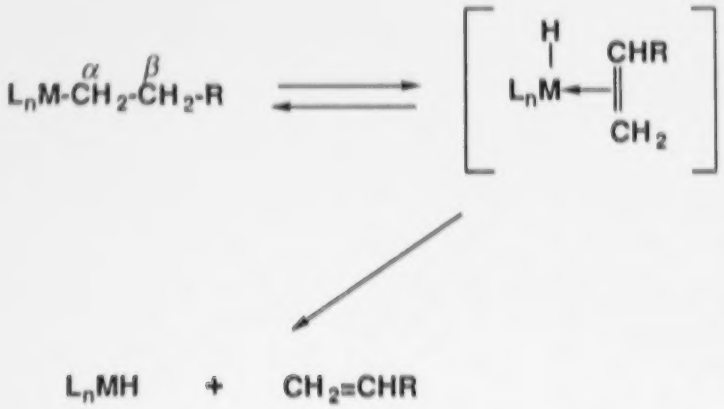

It can be seen that the β-hydrogen transfer involves a change in coordination number of the metal, since the alkyl group occupies only one coordination site, whereas two sites are involved in the intermediate hydrido-alkene, one for the hydride ligand and the other for the olefin coordination. Therefore, one way in which an alkyl can be stabilized against decomposition is by coordinative saturation of the metal. If the sites required for the reaction to proceed are occupied by firmly bound ligands, then there is no possible pathway for such decomposition. The stability of alkyls with π-bonding ligands are prime examples of this situation. Others include Werner type complexes of Co(III), Rh(III), Ir(III), and Cr(III) that are relatively inert to

substitution reactions. A typical example of this class of compounds is the Rh(III) complex ion shown below.[2a] The importance of coordinative

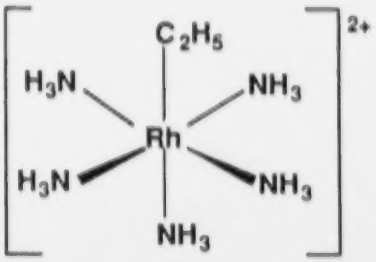

saturationof the metal on the stabilization of alkyl complexes is also illustrated by the observation that [$TiMe_4$] decomposes at *ca.* -50 °C, but on addition of ligands such as bipyridines, which leads to coordinative saturation, a substantial increase in thermal stability results.[4] Thus [Ti(bipy)Me_4], for instance, is stable at *ca.* 15 °C.[4]

Another way by which stable alkyls can be obtained is by the use of alkyl groups having no β-hydrogen atom (such as Me_3CCH_2-, Me_3SiCH_2-, $(Me_3Si)_2CH$- and Ph_3C-), or in which β-elimination would give an intermediate of high energy (such as norbonyl, adamantyl or butane-1,4-diyl groups). This concept was illustrated by Wilkinson and coworkers by use of the trimethylsilylmethyl group allowing them to isolate a number of kinetically stable alkyls such as [$Mo_2(CH_2SiMe_3)_6$].[9] The steric bulk of most of the alkyl groups without β-hydrogen atoms may further enhance the stabilities of the complexes by retarding intermolecular decomposition pathways.

Although hydrogen transfer from an α-carbon atom of a transition metal alkyl complex to produce a hydrido-carbene intermediate (as shown below) as the first step in decomposition is possible, this is less favorable than hydrogen transfer from a β-carbon, and is rarely observed. Methyl

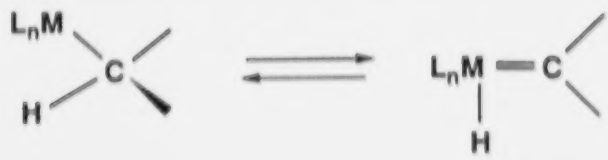

compounds such as $[W(CH_3)_6]$,[10] and $[Ta(CH_3)_5]$[11] are accordingly much more stable than the homologous ethyl compounds. As a result of the development of synthetic methods that effectively block decomposition pathways, alkyl complexes of essentially all the transition metals (usually in conjunction with other ligands) are now known.

A wide variety of methods have been used in the syntheses of transition metal alkyl complexes, including: (1) alkyl transfer reactions, (2) treatment of anionic transition metal complexes with alkyl halides, (3) oxidative addition reactions, (4) insertion reactions, (5) elimination reactions, (6) attack on a coordinated ligand, and (7) reactions of metal complexes with alkylating agents, such as $CH_3SO_3CF_3$.[1c,2a,3b,4,12]

Of the methods listed above alkyl transfer reactions have been most widely used. This method involves the alkylation of metal halides, acetates, alkoxides and so on using Grignard reagents or alkyls of Li, Mg, Zn, Al, Sn and Hg.

$$PdBr_2(PEt_3)_2 + MeMgBr \longrightarrow \textit{trans}\text{-}PdMe(Br)(PEt_3)_2 + MgBr_2$$

$$TiCl_4 + 4MeLi \longrightarrow TiMe_4 + 4LiCl$$

$$WCl_6 + 6AlMe_3 \longrightarrow WMe_6$$

Treatment of anionic metal complexes with alkyl halides is another class of reactions for metal alkyl syntheses. This method is useful when salts of carbonylate and other anions are available or can be readily prepared.

$$Mn_2(CO)_{10} + Na/Hg \longrightarrow 2Na[Mn(CO)_5]$$

$$Na[Mn(CO)_5] + CH_3I \longrightarrow CH_3Mn(CO)_5 + NaI$$

Oxidative-addition reactions, particularly involving alkyl halides, constitute useful routes for synthesizing metal alkyls when the oxidation state of at least one of the constituent metals can be increased by two units.

$$RhCl(PPh_3)_3 + CH_3I \longrightarrow RhCl(I)(CH_3)(PPh_3)_2 + PPh_3$$

$$IrCl(CO)(PPh_3)_2 + CH_3I \longrightarrow Ir(CH_3)Cl(I)(CO)(PPh_3)_2$$

Insertion of olefins or of the methylene group, produced from diazomethane, into M-H bonds of metal hydrides also yield alkyl complexes.

$$\textit{trans}\text{-}PtHCl(PEt_3)_2 + C_2H_4 \longrightarrow \textit{trans}\text{-}Pt(C_2H_5)Cl(PEt_3)_2$$

$$CpMo(CO)_3H + CH_2N_2 \longrightarrow CpMo(CO)_3CH_3 + N_2$$

Elimination reactions, which are the reverse of insertion reactions, are another route to obtaining metal alkyls. They involve the elimination from appropriate compounds such as acyls, sulfinates or carboxylates, of CO, SO_2, and CO_2 by the action of heat or light with concomitant formation of a metal-carbon σ bond.

$$CpFe(CH_3CO)(CO)_2 \xrightarrow{h\nu} CpFe(CH_3)(CO)_2 + CO$$

$$(C_5Me_5)Ir(CO)(Cl)(SO_2CH_3) \xrightarrow[\Delta]{-SO_2} (C_5Me_5)Ir(CH_3)(CO)Cl$$

Another synthetic method which can be employed for the preparation of metal alkyls is by means of reactions involving attack on a coordinated ligand. These usually involve the attack of a nucleophile on a coordinated alkene.

$$[CpPd(C_2H_4)(PPh_3)]^+ + CH_3O^- \longrightarrow [CpPd(PPh_3)CH_2CH_2OCH_3]$$

The last class of reactions for metal alkyl syntheses that will be discussed are those between low-valent, coordinatively unsaturated metal centers and strong, cationic alkylating agents containing weakly coordinating anions, such as CH_3SO_3F, $[(CH_3)_3O][PF_6]$ and $CH_3SO_3CF_3$.

$$Pt(PPh_3)_3 + CH_3SO_3F \longrightarrow [Pt(CH_3)(PPh_3)_3][FSO_3]$$

$$[W(PMe_3)H_5](Cp^2)[Rh(CO)PMe_3] + CH_3SO_3CF_3 \longrightarrow [W(PMe_3)H_5](Cp^2)[Rh(CH_3)(CO)PMe_3][CF_3SO_3]$$

$$(Cp^2 = \eta^5,\eta^5\text{-}Me_4C_5(CH_2)_2C_5Me_4)$$

As mentioned earlier, one of the catalytic processes that involves a transition metal alkyl intermediate is the carbonylation of methanol. There are two commercial processes for making acetic acid from methanol.[1b,4,5a] One is the cobalt-based, high-pressure process that operates under severe conditions (200-250 °C and 500-700 atm.). The other process, which was commercialized in the late 1960s and early 1970s by the Monsanto Company, uses a Rh-based catalyst that is much more reactive than the Co-based catalyst. Furthermore the Monsanto process can be operated at much lower temperatures and pressures (150-200 °C, 1-40 atm.). Based on a number of studies[13] of the reaction, by NMR and IR (eg. using a well characterized 'precatalyst', $[Ph_4As][Rh(CO)_2I_2]$, and methyl iodide), the mechanism shown in Scheme 1.1 has been proposed for this process.[13]

The catalyst precursor, a Rh(III) compound (such as $RhCl_3{\cdot}3H_2O$), is converted to the Rh(I) anion, $[RhI_2(CO)_2]^-$ (**1**), in the presence of CO and an iodide source. Oxidative addition of methyl iodide to the active Rh(I) anion to form a Rh(III) methyl species (**2**) constitutes the rate determining step in the catalytic cycle (although oxidative additions to Rh(I) complexes are well known, this one is extraordinarily fast; evidently the extra electron density in the anionic complex makes it a powerful nucleophile). The methyl iodide for the oxidative addition reaction is formed in situ according to the following reaction.

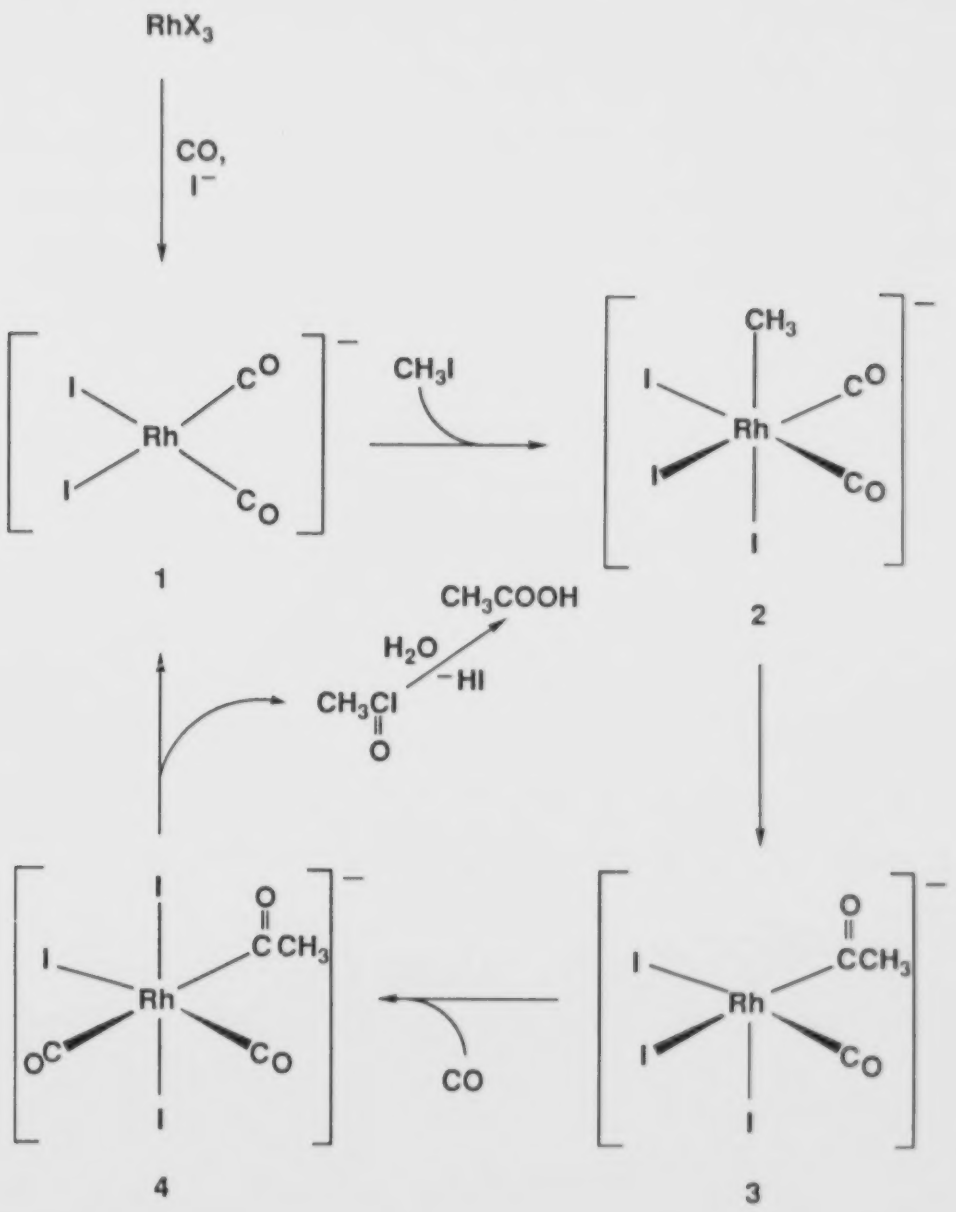

Scheme 1.1.

$$CH_3OH + HI \rightleftharpoons CH_3I + H_2O$$

The methylrhodium complex (**2**) rapidly isomerizes, by means of migratory insertion of the methyl group onto a CO ligand, yielding an isolable acetyl monocarbonyl complex (**3**). This five-coordinate acetyl derivative reacts with CO to produce the labile six-coordinate acetyl complex (**4**), which reductively eliminates acetyl iodide spontaneously, regenerating the $[RhI_2(CO)_2]^-$ (**1**) catalyst. Subsequent hydrolysis of acetyl iodide yields acetic acid. An alternative to the reductive elimination of acetyl iodide is direct hydrolysis of the acetylrhodium species to liberate acetic acid. This process for the production of acetic acid, stands out as one of the technologically most successful examples of homogeneous catalysis.[1] The highly selective reaction (selectivity is 99% based on methanol and 90% based on CO[1b,4,5a]) is extremely rapid with yields of > 90%.[1b]

In spite of the fact that several binuclear transition metal alkyl complexes such as $Li_2[Re_2Me_8]\cdot 2Et_2O$[14] and $[Mo_2Me_4(PMe_3)_4]$[15] were prepared years ago, the vast majority of the early reactivity studies concentrated on mononuclear species. In more recent years, binuclear alkyl complexes such as those of platinum[16] and palladium[17] have been extensively studied, in line with the growing interest in binuclear transition metal complexes in general. This interest has arisen due to the potential of these complexes to display cooperative behavior between the two metal centers and due to the possibility that they might show superior activities and selectivities relative to the mononuclear complexes. Such cooperativity is expected to involve one or more of several processes or situations, including a simple ligand transfer from one metal to the other to create a vacant coordination site for attack by incoming ligands, or the activation of bonds of a ligand which is

coordinated to one of the metal centers by the adjacent metal. There is also the possibility that one or more of the ligands may adopt certain coordination modes that are not possible for mononuclear complexes (such as the bridging of the two metal centers), giving rise to increased reactivity in the binuclear complexes. For example, the movement of a ligand from a bridging to a terminal position could serve as a means of creating a vacant coordination site at one of the metals for attack by an incoming substrate. Also the reverse, which is movement of a ligand from a terminal to a bridging position, could be a means of creating coordinative saturation at the adjacent metal, thus stabilizing the resulting complex. Furthermore, one of the metal centers could act as a source of additional electron density, by means of say a dative bond, enhancing the ability of the adjacent metal to undergo such reactions as oxidative addition. On the other hand, one metal center could reduce electron density build-up at an adjacent metal, by the interaction of the CO ligands bound to the former metal with the latter. Moreover, binuclear complexes are the simplest unit which permit the study of the nature of metal-metal interactions, a first step towards developing theories to explain bonding interactions within higher-nuclearity metal cluster complexes,[18] which themselves can be regarded as model systems for bulk metals.[19] Also binuclear complexes are the simplest systems in which interactions of small molecules at more than one metal center can be studied, a situation that is relevant to heterogenous catalysis, where bonding between the substrate and catalyst is believed to involve several neighboring metal centers in many cases. For example, it is believed that binuclear complexes with bridging methylene ligands could serve as useful models for the Fischer-Tropsch process[20] (the synthesis of multicarbonproducts from CO and H_2), since it has

been suggested that the C-C bonds of the products are formed via polymerization of CH_2 fragments on the metal surface.[21] One significant study that can be cited to support the proposed importance of μ-methylene species in nonstoichiometric CO/H_2 reactions is that by Masters and coworkers,[22] in which coordinated CO was reduced with AlH_3/THF to give high yields of ethylene. The intermediacy of binuclear μ-methylene complexes was postulated, and they are thought to account for carbene dimerization, as shown below.

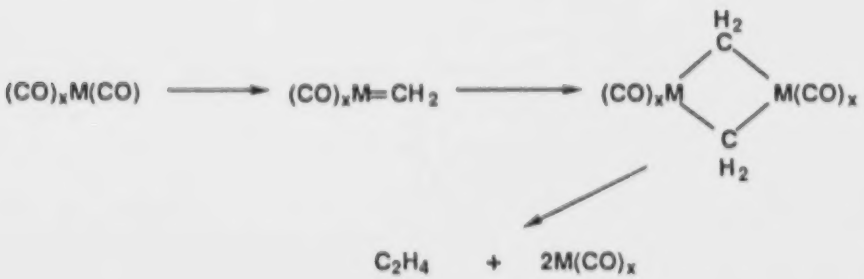

Although initial studies with binuclear complexes involved the use of homobinuclear species, heterobinuclear complexes are gaining much prominence[23,24] in recent times. This is because it is anticipated that the latter complexes will show certain unique reactivity patterns, compared to the analogous homobinuclear complexes, as a result of the different properties contributed by each metal.

Reactions of binuclear complexes frequently lead to cleavage of an existing M-M bond, therefore there is the necessity, in studies with these complexes, to use bridging ligands that effectively hold the two metals in close proximity retaining the integrity of the binuclear framework even in the absence of the M-M bond. One bidentate ligand that has been extensively used for this purpose is bis(diphenyphosphino)methane (dppm = $Ph_2PCH_2PPh_2$),[24,25] which has been found to be a very efficient bridging

ligand, probably as a consequence of its flexibility which allows for considerable variation in the metal-metal separation. The range of M-M separations runs from 2.138(1) Å in the quadruple M-M bonded $[Mo_2Cl_4(dppm)_2]$ to 3.492(1) Å in $[[Pd_2Cl_2(\mu\text{-}C_2R_2)(dppm)_2]$ (R = CF_3)[26] in which there is no Pd-Pd bond. Furthermore, the presence of this ligand in complexes facilitates their characterization by ^{31}P NMR spectroscopy, while its methylene group in ^1H NMR spectra, also gives valuable structural information. The presence of the phenyl groups also tends to facilitate crystallization of compounds for X-ray crystallographic studies.

Although work on mononuclear alkyl complexes of cobalt-triad metals has resulted in an improved understanding of the involvement of metal alkyl species in catalysis,[27] very little has been reported on binuclear derivatives, in spite of the fact that complexes such as $[Rh_2Me_4(SMe)_2(\mu\text{-}I)_2(\mu\text{-}SMe)]$[28] and $[IrMe(Cl)(CO)_2(\mu\text{-}Cl)]_2$[29] were characterized as far back as the 1960s. As mentioned earlier, related binuclear alkyl systems that have been more extensively studied include those of platinum and, to a lesser extent, those of palladium. As part of these studies, compounds such as $[Pt_2Me_3(dppm)_2][PF_6]$,[16k,16l] $[Pt_2Me_4(dppm)_2]$,[16d] $[Pd_2Me_2(\mu\text{-}H)(dppm)_2][BPh_4]$[17b] and $[Pd_2(I)(C_2H_5)(\mu\text{-}I)(dppm)_2][CF_3CO_2]$[17c] have been reported, and results of reactivity studies include the observation that the reaction of the dmpm (dmpm = $(Me_2P)_2CH_2$) analogue of the tetramethyl diplatinum complex, $[Pt_2Me_4(dmpm)_2]$ with halogens results in the migration of one of the methyl groups from one Pt center to the other to give $[Pt_2Me_4(X)(dmpm)][X]$ (X = Cl, Br, I),[16h] as shown below.

Bridging alkyl groups are a common and important feature in main group organometallic chemistry, common examples being $[Li_4(\mu\text{-}Me)_4]$, polymeric $BeMe_2$ and $[Al_2Me_4(\mu\text{-}Me)_2]$.[3c,30] In contrast to these, bridging

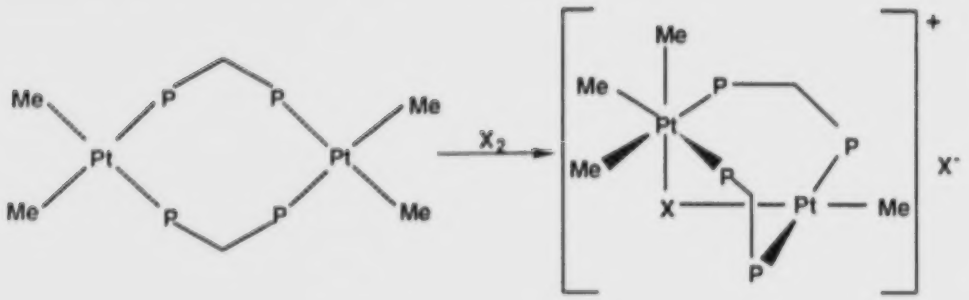

alkyls in transition metal chemistry are relatively rare; examples include $[Os_3(CO)_{10}(\mu\text{-}CH_3)(\mu\text{-}H)]$,[31] $[Cp_2TiPt(CH_3)(\mu\text{-}CH_2)(\mu\text{-}CH_3)(PMe_2Ph)]$[32] and $[Ir_2(CO)_2(\mu\text{-}CH_3)(dmpm)_2][CF_3SO_3]$.[33] As the structures below show, these alkyls either symmetrically bridge the metals, or they are bound by a σ bond to one metal while they engage in an agostic C-H interaction with the adjacent metal (ie. a 3 center-2 electron C-H-M interaction).[34] It is believed that compounds with agostic C-H bonds play an important role in intramolecular activation of these bonds.[35]

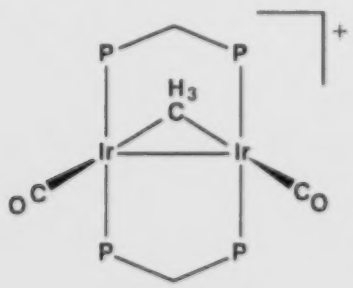

symmetric

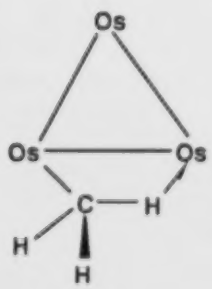

agostic

The first binuclear alkyl complexes characterized within this research group were $[MRe(CH_3)(CO)_4(dppm)_2][CF_3SO_3]$ (M = Rh, Ir).[36] These were synthesized by reacting the appropriate neutral tetracarbonyl compounds, $[MRe(CO)_4(dppm)_2]$, with $CH_3SO_3CF_3$. In these compounds the methyl group was bound to the group 9 metal and it was shown that the chemistry

occurs primarily at this metal in the few reactions that were studied, although the Re carbonyl moieties had an important influence on the stability of the products through their interactions with the former metal. Since this time, related heterobinuclear alkyl complexes such as the methyl species, $[RhOs(CH_3)(CO)_3(dppm)_2]$,[37] $[RhMn(CH_3)(CO)_4(dppm)_2][CF_3SO_3]$,[38] $[RhMo(CH_3)(CO)_4(dppm)_2]$ and $[RhW(CH_3)(CO)_4(dppm)_2]$[39] have also been prepared.

In this thesis, we will concentrate on the 'RhIr' and diiridium complexes, $[RhIr(CO)_3(dppm)_2]$ (I)[40] and $[Ir_2(CO)_3(dppm)_2]$ (II),[41] respectively. Compound I has been characterized by X-ray crystallographic methods,[40] in which it was shown to have the structure diagrammed below, with the dppm phosphorus atoms bound to Ir having a mutually cis disposition, while those bound to Rh adopt the more common mutually trans orientation. On the basis of the asymmetric structure and the coordination

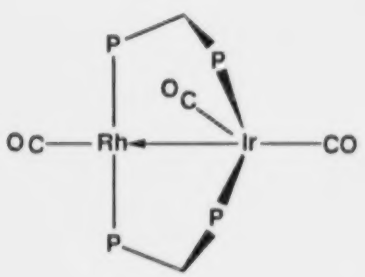

I

environments about each metal, a mixed-valence Rh(I)/Ir(-I) formulation with an accompanying Ir→Rh dative bond was proposed for the complex. The low oxidation states of the metals and the coordinative unsaturation at one of the metals are favorable conditions for oxidative addition reactions, and I has been shown to activate H-H, H-S and H-Se bonds, in reactions with

H_2, H_2S and H_2Se, respectively.[40,42] These reactions yielded [RhIr(H)(μ-X)$(CO)_2(dppm)_2$] (X=H, HS and HSe, respectively). It has also been shown to react with $HBF_4{\cdot}OEt_2$, by apparent electrophilic attack at the metal-metal bond, to give $[RhIr(CO)_3(\mu\text{-}H)(dppm)_2][BF_4]$[40] as shown below.

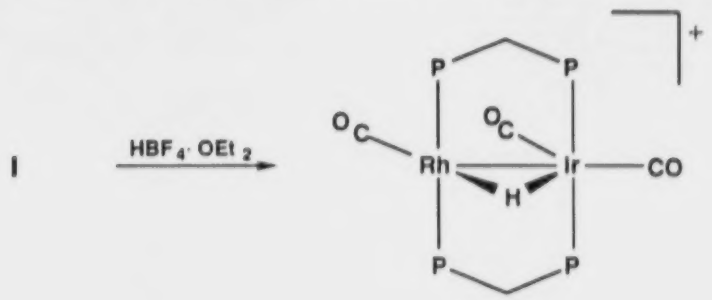

The homobinuclear analogue, $[Rh_2(CO)_3(dppm)_2]$ (**III**) has also been shown by an X-ray structure determination[43] to have an orientation of the dppm ligands similar to that in **I**, such that the phosphorus atoms bound to one metal are mutually cis while those on the other are mutually trans, and it is believed that a similar arrangement exists in **II**. The diiridium and dirhodium complexes react with $HBF_4{\cdot}OEt_2$ in a similar manner to the 'RhIr' analogue, yielding $[M_2(CO)_2(\mu\text{-}CO)(\mu\text{-}H)(dppm)_2][BF_4]$ (M = Ir and Rh, respectively).[41,44] However in contrast to the reactions of the heterobinuclear analogue, those of **II** and **III** with H_2S , result in CO loss and the successive activation of both H-S bonds towards oxidative addition, followed by reductive elimination of H_2 to give the similar compounds [$Ir_2(CO)_2(\mu$-S)$(dppm)_2$] and [$Rh_2(CO)_2(\mu$-S)$(dppm)_2$], respectively (**II** reacts in a similar manner with H_2Se).[42] Several intermediates were characterized in the diiridium reactions, whereas only the final product was observed in the case of the dirhodium reaction. Compounds **II** and **III** were also found to activate the Si-H bonds in reactions with silanes (analogues of methane) yielding the

products $[M_2(H)_2(CO)_2(\mu\text{-SiRR'})(dppm)_2]$ (where M = Rh or Ir ; R and R' are alkyl substituents or hydrogen),[45,46] whereas reactions of compound **I** with the same reagents yielded mixtures of several products. These results and others show clear similarities and differences between heterobinuclear 'RhIr' complexes and their homonuclear analogues.

The first objective of this thesis project was to synthesize alkyl derivatives of the binuclear 'RhIr' complex, $[RhIr(CO)_3(dppm)_2]$ (**I**) and its homonuclear diiridium (**II**) and dirhodium (**III**) analogues. Based on the results of protonation reactions of compounds **I**, **II** and **III** mentioned earlier, it was anticipated that their reactions with the electrophile CH_3^+ (in the form of methyl triflate) might yield the CH_3-bridged analogues of the hydrido-bridged species (these were of interest because of their relevance to C-H activation by an adjacent metal). On obtaining these alkyl derivatives, the second step was to investigate their reactivity with small molecules (such as CO, H_2 and alkynes) in order to obtain information on their potential utility as models for studies of some of the transformations involving metal alkyl complexes in catalysis. It was anticipated that the heterobinuclear complex could combine certain attractive characteristics of each metal (catalytic activity of Rh complexes and the stability of Ir complexes) to give certain unique reactivity patterns compared to its homobinuclear analogues and related mononuclear complexes. These alkyl complexes were expected to undergo a greater variety of reactions than the 'RhRe' and the 'IrRe' systems, in light of the observation that the chemistry in the Re-containing systems occurred primarily at the group 9 metal. Reactions that were of particular interest included insertion reactions (of CO, SO_2, unsaturated organic substrates, etc.), leading to the formation of C-C or C-heteroatom bonds. We were also interested in the potential for two-metal involvement in binuclear

reductive elimination, and in the possibilities of C-H activation of a coordinated alkyl group by the adjacent metal. Furthermore, it was of interest to determine how the reactivities of the 'RhIr' system and its homobinuclear analogues compared with each other, in the expectation that this comparison could shed some light on the roles of the two metals in reactions involving binuclear complexes. During the later stages of this work, it became evident that the alkyl chemistry of **III** was being studied by another research group, so studies with this compound were not pursued.

Metal hydride complexes are inextricably linked to the chemistry of metal alkyls. Not only are they obtained as products in the α- and β-eliminations, but the reverse reactions, the insertions of methylene units or olefins into M-H bonds, yield metal alkyls. Metal hydride complexes are among the most extensively studied in inorganic chemistry, having been shown to play an important role in many stoichiometric and catalytic reactions (complexes containing both hydrido and alkyl ligands are also pivotal intermediates in a large number of metal catalyzed organic transformations). Catalytic reactions in which they are involved include olefin hydrogenation, isomerization and hydroformylation as well as alkyne hydrogenation and the water-gas shift reaction.[1b,2b,3a,4,5] The hydrogenation of olefins has been studied extensively, perhaps more so than any other reaction catalyzed by soluble metal complexes.[5a] The best studied catalyst for this process is Wilkinson's catalyst, $[RhCl(PPh_3)_3]$.[47] The mechanism of olefin hydrogenation by this catalyst[1b,2b,3a,4,5] is shown in Scheme 1.2.

The complex $[RhCl(PPh_3)_3]$ dissociates one of its PPh_3 ligands in solution to give the highly coordinatively unsaturated (14-electron) complex $[RhCl(PPh_3)_2]$ (a solvent molecule may be weakly coordinated to the Rh in this complex). Oxidative addition of H_2 to this complex (in an extremely

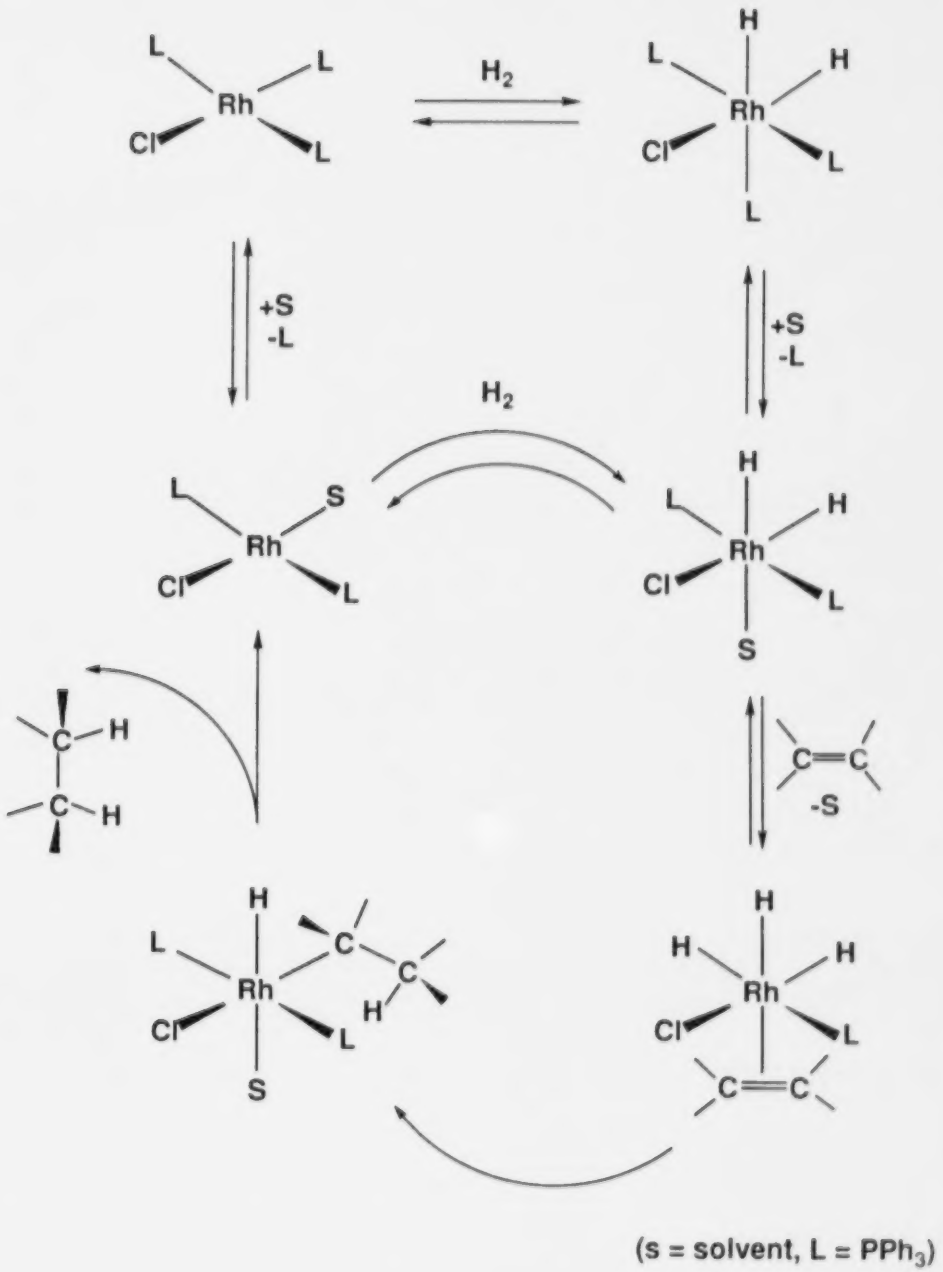
L
L
Rh
Cl
L
H2
H
L
H
Rh
Cl
L
L
+S
-L
+S
-L
H2
L
S
Rh
Cl
L
H
L
H
Rh
Cl
L
S
C
H
C
H
C=C
-S
H
L
C
C
Rh
H
Cl
L
S
H
H
H
Rh
Cl
L
C=C
(s = solvent, L = PPh3)

Scheme 1.2.

rapid step) gives a dihydride complex $[RhCl(H)_2(PPh_3)_2]$ (the same dihydride can also be produced, though much less rapidly, by direct oxidative addition of H_2 to $[RhCl(PPh_3)_3]$, and subsequent dissociation of PPh_3). The octahedral complex $[RhCl(olefin)(H)_2(PPh_3)_2]$ is formed by coordination of the olefin (replacing the coordinated solvent molecule). Insertion of the olefin into a Rh-H bond gives a hydrido alkyl species, which reductively eliminates an alkane to regenerate $[RhCl(PPh_3)_2]$. This complex reacts further with H_2 to continue the catalytic cycle.

Alkynes tend to undergo hydrogenation in a similar manner to olefins, although oxidative addition of H_2 to alkyne compounds tends to be more difficult, as a result of the greater π-acidity of the alkyne ligands.[48] In the case of the alkynes, further hydrogenation to alkanes is possible and the reaction products have to be monitored so that the reaction can be stopped if the olefin is desired. Alkynes also tend to oligomerize and polymerize, especially at high temperatures.

Several studies involving hydride complexes have been carried out in this research group,[37,40,49-57] some of which resulted in insertion of alkynes into M-H bonds of the complexes[51,57] while others gave rise to the hydrogenation of unsaturated substrates.[54] For instance, the reactions of $[Ir_2(H)_2(CO)_2(\mu\text{-}Cl)(dppm)_2][BF_4]$ (**IV**) with phenylacetylene and dimethyl acetylenedicarboxylate (DMAD) result in insertion of the alkynes into both Ir-H bonds to give $[Ir_2(RC{=}C(H)R')_2(CO)_2(\mu\text{-}Cl)(dppm)_2][BF_4]$ (R = H, R' = Ph (**Va**); R = R' = CO_2Me (**Vb**)).[54] Compound **Va** reacts further with H_2 to give styrene and two isomers of the tetrahydride, $[Ir_2(H)_4Cl(CO)_2(dppm)_2][BF_4]$ (see Scheme 1.3), products of the reaction of **IV** with H_2. The dichloro compound, $[Ir_2(H)_2(Cl)_2(CO)_2(dppm)_2]$ (**VI**), on the other hand reacts with DMAD to give insertion of the alkyne into only one of the Ir-H bonds,

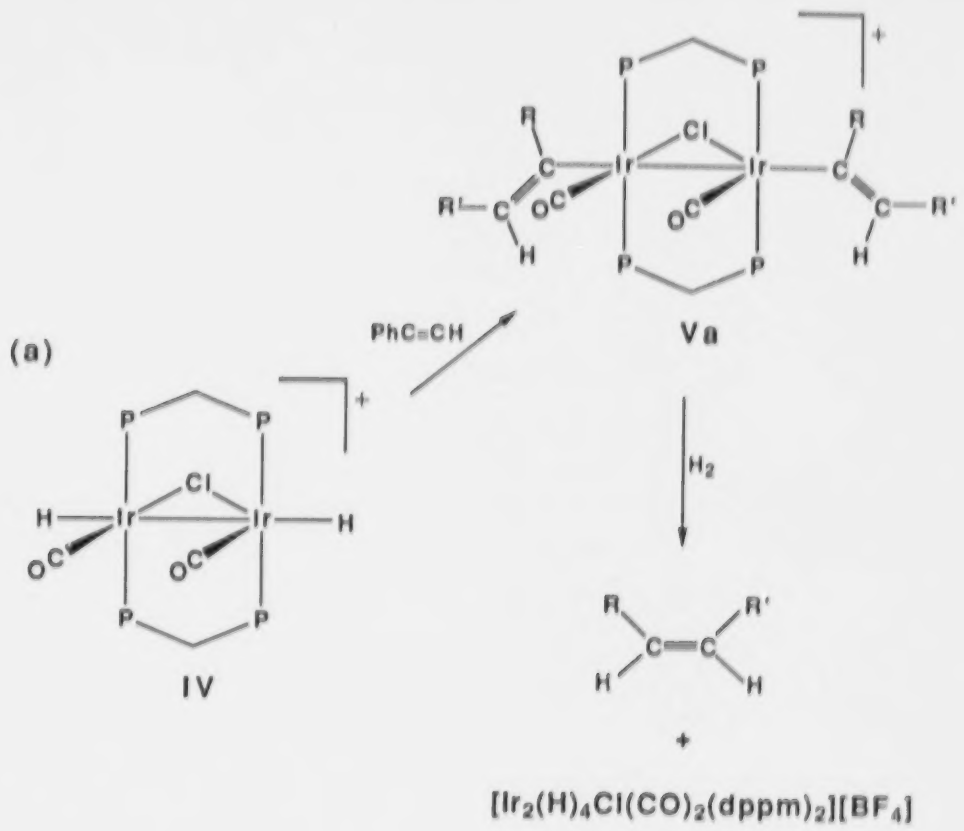

Scheme 1.3.

yielding $[Ir_2(H)(Cl)_2(CH_3O_2CC{=}C(H)CO_2CH_3)(CO)_2(dppm)_2]$ (**VII**), as shown in Scheme 1.3, but does not react any further to give the hydrogenated alkyne.[57] This, presumably because the hydride and the vinyl ligands are on different metals, and the cis orientation of these ligands that is required for reductive elimination does not exist.

A second goal of this thesis project was to extend the alkyne and alkene hydrogenation studies to the trihydride species, $[Ir_2(H)(CO)_2(\mu\text{-}H)_2(dppm)_2][BF_4]$[56] since it was believed that the presence of two adjacent hydride ligands might lead to facile hydrogenation chemistry. This is because on insertion of an alkyne (or alkene) into a M-H bond of this compound, the resulting vinyl (or alkyl) ligand could still be cis to a hydride ligand, thus enhancing the reductive elimination of the hydrogenated substrate. The reactions of this trihydride complex with olefins and alkynes is described in Chapter 5.

References and Footnotes

1. Collman, J. P.; Hegedus, L. S.; Norton, J. R.; Finke, R. G. *Principles and Applications of Organotransition Metal Chemistry;* University Science Books: Mill Valley, CA, 1987, (a) p 100 (b) Chapters 10-12 (c) p 94.
2. Elschenbroich, C; Salzer, A. *Organometallics: A Concise Introduction;* VCH Publishers: New York and Weinheim, Germany, 1989, (a) Chapter 13 (b) Chapter 17.
3. Cotton, F. A.; Wilkinson, G. *Advanced Inorganic Chemistry,* 5th ed.; Wiley: New York, 1988, (a) Chapter 28 (b) Chapter 25 (c) pp 140, 150 and 225.
4. Yamamoto, A. *Organotransition Metal Chemistry: Fundamental Concepts and Applications;* Wiley: New York, 1986.
5. (a) Parshall, G. W. *Homogenous Catalysis;* Wiley: New York, 1980. (b) Gates B. C. *Catalytic Chemistry;* Wiley: New York, 1992.
6. Pope, W. J.; Peachy, S. J. *Proc. Chem. Soc.* **1907**, *23*, 86; *J. Chem. Soc.* **1909**, 371.
7. Chatt, J.; Shaw, B. L. *J. Chem. Soc.*, **1959**, 705.
8. Lappert, M. F.; Patil, D. S.; Pedley, J. B. *J. Chem. Soc., Chem. Commun.* **1975**, 830.
9. Huq, F.; Mowat, W.; Shortland, A.; Skapski, A. C.; Wilkinson, G. *J. Chem. Soc., Chem. Commun.* **1971**, 1079.
10. Shortland, A. J.; Wilkinson, G. *J. Chem. Soc., Dalton Trans.* **1973**, 872.
11. Schrock, R. R.; Meakin, P. *J. Am. Chem. Soc.* **1974**, *96*, 5288.
12. (a) Schrock, R.; Buzinkai, J. F. *Inorg. Chem.* **1989**, *28*, 2837. (b) Pearson, A. J. *Metallo-Organic Chemistry,* Wiley: New York, 1985, Chapter 3.

14. Cotton, F. A.; Gage, L. D.; Mertis, K.; Shive, L. W.; Wilkinson, G. *J. Am. Chem. Soc.* **1976**, *98*, 6922.

15. Andersen, R. A.; Jones, R. A., Wilkinson, G. *J. Chem. Soc. Chem. Commun.* **1977**, 283.

16. See, for example: (a) Hartley; F. R. In *Comprehensive Organometallic Chemistry*; Wilkinson, G., Stone, F. G. A., Abel, E. W., Eds.; Pergamon Press: Oxford, England, 1982; vol. 6, p. 514. (b) Azam, K. A.; Frew, A. A.; Lloyd, B. R.; Manojlovic-Muir, L.; Muir, K. W.; Puddephatt, R. J. *Organometallics* **1985**, *4*, 1400. (c) Brown, M. P.; Yavari, A.; Hill, R. H.; Puddephatt, R. J.; *J. Chem. Soc., Dalton Trans.* **1985**, 2421. (d) Manojlovic-Muir, L.; Muir, K. W.; Frew, A. A.; Ling, S. S. M.; Thomson, M. A.; Puddephatt, R. J.*Organometallics* **1984**, *3*, 1637. (e) Azam, K. A.; Brown, M. P.; Hill, R. H.; Puddephatt, R. J.; Yavari, A. *Organometallics* **1984**, *3*, 697. (f) Azam, K. A.; Hill, R. H.; Puddephatt, R. J. *Can. J. Chem.* **1984**, *62*, 2029. (g) Azam, K. A.; Puddephatt, R. J. *Organometallics* **1983**, *2*, 1396. (h) Manojlovic-Muir, L.; Muir, K. W.; Ling, S. S. M.; Puddephatt, R. J. *J. Organomet. Chem.* **1983**, *255*, C11. (i) Brown, M. P.; Fisher, J. R.; Franklin, S. J.; Puddephatt, R. J.; Thomson, M. A. In *Catalytic Aspects of Metal Phosphine Complexes*; Alyea, E. C., Meek, D. W., Eds.; Advances in Chemistry Series 196; American Chemical Society: Washington, DC, 1982; p 231. (j) Azam, K. A.; Frew, A. A.; Lloyd, B. R.; Manojlovic-Muir, L.; Muir, K. W.; Puddephatt, R. J. *J. Chem. Soc., Chem. Commun.* **1982**, 614. (k) Frew, A. A.; Manojlovic-Muir, L.; Muir, K. W. *J. Chem. Soc., Chem. Commun.* **1980**, 624. (l) Brown, M. P.; Cooper, S.; Puddephatt, R. J.; Thomson, M. A.; Seddon, K. R. *J. Chem. Soc., Chem. Commun.* **1979**, 1117.

17. See, for example: (a) Maitlis, P. M.; Espinet, P.; Russel, M. J. H. In

Comprehensive Organometallic Chemistry; Wilkinson, G., Stone, F. G. A., Abel, E. W., Eds.; Pergamon Press: Oxford, England, 1982; vol. 6, p 279 (b) Young, S. J.; Kellenberger, B.; Riebenspies, J. H.; Himmel, S. E.; Manning, M.; Anderson, O. P.; Stille J. K. *J. Am. Chem. Soc.* **1988**, *110*, 5744. (c) Lee, C.; Hunt, C. T.; Balch, A. L. *Organometallics* **1982**, *1*, 824. (d) Balch, A. L.; Hunt, C. T.; Lee, C.; Olmstead, M. M.; Farr, J. P. *J. Am. Chem. Soc.* **1981**, *103*, 3764.

18. Cotton, F. A. In *Reactivity of Metal-Metal Bonds*; Chisholm, M. H., Ed.; *ACS Symp. Ser.* **1981**, *155*, 1.
19. Mingos, D. M. P. *Chem Soc Rev.* **1986**, *15*, 31.
20. Herrmann, W. A. *Adv. Organomet. Chem.* **1982**, *20*, 159.
21. Brady, R. C. III; Pettit, R. *J. Am. Chem. Soc.* **1980**, *102*, 6182.
22. Masters, C.; van der Wonde, C; van Doorn, J. A. *J. Am. Chem. Soc.* **1979**, *101*, 1633.
23. Geoffroy, G. L. In *Comprehensive Organometallic Chemistry*; Wilkinson, G., Stone, F. G. A., Abel, E. W., Eds.; Pergamon Press: Oxford, England, 1982; vol. 6, p 765.
24. Chaudret, B; Delavaux, B.; Poilblanc, R. *Coord. Chem. Rev.* **1988**, *86*, 191.
25. Puddephatt, R. J. *Chem. Soc. Rev.* **1983**, *12*, 99.
26. Balch, A. L. In *Reactivity of Metal-Metal Bonds*; Chisholm, M. H., Ed.; *ACS Symp. Ser.* **1981**, *155*, 167.
27. Atwood, J. D. *Coord. Chem. Rev.* **1988**, *83*, 93.
28. (a) Fritz, H. P.; Schwarzhans, K. E. *J. Organomet. Chem.* **1966**, *5*, 283. (b) Paulus, E. F.; Fritz, H. P.; Schwarzhans, K. E. *J. Organomet. Chem.* **1968**, *11*, 647.
29. Shaw, B. L.; Singleton, E. *J. Chem. Soc., A.* **1967**, 1683.
30. Davidson, P. J.; Lappert, M. F.; Pearce, R. *Acc. Chem. Res.* **1974**, *7*, 209.

31. Calvert, R. B., Shapley, J. R. *J. Am. Chem. Soc.* **1977**, *99*, 5225.
32. Ozawa, F.; Park, J. W.; Mackenzie, P. B.; Schaefer, W. P.; Henling, L. M.; Grubbs, R. H. *J. Am. Chem. Soc.* **1989**, *111*, 1319.
33. Reinking, M. K.; Fanwick, P. E.; Kubiak, C. P. *Angew. Chem. Int. Ed. Eng.* **1989**, *28*, 1377.
34. Brookhart, M.; Green, M. L. H. *J. Organomet. Chem.* **1983**, *250*, 395.
35. Park, J. W.; Mackenzie, P. B.; Schaefer, W. P.; Grubbs, R. H. *J. Am. Chem. Soc.* **1986**, *108*, 6402.
36. Antonelli, D. M.; Cowie, M. *Organometallics* **1991**, *10*, 2550.
37. Hilts, R. W.; Moro, G.; Sterenberg, B. T.; Cowie, M., manuscript in preparation.
38. Wang, L. S.; Cowie; M., to be submitted for publication.
39. Graham, T.; Mao, T.; Van Gastel, F.; Cowie, M. unpublished work.
40. McDonald, R.; Cowie, M. *Inorg. Chem.* **1990**, *29*, 1564.
41. Sutherland, B. R.; Cowie, M. *Organometallics* **1985**, *4*, 1637.
42. McDonald, R. Ph.D. Thesis, University of Alberta, 1991, Chapter 4.
43. Woodcock, C.; Eisenberg, R. *Inorg.Chem.* **1985**, *24*, 1285.
44. (a) Kubiak, C. P.; Woodcock, C.; Eisenberg, R. *Inorg.Chem.* **1982**, *21*, 2119. (b) Kubiak, C. P.; Eisenberg, R. *J. Am. Chem. Soc.* **1980**, *102*, 3637.
45. McDonald, R.; Cowie, M. *Organometallics* **1990**, *9*, 2468.
46. (a) Wang, W. D.; Hommeltoft, S. I; Eisenberg, R. *Organometallics* **1988**, *7*, 2417. (b) Wang, W. D.; Eisenberg, R. *J. Am. Chem. Soc.* **1990**, *112*, 1833.
47. Osborn, J. A.; Jardine, F. H.; Young, J. F.; Wilkinson, G. *J. Chem. Soc. A.* **1966**, 1711.
48. James, B. R. In *Comprehensive Organometallic Chemistry*; Wilkinson, G., Stone, F. G. A., Abel, E. W., Eds.; Pergamon Press: Oxford, England, 1982; vol. 8, p 285.

49. Hilts, R. W.; Franchuk, R. A.; Cowie, M. *Organometallics* **1991**, *10*, 1297.

50. Hilts, R. W.; Franchuk, R. A.; Cowie, M. *Organometallics* **1991**, *10*, 304.

51. Antonelli, D. M.; Cowie, M. *Inorg. Chem.* **1990**, *29*, 4039.

52. Antonelli, D. M.; Cowie, M. *Inorg. Chem.* **1990**, *29*, 3339.

53. Antonelli, D. M.; Cowie, M. *Organometallics* **1990**, *9*, 1818.

54. Vaartstra, B. A.; Cowie, M. *Organometallics* **1990**, *9*, 1594.

55. Vaartstra, B. A.; Cowie, M. *Inorg. Chem.* **1989**, *28*, 3138.

56. McDonald, R.; Sutherland, B. R.; Cowie, M. *Inorg. Chem.* **1987**, *26*, 3333.

57. Sutherland, B. R.; Cowie, M. *Organometallics* **1985**, *4*, 1801.

Chapter 2

Alkyl Complexes Involving the "$RhIr(dppm)_2$" Framework

Introduction

Alkyl complexes of the Co-triad metals are known to be involved as key intermediates in a variety of important catalytic processes such as the carbonylation of methanol,[1] the hydrogenation of carbon monoxide,[2] and olefin hydrogenation, hydroformylation, and hydrosilation.[3] Although work on mononuclear alkyl complexes of these metals has resulted in an improved understanding of the involvement of the metal alkyl species in catalysis,[4] very little has been reported on binuclear derivatives, in spite of recent interest in utilizing complexes containing adjacent metals as catalysts.[5]

Interest within this research group in utilizing binuclear, dppm-bridged complexes of Rh and Ir as models for transformations occurring at two or more adjacent metal centers[6] led to the investigation of alkyl derivatives of such complexes. As part of this study, the syntheses and reactivities of the complexes, $[MRe(CH_3)(CO)_4(dppm)_2][CF_3SO_3]$ (M = Rh, Ir), have previously been reported.[6c] More recently a series of related alkyl compounds involving the Rh/Os[7], Rh/Mn[8] and Rh/Mo[9] combinations of metals have also been characterized and studied. Interestingly, in all the complexes characterized, the alkyl group was found to be coordinated to the unsaturated group 9 metal. In this chapter, the alkylation of the complex,

$[RhIr(CO)_3(dppm)_2]$ (**1**),[6m] as well as transformations involving the resulting complex are reported.

Experimental Section

All solvents were dried (using the appropriate drying agents listed in the appendix), and distilled before use, and were stored under argon. Deuterated solvents used for NMR experiments were degassed and stored under argon over molecular sieves. Reactions were carried out at room temperature (unless otherwise stated) by using standard Schlenk procedures, and compounds, which were isolated as solids, were purified by recrystallization. A flow rate of *ca.* 0.2 mLs^{-1} was employed for all reactions which involved purging a solution with a gas. Prepurified argon, ethylene and hydrogen were purchased from Linde. Carbon monoxide, sulphur dioxide, propadiene and hydrogen chloride gas were all purchased from Matheson. ^{13}CO (99%) was supplied by Isotec Inc. All gases were used as received. Hydrated Rhodium (III) Chloride was purchased from Engelhard Scientific, whereas triflic acid, methyl triflate, tert-butyl isocyanide, trimethyl phosphine and triphenyl phosphite were obtained from Aldrich. The compound $[RhIr(CO)_3(dppm)_2]$ (**1**)[6m] was prepared as previously reported.

The NMR spectra were recorded on a Bruker AM-400 spectrometer at 400.1 MHz for ^1H, at 161.9 MHz for $^{31}P\{^1H\}$ and at 100.6 MHz for $^{13}C\{^1H\}$ spectra. The $^{13}C\{^1H\}\{^{31}P\}$ NMR spectra were obtained on a Bruker WH-200 spectrometer operating at 50.32 MHz. All $^{13}C\{^1H\}$ NMR spectra were obtained using ^{13}CO-enriched samples unless otherwise stated. Infrared spectra were obtained on a Nicolet 7199 Fourier transform or a Perkin Elmer 883 IR spectrometer, either as nujol mulls on KBr plates, or as solutions in KCl

cells with 0.5 mm-window path lengths. Spectroscopic parameters for the compounds prepared are found in Tables 2.1 and 2.2. Elemental analyses were performed by the microanalytical sevice within the department.

Preparation of Compounds. (a) $[RhIr(CH_3)(CO)_3(dppm)_2][CF_3SO_3]$ (2). The compound $[RhIr(CO)_3(dppm)_2]$ (**1**) (200 mg, 0.174 mmol) was dissolved in 20 mL of benzene, to which was added 1 equiv (19.7 μL, 0.174 mmol) of methyl triflate. The solution was stirred for 3 h during which time the orange solution became cloudy and a brown solid precipitated. The volume of the solvent was reduced to about 5 mL and precipitation was completed by adding 30 mL of diethyl ether. The brown solid was collected and washed with three 10 mL portions of Et_2O and dried under an argon stream and then in vacuo (70-77% yield). Anal. Calcd for $IrRhSP_4F_3O_6C_{55}H_{47}$: C, 50.35; H, 3.61. Found: C, 50.17; H, 3.83.

(b) $[RhIr(CH_3)(CO)_2(\mu\text{-}H)(\mu\text{-}Cl)(dppm)_2][CF_3SO_3]$ (4). Compound **2** (100 mg, 0.076 mmol) was dissolved in 20 mL of CH_2Cl_2. Slightly more than 1 equiv of HCl (in the form of 10 mg N,N-dimethylacetamide·HCl, 0.081 mmol) in 10 mL of CH_2Cl_2 was added, causing an immediate color change from orange to light yellow. The solution was stirred for 2 h during which time the color slowly darkened to a deeper yellow. The solvent was removed under vacuum and the orange solid was recrystallized from CH_2Cl_2/Et_2O giving a 60% yield. Anal. Calcd for $IrRhClSP_4F_3O_5C_{54}H_{48}$: C, 49.12; H, 3.66; Cl, 2.68. Found: C, 48.38; H, 3.43; Cl, 3.93. Analytical results are variable owing to loss of the CH_2Cl_2 of cystallization. The above results, obtained over a short time span, to ensure consistent results among the different elements,

Table 2.1 $^{31}P\{^{1}H\}$ and ^{1}H NMR Spectroscopic Data[a]

Compound	$\delta(^{31}P\{^{1}H\})$[b]	$\delta(^{1}H)$[c,g]
$[RhIr(CH_3)(CO)_3(dppm)_2][CF_3SO_3]$ (2)	29.8 (dm, $^{1}J_{Rh-P}$ = 120.0 Hz), -5.5 (m)	4.33 (m, 4H), -0.08 (t, 3H)
$[RhIr(CH_3)(CO)_3(\mu\text{-}H)(\mu\text{-}Cl)(dppm)_2][CF_3SO_3]$ (4)[d]	22.1 (dm, $^{1}J_{Rh-P}$ = 111.0 Hz), -4.4 (m)	4.40 (m, 2H), 3.83 (m, 2H), -0.25 (t, 3H), -9.50 (m, 1H)
$[RhIr(CH_3)(CO)_2(\mu\text{-}CO)(\mu\text{-}H)(dppm)_2][CF_3SO_3]_2$ (5)[d]	28.0 (dm, $^{1}J_{Rh-P}$ = 98.3 Hz), -11.3 (m)	4.93 (m, 2H), 4.20 (m, 2H), 0.67 (t, 3H), -10.08 (bm, 1H)
$[RhIr(CO)_3(COCH_3)(dppm)_2][CF_3SO_3]$ (6)[d]	26.7 (dm, $^{1}J_{Rh-P}$ = 128.7 Hz), 45.8 (m),	3.60 (b, 4H), 0.83 (bs, 3H)
$[RhIr(CO)_2(\mu\text{-}C(CH_3)=N^{t}Bu)(dppm)_2][CF_3SO_3]$ (8)	15.4 (dm, $^{1}J_{Rh-P}$ = 132.6 Hz), 4.7 (m)	4.10 (m, 2H), 2.95 (m, 2H), 0.82 (s, 3H), 0.80 (s, 9H)

Table 2.1 (continued)

Compound	$\delta(^{31}P\{^1H\})^b$	$\delta(^1H)^{c,g}$
$[RhIr(CH_3)(CO)_2(C_2H_4)(dppm)_2][CF_3SO_3]$ **(9)**	32.6 (dm, $^1J_{Rh-P}$ = 141.1 Hz), 5.4 (m)	3.32 (m, 4H), 0.75 (t, 4H), 0.35 (t, 3H, $^2J_{Rh-H}$ = 3.0 Hz),
$[RhIr(CH_3)(CO)_3(SO_2)(dppm)_2][CF_3SO_3]$ **(11)**	20.9 (m)[f] -1.8 (m)	4.85(m, 2H), 3.45 (m, 2H), 0.33 (t, 3H)
$[RhIr(CH_3)(CO)_2(\mu\text{-}SO_2)(dppm)_2][CF_3SO_3]$ **(12)**	37.7 (dm, $^1J_{Rh-P}$ = 138.2 Hz), -0.8(m)	4.12(m, 2H), 3.50(m, 2H), 1.08 (dt, $^2J_{Rh-H}$ = 3.7 Hz, 3H)
$[RhIr(CO)_2(COCH_3)(\mu\text{-}SO_2)(dppm)_2][CF_3SO_3]$ **(13)**[d]	27.4 (dm, $^1J_{Rh-P}$ = 156.6 Hz), -1.2(m)	4.18 (m, 2H), 3.40 (m, 2H), 1.15 (s, 3H)
$[RhIr(CH_3)(CO)_2(PMe_3)(dppm)_2][CF_3SO_3]$ **(14)**	12.6 (dm, $^1J_{Rh-P}$ = 131.1 Hz), 6.4 (dm, $^1J_{Rh-P}$ = 126.0 Hz), -23.5 (m), -32.7 (m), -62.4 (m)	5.55 (m,1H), 5.08 (m, 1H), 4.82 (m, 1H), 4.77 (m, 1H), 0.33 (dt, 3H), 0.23 (d, 9H)

Table 2.1 (continued)

Compound	$\delta(^{31}P\{^1H\})^b$	$\delta(^1H)^{c,g}$
$[RhIr(CH_3)(CO)_2(P(OPh)_3)(dppm)_2][CF_3SO_3]$ (15)[e]	58.2 (m), 15.7 (dm, $^1J_{Rh-P}$ = 129.0 Hz), 6.9 (dm, $^1J_{Rh-P}$ = 123.0 Hz), -22.9 (m), -23.9 (m)	5.55 (m,1H), 5.06 (m, 1H), 4.65 (m, 1H), 4.60 (m, 1H), 0.50 (m, 3H)

[a] Abbreviations used: s = singlet, d = doublet, t = triplet, m = multiplet, dt = doublet of triplets, dm = doublet of multiplets, b = broad. [b] Vs 85% H_3PO_4, -40°C in CD_2Cl_2 unless otherwise stated. [c] Vs TMS, -40°C in CD_2Cl_2 solvent unless otherwise stated. [d] Data at 25°C. [e] Data at -80°C. [f] Magnitude of Rh-P coupling could not be determined because of the nature of the multiplet. [g] Resonances for phenyl group protons appear as multiplets in the range δ 6.9 - 8.1 for all compounds.

Table 2.2 Infrared and $^{13}C\{^1H\}$ NMR Spectroscopic Data[a]

Compound	IR[b,c], cm^{-1}	$\delta(^{13}C\{^1H\})$[d]
$[RhIr(CH_3)(CO)_3(dppm)_2][CF_3SO_3]$ (2)	1986(s), 1971 (vs), 1912 (vs)	183.7 (dt, 1C, $^1J_{Rh-C}$ = 75.0 Hz), 187.9 (t, 2C)
$[RhIr(CH_3)(CO)_2(\mu\text{-}H)(\mu\text{-}Cl)(dppm)_2][CF_3SO_3]$ (4)[e]	1982 (s), 1932 (s)	189.3 (dt, 1C, $^1J_{Rh-C}$ = 84.5 Hz), 164.4 (t, 1C)
$[RhIr(CH_3)(CO)_3(\mu\text{-}H)(dppm)_2][CF_3SO_3]_2$ (5)[e]	2000 (s), 1977 (vs), 1864 (med)	199.9 (dtt, 1C, $^1J_{Rh-C}$ = 26.2 Hz), 186.0 (dt, 1C, $^1J_{Rh-C}$ = 76.5 Hz), 165.6 (m, 1C)
$[RhIr(CO)_3(COCH_3)(dppm)_2][CF_3SO_3]$ (6)[e]	2003 (med),[f] 1980 (vs), 1623 (med)	227.9 (b, 1C), 194.5 (m, 2C), 187.9 (m, 1C)
$[RhIr(CO)_2(\mu\text{-}C(CH_3)=N^tBu)(dppm)_2][CF_3SO_3]$ (8)	1964 (vs), 1945 (s)	195.0 (dt, 1C, $^1J_{Rh-C}$ = 65.4 Hz), 191.3 (t, 1C)

Table 2.2 (continued)

Compound	IR[b,c], cm^{-1}	$\delta(^{13}C\{^1H\})^d$
$[RhIr(CH_3)(CO)_2(C_2H_4)(dppm)_2][CF_3SO_3]$ (9)	1985 (s)[g]	204.7 (dm, 2C, $^1J_{Rh-C}$ = 20.0 Hz)
$[RhIr(CH_3)(CO)_3(SO_2)(dppm)_2][CF_3SO_3]$ (11)	-	194.9 (dt, 1C, $^1J_{Rh-C}$ = 56.3 Hz), 178.4 (t, 1C), 175.2 (dt, 1C, $^1J_{Rh-C}$ = 63.4 Hz)
$[RhIr(CH_3)(CO)_2(\mu\text{-}SO_2)(dppm)_2][CF_3SO_3]$ (12)	-	180.6 (m, 1C), 170.3 (dt, 1C, $^2J_{C-C}$ = 13.6 Hz)
$[RhIr(CO)_2(COCH_3)(\mu\text{-}SO_2)(dppm)_2][CF_3SO_3]$ (13)[e]	2030 (s), 1986 (vs) 1640 (m), 1055 (m)[h]	255.5 (d, 1C, $^1J_{Rh-C}$ = 34.2 Hz), 172.7 (dt, 1C), 168.7 (dt, 1C, $^2J_{C-C}$ = 12.6 Hz)
$[RhIr(CH_3)(CO)_2(PMe_3)(dppm)_2][CF_3SO_3]$ (14)	2028 (s), 1956 (vs)	182.4 (dm, 1C, $^1J_{Rh-C}$ = 67.9 Hz), 178.7 (m, 1C)

Table 2.2 (continued)

Compound	IR[b,c], cm^{-1}	$\delta(^{13}C[^1H])$[d]
$[RhIr(CH_3)(CO)_2(P(OPh)_3)(dppm)_2][CF_3SO_3]$ (15)[f]	1980 (s), 1955 (vs)	189.9 (m, 1C), 179.9 (bs,1C)

[a] Abbreviations used: med = medium, s = strong, vs = very strong, s = singlet, d = doublet, t = triplet, m = multiplet, dt = doublet of triplets, dm = doublet of multiplets, bs = broad. singlet. [b] Nujol mull on KBr disk unless otherwise stated. [c] Values are ν (CO) . [d] Vs TMS, -40°C in CD_2Cl_2 solvent unless otherwise stated. [e] NMR data at 25°C. [f] NMR data at -80°C. [g] IR in CH_2Cl_2. [h] ν(SO), second SO stretch obscured by triflate anion stretches.

agree well with the calculated values if 0.25 equiv of CH_2Cl_2 is assumed (calcd: C, 48.56; H, 3.64; Cl, 3.96).

(c) $[RhIr(CH_3)(CO)_3(\mu\text{-}H)(dppm)_2][CF_3SO_3]_2$ (5). To a solution of **2** (100 mg, 0.076 mmol) in 10 mL of CH_2Cl_2 was added 1 equiv (6.7 μL, 0.076 mmol) of CF_3SO_3H, causing the dark orange solution to change to a yellow color instantly. After stirring the solution for 1 h, the solvent volume was reduced to ca. 5 mL and the yellow solid was precipitated by the addition of 15 mL of Et_2O. The solid was then collected, washed with Et_2O, and dried under an argon stream. It was then recrystallized from CH_2Cl_2/Et_2O, dried again under an argon stream, and then under vacuo (67% yield). Anal. Calcd for $IrRhS_2P_4F_6O_9C_{56}H_{48}$: C, 46.11; H, 3.30. Found: C, 45.49; H, 2.96.

(d) $[RhIr(CO)_3(COCH_3)(dppm)_2][CF_3SO_3]$ (6). Carbon monoxide (1 atm.) was placed over a 3 mL CH_2Cl_2 solution of **2** (40 mg, 0.030 mmol). The solution, which immediately changed color from orange to yellow, was stirred under a static atmosphere of the gas for 18 h. To obtain NMR spectra, the reaction was carried out in CD_2Cl_2. The product was not isolated because it lost CO in the absence of an atmosphere of the gas.

(e) $[RhIr(CO)_2(\mu\text{-}C(CH_3)=N^tBu)(dppm)_2][CF_3SO_3]$ (8). To a solution of **2** (80 mg, 0.016 mmol) in 10 mL CH_2Cl_2 was added 1 equiv (6.9 μL, 0.061 mmol) of ^{t}BuNC. The color of the solution changed from orange to brown then to purple. After stirring for 3 h, the solvent was taken off under vacuum giving a purple solid. Diethyl ether was layered over a CH_2Cl_2 solution of the purple solid and allowed to diffuse slowly giving purple crystals of the

product in about 2 days. (67% yield). Anal. Calcd for $IrRhSP_4F_3O_5NC_{59}H_{56}$: C, 51.83; H, 4.13; N, 1.02. Found: C, 51.09; H, 4.03; N, 1.13.

(f) $[RhIr(CH_3)(CO)_2(C_2H_4)(dppm)_2][CF_3SO_3]$ (9). Ethylene was passed through a 5 mL CH_2Cl_2 solution of **2** (80 mg, 0.061 mmol) for *ca.* 1 min. The solution was then stirred under a static atmosphere of the gas for 18 h. To obtain NMR spectra, the reaction was carried out in CD_2Cl_2 solution under an ethylene atmosphere. The solid product was not isolated in this reaction.

(g) $[RhIr(CO)_2(COCH_3)(\mu\text{-}SO_2)(dppm)_2][CF_3SO_3]$ (13). Compound **2** (80 mg, 0.061 mmol) was dissolved in 5 mL of CH_2Cl_2. Sulphur dioxide gas was then passed through the solution for about 1 min. The color of the solution changed instantly from orange to dark brown and then to red. The mixture was then stirred under a static atmosphere of the gas for 1.5 h, after which time the product was precipitated, washed with ether, and dried under an argon stream. The solid was then recrystallized from CH_2Cl_2/Et_2O and dried again under a stream of argon (84% yield). Anal. Calcd for $IrRhS_2P_4F_3O_8C_{55}H_{47}$: C, 48.01; H, 3.44; S, 4.66. Found: C, 48.30; H, 3.86; S, 4.58.

(h) $[RhIr(CH_3)(CO)_2(PMe_3)(dppm)_2][CF_3SO_3]$ (14). A solution of 2 equiv of PMe_3 (152 μL of a 1M solution in THF, 0.152 mmol) in 10 mL THF was added to a THF solution of the compound **2** (100 mg, 0.076 mmol in 10 mL). The dark orange solution immediately changed to yellow. The mixture was stirred for 2 h after which the solvent was removed under vacuum. The yellow residue was then recrystallised from THF and ether (68% yield).[10]

(i) $[RhIr(CH_3)(CO)_2(P(OPh)_3)(dppm)_2][CF_3SO_3]$ (15). The procedure was the same as that described for **14** except that 1 equiv of 97% $P(OPh)_3$ was used in place of a 1M THF solution of PMe_3 (70% yield). Anal. Calcd for $IrRhSP_5F_3O_5C_{72}H_{62}$: C, 54.24; H, 3.92. Found: C, 54.19; H, 3.96.

Experiments to Characterize Intermediates in the Reaction of Compound 2 with Sulphur Dioxide. Compound **2** (30 mg, 0.023 mmol) was dissolved in 0.6 mL of CD_2Cl_2 in an NMR tube, capped with a rubber septum, and cooled to *ca.* -60 °C by immersing it in a dry ice/chloroform mixture. Sulphur dioxide gas was passed through the solution for 1 min, and NMR spectra of this solution were obtained immediately afterwards, at -40 °C. The spectra showed the presence of $[RhIr(CH_3)(CO)_3(SO_2)(dppm)_2][CF_3SO_3]$ (**11**). The sample was allowed to warm to room temperature, and maintained at this temperature for another 10 min. The NMR spectra of the solution, obtained afterwards at -40 °C, showed the presence of $[RhIr(CH_3)(CO)_2(\mu\text{-}SO_2)(dppm)_2][CF_3SO_3]$ (**12**). Alternatively, compound **12** was obtained by passing SO_2 gas through a solution of **2** (30 mg, 0.023 mmol) in 0.6 mL CD_2Cl_2, until the solution color changed from orange to red (*ca.* 1 min). The solution was then transfered quickly to an NMR tube, covered with a rubber septum, and the reaction was quenched by immersing the tube in a dry ice/chloroform bath until the NMR spectra were obtained shortly afterwards.

Reaction of Compound 2 with 1,2-Propadiene (Allene). The procedure was the same as that used for the preparation of compound **9**, except that allene was used instead of ethylene, and in this case the solid product was precipitated with Et_2O and dried under argon.

X-ray Data Collection. (a) $[RhIr(CH_3)(CO)_3(dppm)_2][CF_3SO_3]\cdot CH_2Cl_2$ (2). Orange crystals of **2** were obtained by slow diffusion of ether into a concentrated CH_2Cl_2 solution of the compound. Several suitable crystals were mounted and flame sealed in glass capillaries under solvent vapor to minimise decomposition or deterioration due to solvent loss. Data were collected on an Enraf-Nonius CAD4 diffractometer using graphite-monochromated Mo Kα radiation. Unit cell parameters were obtained from a least-squares refinement of the setting angles of 25 reflections in the range $20.0° \leq 2\theta \leq 24.0°$. The monoclinic diffraction symmetry and the systematic absences (*0k0, k = odd)* were consistent with the space groups $P2_1$ or $P2_1/m$; the non-centrosymmetric space group was established by successful refinement of the structure.

Intensity data were collected at 22 °C using the $\theta/2\theta$ scan technique to a maximum $2\theta = 50.0°$, collecting reflections with indices of the form $+h \pm k \pm l$. Backgrounds were scanned for 25% of the peak width on either side of the peak scan. Three reflections were chosen as intensity standards, being remeasured at 120-min intervals of X-ray exposure time. There was no significant systematic decrease in the intensities of these standards thus no decomposition correction was applied. A total of 6760 unique reflections were measured and processed in the usual way, using a value of 0.04 for p[11] to downweight intense reflections; 6248 of these were considered to be observed ($F_o^2 \geq 3\sigma(F_o^2)$) and were used in subsequent calculations. Absorption corrections were applied to the data using the method of Walker and Stuart.[12,13] See Table 2.3 for crystal data and more information on X-ray data collection.

(b) $[RhIr(CO)_2(\mu\text{-}C(CH_3)=N^tBu)(dppm)_2][CF_3SO_3]$ (8). Diffusion of ether into a concentrated CH_2Cl_2 solution of the 8, yielded purple crystals of

Table 2.3. Crystallographic Data for $[RhIr(CH_3)(CO)_3(dppm)_2][CF_3SO_3]\cdot CH_2Cl_2$ (**2**)

formula	$C_{56}H_{49}Cl_2F_3IrO_6P_4RhS$
formula weight	1396.99
crystal shape	monoclinic prism
crystal dimensions, mm	0.60 x 0.38 x 0.32
space group	$P2_1$ (No. 4)
temperature, °C	22
radiation (λ, Å)	graphite-monochromated Mo Kα (0.71069)
unit cell parameters	
a, Å	10.482 (7)
b, Å	25.435 (5)
c, Å	11.391 (3)
β, deg	114.07 (3)
V, Å^3	2773 (4)
Z	2
ρ(calcd), g cm^{-3}	1.673
linear absorption coefficient (μ), cm^{-1}	29.329
range of transmission factors	0.901-1.094
detector aperture, mm	(3.00 + tan θ) wide x 4.00 high
take-off angle, deg	3.0
maximum 2θ, deg	50.0
crystal-detector distance, mm	173
scan type	$\theta/2\theta$

Table 2.3. (continued)

scan rate, deg/min	between 1.43 and 6.71
scan width, deg	0.60 + 0.347tan θ
total unique reflections	6760 ($h \pm k \pm l$)
total observations (NO)	6248 ($Fo^2 \geq 3\sigma(Fo^2)$)
final no. params. varied (NV)	660
error in obs. of unit weight (GOF)[a]	2.157
R[b]	0.041
R_w[c]	0.056

[a] $GOF = \left[\sum w(|F_o| - |F_c|)^2 \,/\, (NO - NV)\right]^{1/2}$ where $w = 4F_o^2 / \sigma^2(F_o^2)$.

[b] $R = \sum ||F_o| - |F_c|| \,/\, \sum |F_o|$. [c] $R_w = \left[\sum \omega(|F_o| - |F_c|)^2 \,/\, \sum \omega F_o^2\right]^{1/2}$.

the complex, several of which were mounted and flame sealed in glass capillaries under solvent vapor to minimise decomposition or deterioration due to solvent loss. Data collection and the derivation of unit-cell parameters proceeded in a manner similar to that above, except that data collection was carried out at a different temperature in this case. The monoclinic diffraction symmetry and the systematic absences (*h0l*, *h+l*=odd; *0k0*, *k*=odd), were consistent with the space group $P2_1/n$.

Intensity data were collected at -65 °C using the $\theta/2\theta$ scan technique to a maximum $2\theta = 50.0°$, collecting reflections with indices of the form $+h +k \pm l$. Of 11042 unique reflections measured, 3029 were considered to be observed and were used in subsequent calculations, with absorption corrections applied as above. See Table 2.4 for crystal data and more information on X-ray data collection.

Structure Solution and Refinement. (a) $[RhIr(CH_3)(CO)_3(dppm)_2]$-$[CF_3SO_3]\cdot CH_2Cl_2$ (2). The structure of **2** was solved in the space group $P2_1$ using standard Patterson and Fourier techniques. Although location of all atoms was straightforward, initial refinements resulted in unusually high thermal parameters for the atoms of the carbonyl groups and the methyl carbon atom. In addition the isotropic thermal parameter for Ir was unusually high and that of Rh was unusually low. A difference Fourier calculation at this stage showed the presence of superimposed methyl and carbonyl groups. This together with the anomalous thermal parameters for the metals led to the model shown below, in which two of the molecules, represented as **A** and **B** in the diagram below (the dppm ligands are omitted for clarity), are disordered in approximately a 60:40 ratio (determined from the relative peak intensities of the ordered and disordered atoms). The two

Table 2.4. Crystallographic Data for $[RhIr(CO)_2(\mu\text{-}C(CH_3)=N^tBu)(dppm)_2][CF_3SO_3]$ (**8**).

formula	$C_{59}H_{49}Cl_2F_3IrNO_6P_4RhS$
formula weight	1367.18
crystal shape	monoclinic prism
crystal dimensions, mm	0.60 x 0.38 x 0.32
space group	$P2_1/n$ (nonstandard setting of $P2_1/c$, No. 14)
temperature, °C	-65
radiation (λ, Å)	graphite-monochromated Mo Kα (0.71069)
unit cell parameters	
a, Å	12.708(2)
b, Å	24.237(3)
c, Å	20.328(2)
β, deg	98.87(2)
V, Å^3	6186(2)
Z	4
ρ(calcd), g cm^{-3}	1.468
linear absorption coefficient (μ), cm^{-1}	25.823
range of transmission factors	0.9129-1.0366
detector aperture, mm	(3.00 + tan θ) wide x 4.00 high
take-off angle, deg	3.0
maximum 2θ, deg	50.0

Table 2.4. (continued)

crystal-detector distance, mm	173
scan type	$\theta/2\theta$
scan rate, deg/min	between 1.43 and 6.71
scan width, deg	0.70 + 0.347 tan θ
total unique reflections	11042 ($+h$ $+k$ $\pm l$)
total observations (NO)	3029 ($Fo^2 \geq 3\sigma(Fo^2)$)
final no. params. varied (NV)	377
error in obs. of unit weight (GOF)[a]	1.542
R^b	0.071
$R_w{}^c$	0.071

[a,b,c] See footnotes of Table 2.4.

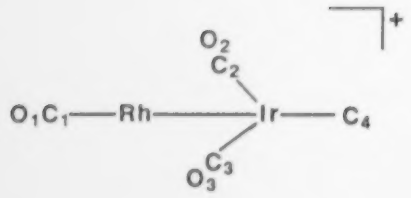

A

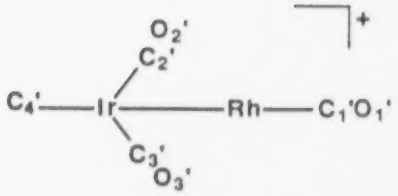

B

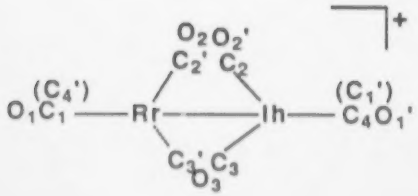

C

molecules, **A** and **B**, are superimposed such that they have the metal atom positions overlapping. This is represented as **C**, in which Rr and Ih indicate the disordered Rh and Ir positions with Rr being 60% Rh and Ih being 60% Ir. The solid lines connect atoms of the major rotomer whereas the dashed lines show the minor one. The disordered atoms are either unprimed or primed, with the former having the higher occupancy. There was no apparent disorder involving the phosphine groups, which appeared to be well behaved. A similar kind of disorder was observed in the X-ray structure determination of $[RhMn(CO)_3(\mu\text{-}CO_3)(dppm)_2]$.[6d]

All non-hydrogen atoms of the complex cation and anion were located. In addition, one molecule of CH_2Cl_2 per formula unit of complex was also located. Atomic scattering factors [14,15] and anomalous dispersion terms[16] were taken from the usual tabulations. Hydrogen atoms, with the exception of the methylene chloride hydrogens, were included as fixed contributions

but not refined. Their idealized positions were calculated from the geometries about the attached carbon atoms, using a C-H bond length of 0.95 Å, and they were assigned thermal parameters 20% greater than the equivalent isotropic B's of their attached C atoms.

The final model, with 660 parameters refined, converged to values of $R = 0.041$ and $R_w = 0.056$. Since the space group $P2_1$ is chiral, refinement of the structure in the opposite hand was also carried out, but this yielded significantly poorer residuals ($R = 0.047$ and $R_w = 0.067$), suggesting that the existing solution is the right one. In the final difference Fourier map the 10 highest residuals (1.8 - 1.1 e/Å^3) were found to be in the vicinity of the metal and carbonyl groups. A typical carbon atom in an earlier synthesis had an electron density of *ca.* 5.9 e/Å^3. The positional and isotropic thermal parameters of the non-hydrogen atoms of **2** are given in Table 2.5.

(b) [RhIr(CO)$_2$(μ-C(CH$_3$)=N^{t}Bu)(dppm)$_2$][CF$_3$SO$_3$] (8). The structure was solved in the space group $P2_1/n$ using standard Patterson and Fourier techniques. Full matrix least-squares refinements proceeded so as to minimize the function $\sum w(|F_o| - |F_c|)^2$, where $w = 4F_o^2 / \sigma^2(F_o^2)$. All non-hydrogen atoms were ultimately located. Atomic scattering factors[14,15] and anomalous dispersion terms[16] were taken from the usual tabulations. Hydrogen atoms, as well as the carbon atom of the triflate anion, were included as fixed contributions but not refined. Their idealized positions were calculated from the geometries about the attached carbon atoms, using a C-H bond length of 0.95 Å, and they were assigned thermal parameters 20% greater than the equivalent isotropic B's of their attached C atoms.

The triflate anion was found to be badly behaved. Although the SO_3 moiety was located and refined well, the CF_3 moiety did not refine well.

Table 2.5. Positional and Thermal Parameters for the Atoms of $[RhIr(CH_3)(CO)_3(dppm)_2][CF_3SO_3]\cdot CH_2Cl_2$ (**2**)[a]

Atom	*x*	*y*	*z*	*B*, Å^{2b}
Ir	0.20140(4)	0.00000	-0.09826(4)	2.39(1)
Rh	0.35373(5)	0.02892(2)	0.15216(4)	2.36(1)
P(1)	0.1539(2)	-0.0847(1)	-0.0479(2)	2.40(6)
P(2)	0.3001(2)	-0.0479(1)	0.2311(2)	2.49(6)
P(3)	0.2529(2)	0.0775(1)	-0.1782(2)	2.54(6)
P(4)	0.4012(2)	0.1131(1)	0.1011(2)	2.53(6)
S[c]	0.3412(3)	0.2947(1)	0.7848(3)	4.75(8)
Cl(1)[d]	0.0640(4)	0.7122(2)	0.1296(4)	8.0(1)
Cl(2)[d]	0.1732(5)	0.7813(2)	0.3464(4)	9.3(2)
O(1)	0.570(2)	0.0549(9)	0.414(2)	10.1(6)*
O(1)'	-0.016(3)	-0.025(1)	-0.363(2)	8.0(7)*
O(2)	0.501(1)	-0.0365(5)	0.018(1)	4.6(3)*
O(2)'	0.531(2)	-0.0346(8)	0.047(2)	4.3(4)*
O(3)	0.0326(8)	0.0662(4)	0.022(1)	7.8(3)
O(4)[c]	0.3959(8)	0.3449(3)	0.8338(7)	5.7(2)
O(5)[c]	0.336(1)	0.2580(4)	0.8787(9)	8.1(3)
O(6)[c]	0.2210(9)	0.2957(5)	0.666(1)	8.5(4)
F(1)[c]	0.5009(8)	0.2972(3)	0.6584(7)	6.4(2)
F(2)[c]	0.5949(8)	0.2627(4)	0.8401(8)	8.5(3)
F(3)[c]	0.441(1)	0.2220(3)	0.6882(9)	9.9(4)
C(1)	0.494(2)	0.0462(8)	0.320(2)	5.0(4)*
C(1)'	0.075(1)	0.0163(6)	0.277(1)	0.1(2)*
C(2)	0.388(2)	-0.0217(8)	-0.048(2)	4.1(4)*
C(2)'	0.470(2)	-0.010(1)	0.084(2)	3.7(5)*
C(3)	0.090(2)	0.0405(6)	-0.030(1)	3.2(3)*
C(3)'	0.141(3)	0.051(1)	0.071(2)	4.1(6)*
C(4)	0.098(3)	0.031(1)	-0.291(3)	8.4(7)*
C(4)'	0.451(3)	0.054(1)	0.337(2)	4.1(6)*
C(5)	0.2655(8)	-0.1024(4)	0.1172(8)	2.5(2)

Table 2.5. (continued)

C(6)	0.2913(8)	0.1318(4)	-0.0648(8)	3.0(2)
C(7)[c]	0.474(1)	0.2677(5)	0.740(1)	5.4(4)
C(11)	-0.0179(9)	-0.0990(4)	-0.0615(8)	3.1(2)
C(12)	-0.116(1)	-0.0599(4)	-0.082(1)	3.8(3)
C(13)	-0.244(1)	-0.0694(5)	-0.077(1)	5.0(3)
C(14)	-0.2750(9)	-0.1197(6)	-0.054(1)	5.6(4)
C(15)	-0.186(1)	-0.1595(4)	-0.040(1)	4.2(3)
C(16)	-0.058(1)	-0.1486(4)	-0.0420(9)	3.4(3)
C(21)	0.1859(9)	0.1353(4)	-0.1474(8)	2.8(2)
C(22)	0.318(1)	-0.1537(5)	-0.1194(9)	3.7(3)
C(23)	0.341(1)	-0.1892(5)	-0.202(1)	4.3(3)
C(24)	0.236(1)	-0.2042(5)	-0.312(1)	5.2(3)
C(25)	0.104(1)	0.1868(5)	-0.338(1)	5.1(4)
C(26)	0.0840(9)	-0.1528(5)	-0.2546(9)	3.8(3)
C(31)	0.434(1)	0.0764(4)	0.3767(8)	2.9(3)
C(32)	0.570(1)	-0.0777(5)	0.3888(9)	4.2(3)
C(33)	0.674(1)	-0.0998(5)	0.494(1)	5.0(3)
C(34)	0.644(1)	-0.1184(5)	0.591(1)	5.3(4)
C(35)	0.509(1)	-0.1192(5)	0.5788(9)	4.6(3)
C(36)	0.405(1)	-0.0986(4)	0.471(1)	3.7(3)
C(41)	0.1491(9)	-0.0412(4)	0.2706(8)	3.0(2)
C(42)	0.1381(9)	0.0042(5)	0.3324(8)	4.0(3)
C(43)	0.029(1)	0.0101(5)	0.373(1)	5.6(4)
C(44)	-0.068(1)	-0.0288(6)	0.349(1)	5.5(4)
C(45)	-0.057(1)	-0.0727(6)	0.290(1)	6.0(4)
C(46)	0.049(1)	-0.0787(5)	0.250(1)	4.6(3)
C(51)	0.1172(9)	0.1072(4)	-0.3195(8)	2.9(2)
C(52)	-0.023(1)	0.1030(5)	-0.342(1)	4.9(3)
C(53)	-0.125(1)	0.1252(6)	-0.445(1)	5.8(4)
C(54)	-0.093(1)	0.1532(5)	-0.534(1)	4.6(3)
C(55)	0.042(1)	0.1585(5)	-0.511(1)	5.4(4)
C(56)	0.145(1)	0.1350(5)	0.408(1)	5.2(3)

Table 2.5. (continued)

C(61)	0.4006(9)	0.0718(4)	-0.2201(9)	3.3(3)
C(62)	0.415(1)	0.0263(4)	-0.284(1)	4.6(3)
C(63)	0.522(1)	0.0206(5)	-0.319(1)	6.1(3)
C(64)	0.623(1)	0.0584(6)	-0.291(1)	6.3(4)
C(65)	0.612(1)	0.1046(5)	-0.230(1)	5.3(3)
C(66)	0.501(1)	0.1099(4)	-0.1965(9)	3.8(3)
C(71)	0.3707(9)	0.1645(4)	0.1969(8)	2.7(2)
C(72)	0.478(1)	0.1846(5)	0.306(1)	5.9(3)
C(73)	0.444(1)	0.2201(7)	0.382(1)	7.9(5)
C(74)	0.316(1)	0.2363(5)	0.354(1)	5.3(3)
C(75)	0.209(1)	0.2184(5)	0.246(1)	5.7(4)
C(76)	0.238(1)	0.1817(5)	0.171(1)	4.8(3)
C(81)	0.5771(9)	0.1253(4)	0.1142(8)	3.0(2)
C(82)	0.673(1)	0.0864(4)	0.137(1)	3.8(3)
C(83)	0.800(1)	0.0948(5)	0.137(1)	5.3(4)
C(84)	0.835(1)	0.1454(6)	0.112(1)	5.2(4)
C(85)	0.743(1)	0.1853(5)	0.093(1)	4.2(3)
C(86)	0.6163(9)	0.1761(4)	0.0946(9)	3.3(3)
C(99)[d]	0.030(1)	0.7448(6)	0.248(1)	6.9(5)

[a]Numbers in parentheses are estimated standard deviations in the least significant digits in this and all subsequent tables. Those parameters without an esd were not refined. The atoms labelled Rh and Ir are actually a 60:40 mix of Rh/Ir and Ir/Rh, respectively, owing to disorder (see Experimental Section). Primed atoms have 40% occupancy and are related to the unprimed (60% occupancy) atoms by the rotational disorder. [b]Starred B values are for atoms refined isotropically. B values for the anisotropically refined atoms are given in the form of the equivalent isotropic Gaussian displacement parameter defined as:
$4/3[a^2\beta_{11} + b^2\beta_{22} + c^2\beta_{33} + ab(\cos\gamma)\beta_{12} + ac(\cos\beta)\beta_{13} + bc(\cos\alpha)\beta_{23}]$. [c]Triflate atoms. [d]Solvent atoms.

49

These atoms were located in the Fourier maps, but the carbon atom invariably refined towards the fluorine atom positions. This carbon atom was fixed at its observed position and was not refined. The thermal parameters for the fluorines were very high, consistent with the smeared out electron density observed in their positions on Fourier maps. The final model, with 377 parameters refined, converged to values of $R = 0.071$ and $R_w = 0.071$. In the final difference Fourier map, the 10 highest residuals (1.6 - 1.0 $e/Å^3$) were found to be in the vicinity of the phenyl rings, the carbonyl groups and the dppm methylene groups. A typical carbon atom in an earlier synthesis had an electron density of *ca.* 3.5 $e/Å^3$. The positional and isotropic thermal parameters of the non-hydrogen atoms are given in Table 2.6.

Results and discussion

(a) Preparation and characterization of $[RhIr(CH_3)(CO)_3(dppm)_2][CF_3SO_3]$ (2). Earlier work in this research group and by Eisenberg and coworkers had shown that protonation of the complexes $[Ir_2(CO)_3(dppm)_2]$, $[Rh_2(CO)_3(dppm)_2]$ and their heterobinuclear analogue, $[RhIr(CO)_3(dppm)_2]$ (**1**), yielded the hydrido-bridged complexes, $[Ir_2(CO)_2(\mu\text{-}CO)(\mu\text{-}H)(dppm)_2][BF_4]$,[6s] $[Rh_2(CO)_2(\mu\text{-}CO)(\mu\text{-}H)(dppm)_2][BF_4]$[17] and $[RhIr(CO)_3(\mu\text{-}H)(dppm)_2][BF_4]$,[6m] respectively, by apparent electrophilic attack at the metal-metal bond. Based on these results, the reaction of **1**[6m] with the electrophile CH_3^+ (in the form of methyl triflate) was attempted, in efforts to obtain a CH_3-bridged analogue of these hydrido-bridged species. Unlike the protonations, the reaction of **1** with 1 equiv of methyl triflate does not yield the product having the electrophile in a bridged position, but gives instead, $[RhIr(CH_3)(CO)_3(dppm)_2][CF_3SO_3]$ (**2**), having the methyl group terminally bound to Ir (see

Table 2.6. Positional and Thermal Parameters for the Atoms of $[RhIr(CO)_2(\mu\text{-}C(CH_3)\text{=}N^tBu)(dppm)_2][CF_3SO_3]$ (8)[a]

50

Table 2.6. Positional and Thermal Parameters for the Atoms of $[RhIr(CO)_2(\mu\text{-}C(CH_3)\text{=}N^tBu)(dppm)_2][CF_3SO_3]$ (8)[a]

Atom	*x*	*y*	*z*	*B*, Å^2[b]
Ir	0.1047(1)	0.92376(4)	0.26515(6)	2.30(2)*
Rh	0.3106(2)	0.93616(8)	0.3534(1)	2.40(6)*
P(1)	0.0579(6)	0.9438(3)	0.3152(4)	2.8(2)*
P(2)	0.2639(6)	0.8601(3)	0.4115(4)	2.9(2)*
P(3)	0.1429(6)	0.9921(3)	0.1942(3)	2.6(2)*
P(4)	0.3441(6)	1.0134(3)	0.2934(4)	2.7(2)*
S[c]	0.6480(8)	0.8601(4)	-0.0605(5)	6.5(3)*
F(1)[c]	0.599(5)	0.866(3)	0.040(2)	61.1(3)*
F(2)[c]	0.443(3)	0.873(3)	-0.069(2)	39.3(3)*
F(3)[c]	0.540(4)	0.910(2)	0.0 (2)	57.7(3)*
O(1)	-0.036(1)	0.9889(7)	0.345(9)	3.9(6)*
O(2)	0.356(2)	1.0009(7)	0.4786(9)	5.0(7)*
O(3)[c]	0.634(2)	0.8043(9)	-0.059(1)	9.9(7)*
O(4)[c]	0.637(3)	0.882(2)	-0.122(2)	18.9(7)*
O(5)[c]	0.733(3)	0.877(2)	-0.015(2)	25.5(7)*
N	0.314(2)	0.8859(7)	0.2675(9)	2.2(6)*
C(1)	0.032(2)	0.967(1)	0.308(1)	3.6(7)
C(2)	0.337(2)	0.977(1)	0.429(1)	3.3(6)
C(3)	0.206(2)	0.843(1)	0.173(1)	3.8(7)
C(4)	0.216(2)	0.878(1)	0.229(1)	3.0(6)
C(5)	0.424(2)	0.858(1)	0.254(1)	3.4(7)
C(6)	0.452(3)	0.875(1)	0.192(2)	5.4(8)
C(7)	0.416(2)	0.798(1)	0.264(1)	4.9(8)
C(8)	0.508(2)	0.876(1)	0.308(1)	4.2(7)
C(9)	0.178(2)	0.8117(9)	0.362(1)	1.8(5)
C(10)	0.278(2)	1.009(1)	0.207(1)	2.9(6)
C(11)	-0.043(2)	0.8469(9)	0.369(1)	2.7(6)
C(12)	-0.042(2)	0.812(1)	0.422(1)	3.9(7)
C(13)	-0.126(3)	0.812(1)	0.457(2)	5.1(8)

Table 2.6. (continued)

C(14)	-0.205(3)	0.850(1)	0.443(2)	6.3(9)
C(15)	-0.212(3)	0.884(1)	0.392(2)	6.7(9)
C(16)	-0.133(2)	0.881(1)	0.356(1)	3.8(7)
C(21)	0.0 (2)	0.789(1)	0.260(1)	3.7(7)
C(22)	-0.002(2)	0.736(1)	0.276(1)	4.0(7)
C(23)	-0.061(2)	0.695(1)	0.236(1)	4.5(7)
C(24)	-0.107(3)	0.714(1)	0.175(2)	6.3(9)
C(25)	-0.102(3)	0.763(1)	0.155(2)	5.5(8)
C(26)	-0.055(2)	0.807(1)	0.197(1)	4.5(7)
C(31)	0.377(2)	0.819(1)	0.451(1)	2.9(6)
C(32)	0.386(2)	0.762(1)	0.449(1)	3.4(6)
C(33)	0.474(2)	0.737(1)	0.494(1)	3.7(7)
C(34)	0.552(3)	0.767(1)	0.521(2)	5.4(8)
C(35)	0.542(2)	0.820(1)	0.525(1)	4.1(7)
C(36)	0.458(2)	0.848(1)	0.499(1)	3.5(7)
C(41)	0.192(2)	0.8731(9)	0.481(1)	1.7(5)
C(42)	0.193(2)	0.833(1)	0.530(1)	3.9(7)
C(43)	0.137(2)	0.843(1)	0.581(1)	4.4(7)
C(44)	0.091(2)	0.892(1)	0.587(1)	4.8(8)
C(45)	0.086(2)	0.931(1)	0.539(1)	3.4(6)
C(46)	0.140(2)	0.921(1)	0.494(1)	3.2(6)
C(51)	0.116(2)	0.9683(9)	0.108(1)	2.7(6)
C(52)	0.020(2)	0.946(1)	0.088(1)	4.1(7)
C(53)	-0.010(2)	0.922(1)	0.023(1)	3.8(6)
C(54)	0.066(2)	0.925(1)	-0.016(1)	4.4(6)
C(55)	0.161(3)	0.948(1)	0.001(2)	7(1)
C(56)	0.185(2)	0.972(1)	0.066(1)	3.7(7)
C(61)	0.074(2)	1.0579(9)	0.193(1)	2.3(6)
C(62)	-0.033(2)	1.057(1)	0.200(1)	4.0(7)
C(63)	-0.093(2)	1.105(1)	0.196(1)	4.7(8)
C(64)	-0.045(2)	1.153(1)	0.185(1)	4.1(7)
C(65)	0.055(2)	1.157(1)	0.175(1)	4.0(7)
C(66)	0.109(2)	1.107(1)	0.178(1)	3.4(6)

Table 2.6. (continued)

52

C(71)	0.479(2)	1.0274(9)	0.291(1)	2.1(5)
C(72)	0.550(3)	1.031(1)	0.351(2)	5.7(9)
C(73)	0.656(3)	1.041(1)	0.355(1)	5.1(8)
C(74)	0.698(3)	1.042(1)	0.300(2)	6.1(9)
C(75)	0.636(3)	1.038(1)	0.239(1)	5.5(8)
C(76)	0.528(2)	1.031(1)	0.235(1)	3.1(6)
C(81)	0.293(2)	1.080(1)	0.319(1)	2.3(5)
C(82)	0.329(2)	1.128(1)	0.297(1)	3.3(6)
C(83)	0.291(2)	1.176(1)	0.312(1)	3.7(7)
C(84)	0.222(2)	1.181(1)	0.352(1)	3.7(7)
C(85)	0.182(2)	1.134(1)	0.375(1)	3.6(7)
C(86)	0.219(2)	1.0839(9)	0.360(1)	2.4(5)
C(99)[c]	0.540(0)	0.884(0)	-0.036(0)	20.0

[a]Numbers in parentheses are estimated standard deviations in the least significant digits in this and all subsequent tables. Those parameters without an esd were not refined. [b]Starred B values are for atoms refined anisotropically. B values for the anisotropically refined atoms are given in the form of the equivalent isotropic Gaussian displacement parameter defined as:

$4/3[a^2\beta_{11} + b^2\beta_{22} + c^2\beta_{33} + ab(\cos\gamma)\beta_{12} + ac(\cos\beta)\beta_{13} + bc(\cos\alpha)\beta_{23}]$. [c]Triflate atoms.

Scheme 2.1). Although initial attack may occur at the Rh-Ir bond, this cannot be confirmed, since reactions performed at low temperature yielded **2** as the only product. In contrast to this, the reaction of methyl triflate with $[Ir_2(CO)_3(dppm)_2]$[86] does show evidence of a methyl-bridged species (see Chapter 3 and elsewhere[19]).

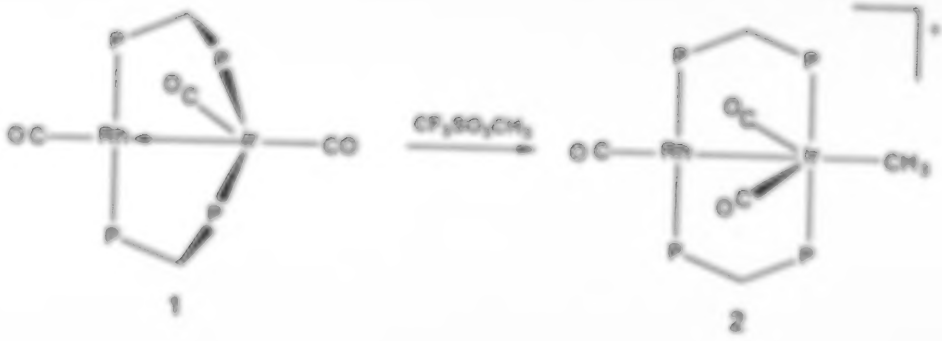

Scheme 2.1.

The ^1H NMR spectrum of **2** shows the methyl resonance as a triplet at δ -0.08, and selective ^{31}P-decoupling experiments confirm that the methyl protons are coupled only to the phosphorus nuclei on Ir. Upon selectively decoupling the Ir-bound phosphorus resonance, the methyl triplet in the ^1H NMR spectrum collapses to a singlet, whereas decoupling the Rh-bound phosphorus resonance does not alter its appearance. The absence of Rh coupling to the methyl protons also supports the model in which the methyl group is bound to Ir, but is equivocal since such coupling is only 2-4 Hz at most in related Rh-bound methyl species (*vide infra*).[6c,7,8,9] The $^{13}C\{^1H\}$ NMR spectrum, which shows a doublet of triplets at δ 183.7 ($^1J_{Rh\text{-}C}$ = 75.0 Hz) and a triplet at δ 187.9, with intensity ratios 1:2, respectively, indicates that compound **2** has one terminal carbonyl group on Rh and two on Ir. Taken

together the NMR spectroscopic data clearly establish the structure of 2, having one terminal carbonyl group bound to Rh and the methyl group as well as two terminal carbonyl groups bound to Ir as shown in Scheme 2.1.

The proposed structure is confirmed by the X-ray structure determination. The asymmetric unit of compound 2 contains the complex cation, a triflate anion and one molecule of CH_2Cl_2 solvent. The geometries of the triflate anion and the solvent molecule are as expected, and there are no unusual contacts involving the solvent and the ions. A perspective drawing of the cation of this compound is shown in Figure 2.1, with the dppm ligands bridging the metal nuclei in a typical manner. Although as noted earlier, the non-phosphine components of the cation are disordered in a 60:40 ratio, only the molecule having the larger occupancy is shown. In Tables 2.7 and 2.8 the parameters involving both disordered molecules are shown, with the atoms of the minor species being primed; however, in this discussion only the parameters of the major species are discussed, since they are more reliable.

Owing to the disorder, there will be some uncertainty in the metal-ligand parameters; nevertheless the crystal structure does confirm the gross overall structure of compound 2. As is observed in most other binuclear dppm-bridged systems, the diphosphine groups are oriented trans to each other about the metal centers (P(1)-Ir-P(3) = 170.17(7)° and P(2)-Rh-P(4) = 170.22(7)°) and are both cis to the other atoms coordinated to the metal nuclei. The Rh metal has the distorted square planar geometry expected for Rh(I) species, while the Ir metal has a distorted trigonal bipyramidal geometry (ignoring the metal-metal bond). The discussion of the nature of the metal-metal bond requires a concomitant consideration of metal oxidation states. If the positive charge is considered to be localized on Ir, then the oxidation state assignment is Ir(+2)/Rh(0) and this d^7/d^9 system would require a metal-metal

55

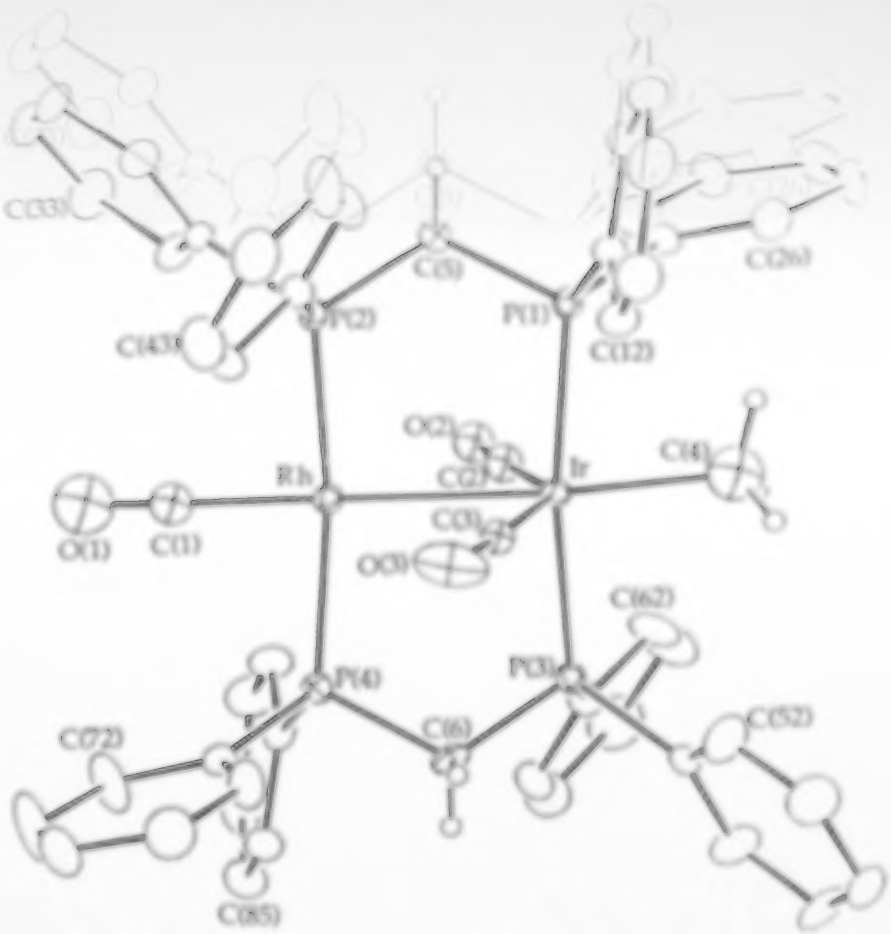

Figure 2.1. A perspective view of the $[RhIr(CH_3)(CO)_3(dppm)_2]^+$ cation, showing the numbering scheme. Thermal ellipsoids are shown at the 20% level except for the methyl and methylene hydrogens, which are shown artificially small and the phenyl hydrogens, which are omitted.

Table 2.7. Selected Distances in (Å) in $[RhIr(CH_3)(CO)_3(dppm)_2][CF_3SO_3]\cdot CH_2Cl_2$ (2)[a]

56

Table 2.7. Selected Distances in (Å) in $[RhIr(CH_3)(CO)_3(dppm)_2][CF_3SO_3]\cdot CH_2Cl_2$ (2)[a]

(a) Bonded			
Ir-Rh	2.743(1)	P(2)-C(41)	1.820(8)
Ir-P(1)	2.336(2)	P(3)-C(6)	1.821(9)
Ir-P(3)	2.327(2)	P(3)-C(51)	1.819(8)
Ir-C(1)′	1.97(1)	P(3)-C(61)	1.803(8)
Ir-C(2)	1.88(2)	P(4)-C(6)	1.830(8)
Ir-C(3)	1.94(1)	P(4)-C(71)	1.813(8)
Ir-C(4)	2.16(3)	P(4)-C(81)	1.816(8)
Rh-P(2)	2.316(2)	O(1)-C(1)	1.06(2)
Rh-P(4)	2.326(2)	O(1)-C(4)′	1.19(3)
Rh-C(1)	1.93(2)	O(1)′-C(1)′	1.07(3)
Rh-C(2)′	1.96(2)	O(1)′-C(4)	1.14(3)
Rh-C(3)′	2.11(2)	O(2)-C(2)	1.15(2)
Rh-C(4)′	2.04(3)	O(2)-C(2)′	1.49(2)
P(1)-C(5)	1.820(8)	O(2)′-C(2)	1.49(2)
P(1)-C(11)	1.782(8)	O(2)′-C(2)′	1.09(2)
P(1)-C(21)	1.834(8)	O(3)-C(3)	1.20(1)
P(2)-C(5)	1.831(8)	O(3)-C(3)′	1.11(2)
P(2)-C(31)	1.827(7)		
(b) Non-bonded			
Rh-C(2)	2.77(1)	P(1)-P(2)	3.060(3)
Rh-C(3)	2.71(1)	P(3)-P(4)	3.055(3)
C(2)-C(2)′	1.43 (2)	C(3)-C(3)′	1.09 (2)

[a]The atoms labelled Rh and Ir are actually a 60:40 mix of Rh/Ir and Ir/Rh, respectively, owing to disorder (see Experimental Section). Primed atoms have 40% occupancy and are related to the unprimed (60% occupancy) atoms by the rotational disorder.

57

Table 2.8. Selected Angles (deg) in $[RhIr(CH_3)(CO)_3(dppm)_2][CF_3SO_3]\cdot CH_2Cl_2$ (2)[a]

Table 2.8. Selected Angles (deg) in
$[RhIr(CH_3)(CO)_3(dppm)_2][CF_3SO_3]\cdot CH_2Cl_2$ (2)[a]

Rh-Ir-P(1)	94.95(5)	C(5)-P(1)-C(11)	103.8(3)
Rh-Ir-P(3)	92.74(5)	C(5)-P(1)-C(21)	105.3(4)
Rh-Ir-C(1)'	173.7(4)	C(11)-P(1)-C(21)	103.5(4)
Rh-Ir-C(2)	70.7(5)	Rh-P(2)-C(5)	112.0(2)
Rh-Ir-C(3)	68.2(4)	Rh-P(2)-C(31)	117.8(3)
Rh-Ir-C(4)	173.2(7)	Rh-P(2)-C(41)	113.1(3)
P(1)-Ir-P(3)	170.17(7)	C(5)-P(2)-C(31)	101.6(3)
P(1)-Ir-C(1)'	86.4(4)	C(5)-P(2)-C(41)	107.6(3)
P(1)-Ir-C(2)	87.6(5)	C(31)-P(2)-C(41)	103.6(4)
P(1)-Ir-C(3)	99.6(4)	Ir-P(3)-C(6)	112.7(2)
P(1)-Ir-C(4)	81.0(7)	Ir-P(3)-C(51)	118.3(2)
P(3)-Ir-C(1)'	86.6(4)	Ir-P(3)-C(61)	113.5(3)
P(3)-Ir-C(2)	89.2(5)	C(6)-P(3)-C(51)	100.5(3)
P(3)-Ir-C(3)	88.9(4)	C(6)-P(3)-C(61)	106.3(4)
P(3)-Ir-C(4)	90.7(7)	C(51)-P(3)-C(61)	104.1(4)
C(2)-Ir-C(3)	138.8(6)	Rh-P(4)-C(6)	112.8(3)
C(2)-Ir-C(4)	103.5(8)	Rh-P(4)-C(71)	113.9(2)
C(3)-Ir-C(4)	117.8(8)	Rh-P(4)-C(81)	117.1(3)
Ir-Rh-P(2)	92.56(5)	C(6)-P(4)-C(71)	104.2(4)
Ir-Rh-P(4)	94.73(5)	C(6)-P(4)-C(81)	103.3(3)
Ir-Rh-C(1)	167.9(6)	C(71)-P(4)-C(81)	104.3(4)
Ir-Rh-C(2)'	69.1(6)	Rh-C(1)-O(1)	178(2)
Ir-Rh-C(3)'	63.5(6)	Ir-C(1)'- O(1)'	163(2)
Ir-Rh-C(4)'	174.8(8)	Ir-C(2)-O(2)	178(1)
P(2)-Rh-P(4)	170.22(7)	P(4)-Rh-C(1)	83.1(5)
P(2)-Rh-C(1)	91.0(5)	P(4)-Rh-C(2)'	97.9(6)
P(2)-Rh-C(2)'	90.8(6)	P(4)-Rh-C(3)'	86.9(6)
P(2)-Rh-C(3)'	90.5(6)	P(4)-Rh-C(4)'	84.1(7)
P(2)-Rh-C(4)'	88.0(7)	C(2)'-Rh-C(3)'	132.6(9)
Ir-P(1)-C(5)	111.6(2)	C(2)'-Rh-C(4)'	116(1)

58

Table 2.8 (continued)

Table 2.8 (continnued)

Ir-P(1)-C(11)	118.7(3)	C(3)'-Rh-C(4)'	111(1)
Ir-P(1)-C(21)	112.6(2)	Rh-C(2)'-O(2)'	176(2)
Ir-C(3)-O(3)	174(1)	P(3)-C(6)-P(4)	113.6(4)
P(1)-C(5)-P(2)	113.9(4)		

[a]Labelling as in footnote of Table 2.6.

bond to give a diamagnetic compound. The other possibility places the positive charge on Rh yielding d^8/d^8 Ir(+1)/Rh(+1) centers. In this situation, the Ir has an 18-electron configuration and the trigonal bipyramidal geometry observed is as expected. However the Rh center would only have 14 valence electrons, requiring an Ir→Rh dative bond to give a square planar 16-electron configuration at this atom. This latter view appears to be the more appropriate one. A dative bond would utilize the filled d_{xy} or $d_{x^2-y^2}$ orbitals of Ir, and would require no rehybridization of the trigonal bipyramidal Ir center, whereas one would expect that the Ir(+2)/Rh(0) system, having a normal covalent bond, would result in rehybridization of Ir to give an octahedral geometry at this metal. In addition, the carbonyl stretches, which are all lower than 1990 cm^{-1}, are not consistent with Ir(+2). The Rh-Ir distance (2.743(1) Å), which is significantly shorter than the intraligand P(1)-P(2) and P(3)-P(4) distances (3.060(3) Å and 3.055(3) Å respectively), indicates substantial attraction of the adjacent metal centers, and is therefore consistent with some form of metal-metal bond. This distance is similar to that observed in the precursor, $[RhIr(CO)_3(dppm)_2]$ (2.7722(7) Å),[6m] which was also proposed to have a dative metal-metal bond. The distortion of the geometry around each metal is caused by the two metals being drawn inwards as a result of the strong dative interaction.

The assignment of the methyl group as being bound to Ir is supported by the successful refinement of the structure with a 60% and 40% occupancy for O(1) and O(1)' respectively, which indicates that O(1) is associated with the major rotomer. Consequently, this rotomer has the carbonyl group which is trans to the metal-metal bond, bound to Rh, and hence it has the methyl group bound to Ir. The essentially linear Ir-C-O linkages, as well as the magnitude of the contacts between Rh and C(2) and C(3) (2.77(1) and 2.71(1)

Å respectively), preclude any significant semibridging interaction between Rh and the carbonyls C(2)-O(2) and C(3)-O(3). This is supported by the lack of Rh coupling for these carbonyl resonances in the ^{13}C NMR spectrum.

One of the interesting features of compound **2** is that it has the methyl group bound to the saturated Ir metal. This is unlike the analogous alkyl complexes of Rh/Re,[6c] Rh/Os,[7] Rh/Mn[8] and Rh/Mo[9] all of which have the alkyl groups bound to the unsaturated Rh metal. In all cases in which the alkyl group is bound to Rh, there is at least one accompanying semibridging CO group, apparently to alleviate the electron-density buildup at the metal due to the good donor alkyl group. There are no such semibridging carbonyls in compound **2**, on the other hand, since any such electron density buildup is effectively reduced by the terminal CO ligands. It is not clear why the alkyl group should be bound to Rh in the large number of compounds while being bound to Ir in the case of **2**, especially considering the fact that **2** is isoelectronic with the related complex, $[RhOs(CH_3)(CO)_3(dppm)_2]$,[7] which has a Rh-bound methyl group.

Hence the 'RhIr' species behaves very differently from the diiridium system, as is shown in the next chapter. This is one of the several cases[6h,6j,6m-p,6r-t,17,19] (see also subsequent chapters of this thesis) in which analogous dirhodium, 'RhIr' and diiridium complexes show different reactivity patterns demonstrating the unique properties conferred on the 'RhIr' heterobinuclear systems as a result of the combination of the two different metals.

(b) Reactivity studies. Having successfully prepared the 'RhIr' methyl species, **2**, there were several aspects of its potential reactivity that were of interest. The first aspect was to establish its reductive elimination pathways (of methane etc.); the potential for two-metal involvement in binuclear

reductive elimination was of interest, and had been shown to occur in $[Pd_2(CH_3)(H)(\mu\text{-}Cl)(dppm)_2][Cl]$ (which eliminates methane at -20 °C), and $[Pd_2(CH_3)_2(\mu\text{-}H)(dppm)_2][Cl]$ (which eliminates methane and ethane at room temperature).[20] Although pathways were proposed for these dipalladium systems whereby the methyl and hydride or the two methyl groups become attached to the same metal in a cis orientation before elimination, no intermediates with such an orientation of the ligands were observed. The second aspect of interest was to induce C-C and C-heteroatom bond formation through migratory insertions of ligands such as isocyanides and carbon monoxide as well as unsaturated hydrocarbons, such as ethylene, into the M-CH_3 bond (reactions of compound **2** with a variety of alkynes were also investigated with the same aim of C-C bond formation, and these are discussed in Chapter 4).

Other aspects that were of interest included the possibilities of C-H activation of the CH_3 group by the adjacent metal and insertion of ligands such as SO_2 into the M-CH_3 bond. Such SO_2 insertions have been shown to involve direct attack of the SO_2 ligand at the alkyl group,[21] a different mechanism from that involving insertion of ligands such as carbon monoxide which proceed through the migration of the alkyl group to the carbonyl carbon. C-H activation of a coordinated methyl group by the adjacent metal has been shown to occur in the diiridium system (see chapter 3 and elsewhere[18]). Results on the reactivity of **2** are described in detail in what follows.

Reaction of **2** with H_2 yields the known trihydride species $[RhIr(H)\text{-}(CO)_2(\mu\text{-}H)_2(dppm)_2]^+$ (**3**),[6m] through methane and CO evolution, as shown in Scheme 2.2. Although no methyl hydride intermediate was observed in this reaction, even at low temperature, a related species can be obtained in the

reaction of **2** with 1 equiv of HCl to give $[RhIr(CH_3)(CO)_2(\mu\text{-}H)(\mu\text{-}Cl)(dppm)_2][CF_3SO_3]$ (**4**). Compound **4** represents a rare example in which a hydrido-methyl complex is stable to methane elimination at room temperature to the extent that it can be isolated as a solid. Although the relative positions of the equatorial ligands are not known, it is assumed that the hydride and methyl groups are not adjacent, therefore reductive elimination is inhibited.

The hydride ligand in **4** is clearly bridging, as shown by the hydride signal in the ^1H NMR spectrum, appearing as a multiplet at δ - 9.50, which collapses to a doublet of triplets on selectively decoupling each of the Rh-bound and Ir-bound phosphorus resonances, and a doublet ($^1J_{Rh\text{-}H}$ = 22.0 Hz) on broadband decoupling. The methyl group remains coordinated to Ir as demonstrated by these ^1H NMR experiments. The formation of **4** is accompanied by CO loss, as indicated by its $^{13}C\{^1H\}$ NMR spectrum, which shows a doublet of triplets at δ 189.3 ($^1J_{Rh\text{-}C}$ = 84.5 Hz) and an equal intensity triplet at δ 164.4, indicating the presence of only one CO ligand each on Rh and Ir. A similar product to **4**, $[RhIr(CH_3)(CO)_2(\mu\text{-}CO)(\mu\text{-}H)(dppm)_2][CF_3SO_3]$ (**5**), is obtained on reacting **2** with CF_3SO_3H, except that the bridging chloride ligand in **4** is replaced by a bridging CO ligand. The $^{13}C\{^1H\}$ NMR spectrum of compound **5** shows a doublet of triplets of triplets at δ 199.9 ($^1J_{Rh\text{-}C}$ = 26.2 Hz), a doublet of triplets at δ 186.0 ($^1J_{Rh\text{-}C}$ = 76.5 Hz), and a multiplet at δ 165.6,[22] indicating the presence of a bridging carbonyl group (the coupling to Rh of 26.2 Hz is slightly less than that expected for a symmetrically bridging carbonyl[18] and hence this carbonyl probably interacts slightly more strongly with Ir than with Rh) and a terminal carbonyl group each on Rh and Ir.

Reaction of compound **2** with CO yields the acyl complex,

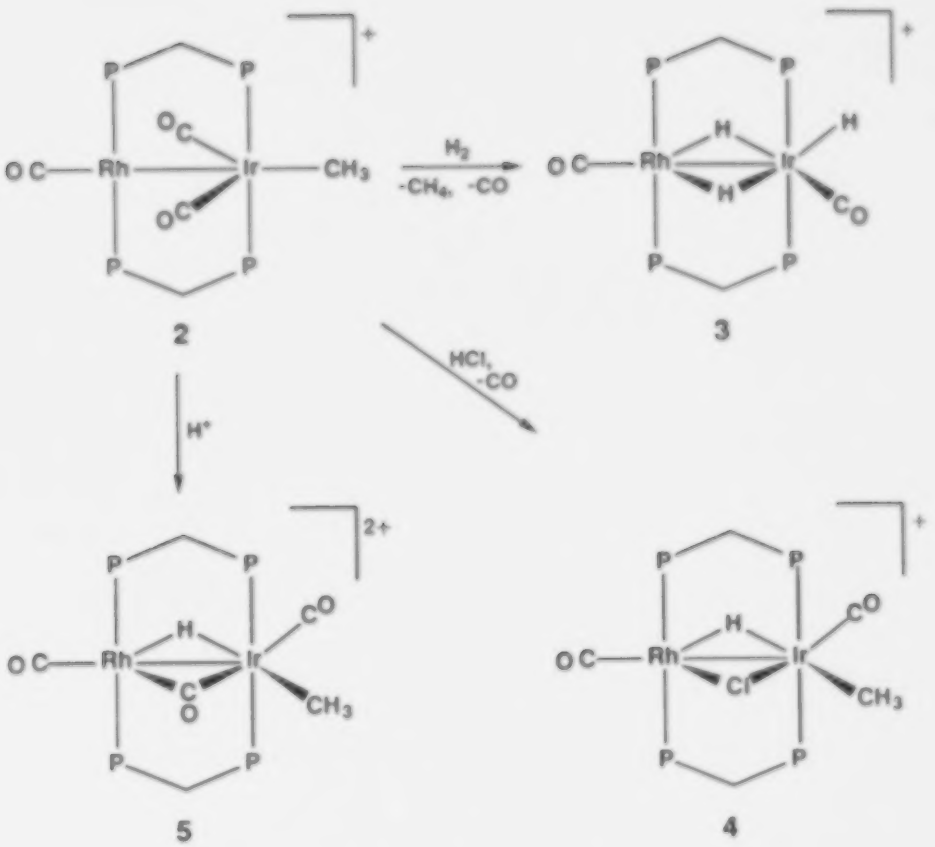

Scheme 2.2.

$[RhIr(CO)_3(COCH_3)(dppm)_2]^+$ (**6**), which is analogous to the methyl precursor. The acyl stretch in the IR spectrum of **6** appears at 1623 cm^{-1} together with CO stretches at 2003 and 1980 cm^{-1}, and the ^{13}C NMR spectrum shows the acyl carbon resonance at δ 227.9, as well as resonances at δ 194.5 and 187.9. The formation of the acyl complex **6**, is accompanied by the shift of the methyl resonance to lower field (from δ -0.08 in compound **2** to δ 0.83 in compound **6**) in the ^1H NMR spectrum as expected. This spectrum also shows a single resonance for the four dppm methylene protons, indicating that they are equivalent, which is consistent with the assigned structure of **6**, which is shown in Scheme 2.3. Compound **6**, which is unstable in the absence of an excess CO atmosphere, reverts to the precursor complex, **2**, under these conditions, making it difficult to isolate it as the triflate salt.

Reaction of compound **2** with ^{t}BuNC also results in C-C bond formation, yielding $[RhIr(CO)_2(\mu\text{-}C(CH_3)=N^tBu)(dppm)_2][CF_3SO_3]$ (**8**), the product of isocyanide insertion into the Ir-methyl bond. This insertion reaction results in loss of CO and movement of the iminoacyl group to the bridging position. The ^1H NMR spectrum of **8** shows the methyl and ^{t}butyl resonances as singlets at δ 0.82 and 0.80, respectively. The transformation of the methyl resonance from a triplet at δ -0.08 in compound **2** to a sharp singlet at lower field (δ 0.82) in **8** is consistent with the insertion of the ^{t}BuNC ligand into the M-CH_3 bond. In fact the chemical shift of the methyl group in **8** is very similar to that in the acyl complex, **6** (δ 0.82 in the former and δ 0.83 in the latter). The structure shown in Scheme 2.3 has the iminoacyl nitrogen bound to Rh rather than to Ir. This geometry could not be established from the spectroscopic data, but has been established crystallographically (vide infra). In both compounds **6** and **8**, the methyl group is one atom removed from Ir so does not show coupling to the metal-bound phosphorus nuclei.

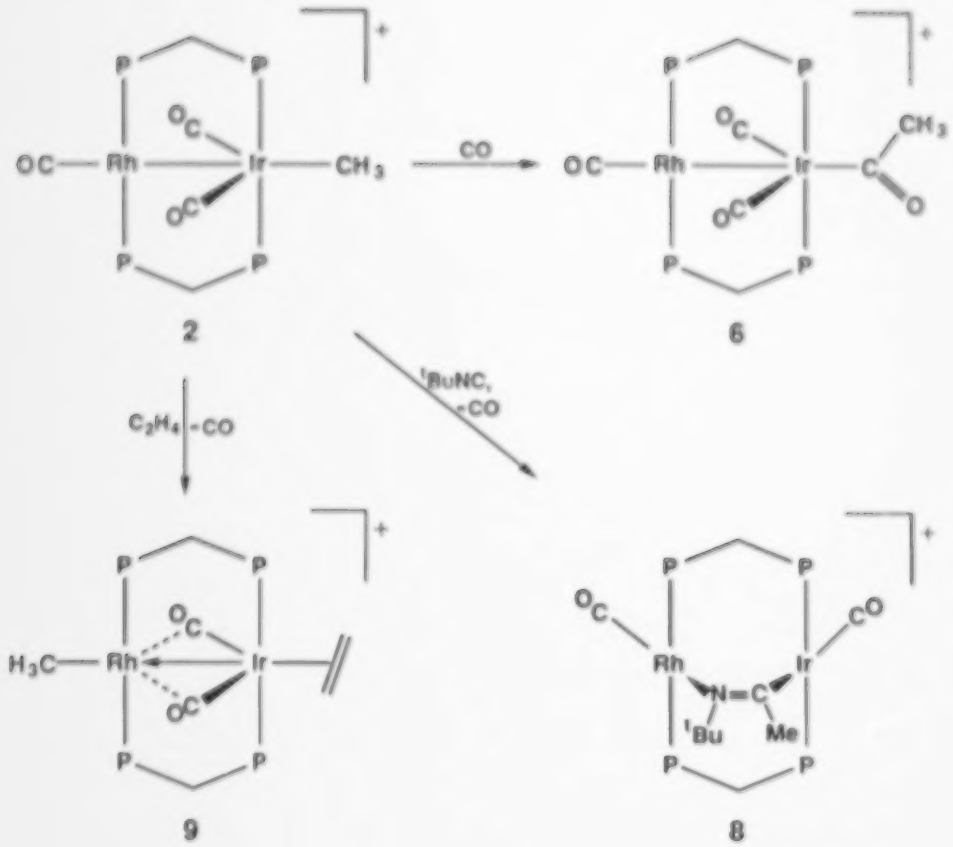

Scheme 2.3.

The $^{13}C\{^1H\}$ spectrum of **8** shows a doublet of triplets at δ 195.0 ($^1J_{Rh-C}$ = 65.0 Hz) and a triplet at δ 191.3, while the IR spectrum shows CO stretches at 1964 and 1945 cm^{-1}, indicating that there is one terminally bound carbonyl on each metal. The absence of an absorption in the 2000 to 2190 cm^{-1} range (the expected range for a C≡N stretch[23]), in the IR spectrum, is consistent with the insertion of the isocyanide ligand into the M-CH_3 bond, reducing the C-N bond order. The expected C=N stretch is probably obscured by the absorptions due to the dppm phenyl groups and is not observed. All these observations are consistent with the structure assigned to compound **8**, as shown in Scheme 2.3.

The structure of **8**, having a bridging iminoacyl ligand, was confirmed by an X-ray crystal structure determination. This structure conclusively establishes that the iminoacyl group is N-bound to Rh and C-bound to Ir. Figure 2.2 shows a perspective view of the cation of this complex, with the dppm ligands bridging the metal nuclei in a typical manner. Relevant bond lengths and angles are given in Tables 2.9 and 2.10. Within the complex cation, the diphosphine groups are oriented approximately trans to each other about the metal centers (P(1)-Ir-P(3) = 167.3(2)° and P(2)-Rh-P(4) = 175.8(3)°) and are both cis to the other atoms coordinated to the metal nuclei, resulting in a distorted square planar geometry about both metals. Formation of the iminoacyl complex **8**, is accompanied by elongation of the Rh-Ir separation from 2.743(1) Å in the precursor complex, **2** (vide supra), to 2.950(2) Å. Although the Rh-Ir separation in **8** is intermediate between those in compounds **1** (2.7722(7) Å)[6m] and **2**, which both have M-M bonds, and those in $[RhIr(H)_2(CO)_2(\mu\text{-}Cl)(dppm)_2][BF_4]$ (3.0651(5)),[6n] and $[RhIr(C{\equiv}CPh)_2(CO)_2(\mu\text{-}H)(dppm)_2][CF_3SO_3]$ (3.0582(8) Å; see Chapter 4) which have no M-M bond, it is suggested that there is no Rh-Ir bond in **8**, since this situation is

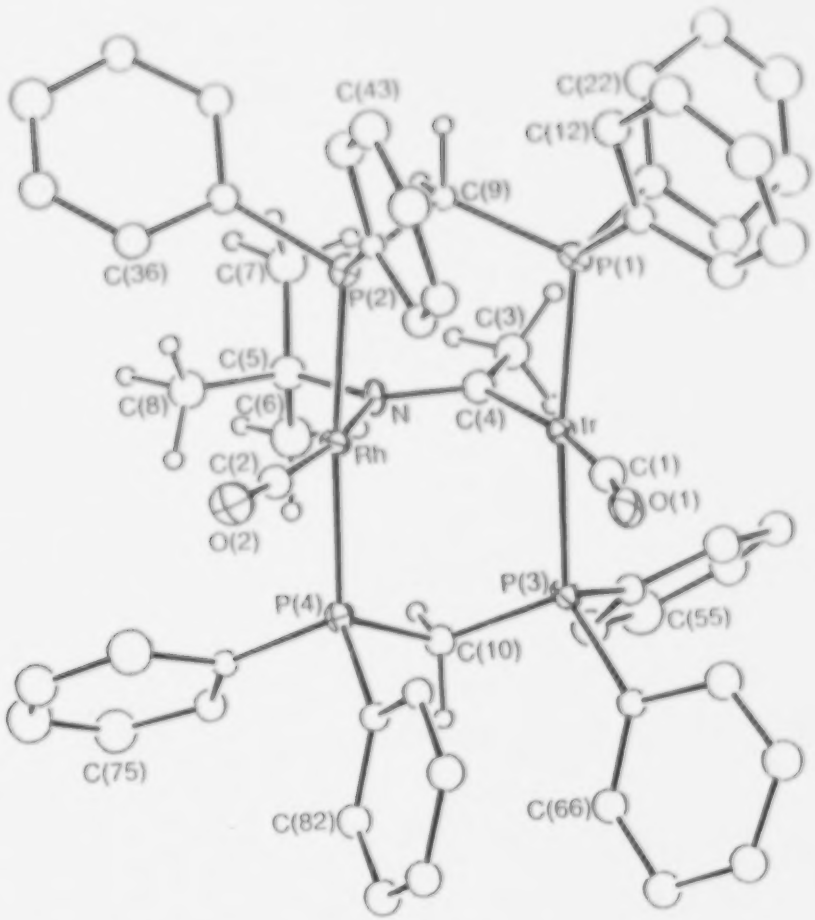

Figure 2.2. A perspective view of the $[RhIr(CO)_2(\mu\text{-}C(CH_3)=N^tBu)(dppm)_2]^+$ cation, showing the numbering . Thermal ellipsoids are shown at the 20% level except for the methyl, ^{t}butyl and methylene hydrogens, which are shown artificially small and the phenyl hydrogens, which are omitted.

Table 2.9. Selected Distances in (Å) in $[RhIr(CO)_2(\mu\text{-}C(CH_3)\text{=}N^tBu)(dppm)_2][CF_3SO_3]$ (8)

(a) Bonded

Ir-Rh	2.950(2)	P(3)-C(10)	1.75(2)
Ir-P(1)	2.310(6)	P(3)-C(51)	1.82(2)
Ir-P(3)	2.297(6)	P(3)-C(61)	1.82(2)
Ir-C(1)	1.72(3)	P(4)-C(10)	1.83(2)
Ir-C(4)	2.02(2)	P(4)-C(71)	1.76(2)
Rh-P(2)	2.316(7)	P(4)-C(81)	1.85(2)
Rh-P(4)	2.310(7)	O(1)-C(1)	1.23(3)
Rh-N	2.14(2)	O(2)-C(2)	1.16(2)
Rh-C(2)	1.82(2)	N-C(4)	1.38(2)
P(1)-C(9)	1.84(2)	N-C(5)	1.60(3)
P(1)-C(11)	1.80(2)	C(3)-C(4)	1.42(3)
P(1)-C(21)	1.83(2)	C(5)-C6	1.42(3)
P(2)-C(9)	1.80(2)	C(5)-C(7)	1.47(3)
P(2)-C(31)	1.82(2)	C(5)-C(8)	1.47(3)
P(2)-C(41)	1.81(2)		

(b) Non-bonded

P(1)-P(2)	3.04(1)	P(3)-P(4)	3.05(1)

Table 2.10. Selected Angles (deg) in $[RhIr(CO)_2(\mu\text{-}C(CH_3)\text{=}N^tBu)(dppm)_2][CF_3SO_3]$ (8)

(a) Bond Angles

Rh-Ir-P(1)	94.7(2)	Ir-P(3)-C(10)	112.2(7)
Rh-Ir-P(3)	93.2(2)	Ir-P(3)-C(51)	110.3(7)
Rh-Ir-C(1)	97.0(8)	Ir-P(3)-C(61)	119.3(8)
Rh-Ir-C(4)	71.0(6)	C(10)-P(3)-C(51)	104(1)
P(1)-Ir-P(3)	167.3(2)	C(10)-P(3)-C(61)	105(1)
P(1)-Ir-C(1)	95.1(8)	C(51)-P(3)-C(61)	104.6(9)
P(1)-Ir-C(4)	86.6(6)	Rh-P(4)-C(10)	111.6(7)
P(3)-Ir-C(1)	93.7(8)	Rh-P(4)-C(71)	115.6(7)
P(3)-Ir-C(4)	86.6(6)	Rh-P(4)-C(81)	117.3(8)
C(1)-Ir-C(4)	168(1)	C(10)-P(4)-C(71)	106(1)
Ir-Rh-P(2)	87.4(2)	C(10)-P(4)-C(81)	101.2(9)
Ir-Rh-P(4)	88.8(2)	C(71)-P(4)-C(81)	103(1)
Ir-Rh-N	64.8(5)	O(3)-P(5)-O(4)	115 (2)
Ir-Rh-C(2)	126.8(8)	O(3)-P(5(-O(5)	112(2)
P(2)-Rh-P(4)	175.8(3)	Rh-N-C(4)	114(1)
P(2)-Rh-N	90.1(5)	Rh-N-C(5)	120(1)
P(2)-Rh-C(2)	91.5(7)	C(4)-N-C(5)	125(2)
P(4)-Rh-N	90.1(5)	Ir-C(1)-O(1)	171(2)
P(4)-Rh-C(2)	89.1(7)	Rh-C(2)-O(2)	177(2)
N-Rh-C(2)	168.4(9)	Ir-C(4)-N	110(1)
Ir-P(1)-C(9)	109.5(7)	Ir-C(4)-C(3)	130(2)
Ir-P(1)-C(11)	119.0(7)	N-C(4)-C(3)	120(2)
Ir-P(1)-C(21)	116.5(8)	N-C(5)-C(6)	112(2)
C(9)-P(1)-C(21)	104(1)	N-C(5)-C(7)	108(2)
C(11)-P(1)-C(21)	98(1)	N-C(5)-C(8)	108(2)
Rh-P(2)-C(9)	114.6(7)	C(6)-C(5)-C(7)	116(2)
Rh-P(2)-C(31)	114.1(8)	C(6)-C(5)-C(8)	109(2)

Table 2.10. (continued)

Rh-P(2)-C(41)	117.0(7)	C(7)-C(5)-C(8)	104(2)
C(9)-P(2)-C(31)	105(1)	P(1)-C(9)-P(2)	113(1)
C(9)-P(2)-C(41)	102(1)	P(3)-C(10)-P(4)	116(1)
C(31)-P(2)-C(41)	102(1)	C(9)-P(1)-C(11)	108(1)

(b) Torsion Angles

P(1)-Ir-Rh-N	87.2(6)	C(4)-Ir-Rh-P(4)	93.1(7)

more consistent with electron counting. Even though the two metals are drawn together to some extent, as indicated by the longer intraligand P-P separations of 3.04(1) Å (P(1)-P(2)) and 3.05(1) Å (P(3)-P(4)), this is apparently due to non-bonded interactions between the ^{t}butyl group and the phenyl groups bound to P(4) and not a Rh-Ir bond. The iminoacyl bridge is perpendicular to the metal phosphorus plane (the torsion angles are P(1)-Ir-Rh-N = 87.2(6)° and C(4)-Ir-Rh-P(4) = 93.1(7)°), and the Ir-C(4) and Rh-N distances of 2.02(2) Å and 2.14 (2) Å, respectively, are within the expected range for Ir-C and Rh-N single bonds. Also the C-C bonds within the iminoacyl ligand are consistent with single bonds involving either sp2 or sp3 carbon atoms. The N-C(4) separation of 1.38(2) Å is longer than those of the bridging iminoacyl ligands in $[Os_3(CO)_{10}(\mu\text{-H})(\mu\text{-}\eta^2\text{-}C_6H_5C{=}NCH_3]$ (1.278(10) Å),[24] and $[Fe_2\{\eta^2\text{-C(Mes)N}^t\text{Bu}\}_2(\mu\text{-C(Mes)}{=}\text{N}^t\text{Bu})_2]$ (Mes = 2,4,6-$Me_3C_6H_2$-; 1.295(10) Å),[25] and is also longer than a normal N=C bond (*ca.* 1.30 Å[26]). The geometries around C(4) and N are the normal trigonal planar geometries, with the Ir-C(4)-C(3) angle (130(2)°) slightly increased at the expense of the Ir-C(4)-N angle (110(1)°), while the ^{t}butyl group adopts a normal tetrahedral geometry. The carbonyl geometries and distances are normal for such terminally bound groups.

The insertion of an isocyanide ligand into a M-C σ bond is well documented.[25,27] Whether the resulting iminoacyl formed is bonded in a mono- or bidentate manner depends ultimately on the electronic configuration and the required coordination geometry of the metals in the complex.[27a] In **8**, coordination of the lone pair on the nitrogen atom to Rh gives it the square planar geometry characteristic of Rh (I). Compound **8** is very similar to $[Pd_2(\mu\text{-}CH_3N{=}CCH_3)(CNCH_3)_2(dppm)_2]^{3+}$,[27c] which is also obtained by the insertion of an isocyanide into a M-CH_3 bond. Other

examples of bridging iminoalkyl ligands,[28] and closely related bridging formimidoyl[29] ligands are known.

Although the reaction of compound **2** with ethylene does not result in insertion of the unsaturated ligand into the Ir-methyl bond, it nevertheless gives a very interesting species. This reaction results in the migration of the methyl group from Ir to Rh to give $[RhIr(CH_3)(CO)_2(C_2H_4)(dppm)_2][CF_3SO_3]$ (**9**), a compound which is analogous to $[RhOs(CH_3)(CO)_3(dppm)_2]$,[7] in having the methyl group coordinated to the unsaturated Rh rather than to the saturated Ir or Os center, as shown earlier in Scheme 2.3. The four ethylene protons of compound **9** are equivalent giving rise to a triplet at δ 0.75, while the methyl group resonance appears as a doublet of triplets at δ 0.35 ($^2J_{Rh-H}$ = 3.0 Hz)[30] in the ^1H NMR spectrum, and selective ^{31}P-decoupling experiments confirm that the ethylene protons are coupled to the Ir-bound phosphorus nuclei whereas the methyl protons are coupled to the phosphorus nuclei bound to Rh. Both carbonyls are semibridging, as shown by the ^{13}C NMR spectrum in which coupling to Rh of 20 Hz is observed. Ethylene adducts of dppm-bridged binuclear complexes of Rh or Ir are extremely rare (to our knowledge the complexes, $[Ir_2(CO)(C_2H_4)(\mu\text{-}I)(\mu\text{-}CO)(dppm)_2][X]$ (X = I, BF_4),[6b] $[Ir_2(CH_3)(CO)_2(C_2H_4)(dppm)_2][BF_4]$ (see Chapter 3 and elsewhere[18]) and $[Ir_2(C_2H_4)(CO)_2(\mu\text{-}H)(dppm)_2][BF_4]$[31] are the only other examples) thus compound **9** and that described in Chapter 3, both of which have an accompanying alkyl group are unprecedented.

The reaction of compound **2** with 1,2-propadiene (allene) gives a single product $[RhIr(CH_3)(CO)_2(C_3H_4)(dppm)_2][CF_3SO_3]$ (**10**). The ^1H NMR spectrum of compound **10** shows only two signals for the allene protons at δ 4.00 and 3.46, indicating the presence of two pairs of equivalent protons for this ligand in the product. It also shows the methyl resonance at δ 1.05. The

$^{13}C\{^1H\}$ NMR spectrum shows a doublet of triplets at δ 186.8 ($^1J_{Rh-C}$ = 63.4 Hz) and a triplet at δ 170.7, indicating that there is a terminally bound CO ligand each on Rh and Ir in this compound, and that this reaction of **2** with allene is accompanied by CO loss. The CO stretches at 2001 cm^{-1} and 1980 cm^{-1} in the IR spectrum confirm that the CO ligands are terminally bound. The chemical shifts of the allene protons in this product are similar to those in $[W_2(O\text{-}t\text{-}Bu)_6(C_3H_4)(CO)_2]$ (δ 4.05 and 3.60),[32] suggesting that the allene ligand adopts a similar bridging coordination mode in the two compounds. However the available spectroscopic evidence is not sufficient to establish the coordination geometry about the metals in the case of **10**. The structure could also not be ascertained by means of an X-ray structure determination because of serious disorder problems.

The reaction of compound **2** with SO_2 leads to the formation of the acyl complex $[RhIr(CO)_2(COCH_3)(\mu\text{-}SO_2)(dppm)_2][CF_3SO_3]$ (**13**). The ^1H NMR spectrum of compound **13** shows the resonance of the acyl protons as a singlet at δ 1.15. The $^{13}C\{^1H\}$ spectrum shows three resonances of equal intensity. The two doublets of triplets at δ 172.7 and 168.7 ($^2J_{C-C}$ = 12.6 Hz) are due to the carbonyl groups on Ir. The coupling of 12.6 Hz between the carbon nuclei of these two CO ligands, which is intermediate between that reported for CO ligands that are trans to each other (*ca.* 35.0 Hz[33a]) and those for CO ligands that are cis to each other (2.0-3.5 Hz[33b]), suggests an orientation of the two ligands in **13** that deviates significantly from trans. The third resonance at δ 255.5 appears as a doublet ($^1J_{Rh-C}$ = 34.2 Hz) and is assigned to the acyl carbonyl, which is bound to Rh. The chemical shift and magnitude of the Rh-C coupling of this carbonyl group is similar to that of $[RhRe(COCH_3)(CO)_4(dppm)_2][CF_3SO_3]$.[6c] The acyl stretch in the IR spectrum of compound **13** appears at 1640 cm^{-1}. This spectrum also shows one of the

SO stretches at 1055 cm^{-1}, with the second one presumably obscured by the triflate anion stretches. All the NMR data are consistent with the structure of **13** shown in Scheme 2.4.

When the reaction of **2** with SO_2 is started at *ca.* -60 °C, the intermediate, $[RhIr(CH_3)(CO)_3(SO_2)(dppm)_2][CF_3SO_3]$ (**11**), is observed in solution. On standing at room temperature for about 10 min, compound **11** is transformed to a second intermediate, $[RhIr(CH_3)(CO)_2(\mu\text{-}SO_2)(dppm)_2][CF_3SO_3]$ (**12**), which in turn is transformed to the acyl product, **13**, on standing at room temperature for about 1 h.

In the ^1H NMR spectrum of compound **11**, the methylene resonances appear as multiplets at δ 4.85 and 3.45, while the methyl resonance appears as a broad signal at δ 0.33. Selective ^{31}P decoupling experiments show that the methyl group is bound to Ir, as decoupling the resonance due to the Ir-bound phosphorus nuclei, leads to the collapse of the broad methyl resonance into a sharp singlet, while decoupling the other ^{31}P resonance has no effect. The $^{13}C\{^1H\}$ NMR spectrum shows two doublets of triplets at δ 194.9 ($^1J_{Rh\text{-}C}$ = 56.3 Hz) and 175.2 ($^1J_{Rh\text{-}C}$ = 63.4 Hz), as well as a triplet at δ 178.4, indicating the presence of two terminal CO ligands on Rh and one on Ir. A terminal coordination mode is proposed for compound **11**, on the basis of the structure of the second intermediate **12** (vide infra). A bridging SO_2 in **11**, would inhibit methyl transfer from Ir to Rh, accompanied by CO transfer in the reverse direction.

The ^1H NMR spectrum of compound **12** shows the dppm methylene resonances as multiplets at δ 4.12 and 3.50, as well as the methyl resonance as a doublet of triplets at δ 1.08 ($^2J_{Rh\text{-}H}$ = 3.7 Hz). The presence of Rh coupling to the methyl protons indicates that the methyl group has migrated to Rh, as

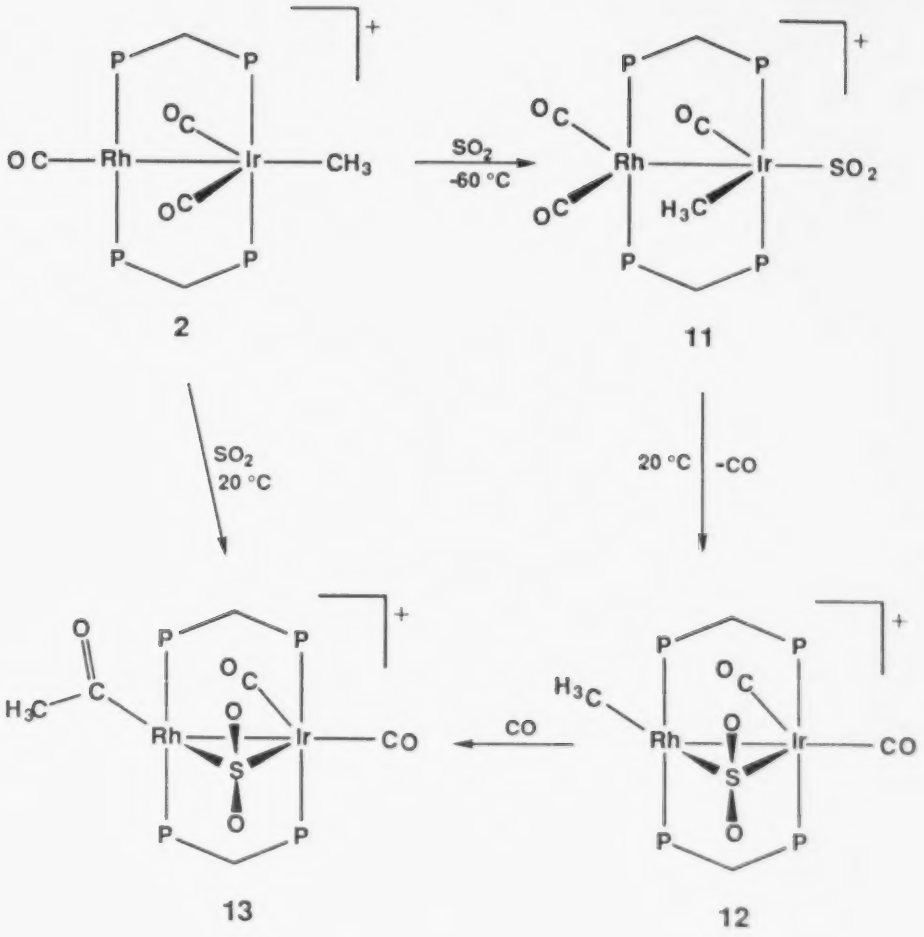

Scheme 2.4.

was observed in the reaction of **2** with ethylene. This is confirmed by selective ^{31}P decoupling experiments. The $^{13}C\{^1H\}$ NMR spectrum shows two doublets of triplets at δ 180.6 and 170.3 ($^2J_{C-C}$ = 13.6 Hz), indicating the presence of two CO ligands on Ir, and implying that the transformation from **11** to **12** involves CO loss. The coupling of 13.6 Hz between the carbon nuclei of these two CO ligands suggests that they have an orientation with respect to each other that is similar to that of the terminal CO ligands in **13**, which is probably intermediate between exactly cis and trans. The change of the methyl resonance from a doublet of triplets in **12** to a sharp singlet in **13** is consistent with the assignment of the latter as an acyl complex in which four-bond coupling between the methyl protons and the phosphorus nuclei are not observed.

On the basis of the intermediates and the acyl product observed in the reaction of **2** with SO_2, the reaction pathway shown in Scheme 2.4 is proposed. Apparently there is migration of one CO ligand from Ir to Rh accompanied by the coordination of SO_2 to the former metal to yield compound **11**. This compound then loses one CO ligand, undergoes CO migration from Rh to Ir, concomitant with methyl migration from Ir to Rh, and movement of the SO_2 ligand into the more favored bridging position[34] to yield compound **12**. The latter compound combines with another CO molecule, resulting in migratory insertion of the methyl group onto a CO ligand to give the acyl product, **13**. No insertion of the SO_2 ligand into the Ir-methyl bond is observed in this reaction of compound **2** with SO_2. Apparently the methyl group of **2** is not nucleophilic enough to result in direct attack by the SO_2 electrophile; instead attack at the metal occurs ultimately yielding the acyl product.

It was anticipated that increasing the electron density at the metals could enhance their tendency to induce C-H activation of the methyl group. However, reaction of compound **2** with PMe_3 has only resulted in CO substitution to yield $[RhIr(CH_3)(CO)_2(PMe_3)(dppm)_2][CF_3SO_3]$ (**14**), in which the methyl group remains terminally bound to Ir. The ^{31}P NMR spectrum of compound **14** shows a pattern characteristic of an ABCDMX spin system with two doublets of multiplets at δ 12.6 and 6.4 ($^1J_{Rh-P}$ = 131 and 126 Hz, respectively) and multiplets at δ -23.5, -32.7 and -62.4 (PMe_3). It is believed that the phosphorus atoms in compound **14** are oriented in such a way as to minimize steric interactions between the PMe_3 group and the phenyl rings attached to the Ir-bound dppm phosphorus atoms, resulting in the five phosphorus atoms having different chemical environments and giving rise to the observed spin system. It is proposed that one of the Ir-bound phosphorus atoms is bent slightly out of the plane of the other three away from the PMe_3 phosphorus as shown below.

The ^1H spectrum of compound **14** shows four multiplets for the four dppm methylene protons at δ 5.55, 5.08, 4.82, and 4.77, as well as an apparent doublet of triplets at δ 0.33, and a doublet at δ 0.23 ($^3J_{P-H}$ = 10.2 Hz), representing the methyl and the PMe_3 group proton resonances. Selective ^{31}P decoupling experiments show that the methyl proton resonance at δ 0.33 is actually a doublet of doublets of doublets ($^3J_{P-H}$ = 5.0, 6.0, and 14.0 Hz; the largest coupling is due to the PMe_3 phosphorus). It also shows that the methyl group is bound to Ir, as decoupling each of the Ir-bound dppm phosphorus resonances leads to the collapse of the methyl resonance to a doublet of doublets, whereas decoupling each of the Rh-bound phosphorus resonances has no effect. Decoupling the PMe_3 phosphorus resonance leads

to the collapse of the methyl resonance to a pseudotriplet. The $^{13}C\{^1H\}$

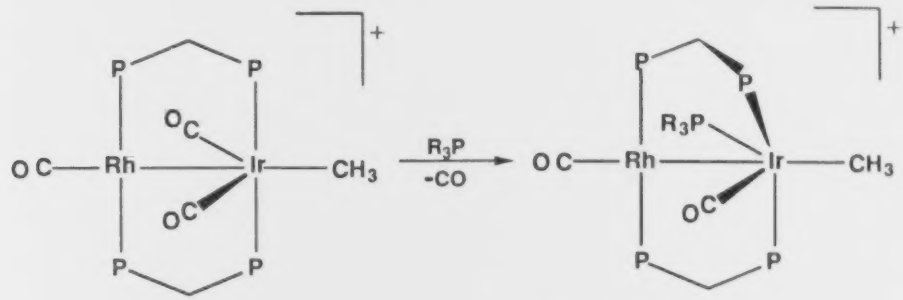

2 **R = Me (14), OPh (15)**

NMR spectrum shows a doublet of multiplets at δ 182.4 ($^1J_{Rh-C}$ = 67.9 Hz) and a multiplet at 178.7, indicating the presence of one terminal CO ligand on each metal. The absence of any substantial phosphorus coupling to the CO carbon nuclei, indicates that both CO ligands are cis to dppm, and that the CO ligand which is bound to Ir is also cis to the PMe_3 ligand.

The reaction of compound **2** with $P(OPh)_3$ yields $[RhIr(CH_3)(CO)_2(P(OPh)_3)(dppm)_2][CF_3SO_3]$ (**15**), the $P(OPh)_3$ analogue of compound **14**. Compounds **14** and **15** show similar ABCDMX patterns in their $^{31}P\{^1H\}$ spectra and similar chemical shifts in the $^{13}C\{^1H\}$ and ^1H spectra (apart from the chemical shifts of the $P(OPh)_3$ and the PMe_3 groups) indicating that they have similar structures.

Conclusions

As mentioned previously, we were interested in preparing a methyl derivative of the 'RhIr' complex, $[RhIr(CO)_3(dppm)_2]$ (**1**) (preferably a methyl-bridged complex). The second step after obtaining this product, was to undertake its reactions with small molecules such as phosphines, CO, etc to

study different aspects of its reactivity. The first aspect was to establish its reductive elimination pathways (of methane etc.); the potential for two-metal involvement in binuclear reductive elimination was of particular interest. The second aspect of interest was to induce C-C and C-heteroatom bond formation through migratory insertions of ligands such as isocyanides and carbon monoxide as well as unsaturated hydrocarbons, such as ethylene, into the M-CH_3 bond. Other aspects that were of interest included the possibilities of C-H activation of the CH_3 group by the adjacent metal and insertion of ligands such as SO_2 into the M-CH_3 bond.

Electrophilic attack of the low valent mixed-metal complex, **1** by CH_3^+ does not yield the methyl-bridged species analogous to the protonation product. Instead the complex, $[RhIr(CH_3)(CO)_3(dppm)_2][CF_3SO_3]$ (**2**), having the methyl group terminally bound to the saturated Ir center is obtained. Although a product having the alkyl group bound to Ir, which should have stronger metal-carbon bonds than does Rh,[23] is not surprising per se, it is surprising in view of the large number of related complexes of Rh/Mo,[9] Rh/Mn,[8] Rh/Re[6c] and Rh/Os,[7] all of which have the alkyl groups bound to the unsaturated Rh center. In particular, $[RhOs(CH_3)(CO)_3(dppm)_2]$ is isoelectronic with **2**, yet has the methyl group terminally bound to the unsaturated Rh center. It is not clear why this is the case. Adding to this puzzle, the substitution of one CO by ethylene in **2** results in migration of the methyl group to the unsaturated Rh atom yielding a product that is analogous to the large number of mixed-metal alkyl complexes (a similar methyl migration is also observed in the reaction of **2** with SO_2).

The reaction of compound **2** with H_2, shows that the former can be induced to reductively eliminate methane, using the appropriate reagent, although our inability to observe intermediates in this reaction does not allow

us to determine a pathway for this reaction. In the case of the reaction of **2** with HCl, reductive elimination of methane is inhibited, apparently by the orientation of the methyl and hydride ligands, which are not adjacent to each other. Moreover it seems that rearrangement of the ligands to give this cis orientation is unfavorable and does not occur. It is possible that this is because such a rearrangement would involve the breaking of at least one bond. In the case of the dipalladium systems, in which rearrangement to give a cis orientation of the methyl and hydride or the two methyl ligands is proposed, such a cis orientation can be achieved by the simple movement of a ligand from a terminal to a bridging position or vice versa, making it a very facile process.[20] In fact the dipalladium complexes are fluxional, in one case down to -100 °C.

The realization of our goal of inducing C-C bond formation resulted from migratory insertion of the methyl group in compound **2**, onto CO and ^{t}BuNC, as is seen in the formation of $[RhIr(CO)_3(COCH_3)(dppm)_2][CF_3SO_3]$ (**6**), $[RhIr(CO)_2(COCH_3)(\mu\text{-}SO_2)(dppm)_2][CF_3SO_3]$ (**13**), and $[RhIr(CO)_2(\mu\text{-}C(CH_3)=N^{t}Bu)(dppm)_2][CF_3SO_3]$ (**8**). Evidently, in the formation of **13**, migratory insertion onto CO occurs in preference to the insertion of SO_2. While the reaction of **2** with ethylene does not result in insertion of the unsaturated substrate into the M-CH_3 bond, a similar insertion occurs on reacting **2** with activated alkynes as shown in Chapter 4.

The migration of the methyl group from Ir to Rh, in the reaction of compound **2** with ethylene as well as in its reaction with SO_2, clearly demonstrates the cooperativity that is exhibited by the two metals in the complex. Such cooperativity permits the movement of ligands between the two metals and this frequently results in reactivity patterns that might not be possible with mononuclear species. For example, migration of a CO ligand

from Ir to Rh in the reaction with SO_2, allows attack of the incoming ligand at the originally coordinatively saturated Ir center. In mononuclear complexes, such attack at a coordinatively saturated metal center would require the initial dissociation of one of the ligands, which might not always be possible. Also the migration of the methyl group from Ir to Rh in the reaction with SO_2 apparently allows the formation of an acyl species, on reacting with one reagent, since migratory insertion is more favored by Rh than by Ir[23] (as is shown in the next chapter).

The tendency of **2** to form acyl (and iminoacyl in one case) complexes, leading to C-C bond formation suggests that it has the potential for effective application in organic synthesis.

The reactions of **2** with PMe_3 and $P(OPh)_3$ did not result in activation of a C-H bond of the methyl group, but rather led to a simple CO replacement. However such activation has been found to occur in the analogous diiridium system, as shown in the next chapter.

References and Footnotes

1. Forster, D. *Adv. Organomet. Chem.* **1979**, *17*, 255.
2. Dombek, B. D. *Adv. Catal.* **1983**, *32*, 325.
3. (a) James, B. R. *Adv. Organomet. Chem.* **1979**, *17*, 319. (b) Pruet, R. L. *Adv. Organomet. Chem.* **1979**, *17*, 1. (c) Masters, C. *Homogeneous Transition-Metal catalysis: A Gentle Art*; Chapman and Hall: London, 1980. (d) Speier, J. L. *Adv. Organomet. Chem.* **1979**, *17*, 407.
4. (a) Parshall, G. W.; Mrowca, J. J. *Adv. Organomet. Chem.* **1968**, *7*, 157. (b) Atwood, J. D. *Coord. Chem. Rev.* **1988**, *83*, 93.
5. (a) Balch, A. L. In *Homogeneous Catalysis with Metal Phosphine Complexes;* Pignolet, L. H., Ed.; Plenum: New York, 1983. (b) Brown, M. P.; Fisher, J. R.; Franklin, S. J.; Puddephatt, R. J.; Thomson, M. A. In *Catalytic Aspects of Metal Phosphine Complexes;* Alyea, E. C., Meek, D. W., Eds.; Advances in Chemistry Series 196; American Chemical Society: Washington, DC, 1982; p 231. (c) Poilblanc, R. *Inorg. Chim. Acta* **1982**, *62*, 75. (d) Muetterties, E. L.; Krause, M. J. *Angew. Chem. Int. Ed. Eng.* **1983**, *22*, 135. (e) Ertl, G. In *Metal Clusters in Catalysis;* Gates, B. C., Guczi, L., Knozinger, H., Eds.; Elsevier: New York, 1986; Chapter 11. (f) Levigne, G.; Kaesz, H. D. In ref 5e, Chapter 4. (g) Marko, L.; Vizi-Orosz, A. In ref 5e, Chapter 5.
6. See, for example: (a) Xiao, J.; Cowie, M. *Organometallics* **1993**, *12*, 463. (b) Vaartstra, B. A.; Xiao, J.; Jenkins, J. A.; Verhagen, R.; Cowie, M. *Organometallics* **1991**, *10*, 2708. (c) Antonelli, D. M.; Cowie, M. *Organometallics* **1991**, *10*, 2550. (d) Antonelli, D. M.; Cowie, M. *Organometallics* **1991**, *10*, 2173. (e) Hilts, R. W.; Franchuk, R. A.; Cowie,

M. *Organometallics* **1991**, *10*, 1297. (f) Hilts, R. W.; Franchuk, R. A.; Cowie, M. *Organometallics* **1991**, *10*, 304. (g) Vaartstra, B. A.; Xiao, J.; Cowie, M. *J. Am. Chem. Soc.* **1990**, *112*, 9425. (h) McDonald, R.; Cowie, M. *Organometallics* **1990**, *9*, 2468. (i) Antonelli, D. M.; Cowie, M. *Organometallics* **1990**, *9*, 1818. (j) Vaartstra, B. A.; Cowie, M. *Organometallics* **1990**, *9*, 1594. (k) Antonelli, D. M.; Cowie, M. *Inorg. Chem.* **1990**, *29*, 4039. (l) Antonelli, D. M.; Cowie, M. *Inorg. Chem.* **1990**, *29*, 3339. (m) McDonald, R.; Cowie, M. *Inorg. Chem.* **1990**, *29*, 1564. (n) Vaartstra, B. A.; Cowie, M. *Inorg. Chem.* **1989**, *28*, 3138. (o) Vaartstra, B. A.; Cowie, M. *Organometallics* **1989**, *8*, 2388. (p) McDonald, R.; Sutherland, B. R.; Cowie, M. *Inorg. Chem.* **1987**, *26*, 3333. (q) Cowie, M.;Vasapollo, G.; Sutherland, B. R.; Ennett, J. P. *Inorg. Chem.* **1986**, *25*, 2648. (r) Sutherland, B. R.; Cowie, M. *Organometallics* **1985**, *4*, 1801. (s) Sutherland, B. R.; Cowie, M. *Organometallics* **1985**, *4*, 1637. (t) Sutherland, B. R.; Cowie, M. *Organometallics* **1984**, *3*, 1869.

7. Hilts, R. W.; Moro, G.; Sterenberg, B. T.; Cowie, M., manuscript in preparation.
8. Wang, L. S.; Cowie; M., to be submitted for publication.
9. Graham, T.; Mao, T.; Van Gastel, F.; Cowie, M., unpublished work.
10. Microanalyses, carried out on compound **14**, consistently yielded lower percentages of carbon and hydrogen than those calculated since it could not be obtained free from traces of starting material, **2**.
11. Doedens, R. J.; Ibers, J. A. *Inorg. Chem.* **1967**, *6*, 204.
12. Walker, N.; Stuart, D. *Acta Crystallogr., Sect. A: Found Crystallogr.* **1983**, *A39*, 1581.
13. Programs used were those of the Enraf-Nonius Structure Determination Package by B. A. Frenz, in addition to local programs by R. G. Ball.

14. Cromer, D. T.; Waber, J. T. *International Tables for Crystallography;* Kynoch Press: Birmingham, England, 1974; Vol. IV, Table 2.2A.

15. Stewart, R. F.; Davidson, E. R.; Simpson, W. T. *J. Chem. Phys.* **1965**, *42*, 3175.

16. Cromer, D. T.; Liberman, D. *J. Chem. Phys.* **1970**, *53*, 1891.

17. (a) Kubiak, C. P.; Woodcock, C.; Eisenberg, R. *Inorg.Chem.* **1982**, *21*, 2119. (b) Kubiak, C. P.; Eisenberg, R. *J. Am. Chem. Soc.* **1980**, *102*, 3637.

18. Antwi-Nsiah, F.; Cowie, M. *Organometallics* **1992**, *11*, 3157.

19. (a) McDonald, R. Ph.D. Thesis, University of Alberta, 1991, Chapter 4. (b) Wang, W. D.; Hommeltoft, S. I; Eisenberg, R. *Organometallics* **1988**, *7*, 2417. (c) Wang, W. D.; Eisenberg, R. *J. Am. Chem. Soc.* **1990**, *112*, 1833. (d) Vaartstra, B. A. Ph.D. Thesis, University of Alberta, 1989, Chapter 6. (e) Berry, D. H.; Eisenberg, R. *Organometallics* **1987**, *6*, 1796. (f) Berry, D. H.; Eisenberg, R. *J. Am. Chem. Soc.* **1985**, *107*, 7181. (g) Woodcock, C.; Eisenberg, R. *Inorg.Chem.* **1984**, *23*, 4207. (h) Sutherland, B. R.; Cowie, M. *Organometallics* **1984**, *3*, 1869.

20. Young, S. J.; Kellenberger, B.; Riebenspies, J. H.; Himmel, S. E.; Manning, M.; Anderson, O. P.; Stille J. K. *J. Am. Chem. Soc.* **1988**, *110*, 5744.

21. (a) Mils, S. L.; Mils, D. L.; Bau, R.; Flood, T. C. *J. Am. Chem. Soc.* **1978**, *100*, 7278. (b) Attig, T. G.; Teller, R. G.; Wu, S. -M.; Bau, R.; Wojcicki, A. *J. Am. Chem. Soc.* **1979**, *101*, 619. (c) Wojcicki, A. *Adv. Organomet. Chem.* **1974**, *12*,

31. (d) Wojcicki, A. *Acc. Chem. Res.* **1971**, *4*, 344.

22. All NMR signals have the appropriate ratios of intensity.

23. Collman, J. P.; Hegedus, L. S.; Norton, J. R.; Finke, R. G. *Principles and Applications of Organotransition Metal Chemistry;* University Science Books: Mill Valley, CA, 1987, pp 148 and 372.

24. Adams, R. D.; Golembeski, N. M. *Inorg. Chem.* **1978**, *17*, 1969.

25. Klose, A.; Solari, E.; Ferguson, R.; Floriani, C.; Chiesi-Villa, A.; Rizzoli, C. *Organometallics* **1993**, *12*, 2414.

26. Allen, F. H.; Kernard, O.; Watson, D. G.; Brammer, L.; Orpen, G. A.; Taylor, R. *J. Chem. Soc., PerkinTrans. II* **1987**, S1.

27. (a) Werner, H. *Angew. Chem. Int. Ed. Eng.* **1990**, *29*, 1077. (b) Singleton, E.; Oosthuizen, H. E. *Adv. Organomet. Chem.* **1983**, *22*, 209 and references therein. (c) Lee, C.; Hunt, C. T.; Balch, A. L. *Organometallics* **1982**, *1*, 824. (d) Yamamoto, Y.; Yamazaki, H. *Coord. Chem. Rev.* **1972**, *8*, 225.

28. Yin, C. C.; Deeming, A. J. *J. Organomet. Chem.* **1977**, *133*, 123.

29. (a) Alonso, F. J. G.; Sanz, M. G.; Riera, V. *Organometallics* **1992**, *11*, 801. (b) Adams, R. D.; Golembeski, N. M. *J. Am. Chem. Soc.* **1979**, *101*, 3637.

30. This Rh-H coupling is not always resolved; sometimes the methyl resonance appears as a broad triplet.

31. See Chapter 5 of this thesis.

32. Chacon, S. T.; Chisholm, M. H.; Folting, K.; Huffman, J. C.; Hampden-Smith, M. J.*Organometallics* **1991**, *10*, 3722.

33. (a) Tachikawa, M.; Richter, S. I.; Shapley, J. R. *J. Organomet. Chem.* **1977**, *128*, C9. (b) Aime, S.; Osella, D.; *J. Chem. Soc. Chem. Commun.* **1981**, 300.

34. See, for example: (a) Uson, R.; Fornies, J.; Espinet, P.; Fortuno, C. *J. Chem. Soc., Dalton Trans.* **1986**, 1849. (b) Cowie, M.; Dickson, R. S.; Hames B. W. *Organometallics* **1984**, *3*, 1879. (c) Kubas, G. J. *Inorg. Chem.* **1979**, *18*, 182. (d) Dwight, S. K.; Cowie, M. *Inorg. Chim. Acta* **1978**, *31*, L407. (e) Mingos, D. M. P. *Transition Met. Chem.* **1978**, *3*, 1. (f) Benner, L. S.; Olmstead, M. M.; Hope, H.; Balch, A. L. *J. Organomet. Chem.* **1978**, *153*, C81. (g) Angoletta, M.; Malatesta, L.; Caglio, G. *J. Chem. Soc., Dalton Trans.* **1977**, 2131. (h) Angoletta, M.; Bellon, P. L.; Manassero, M.;

Sansoni, M. *J. Organomet. Chem.* **1974**, *81*, C40. (i) Churchill, M. R.; Krishan, L. K. *Inorg. Chem.* **1973**, *12*, 1650. (j) Churchill, M. R.; DeBoer, B. G.; Kalra, K. L. *Inorg. Chem.* **1973**, *12*, 1646. (k) Churchill, M. R.; DeBoer, B. G.; Kalra, K. L.; Reich-Rohrwig, P.; Wojcicki, A. *J. Chem. Soc., Chem. Commun.* **1972**, 981.

Chapter 3

Alkyl Complexes Involving the "$Ir_2(dppm)_2$" Framework

Introduction

In the previous chapter, the synthesis and reactivity of the heterobinuclear alkyl complex $[RhIr(CH_3)(CO)_3(dppm)_2][CF_3SO_3]$,[1] was described. Since it was of interest to establish how the reactivity of group 9 alkyl species might vary with different metals within the triad, the attempted synthesis of the homobinuclear, diiridium analogue, $[Ir_2(CH_3)(CO)_3(dppm)_2][CF_3SO_3]$, was undertaken, with the subsequent intent of comparing its reactivity to that of the 'RhIr' analogue.

Previous studies in related hydride complexes had shown that the heterobinuclear 'RhIr' system displays some differences in its chemistry, as compared to those of the dirhodium and diiridium systems.[2-8] For instance, in the 'RhIr' system, no species containing more than three hydrides is observed,[3] in contrast to the diiridium chemistry, where several tetrahydride complexes,[2,4] and as is shown in this chapter, a pentahydride complex,[9] are observed. Also it has been shown that protonation of $[RhIr(H)(CO)_2(\mu\text{-}H)(dppm)_2]$, leads to the cationic trihydride, $[RhIr(H)(CO)_2(\mu\text{-}H)_2(dppm)_2][BF_4]$,[3] quite unlike the product reported in the dirhodium chemistry, where H_2 loss apparently occurs, yielding $[Rh_2(CO)_2(\mu\text{-}H)(dppm)_2]^+$.[5]

In this chapter, the alkylation of $[Ir_2(CO)_3(dppm)_2]$[8] and some of the unusual transformations that occur, are reported.

Experimental Section

General experimental conditions were as described in Chapter 2. Dimethylphenylphosphine, triphenylphosphine and anhydrous trimethylamine *N*-oxide were purchased from Aldrich, while $[Ir_2(CO)_3(dppm)_2]$ was prepared as previously reported.[8] The solid state $^{13}C\{^1H\}$ NMR spectrum was recorded on a Bruker AMR-300 spectrometer (with MAS accessory) operating at 75.5 MHz, while the conductivity measurement was carried out using a Yellow Springs Instrument Co. Model 31 conductivity bridge, with a solution of approximately 10^{-3} M concentration. Spectroscopic parameters for the compounds prepared are found in Tables 3.1 and 3.2.

Preparation of Compounds. (a) $[Ir_2(H)(CO)_3(\mu\text{-}CH_2)(dppm)_2][CF_3SO_3]$ (2). The compound $[Ir_2(CO)_3(dppm)_2]$ (**1**) (100 mg, 0.081 mmol) was dissolved in 10 mL of benzene, to which was added 1 equiv of methyl triflate (9.1 μL, 0.081 mmol). The light yellow solution immediately darkened to orange and started turning cloudy after about 10 min. The mixture was stirred for 3 h by which time a yellow precipitate had formed. The solvent was removed under vacuum leaving a yellow product which was then recrystallized from CH_2Cl_2 / Et_2O. The solid was then dried under a stream of argon and put under vacuum for about 18 h during which time the color changed from yellow to light brown (86% yield). Anal. Calcd for $Ir_2SP_4F_3O_6C_{55}H_{47}$: C, 47.20; H, 3.37. Found: C, 47.32; H, 3.40.

(b) $[Ir_2(H)(CO)_2(PMe_3)(\mu\text{-}CH_2)(dppm)_2][CF_3SO_3]$ (5a). A solution of PMe_3 (71.4 μL or 0.071 mmol, of a 1 M solution in THF) in 10 mL THF, was added to a THF solution of compound **2** (100 mg, 0.071 mmol). The orange solution immediately changed color to bright yellow. The solution was

Table 3.1 $^{31}P\{^{1}H\}$ **and** ^{1}H **NMR Spectroscopic Data**[a]

Compound	$\delta(^{31}P\{^{1}H\})$[b]	$\delta(^{1}H)$[c,d]
$[Ir_2(H)(CO)_3(\mu\text{-}CH_2)(dppm)_2][CF_3SO_3]$ (2)	-0.9 (m), -12.5 (m)	5.19 (m, 2H), 4.60 (m, 2H), 3.59(m, 2H), -11.35 (t, 1H)
$[Ir_2(CH_3)(CO)_4(dppm)_2][CF_3SO_3]$ (4)[e]	-8.9 (m), -16.0 (m)	4.59 (m, 4H), 0.38 (t, 3H)
$[Ir_2(H)(CO)_2(PMe_3)(\mu\text{-}CH_2)(dppm)_2][CF_3SO_3]$ (5a)	-7.7 (m), -11.3 (m), -79.2 (b)	4.05 (m, 2H), 3.45(m, 2H), 3.05 (m, 2H), 0.75 (d, 9H), -12.35 (dm, $^{2}J_{P\text{-}H}$ = 21.2, 13.5 Hz, $^{3}J_{P\text{-}H}$ = 4.8 Hz, 1H)
$[Ir_2(H)(CO)_2(PPh_3)(\mu\text{-}CH_2)(dppm)_2][CF_3SO_3]$ (5b)	-4.1 (m), -13.7 (m), -33.9 (b)	3.84 (m, 2H), 3.71 (m, 2H), 3.13 (m, 2H), -13.25 (dm, $^{2}J_{P\text{-}H}$ = 22.3 Hz, 1H)
$[Ir_2(H)(CO)_2(PMe_2Ph)(\mu\text{-}CH_2)(dppm)_2][CF_3SO_3]$ (5c)	-5.7 (m), -12.1 (m), -71.6 (b)	3.82 (m, 2H), 3.35 (m, 2H), 3.30 (m, 2H), 1.12 (d, 6H), -12.20 (dm, $^{2}J_{P\text{-}H}$ = 21.6 Hz, 1H)

Table 3.1 (continued)

Compound	$\delta(^{31}P\{^1H\})^b$	$\delta(^1H)^{c,d}$
$[Ir_2(H)(CO)_2(P(OPh)_3)(\mu\text{-}CH_2)(dppm)_2][CF_3SO_3]$ (6)	43.9(m), -4.1 (m), -12.6 (m)	3.88 (m, 2H), 3.85 (m, 2H), 3.82 (m, 2H), -12.69 (dm, $^2J_{P\text{-}H}$ = 37.3 Hz, 1H)
$[Ir_2(CO)_4(COCH_3)(dppm)_2][CF_3SO_3]$ (7)[e]	-9.6 (m), -25.5 (m)	4.61 (b, 4H), 0.63(s, 3H)
$[Ir_2(CH_3)(CO)_3(\mu\text{-}SO_2)(dppm)_2][CF_3SO_3]$ (8)[e]	-0.4 (m), -14.7 (m)	4.90 (m, 2H), 3.40 (m, 2H), 0.01 (t, 3H)
$[Ir_2(CH_3CO)(CO)_3(\mu\text{-}SO_2)(dppm)_2][CF_3SO_3]$ (9)[e]	-5.0 (m), -13.8 (m)	5.03(m, 2H), 3.18 (m, 2H), 1.28 (s, 3H)
$[Ir_2(H)(CO)_2(CN^tBu)(\mu\text{-}CH_2)(dppm)_2][CF_3SO_3]$ (10)	-6.6 (m), -8.5 (m)	3.92 (m, 2H), 3.58 (m, 2H), 3.57 (m, 2H), 0.60 (s, 9H), -11.46 (t, 1H)

Table 3.1 (continued)

Compound	$\delta(^{31}P\{^1H\})^b$	$\delta(^1H)^{c,d}$
$[Ir_2(CH_3)(CO)_2(C_2H_4)(dppm)_2][CF_3SO_3]$ **(11)**[e]	19.0 (m), 5.7 (m)	3.25 (m, 4H), 1.05 (t, 4H), 0.70 (t, 3H)
$[Ir_2(CO)_2(\mu\text{-}CH_3)(OSO_2CF_3)(dppm)_2]$ **(13)**[e]	22.1 (s)	4.45 (m, 2H), 3.78 (m, 2H), 0.58 (q, $^3J_{P\text{-}H}$ = 4.1 Hz, 3H)
$[Ir_2(CO)_2(\mu\text{-}CH_3)(\mu\text{-}SO_2)(dppm)_2][CF_3SO_3]$ **(14)**[e]	-1.0 (s)	4.50 (m, 2H), 3.94 (m, 2H), -2.15 (b, 3H)
$[Ir_2(CO)_3(OSO_2CF_3)(dppm)_2][CF_3SO_3]$ **(15)**	1.7 (m), -17.0 (m)	5.40 (m, 2H), 5.35 (m, 2H)
$[Ir_2(H)_2(CH_3)(CO)_3(dppm)_2][CF_3SO_3]$ **(17)**	-2.0 (m), -14.5 (m)	5.73 (m, 2H), 4.15 (m, 2H), 0.42 (t, 3H), -9.43 (t, 1H), -10.81 (t, 1H)
$[Ir_2(H)_3(CO)_3(dppm)_2][CF_3SO_3]$ **(19)**	-6.3 (m), -16.0 (m)	5.58 (m, 2H), 4.33 (m, 2H), -10.25 (t, 1H), -10.40 (t, 1H), -12.48 (t, 1H)

Table 3.1 (continued)

Compound	$\delta(^{31}P\{^1H\})^b$	$\delta(^1H)^{c,d}$
$[Ir_2(H)_4(CO)_2(\mu\text{-}H)(dppm)_2][CF_3SO_3]$ **(21)**^{f}	-6.6 (m)	5.75(m, 2H), 3.82 (m, 2H), -10.72 (b, 2H), -12.90 (b, 2H), -16.31 (b, 1H)

[a] Abbreviations used: s = singlet, d = doublet, t = triplet, m = multiplet, dm = doublet of multiplets, b = broad. [b] Vs 85% H_3PO_4, -40 °C in CD_2Cl_2 unless otherwise stated. [c] Vs TMS, -40 °C in CD_2Cl_2 solvent unless otherwise stated. [d] Resonances for dppm phenyl group protons appear as multiplets in the range δ 6.9 - 8.1 for all compounds. [e] Data at 25°C. [f] Data at -80°C.

Table 3.2 Infrared and $^{13}C\{^1H\}$ NMR Spectroscopic Data

Compound	IR[b,c], cm^{-1}	$\delta(^{13}C\{^1H\})$[d]
$[Ir_2(H)(CO)_3(\mu\text{-}CH_2)(dppm)_2][CF_3SO_3]$ (2)	2018 (vs), 2000 (vs), 1970 (vs)	177.4 (t, 1C), 177.0 (t, 1C), 162.0 (t, 1C)
$[Ir_2(CH_3)(CO)_4(dppm)_2][CF_3SO_3]$ (4)	–	194.2 (b, 2C), 182.9 (t, 2C)
$[Ir_2(H)(CO)_2(PMe_3)(\mu\text{-}CH_2)(dppm)_2][CF_3SO_3]$ (5a)	1961 (vs), 1950 (vs)	183.0 (t, 1C), 180.1 (b, 1C)
$[Ir_2(H)(CO)_2(PPh_3)(\mu\text{-}CH_2)(dppm)_2][CF_3SO_3]$ (5b)	1975 (vs), 1948 (vs)	183.4 (t, 1C), 180.5 (b, 1C)
$[Ir_2(H)(CO)_2(PMe_2Ph)(\mu\text{-}CH_2)(dppm)_2][CF_3SO_3]$ (5c)	1963 (vs), 1952 (s)	182.6 (t, 1C), 180.6 (b, 1C)
$[Ir_2(H)(CO)_2(P(OPh)_3)(\mu\text{-}CH_2)(dppm)_2][CF_3SO_3]$ (6)	1975 (vs), 1951 (vs)	180.4 (b, 1C), 179.7 (t, 1C)
$[Ir_2(CO)_4(COCH_3)(dppm)_2][CF_3SO_3]$ (7)[f]	2049 (med), 1959 (s), 1622 (w)	225.1 (t, 1C), 195.6 (b, 2C), 179.9 (t, 2C)

Table 3.2 (continued)

Compound	IR[b,c], cm^{-1}	$\delta(^{13}C\{^1H\})$[d]
$[Ir_2(CH_3)(CO)_3(\mu\text{-}SO_2)(dppm)_2][CF_3SO_3]$ **(8)**[f]	2042 (s), 2010 (vs), 1987 (s), 1070 (m)[i]	177.9 (t, 1C), 177.8 (t, 1C), 160.2 (t, 1C)
$[Ir_2(CH_3CO)(CO)_3(\mu\text{-}SO_2)(dppm)_2][CF_3SO_3]$ **(9)**[e,f]	2013 (s), 1990 (vs), 1646 (med)[k]	
$[Ir_2(H)(CO)_2(CN^tBu)(\mu\text{-}CH_2)(dppm)_2][CF_3SO_3]$ **(10)**	2163 (s),[h] 1975 (s), 1970 (sh)	179.2 (b, 1C), 179.1 (t, 1C)
$[Ir_2(CH_3)(CO)_2(C_2H_4)(dppm)_2][CF_3SO_3]$ **(11)**[e]	1971 (vs), 1787 (s)	204.0 (t, 2C)
$[Ir_2(CO)_2(\mu\text{-}CH_3)(OSO_2CF_3)(dppm)_2]$ **(13)**[e,f]	1964 (s), 1886 (w), 1347 (s)[j]	171.4 (b, 2C)
$[Ir_2(CH_3)(CO)_2(dppm)_2][CF_3SO_3]$ **(13a)**[f]	1974 (vs), 1832 (s)	187.8 (m, 1C), 167.0 (m, 1C)
$[Ir_2(CO)_2(\mu\text{-}CH_3)(\mu\text{-}SO_2)(dppm)_2][CF_3SO_3]$ **(14)**[e,f]	2044 (vs), 1997 (vs)	170.8 (t, 2C)

Table 3.2 (continued)

Compound	IR[b,c], cm^{-1}	$\delta(^{13}C\{^1H\})$[d]
$[Ir_2(CO)_3(OSO_2CF_3)(dppm)_2][CF_3SO_3]$ **(15)**	2023 (sh),2004 (s), 1964 (med), 1323 (med),[j] 1272 (vs),[j] 1260 (vs),[j] 1161 (s)[j]	168.9 (m, 1C), 168.7 (b, 1C), 165.0 (b, 1C)
$[Ir_2(H)_2(CH_3)(CO)_3(dppm)_2][CF_3SO_3]$ **(17)**	-	181.3 (b, 2C), 157.0 (b, 1C)
$[Ir_2(H)_3(CO)_3(dppm)_2][CF_3SO_3]$ **(19)**	-	180.4 (b, 1C), 179.6 (b, 1C), 155.2 (b, 1C)
$[Ir_2(H)_4(CO)_2(\mu\text{-}H)(dppm)_2][CF_3SO_3]$ **(21)**[e,g]	2020 (vs), 1963 (s)	170.9 (b, 2C)

[a] Abbreviations used: med = medium, s = strong, vs = very strong, t = triplet, m = multiplet, b = broad. [b] Nujol mull on KBr disk unless otherwise stated. [c] Values are ν(CO). [d] Vs TMS, -40 °C in CD_2Cl_2 solvent unless otherwise stated. [e] IR in CH_2Cl_2. [f] NMR data at 25 °C. [g] NMR data at -80 °C. [h] ν(CN). [i] ν(SO), second SO stretch obscured by triflate anion stretches. [j] Stretch due to triflate group. [k] Acyl stretch.

stirred for 2 h during which time a yellow precipitate formed. The solvent was then removed under vacuum giving a light yellow microcrystalline solid, which was then recrystallized from THF/Et_2O (70% yield). Anal. Calcd for $Ir_2SP_5F_3O_5C_{57}H_{56}$: C, 47.23; H, 3.89. Found: C, 47.12; H, 4.12.

(c) $[Ir_2(H)(CO)_2(PPh_3)(\mu\text{-}CH_2)(dppm)_2][CF_3SO_3]$ (5b). Compound **2** (100 mg, 0.071 mmol) was dissolved in 20 mL of THF, to which was added 1 equiv of PPh_3 (19 mg, 0.071 mmol) dissolved in 10 mL of THF. The solution color changed from orange to yellow. After stirring for 2 h, the solvent was removed under vacuum, and the yellow solid was recrystallized from CH_2Cl_2/Et_2O.[10]

(d) $[Ir_2(H)(CO)_2(PMe_2Ph)(\mu\text{-}CH_2)(dppm)_2][CF_3SO_3]$ (5c). The procedure was the same as that described for **5a** except that PMe_2Ph (99%) was used instead of a 1 M THF solution of PMe_3 (67% yield). Anal. Calcd for $Ir_2SP_5F_3O_5C_{62}H_{58}$: C, 49.27; H, 3.87. Found: C, 49.08; H, 3.71.

(e) $[Ir_2(H)(CO)_2(P(OPh)_3)(\mu\text{-}CH_2)(dppm)_2][CF_3SO_3]$ (6). The procedure was the same as that described for **5a** except that $P(OPh)_3$ (97%), was used instead of a 1 M THF solution of PMe_3, and the mixture was stirred for 3 h instead of 2 h (60% yield). Anal. Calcd for $Ir_2SP_5F_3O_8C_{72}H_{62}$: C, 51.36; H, 3.71. Found: C, 51.40; H, 3.82.

(f) $[Ir_2(CH_3)(CO)_3(\mu\text{-}SO_2)(dppm)_2][CF_3SO_3]$ (8). Sulphur dioxide gas was passed through a 5 mL CH_2Cl_2 solution of **2** (80 mg, 0.057 mmol) for about 2 min, resulting in a color change from orange to light yellow, then to green. The solution was then stirred under a static atmosphere of the gas for

15 min, after which time the green solid was precipitated with Et_2O. The solid was collected, washed with Et_2O and dried under an argon stream. It was then recrystallized from CH_2Cl_2/Et_2O (64% yield). Anal. Calcd for $Ir_2S_2P_4F_3O_8C_{55}H_{47}$: C, 45.19; H, 3.23; S, 4.37. Found: C, 44.54; H, 3.21; S, 4.77.

(g) $[Ir_2(H)(CO)_2(^tBuNC)(\mu\text{-}CH_2)(dppm)_2][CF_3SO_3]$ (10). To a solution of compound **2** (100 mg, 0.071 mmol) in 5 mL CH_2Cl_2, was added 1 equiv of ^tBuNC (8.1 μL, 0.071 mmol), causing an immediate color change from orange to yellow. The mixture was stirred for 2 h by which time the color was green. The solvent volume was reduced to about 2 mL, and the green product was precipitated and washed with ether. After drying under an argon stream, the solid was recrystallized from CH_2Cl_2/Et_2O (70 % yield).[11]

(h) $[Ir_2(CO)_2(\mu\text{-}CH_3)(dppm)_2][CF_3SO_3]$ (13a). Compound **2** (80 mg, 0.057 mmol) was dissolved in 5 mL CH_2Cl_2. 1 equiv of anhydrous Me_3NO (4.3 mg, 0.057 mmol) dissolved in 5 mL of CH_2Cl_2 was added to this solution, dropwise (by means of an addition funnel, over a 15 min time span), while maintaining a slow stream of argon. The mixture was than stirred for 45 min, and the solvent was removed under vacuo. The solid was then recrystallized from CH_2Cl_2 and Et_2O, dried under argon, and then under vacuo giving a 78% yield (NMR and IR spectroscopic data suggest that compound **13a** exists as $[Ir_2(CO)_2(\mu\text{-}CH_3)(OSO_2CF_3)(dppm)_2]$ (**13**) in solution). Anal. Calcd for $Ir_2SP_4F_3O_5C_{54}H_{47}$: C, 47.23; H, 3.45. Found: C, 46.81; H, 3.24.

(i) $[Ir_2(CO)_3(OSO_2CF_3)(dppm)_2][CF_3SO_3]$ (15). Compound **2** (80 mg, 0.057 mmol) was dissolved in 20 mL of CH_2Cl_2 to which was added 1 equiv of CF_3SO_3H (5.1 μL, 0.057 mmol). The color of the solution immediately

changed from orange to yellow. After stirring the solution for 1 h, the volume of the solvent was reduced to about half. Addition of 30 mL of Et_2O resulted in the precipitation of a yellow solid, which was washed with Et_2O, and dried under an argon stream. It was then recrystallized from CH_2Cl_2/Et_2O (61% yield). Conductivity measurements in nitromethane indicate that **15** is a 1:1 electrolyte (Λ (10^{-3}M) = 107.6 $\Omega^{-1}cm^2mol^{-1}$). Anal. Calcd for $Ir_2S_2P_4F_6O_9C_{55}H_{44}$: C, 43.14; H, 2.88. Found: C, 42.68; H, 2.74.

Low Temperature Reaction of Compound 1 with Methyl Triflate. Compound **1** (30 mg, 0.024 mmol) was dissolved in 0.6 mL of CD_2Cl_2, transferred to an NMR tube and covered with a rubber septum. The solution was then cooled, under argon, to -78 °C by immersing the NMR tube in a dry-ice/acetone mixture. One equiv of methyl triflate (2.7 μL, 0.024 mmol) was then added to the solution, and the NMR spectra of the reaction mixture were obtained immediately. The spectra were obtained in the temperature range, -80 °C to 0 °C, starting at the lowest temperature and warming gradually (the sample was allowed to stand for 20 min at each temperature before the spectra were obtained). Finally the NMR spectra were obtained at -40 °C (because of fluxionality at room temperature) after the mixture had been allowed to stand at room temperature for 1 h.

Reaction of Compound 2 with CO. Carbon monoxide was passed through a 5 mL CH_2Cl_2 solution of compound **2** (80 mg, 0.057 mmol) for about 1 min. The solution was then stirred under a static atmosphere of the gas for 18 h during which time the color of the solution changed from orange to yellow. To obtain NMR spectra, the reaction was carried out in CD_2Cl_2 solution under an atmosphere of CO. The NMR spectra showed that the reaction mixture contained $[Ir_2(CH_3)(CO)_4(dppm)_2][CF_3SO_3]$ (4) and

$[Ir_2(CO)_4(COCH_3)(dppm)_2][CF_3SO_3]$ (**7**). However, the products were not isolated as solids, because they are unstable in the absence of a CO atmosphere.

Reaction of Compound 2 with Ethylene. Ethylene was passed through a 10 mL CH_2Cl_2 solution of **2** (150 mg, 0.107 mmol) for about 1 min. The solution was then stirred under a static atmosphere of the gas for 18 h. To obtain NMR spectra, the reaction was carried out in CD_2Cl_2 solution under an ethylene atmosphere. The NMR spectra showed that the reaction mixture consisted of compound **2** and $[Ir_2(CH_3)(CO)_2(C_2H_4)(dppm)_2][CF_3SO_3]$ (**11**), but the solid was not isolated. Compound **11** was however obtained as a pure product by an alternative method (vide infra).

Reaction of 2 with 1,2-Propadiene (allene). Allene was passed through a 5 mL CH_2Cl_2 solution of compound **2** (80 mg, 0.057 mmol) for 2 min. The solution was then stirred under a static atmosphere of the gas for 2 h, after which the yellow solid was precipitated with Et_2O. After it was washed with Et_2O and dried under an argon stream, the solid was recrystallized from CH_2Cl_2/Et_2O.

Reaction of Compound 8 with CO. The procedure was the similar to that used for the reaction of compound **2** with CO. The NMR spectrum of the reaction mixture showed that it contained compound **8** and $[Ir_2(CH_3)(CO)_3(\mu\text{-}SO_2)(dppm)_2][CF_3SO_3]$ (**9**), in a typical ratio of 3:1. However the product was not isolated as a solid, since **9** reverts to **8** in the absence of a CO atmosphere.

Reaction of Compound 13 with CO. To a solution of compound **13** (30 mg, 0.022 mmol) in 0.6 mL of CD_2Cl_2, in an NMR tube which was capped with a rubber septum, was added 2 mL of CO, by means of a gas-tight syringe, leading to an immediate color change of the solution from red to

yellow. The NMR spectra of the solution showed that the product was a mixture of compounds **5** and **8** in a typical ratio of 1:0.2.

Reaction of Compound 13 with PMe_2Ph. To a solution of compound **13** (30 mg, 0.022 mmol) in 0.6 mL of CD_2Cl_2, in an NMR tube which was capped with a rubber septum, was added 1 equiv (3.1 μL, 0.022 mmol) of PMe_2Ph, leading to an immediate color change of the solution from red to yellow. The NMR spectra of the solution showed that the product was compound **5c**.

Reactions of Compound 13 with ^{t}BuNC and Ethylene. The procedures used were the same as those used for preparing compounds **10** and **11**, respectively, from compound **2**, except that **13** was used instead of **2**, and the solid was isolated in this case in the reaction with ethylene. The NMR spectra of the products obtained showed that they were **10** and **11**, respectively.

Reaction of 13 with SO_2. Sulphur dioxide gas was passed through a solution of compound **13** (30 mg, 0.022 mmol) in 0.6 mL of CD_2Cl_2 in an NMR tube which was covered with a rubber septum, leading to an immediate color change of the solution from red to dark red. The NMR spectra of the solution showed that the product was $[Ir_2(CO)_2(\mu\text{-}CH_3)(\mu\text{-}SO_2)(dppm)_2][CF_3SO_3]$ (**14**).

Reaction of 2 with H_2. Hydrogen was passed through a solution of compound **2** (100 mg, 0.071 mmol) in 10 mL of CH_2Cl_2 for about 2 min. The solution was then stirred under a static atmosphere of the gas for 18 h, leading to a change of the solution color from orange to yellow. The volume of the solvent was reduced to about 5 mL under a stream of H_2. The yellow product was then precipitated with Et_2O. The solid was then dried under a stream of H_2, and under vacuo yielding, $[Ir_2(H)(CO)_2(\mu\text{-}H)_2(dppm)][CF_3SO_3]$ (**20**). In a second reaction the product was not put under vacuum after drying

under a stream of H_2, in which case it yielded, $[Ir_2(H)_4(CO)_2(\mu\text{-}H)(dppm)_2]$-$[CF_3SO_3]$ (**21**).

In the experiments to characterize intermediates in this reaction, compound **2** (25 mg, 0.018 mmol), was dissolved in 0.6 mL of CD_2Cl_2 and transferred to an NMR tube, which was then covered with a rubber septum. The reaction with H_2 was done under three different conditions. In the first case, H_2 gas was passed through the solution at room temperature and the NMR spectra were obtained immediately afterwards. In another case, after passing the gas through the solution, the reaction was quenched by immersing the NMR tube in a dry ice/acetone mixture in a dewar flask until the NMR spectra were obtained shortly afterwards, while in the third case the solution in the NMR tube was cooled to -78 °C by immersing it in a dry-ice/acetone mixture in a dewar flask before passing the gas through it.

^{1}H NMR Magnetization Transfer Experiments on Compound 2. Magnetization transfer between the hydride and the methylene ligand protons was examined by selective inversion. The hydride signal was selectively inverted by means of a DANTE[12] pulse sequence. Typically, after a delay of 1.5 s, a series of eighteen, 5 μs pulses, each separated by a 550 μs delay was used. The relaxation of this signal following the inversion was monitored using a 90° nonselective observation pulse, applied at variable delays of between 0.001 s and 2.5 s, after the selective pulse.

Non-selective inversion recovery experiments were performed initially, in order to measure the relaxation time (T_1) for the hydride as well as that for the methylene ligand protons. The nonselective 90° pulse width for ^{1}H, with an attenuator set at 10 dB, was 44.75 μs. This pulse width was calibrated at the beginning of the experiment. NMR probe temperatures were

measured with an independently calibrated thermocouple immersed in the appropriate volume of toluene in an NMR tube before and after the experiments.

Results and Discussion

(a) Preparation and Characterization of $[Ir_2(H)(CO)_3(\mu\text{-}CH_2)(dppm)_2][CF_3SO_3]$ (2). Replacing the Rh atom in $[RhIr(CO)_3(dppm)_2]$[3] by the more basic Ir atom, to give $[Ir_2(CO)_3(dppm)_2]$ (**1**),[8] results in a dramatic change in reactivity upon alkylation by methyl triflate. Instead of yielding the analogous methyl complex, $[Ir_2(CH_3)(CO)_3(dppm)_2][CF_3SO_3]$, the reaction of compound **1** with this alkylating reagent gives the novel hydrido, methylene-bridged species, $[Ir_2(H)(CO)_3(\mu\text{-}CH_2)(dppm)_2][CF_3SO_3]$ (**2**) as shown in Scheme 3.1.

The ^1H NMR spectrum of compound **2** shows three resonances at δ 5.19, 4.60 and 3.59 respectively, each integrating as two protons and corresponding to the three methylene groups in the complex, and a hydride resonance at δ -11.35, integrating as one proton. Selective and broad-band ^{31}P decoupling experiments clearly differentiate the two methylene resonances of the dppm groups from that bridging the metals (δ 4.60). This latter resonance, which appears as a poorly resolved quintet in the ^{31}P-coupled ^1H NMR spectrum, simplifies to a triplet, which is not well resolved, upon selectively decoupling *either* ^{31}P resonance and to a singlet upon broad-band decoupling, whereas the dppm methylene proton resonances appear as two doublets (at δ 5.19 and 3.59) upon ^{31}P broad-band decoupling (see Figure 3.1). The hydride resonance, which appears as a triplet, collapses into a singlet on selectively decoupling the lower-field ^{31}P resonance, while it is unchanged on decoupling the other ^{31}P resonance, showing that it is terminally bound to

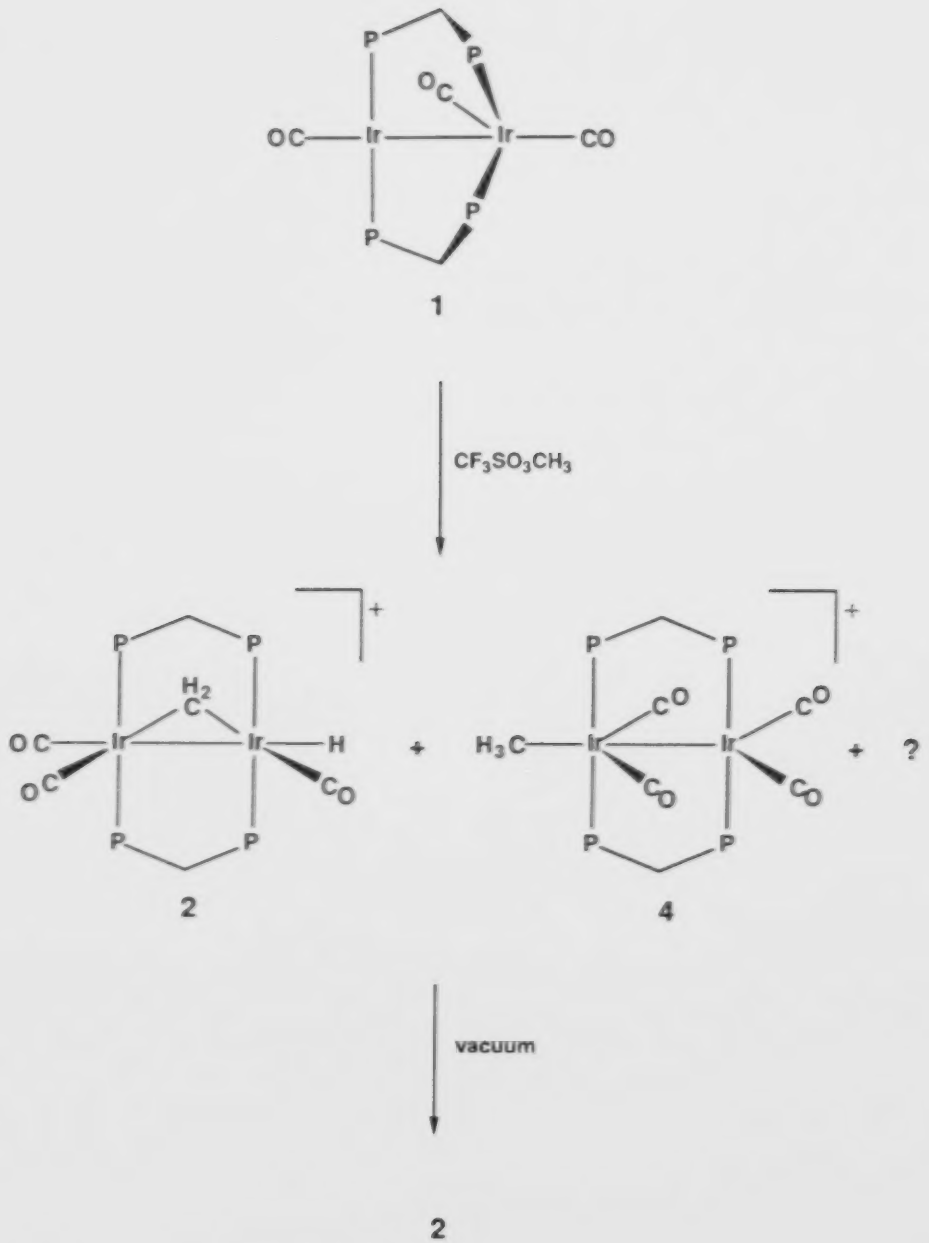
P
P
OC
OC
Ir
Ir
CO
P
P
1
CF3SO3CH3
+
P
P
H2
C
OC
Ir
Ir
H
OC
CO
P
P
2
+
P
P
CO
CO
H3C
Ir
Ir
CO
CO
P
P
4
+
?
vacuum
2

Scheme 3.1.

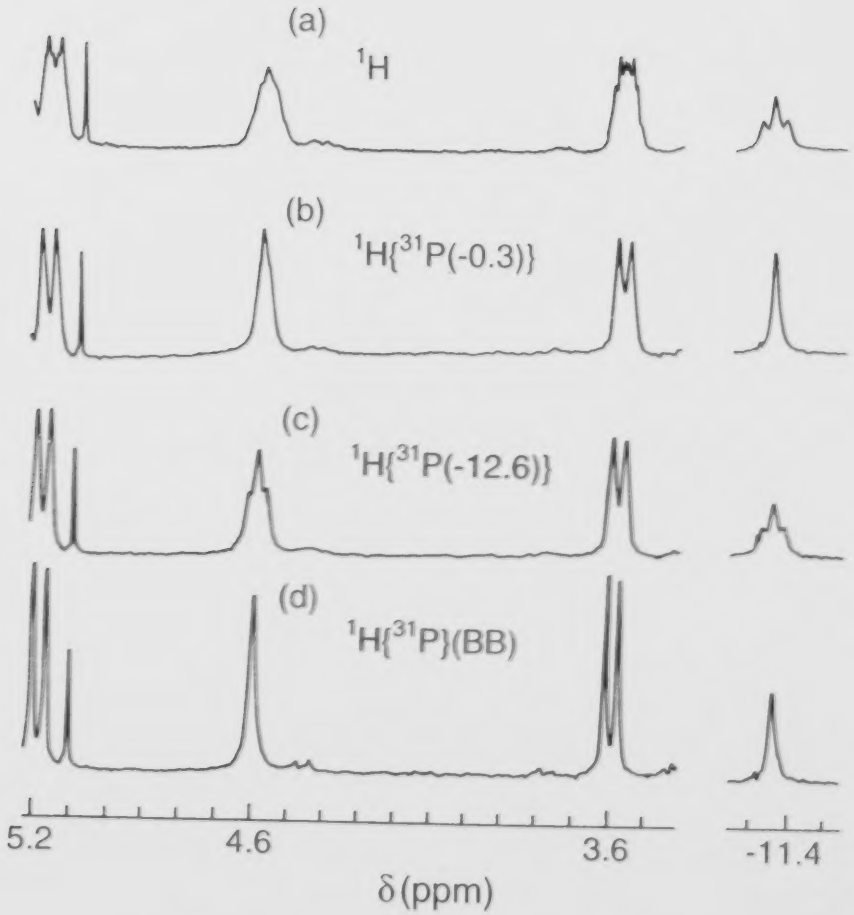

Figure 3.1. ^{1}H and $^{1}H\{^{31}P\}$ NMR spectra of compound **2** at -40 °C.

one of the metal centers, coupling to only the two phosphorus nuclei bound to that metal.

Although the chemical shift for the dimetalated methylene protons is slightly outside the wide range quoted for such groups when they bridge a metal-metal bond (δ 5-11),[13] the significance of this observation is not clear, since there are at least two previous reports in which methylene protons in related species resonate at even higher field (δ 4.32, 4.78, 4.08)[14] than for **2**, and subsequent work to be described herein has shown even higher-field shifts in related species (vide infra).

The $^{13}C\{^1H\}$ NMR spectrum[15] of **2** shows triplets at δ 177.4, 177.0 and 162.0 respectively, corresponding to the three carbonyl groups, each coupling to two phosphorus nuclei. Selectively decoupling the higher-field phosphorus resonance leads to the collapse of the ^{13}C resonances at δ 177.4 and 162.0 into singlets, while the third resonance remains as a triplet. Similarly, selectively decoupling the other phosphorus resonance leads to the collapse of the carbon resonance at δ 177.0 into a singlet, while the other two remain as triplets. This demonstrates that two of the CO ligands are bound to one metal center while the third one is bound to the other metal to which the hydride is also bound. Unfortunately, identification of the ^{13}C resonance of the methylene group in samples prepared using nonenriched methyl triflate has not been possible. However the NMR data obtained clearly establish the structure of compound **2** as that shown in Scheme 3.1.

Compound **2** is the unusual result of C-H activation of a coordinated methyl group by an adjacent metal center - a transformation that has only rarely been observed. In addition, it appears that this reversible transformation is unusually facile. Presumably the formation of **2** proceeds through the initial formation of an intermediate methyl complex,

$[Ir_2(CH_3)(CO)_3(dppm)_2][CF_3SO_3]$ (**3**)[16] followed by C-H activation to give compound **2**. Reports of similar C-H activation processes include those by Muetterties and coworkers,[17] and Shapley and coworkers.[14a] Muetterties' work involved the reaction of $[(COD)Ir(\mu\text{-}Cl)]_2$ (COD = 1,5-cyclooctadiene) with CH_3Li, at -78 °C, to give $[(COD)Ir(\mu\text{-}CH_2)]_2$. Apparently in forming the methylene-bridged complex, there was initial replacement of the bridging chloride ligands by methyl ligands, followed by activation of one of the C-H bonds of each methyl group with concomitant elimination of hydrogen. Shapley's work, on the other hand, involved the reaction of $[H_2Os_3(CO)_{10}]$ with diazomethane at -20 °C to give first, $[HOs_3(CO)_{10}(CH_3)]$, followed by C-H activation to give an equilibrium mixture of this hydrido methyl compound and the dihydrido methylene compound, $[H_2Os_3(CO)_{10}(\mu\text{-}CH_2)]$, as the temperature was raised. A more recent report is that by Bergman and coworkers,[18] regarding the complex, $[Cp_2TaPt(H)(\mu\text{-}CH_2)_2(PMe_3)]$. ^1H NMR spin-saturation-transfer experiments demonstrated that exchange between the hydride and methylene hydrogens occurs in this complex, and an intermediate methyl complex, $[Cp_2TaPt(CH_3)(\mu\text{-}CH_2)(PMe_3)]$ was suggested as accounting for this exchange. Apparently the methyl and the hydrido-methylene complexes are interconverting by means of methyl C-H activation and hydride migratory insertion onto the methylene ligand.

At temperatures above -40 °C, the ^1H resonances of the bridging methylene and hydride ligands of **2** are broad suggesting an exchange between the two, presumably via the intermediate methyl complex, $[Ir_2(CH_3)(CO)_3(dppm)_2][CF_3SO_3]$ (**3**), as shown in Scheme 3.2. This exchange has been confirmed by a ^1H NMR spin-saturation-transfer experiment at -30 °C, in which saturation of one signal causes a corresponding decrease in the intensity of the other. Furthermore, broadening of the carbonyl

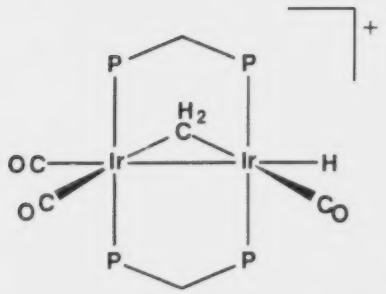

2

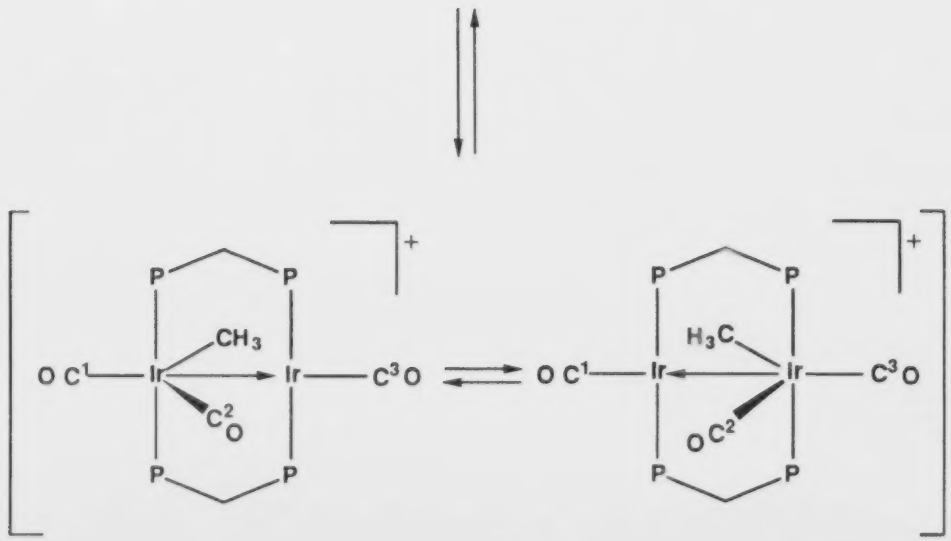

3

Scheme 3.2.

resonances at δ 177.0 and 162.0 at -20 °C and higher temperatures (see Figure 3.2) indicates that there is exchange between the CO group on the metal bearing the hydride ligand and one of the two on the other metal. The extent of broadening of these resonances increases as the temperature is raised from -20 °C, and at room temperature they are not resolved from the baseline. Although the approximate rate of this exchange process, determined at different temperatures by simulation of the $^{13}C\{^1H\}$ spectra of **2** at those temperatures[19] is comparable to that involving the methylene protons and hydride ligand (vide infra), it is suggested that they are different processes. It is proposed that the carbonyl exchange process occurs via the intermediate complex **3**, and that it involves the migration of one of the CO ligands as well as the methyl group in this intermediate complex from one metal to the other as shown in Scheme 3.2 (if the methyl group in **3** is bridging, then the process involves migration of only the CO ligand).

The rate of exchange between the bridging-methylene protons and the hydride ligand in **2** was determined from the results of the ^1H NMR selective inversion-recovery experiments. The FIDs obtained in this experiment, were transformed without using any line broadening, and all spectra were normalized with respect to the spectrum which corresponds to the longest delay time. Data analysis was carried out according to the method of McClung and coworkers,[20] by Mrs. G. Aarts and Dr. McClung, who are acknowledged for their assistance with the magnetization transfer experiments and the interpretation of the results obtained.

The resulting plots obtained from this analysis are shown in Figure 3.3, and Table 3.3 shows the variation of the calculated rate constant for the exchange process with temperature. The activation parameters for this

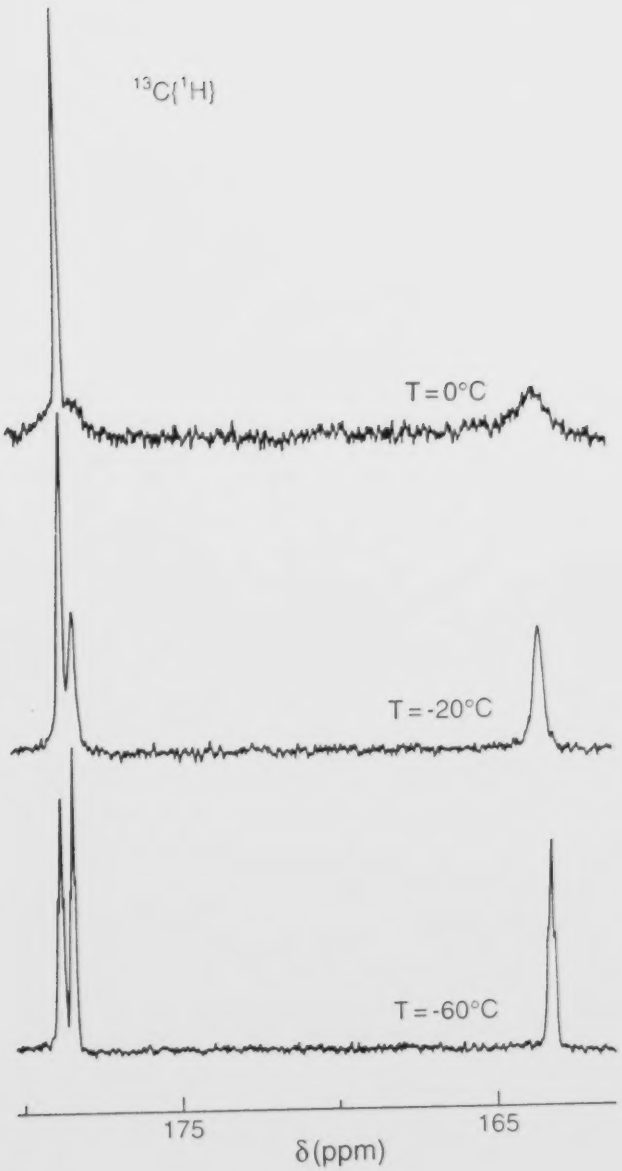

Figure 3.2. Carbonyl region of the $^{13}C\{^{1}H\}$ NMR spectra of compound **2** at temperatures between -60 °C and 0 °C.

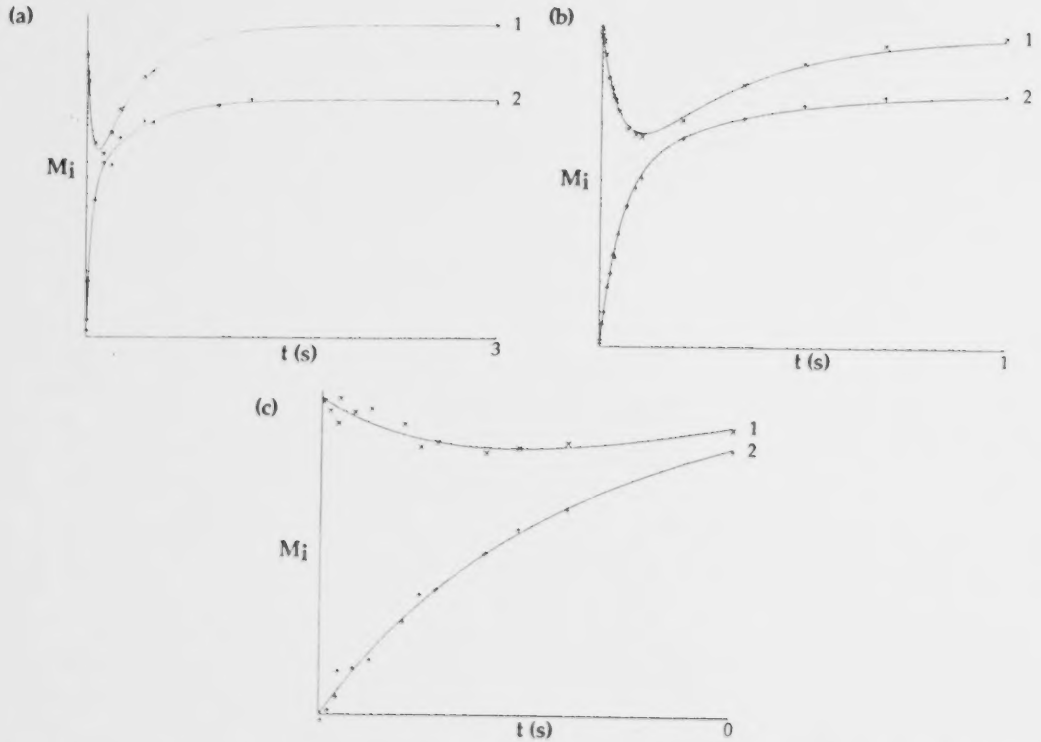

Figure 3.3. (+,-) Magnetizations, $M_i(t)$ (arbitrary units) at the CH_2 (1) and hydride (2) sites of compound **2**, following a selective inversion of site 2 magnetization. Curves represent least-squares fit for (a) k = 10.28 s^{-1} (-29.7 °C), (b) k = 5.86 s^{-1} (-40.6 °C), (c) k = 2.17 s^{-1} (-46.9 °C), (d) k = 1.23 s^{-1} (-50.6 °C) and (e) k = 0.81 s^{-1} (-56.4 °C).

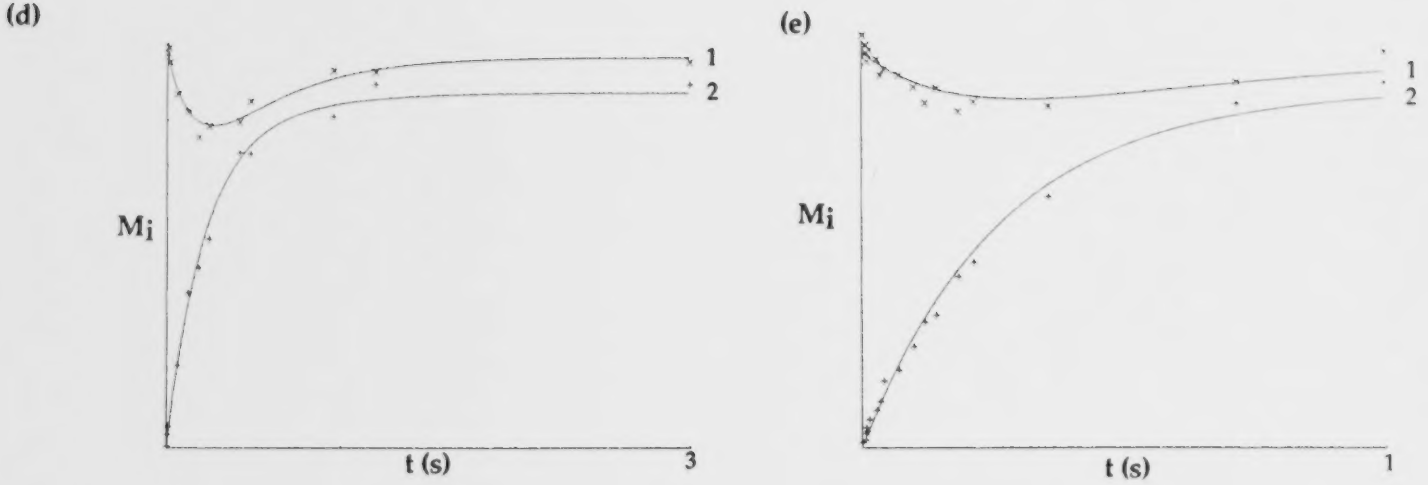

Figure 3.3. contd.

Table 3.3. Values used for the Eyring plot in Figure 3.4.

Rate (k)	T (°C)	T (K)	1/T	ln k/T
10.28	-29.7	243.43	4.11×10^{-3}	-3.165
5.86	-40.6	232.53	4.30×10^{-3}	-3.681
2.17	-46.9	226.23	4.42×10^{-3}	-4.647
1.23	-50.6	222.53	4.49×10^{-3}	-5.198
0.81	-56.4	216.73	4.61×10^{-3}	-5.589

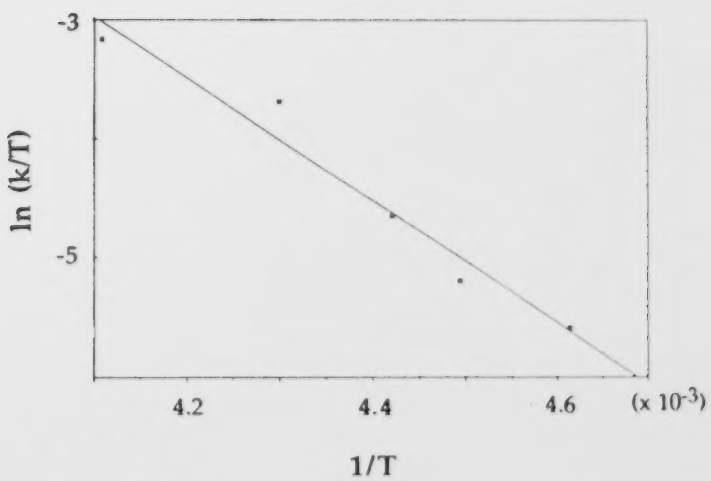

Figure 3.4. Eyring plot for the methylene-hydride exchange process in compound **2**.

process were calculated from the rate constants (k) and the temperatures as explained below. From the Eyring equation,[21]

$$k = (\kappa T/h)\, e^{-\Delta G^{\neq}/RT} = (\kappa T/h)\, e^{-\Delta H^{\neq}/RT}\, e^{\Delta S^{\neq}/R} \quad \text{....(1)}$$

Hence, $$\ln(k/T) = \ln(\kappa/h) - \Delta H^{\neq}/RT + \Delta S^{\neq}/R \quad \text{....(2)}$$

where R = gas constant

κ = Boltzmann's constant

h = Plank's constant

T = temperature in K

and a plot of ln(k/T) against 1/T gives a straight line with slope equal to $-\Delta H^{\neq}/R$, and intercept equal to $\Delta S^{\neq}/R$ (see Figure 3.4 on the previous page). From the plot, the activation parameters for the process have been calculated to be $\Delta H^{\neq} = 10.3 \pm 0.4$ kcal/mol and $\Delta S^{\neq} = -11.2 \pm 1.5$ eu.[22] The activation energy for the methylene proton-hydride exchange that occurs in compound **2** is therefore less than that determined for a similar process in the complex, $[Cp_2TaPt(H)(\mu\text{-}CH_2)_2(PMe_3)]$,[18] which was mentioned earlier. In the latter compound, it was ascertained that exchange occurred between the hydride ligand and the methylene protons cis to it, and the calculated activation parameters for the process were, $\Delta H^{\neq} = 18.2 \pm 0.4$ kcal/mol and $\Delta S^{\neq} = -0.1 \pm 1.1$ eu.

The differing behavior of the 'RhIr' and diiridium systems in their alkylation reactions can be attributed to the properties of the metal adjacent to that to which the methyl group is bound (assuming that the methyl group is terminally bound in **3**). In the diiridium compound, **3**, the more electron rich adjacent Ir metal favors oxidative addition of a C-H bond of the methyl more than does the adjacent Rh metal, in the analogous 'RhIr' complex, $[RhIr(CH_3)(CO)_3(dppm)_2][CF_3SO_3]$.[23] That C-H activation occurs for the

diiridium compound but not for the 'RhIr' analogue, can be rationalized in terms of the resulting M-C and M-H bonds, both of which are stronger for Ir than for Rh.[24,25]

Attempts to deprotonate compound **2** to yield a neutral methylene-bridged species have so far failed. Similarly attempts to replace the hydride ligand in **2**, through the reaction with $CHCl_3$ (or CCl_4), also failed. It was reasoned that the methylene-bridged chloro species resulting from this latter reaction could be used to generate a methylene-bridged alkyl complex by reaction with Grignard reagents. The failure of **2** to react as a typical metal-hydride species is possibly not surprising considering the rapid exchange that occurs between the methylene-hydride species **2** and the methyl complex, **3**.

In an attempt to observe the initial product of alkylation of compound **1**, the reaction of **1** with methyl triflate was started at -78 °C, in CD_2Cl_2, and monitored by NMR while gradually warming the mixture. However, the only two characterizable species observed were compound **2** and, $[Ir_2(CH_3)(CO)_4(dppm)_2][CF_3SO_3]$ (**4**), in a typical ratio of 1:0.4. Small amounts of unidentified decomposition products were also detected above the baseline in the $^{31}P\{^1H\}$ NMR spectra. Compound **4** can be obtained quantitatively from **2** by addition of CO; removal of CO reverses the reaction, giving compound **2**. The failure to observe the initial alkylation product is consistent with the facility of the C-H activation process that transforms it to compound **2**.

In the ^1H NMR spectrum[26] of compound **4**, the methyl resonance appears as a triplet at δ 0.38, while the four dppm methylene protons, which are all equivalent, give rise to a multiplet at δ 4.59, indicating that compound **4** is symmetric on either side of the metal-phosphorus plane. The $^{13}C\{^1H\}$ NMR spectrum of **4** shows a broad resonance at δ 194.1 and a triplet at

δ 182.9. Comparing the intensities of the carbonyl resonances of compounds **2** and **4** in the $^{13}C\{^1H\}$ NMR spectrum of the mixture, indicates that each of the resonances of the latter compound represents two CO ligands. All the NMR data are consistent with the structure of **4** shown in Schemes 3.1 and 3.3. Apparently compound **4** is stable as a methyl complex, as opposed to a hydrido-methylene complex, because the additional π-acceptor carbonyl deactivates this species to subsequent oxidative addition. In addition, **4** is coordinatively saturated, negating the possibility of C-H activation.

(b) Reactivity studies. Compound **2**, being the product of C-H activation, offered a unique opportunity for the investigation of the stepwise transformations involved in such an activation by an adjacent metal and also presented several possibilities in reactivity that were of interest. It was anticipated that by varying the ancillary ligands in compound **2**, it should be possible to fine-tune the electron density at the metals such that the transformation from terminal methyl to bridged methyl to hydrido-methylene species could be effected. In this respect, the study of the reactivity of **2** with a variety of ligands of different σ-donor and π-acceptor strengths was of interest.

It was also of interest to investigate the reactivity of this hydrido-methylene complex with unsaturated substrates, such as ethylene, owing to the obvious relevance to reactions leading to the coupling of organic substrates. Such coupling in reactions with unsaturated compounds such as olefins, may occur via alkyl migration to the olefin ligand,[27] by insertion of the olefin into an Ir-C bond of the bridging methylene group,[28] or by olefin insertion into the metal-hydride bond to give a methylene-bridged alkyl complex,[29] which may then undergo coupling of the alkyl and methylene moieties. Furthermore, it was of interest to see how the reactivity of

compound **2** compared with that of the closely related 'RhIr' complex, $[RhIr(CH_3)(CO)_3(dppm)_2][CF_3SO_3]$.[23]

Reagents with which compound **2** was reacted included phosphines, with the anticipation that increasing the electron density on the metals with these strong σ-donor ligands should increase the stability of the C-H activated products. A similar reaction was carried out with triphenylphosphite, since it was of interest to determine how this ligand of intermediate donor/acceptor properties would react (phosphites, such as $P(OPh)_3$, are better π-acceptors than the phosphine analogues, but are still less effective than CO ligands). Reactions with CO and ^tBuNC were also undertaken because of interest in the possibility of migratory insertion involving these ligands, and the reaction with SO_2 was carried out to investigate the possibility of electrophilic attack[30] and subsequent insertion into either the Ir-methylene bond of **2** or the Ir-methyl bond of the reactive intermediate, **3**, as has previously been observed in other metal alkyl complexes.

Compound **2** reacts with phosphines to give the phosphine-substitution products, $[Ir_2(H)(CO)_2(PR_2R')(\mu\text{-}CH_2)(dppm)_2][CF_3SO_3]$ (R = R' = Me (**5a**), Ph (**5b**) and R = Me, R' = Ph (**5c**)) in which the substitution of one CO by a phosphine ligand has occurred (see Scheme 3.3). The $^{31}P\{^1H\}$ NMR spectrum of compound **5a** shows multiplets at δ -7.7, -11.3 and a broad resonance at δ -79.2 (representing the two sets of dppm phosphines and the PMe_3 group, respectively), in a pattern that is consistent with an AA'BB'M spin system. The ^1H NMR spectrum of **5a** shows the hydride resonance as a doublet of multiplets at δ -12.35 ($^2J_{P\text{-}H}$ = 21.2, 13.5 Hz ; $^3J_{P\text{-}H}$ = 4.8 Hz) and the PMe_3 methyl resonance as a doublet at δ 0.75 ($^2J_{P\text{-}H}$ = 9.6 Hz). It also shows three multiplets at δ 4.05, 3.45 and 3.05. Selective ^{31}P decoupling experiments indicate that the multiplet at δ 3.05 is the resonance for the methylene group

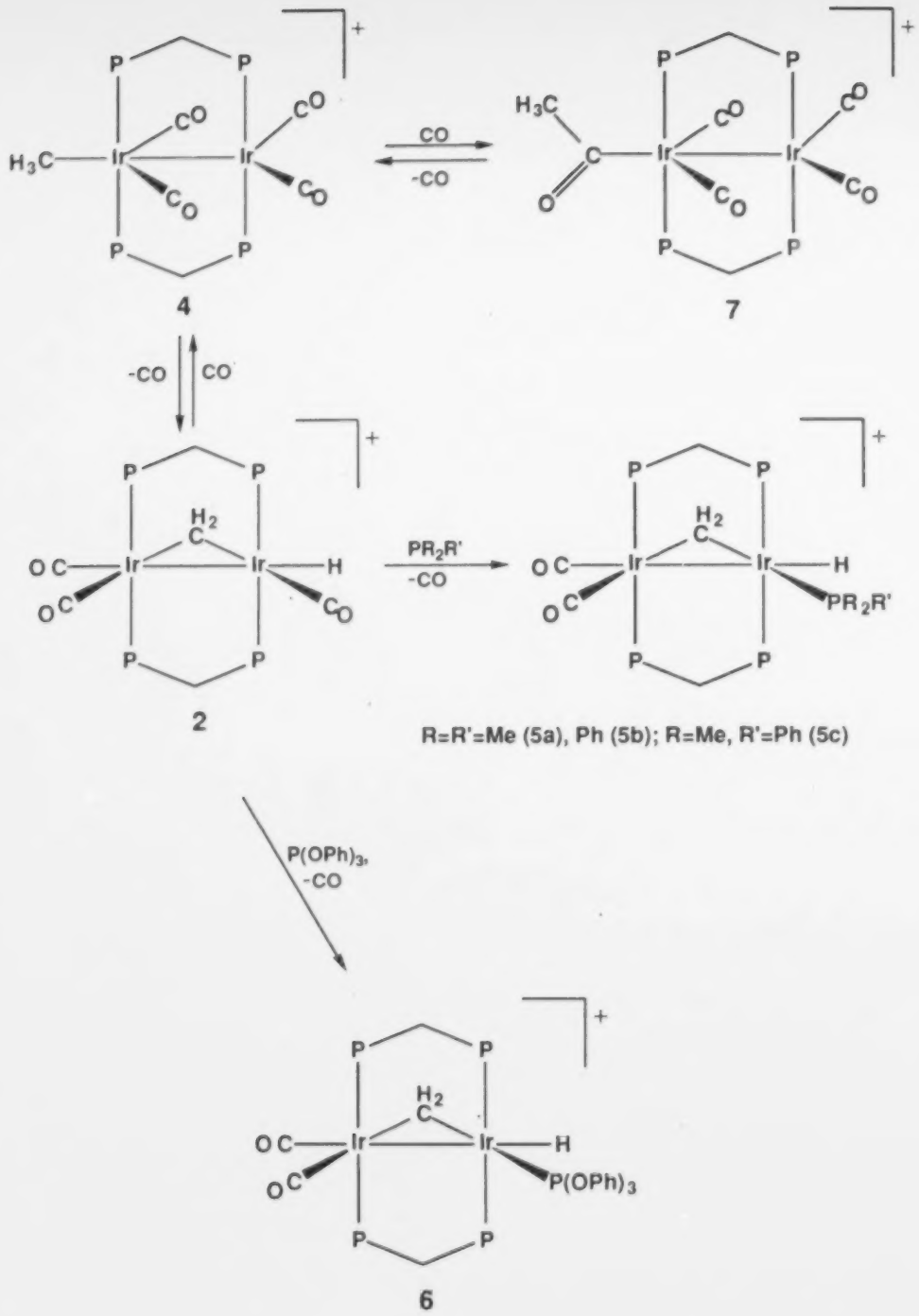

Scheme 3.3.

bridging the two metals, while the other two (δ 4.05, 3.45) are those of the dppm methylene protons. The $^{13}C\{^1H\}$ NMR spectrum shows a triplet and a broad resonance of equal intensity at δ 183.0 and 180.1, respectively, indicating the presence of two CO groups in **5a**. The IR spectrum shows CO stretches at 1961 and 1950 cm^{-1}, precluding any bridging interaction of the carbonyls with the adjacent metal. Compounds **5b** and **5c** have similar spectroscopic parameters to those of **5a** (apart from the resonances due to the phosphines) indicating that they have similar structures.

It is interesting to note that the dimetalated methylene protons of the products **5a-c** resonate at even higher field than in compound **2** (ie. δ 3.05 (**5a**), 3.71 (**5b**) and 3.35 (**5c**)). These values suggest that the chemical shift of these methylene protons is directly related to the electron density at the metals. Hence the strong σ-donating and poor π-back-accepting phosphine groups that increase the electron density at the metals more than the CO groups, bring about further shielding of the methylene protons. Also, as shown in Table 3.1, the more electron donating the phosphine is, the more shielded the methylene protons are (PMe_3 > PMe_2Ph > PPh_3). Furthermore, increasing the electron density at the metals by replacing one CO ligand with a phosphine ligand leads to increased stability of the C-H activated product, as expected. This is consistent with increased electron density favoring oxidative-addition. The apparent absence of exchange between the hydride ligand and the methylene protons at 20 °C in compound **5a** (inferred from ^1H NMR spin-saturation-transfer experiments), seems to be a consequence of the increased stability of such a C-H activated product, compared to compound **2**. It was anticipated that compound **5a** would be more prone both to deprotonation, and to exchange of the hydride ligand by a chloride ligand, in contrast to **2**, since **5a** appears to be a classical hydride and is not exhibiting exchange

between the hydride ligand and the methylene protons as was the case for **2**. However such experiments have not yielded any positive results so far.[31]

The phosphine-substituted products **5a-c** are structurally different from $[RhIr(CH_3)(CO)_2(PMe_3)(dppm)_2][CF_3SO_3]$,[23] as shown by the $^{31}P\{^1H\}$ NMR spectra. Whereas the diiridium products give rise to AA'BB'M type patterns, typical of two dppm phosphorus chemical environments, the mixed 'RhIr' species has four chemically distinct dppm phosphorus nuclei and gives rise to an ABCDMX type pattern (X = Rh). It is assumed that some subtle steric differences between compounds **5a-c**, on one hand, and $[RhIr(CH_3)(CO)_2(PMe_3)(dppm)_2][CF_3SO_3]$, on the other, lead to the structural difference in which one of the dppm phosphines of the 'RhIr' compound bends out of the plane of the others, while the analogous atoms in the diiridium compounds are in the same plane.

Reaction of compound **2** with $P(OPh)_3$, also results in substitution of one of the CO ligands in the former to give, $[Ir_2(H)(CO)_2(P(OPh)_3)(\mu\text{-}CH_2)(dppm)_2][CF_3SO_3]$ (**6**), the $P(OPh)_3$ analogue of compounds **5a-c**. The spectroscopic parameters of **6** suggest a structure similar to those of the compounds **5a-c**.

Compound **2** reacts with CO to give a mixture of compound **4** (as noted earlier) and the labile acyl complex, $[Ir_2(CO)_4(COCH_3)(dppm)_2][CF_3SO_3]$ (**7**). In the ^1H NMR spectrum of **7**, the methyl resonance appears as a singlet at δ 0.63, and the four dppm methylene protons give rise to a single resonance at δ 4.61. The $^{13}C\{^1H\}$ spectrum shows the acyl carbonyl resonance as a triplet at δ 225.1 together with a broad singlet and a triplet at δ 195.6 and 180.0, respectively, while the IR spectrum shows the acyl stretch at 1622 cm^{-1}, as well as CO stretches at 2049 and 1959 cm^{-1}. These NMR and IR data are consistent with the structure assigned to compound **7**, with two CO ligands

terminally bound to each metal (see Scheme 3.3). Furthermore, the transformation of the methyl resonance from a triplet in compound **4** (δ 0.38) to a singlet at lower field in compound **7** is consistent with the latter compound being an acyl complex, in which the methyl protons no longer display coupling to phosphorus, being one additional atom further removed from them.

Compound **7** is the result of migratory insertion of the CH_3 group to a carbonyl of compound **4**, accompanied by incorporation of an additional CO ligand. Compound **7** loses CO in the absence of an atmosphere of the gas to yield the precursor, compound **4**.

The behavior of **2** in its reaction with CO is different from that of $[RhIr(CH_3)(CO)_3(dppm)_2][CF_3SO_3]$.[23] The latter complex picks up only one CO ligand to give an acyl complex whereas the former requires two CO ligands. This is consistent with the ability of the more electron rich Ir metal to bind more CO ligands than Rh.[32]

Compound **2** reacts with SO_2 to give $[Ir_2(CH_3)(CO)_3(\mu\text{-}SO_2)(dppm)_2][CF_3SO_3]$ (**8**), as shown in Scheme 3.4. In the ^1H NMR spectrum of compound **8** the methyl resonance appears as a triplet at δ 0.01. The $^{13}C\{^1H\}$ NMR spectrum shows triplets at δ 177.9, 177.8 and 160.2, while the IR spectrum shows CO stretches at 2042, 2010 and 1987 cm^{-1}, indicating that there are three terminally bound carbonyl ligands in compound **8**. The IR spectrum also shows one of the two S-O stretches at 1070 cm^{-1} (the other one is presumably overshadowed by similar stretches due to the triflate anion). A bridging mode is proposed for the SO_2 ligand in **8**, because it is the mode of coordination that has been observed in several related binuclear SO_2 adducts.[33] In addition, the identification of the CH_3 and CO ligands as being

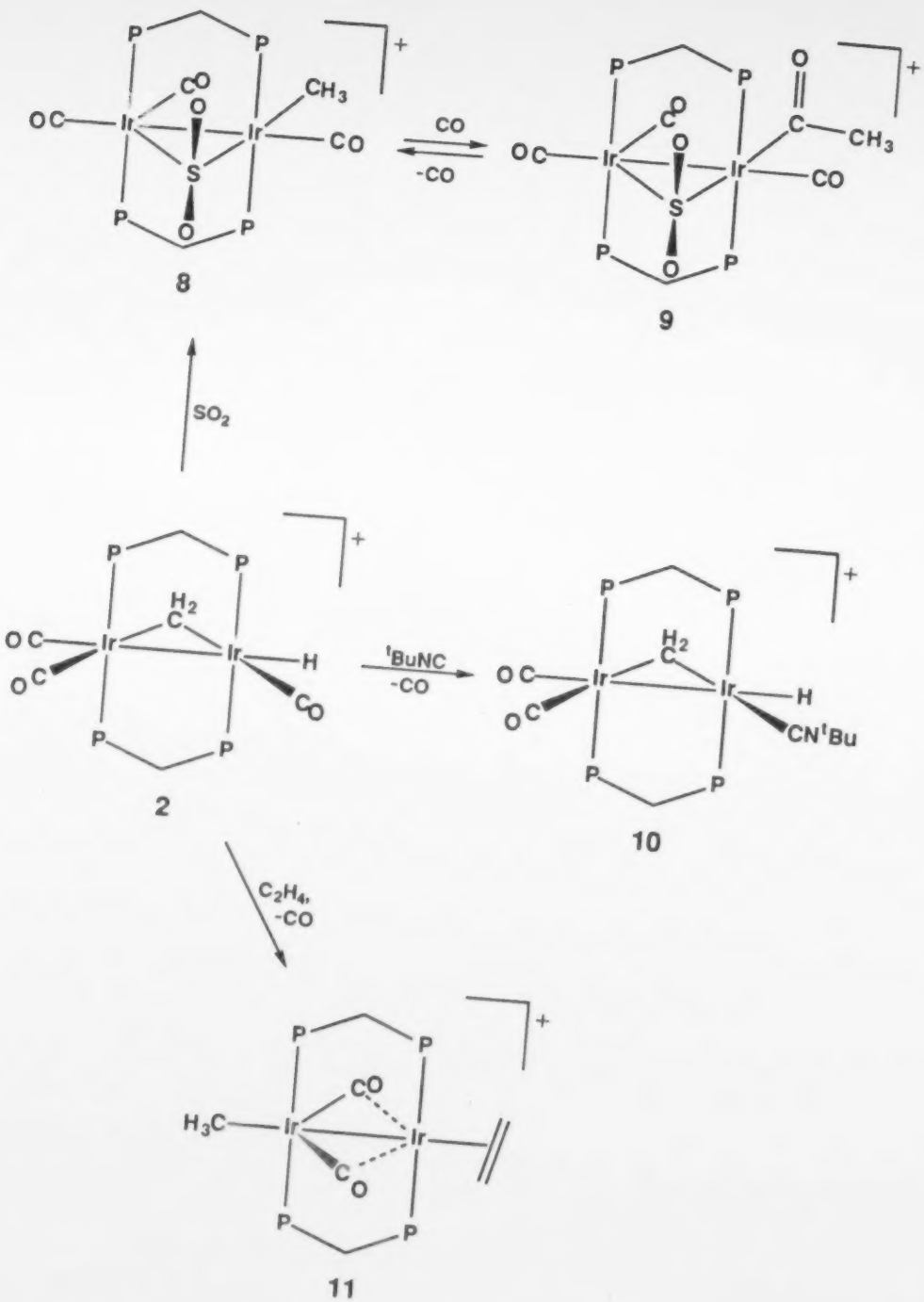

Scheme 3.4.

terminally bound supports a bridging arrangement for the SO_2 group, giving both metals similar geometries.

If the reaction of compound **2** with SO_2 is carried out for a longer time (eg. for 2 h instead of 15 min), it yields some amount of a product that was later characterized as $[Ir_2(CO)_2(\mu\text{-}CH_3)(\mu\text{-}SO_2)(dppm)_2][CF_3SO_3]$ (**14**), (vide infra), in addition to compound **8**. A typical ratio of compounds **8** and **14** obtained under these conditions is 4:1. Apparently compound **14** is obtained from **8** by CO loss under these conditions.

The behavior of compound **2** in its reaction with SO_2 is similar to that observed for the complex, $[RhIr(CH_3)(CO)_3(dppm)_2][CF_3SO_3]$,[23] in that it does not lead to insertion of the SO_2 ligand into a M-C (methylene or alkyl) bond. Although the reaction with the 'RhIr' compound eventually resulted in migratory insertion of the CH_3 group onto a carbonyl, no subsequent migratory insertion takes place in **8** (as mentioned earlier, CO loss actually occurs on prolonging the reaction with **2**). Such migratory insertion can be induced by reacting compound **8** with CO, giving the acyl product $[Ir_2(CH_3CO)(CO)_3(\mu\text{-}SO_2)(dppm)_2][CF_3SO_3]$ (**9**) and compound **8** in a typical ratio of 1:3 (using 1 atm. of CO). Compound **9** reverts to **8** in the absence of an atmosphere of CO. This difference in the reactivities of the 'RhIr' and diiridium complexes is consistent with the ability of the electron rich Ir metal to bind more CO ligands compared to Rh,[32] the lower tendency of Ir alkyls to undergo migratory insertions than their Rh analogues,[24b] and the lesser tendency of Ir, compared to Rh, to adopt a stable coordinatively unsaturated configuration.[3,4]

It was anticipated that it would be possible to abstract one of the CO ligands in compound **8**, using Me_3NO, since two of its CO stretches were above 2000 cm^{-1}, and that such an abstraction might lead to C-H activation of

the methyl ligand. Although reaction of **8** with 1 equiv of anhydrous Me_3NO did result in loss of a CO ligand, to yield a product which was later characterized as compound **14**, this method gave a mixture of several products and so was not pursued. Compound **14** is best prepared by an alternative route (vide infra).

Reaction of compound **2** with ^{t}BuNC results in substitution of one carbonyl to give $[Ir_2(H)(CO)_2(^t\text{BuNC})(\mu\text{-}CH_2)(dppm)_2][CF_3SO_3]$ (**10**), which is not unlike the products in the reactions of **2** with phosphines and triphenylphosphite. The ^{1}H NMR spectrum of compound **10** shows the hydride resonance as a triplet at δ -11.46 and the resonance for the t-butyl group protons as a singlet at δ 0.60, as well as three multiplets at δ 3.92, 3.58 and 3.57. Selective ^{31}P decoupling experiments establish that the multiplet at δ 3.58 is the signal for the methylene group that bridges the two metals, while the other two are those of the bridging dppm methylene groups. These experiments also confirm that the hydride ligand is terminally bound to one metal. The $^{13}C\{^1H\}$ NMR spectrum shows a multiplet and a triplet at δ 179.2 and 179.1, respectively, and the IR spectrum shows CO stretches at 1975 and 1970 cm^{-1}, indicating that there are two terminal CO ligands in compound **10**, as well as a characteristic C≡N stetch at 2163 cm^{-1}, consistent with a terminally bound isocyanide ligand.[24b] The increase in frequency of the C≡N stretch in **10** compared to the value of 2125 cm^{-1} observed in free ^{t}BuNC, is consistent with strong RNC→Ir σ donation and little Ir→CNR π backbonding.[34] Thus it is not surprising that the methylene-hydride structure is maintained in compound **10**, as opposed to a methyl structure, since the predominantly σ-donor property of the isocyanide in this case will give rise to increased electron density at the metals, leading to increased stability of the C-H activated product. The reaction of ^{t}BuNC with compound **2** contrasts with its

reaction with $[RhIr(CH_3)(CO)_3(dppm)_2][CF_3SO_3]$ which results in isocyanide insertion into the Ir-CH_3 bond.[23] This difference is consistent with the greater tendency for migratory insertions involving Rh, than Ir,[24b] assuming that an intermediate in the 'RhIr' species has the methyl and the isocyanide ligands bound to Rh.

The reaction of compound **2** with ethylene does not result in any products of insertion involving the unsaturated substrate. Instead it yields a mixture of the starting compound, **2**, and an unusual methyl-ethylene complex $[Ir_2(CH_3)(CO)_2(C_2H_4)(dppm)_2][CF_3SO_3]$ (**11**) in a typical ratio of 1:1.3. The ^1H NMR spectrum of compound **11** shows the methyl resonance as a triplet at δ 0.70, and the resonance for the four ethylene protons, which are all equivalent, as a triplet at δ 1.05. Similarly the resonance for the four dppm methylene protons appears as a multiplet at δ 3.25, indicating that they are all equivalent. Selective ^{31}P decoupling experiments show that the methyl and ethylene ligands are terminally bound to different metal centers. The $^{13}C\{^1H\}$ NMR spectrum of a mixture of compounds **2** and **11** displays a single resonance for the two CO ligands in **11** at δ 204.0, indicating that they are equivalent. Selective ^{31}P decoupling experiments show that these two carbonyl ligands are bound to the same Ir center to which the methyl group is also bound. These experiments also suggest that the CO ligands in **11**, maintain a weak semibridging interaction with the second Ir metal, as selectively decoupling one phosphorus resonance leads to the sharpening of the broad triplet resonance for these ligands, while decoupling the other resonance leads to the collapse of the triplet into a broad singlet resonance. Moreover, the resonance for the CO ligands appears at lower field than that normally observed for terminally bound ones in these systems.[35]

It is perhaps surprising that substitution of one CO by C_2H_4 has resulted in a stable methyl compound as opposed to a hydrido-methylene compound, since C_2H_4 is usually thought of as being a poorer π-acid than CO.[36] However calculations involving the complexes $[Pt(bipy)(L)F_2]$ (bipy = bipyridyl, L = C_2H_4, CO, ONMe, PH_3), suggested that, for these compounds, the π-accepting capability of the ligands, L, varied along the series, C_2H_4 > CO > PH_3 > ONMe,[37] and it is possible that this observed behavior of C_2H_4 as a better π-acceptor than CO, is the situation in **11**. It may also be that steric differences between C_2H_4 and CO result in subtle geometric differences that favor a methyl compound over a methylene-bridged hydride.

Compound **11** is subtly different from the 'RhIr' analogue, $[RhIr(CH_3)(CO)_2(C_2H_4)(dppm)_2][CF_3SO_3]$,[23] having the two CO ligands bound to the same metal as the methyl group, whereas for the 'RhIr' analogue the two carbonyls and the ethylene ligand are bound to one metal, while the methyl group is bound to the other. As such compound **11** actually resembles the complex, $[RhIr(CH_3)(CO)_3(dppm)_2][CF_3SO_3]$,[23] having the methyl group on the saturated metal. The reason for such subtle differences between the two systems is not clear.

Compound **2** also reacts with 1,2-propadiene (allene), to give $[Ir_2(CH_3)(CO)_2(C_3H_4)(dppm)_2][CF_3SO_3]$ (**12**). The ^1H NMR spectrum of this product shows only two signals for the allene protons at δ 4.20 and 3.45 (both signals are multiplets), indicating the presence of two pairs of equivalent protons for this ligand in the product. It also shows the methyl resonance as a triplet at δ 1.05. The $^{13}C\{^1H\}$ NMR spectrum shows a triplet at δ 179.1 and a broad resonance at δ 170.7, indicating that there are only two CO ligands remaining in this compound. The CO stretches at 2003 and 1970 cm^{-1} in the IR spectrum of the allene product argue against any bridging interaction of

these ligands. The chemical shifts of the allene protons in this product are similar to those in $[W_2(O\text{-}t\text{-}Bu)_6(C_3H_4)(CO)_2]$ (δ 4.05 and 3.60),[38] as well as those in $[RhIr(CH_3)(CO)_2(C_3H_4)(dppm)_2][CF_3SO_3]$ (δ 4.00 and 3.46),[23] suggesting that the allene ligand adopts a similar coordination mode in the three compounds (μ-η^1:η^3- coordination mode). However the available spectroscopic evidence is not sufficient to establish the coordination geometry about the metals in the case of **12** (the structure of the 'RhIr' product could also not be determined from the spectroscopic evidence[1]). Furthermore the closeness of the phosphorus resonances in the $^{31}P\{^1H\}$ spectrum of **12** makes it impossible to selectively decouple these resonances, making it difficult to obtain further information concerning the coordination mode of the allene.

(c) Bridging Methyl Complexes. The high frequencies of two of the CO stretches in compound **2** (2018 and 2000 cm^{-1}) suggested that reaction with Me_3NO might result in abstraction of a CO ligand. This proved to be the case, yielding $[Ir_2(CO)_2(\mu\text{-}CH_3)(OSO_2CF_3)(dppm)_2]$ (**13**). At room temperature, the $^{31}P\{^1H\}$ NMR spectrum of compound **13** shows a singlet at δ 22.1, indicating that the four phosphorus nuclei are equivalent. The ^1H NMR spectrum at this temperature shows the methyl resonance as a quintet at δ 0.58, suggesting that the methyl ligand bridges the two metals, since it couples equally to the four phosphorus nuclei, while the dppm methylene resonances appear as two multiplets at δ 4.45 and 3.78 (see Figure 3.5). The $^{13}C\{^1H\}$ NMR spectrum at this temperature shows a broad resonance at δ 171.4, suggesting that the two CO ligands are equivalent.

NMR spectroscopic data obtained at low temperature, for **13**, in solution, show that this compound is fluxional. At -40 °C, the $^{31}P\{^1H\}$ NMR spectrum shows a single, very broad, featureless resonance, centered at δ 22.3, while the $^{13}C\{^1H\}$ NMR spectrum also shows a similar featureless resonance,

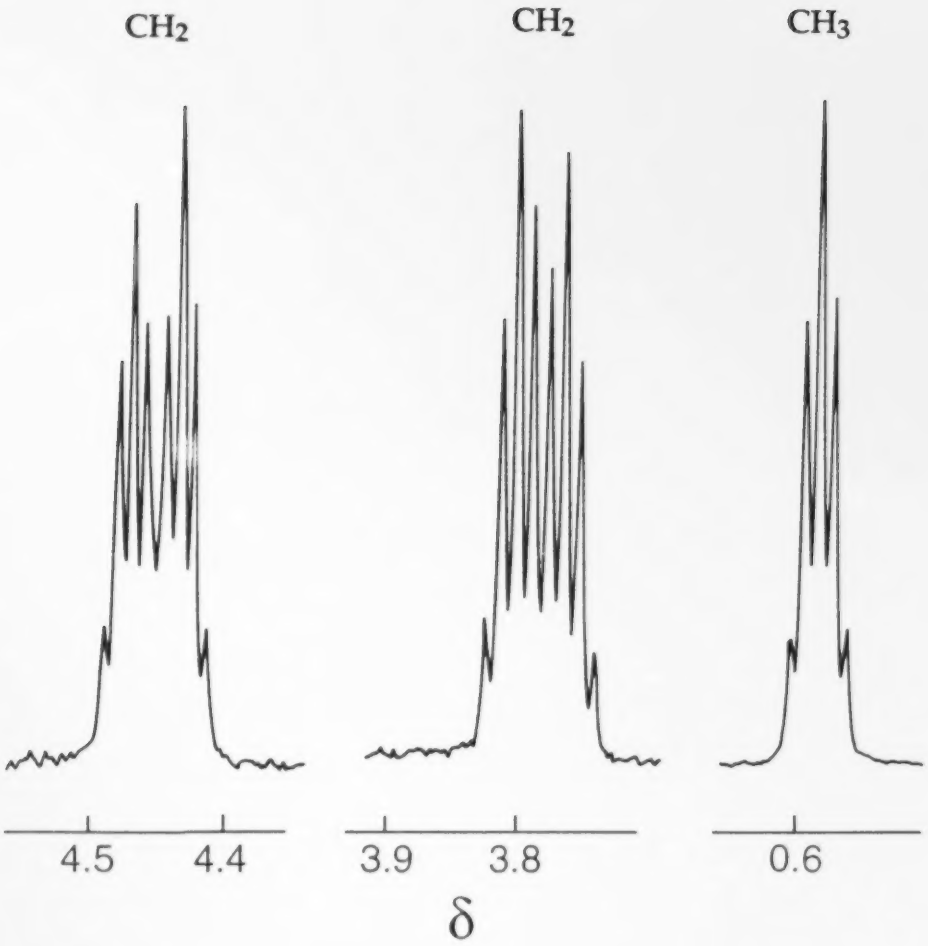

Figure 3.5. ^{1}H NMR spectrum of compound **13**, at 20 °C, showing the dppm methylene and the methyl resonances.

centered at δ 173.3, in the carbonyl region. The two methylene and the methyl resonances, on the other hand, are well resolved in the ^{1}H NMR spectrum, appearing as two multiplets at δ 4.47 and 3.38 and a quintet at δ 0.57, respectively. At -80 °C, however, the respective NMR spectra show that two separate phosphorus and CO carbon environments exist. The $^{31}P\{^{1}H\}$ NMR spectrum at this temperature shows two multiplets (typical of an AA'BB' spin system) at δ 26.2 and 17.6, and the $^{13}C\{^{1}H\}$ NMR spectrum shows two broad resonances at δ 182.5 and 162.1. In the ^{1}H NMR spectrum, the methyl resonance appears as a poorly resolved quintet at δ 0.51. The IR spectrum in CH_2Cl_2 shows a strong CO stretch at 1964 cm^{-1}, a weak one at 1886 cm^{-1}, and a stretch at 1347 cm^{-1} due to the triflate group. The frequency of this triflate stretch, is consistent with the presence of a coordinated triflate group in this compound in solution.[39]

The IR spectrum of the dicarbonyl compound, obtained using a nujol mull of the sample, shows two CO stretches at 1974 and 1832 cm^{-1}, while the solid state ^{13}C NMR spectrum shows two multiplets at δ 187.8 and 167.0, suggesting the presence of a semibridging CO ligand in the solid state structure (since none of the ^{13}C resonances are sufficiently low-field to indicate the presence of a symmetrically bridging CO ligand, although the IR stretch at 1832 cm^{-1} suggests some bridging interaction by one of the carbonyls). However preliminary work on an X-ray structure determination of this compound, shows that the two carbonyls are terminally bound, and the methyl group symmetrically bridges the two metals. Furthermore, the IR spectrum, obtained using a CH_2Cl_2 cast of the sample, shows a single strong CO stretch at 1960 cm^{-1}.[40] It is not clear why the spectrum obtained using a nujol mull of the sample shows a second CO stretch at a frequency which is typical for bridging CO ligands. Also, the observation that there are no

stretches higher than 1275 cm^{-1}, in the IR spectrum, due to the triflate group, is consistent with the fact that the methyl compound is cationic in the solid state, having a triflate counterion.[39] This contrasts with the IR spectrum in solution, which indicates the presence of a coordinated triflate ligand, as mentioned earlier.

While bridging methyl ligands can be σ-bound to one metal and engage in an agostic interaction of one of their C-H bonds with the second metal, but still give one signal for all the three protons, due to rapid exchange of these nuclei, the methyl resonance is usually high-field in these cases.[41] The chemical shift and the resolution of the quintet of the methyl resonance in **13**, in solution, therefore suggest that the methyl group symmetrically bridges the two metals under these conditions. Shapley and coworkers[42] have developed a method for distinguishing between a symmetrically bridging methyl group and an agostic C-H-M interaction by means of deuterium incorporation into one of the proton sites. Unfortunately, it has not yet been possible to incorporate a deuterium into compound **13**.

On the basis of the above information, it appears that the dicarbonyl compound, obtained from **2** by abstraction of one of its CO ligands, has the structure shown below (numbered **13a**), in the solid state. This compound is

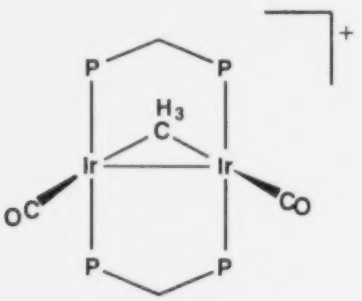

13a

very similar to $[Ir_2(CO)_2(\mu\text{-}CH_3)(dmpm)_2][CF_3SO_3]$ (dmpm = bis(dimethylphosphino)methane),[43] which varies only in the nature of the substituents on the bridging phosphine groups. The spectroscopic data are consistent with a different structure of the compound in solution. The structure shown below (numbered **13** to distinguish it from the solid state structure) is proposed for

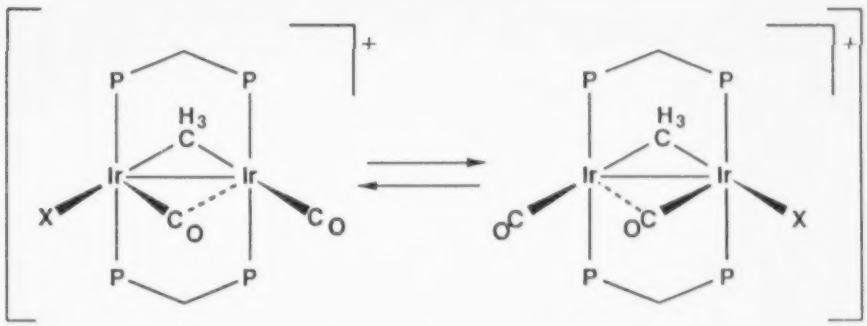

13 ($X = OSO_2CF_3$)

the compound in solution. It is suggested that a fluxional process such as that shown below accounts for the observed NMR spectroscopic results. This process is slow on the NMR time scale at -80 °C such that two different phosphorus environments are distinguishable. The high resolution of the methyl resonance at room temperature and -40 °C supports the presumption that movement of the methyl ligand is not part of the fluxional process.

It is not clear why ligand loss from **2** should stabilize a methyl product; one would expect that creating a vacant coordination site by the abstraction of a ligand would rather favor a methylene-hydride product. In addition the removal of a π-withdrawing CO group should stablize the higher oxidation state, methylene-hydride species.

Preliminary studies of the reactivity of compound **13** indicate that its reactions with phosphines, CO, ethylene and ^{t}BuNC give the same products

as those given by compound **2** with the same reagents, as shown in Scheme 3.5. Thus compound **13** reacts with CO to yield **2**, which reacts further with CO to give a mixture of compounds **4** and **7**, as shown in Schemes 3.5 and 3.3, in a typical ratio of 6:1 (the ratio depends on the quantity of CO added to **13**). This shows that the formation of **13** from **2** is a reversible process. The reaction of **13** with PMe_2Ph yields **5c**, while with ^tBuNC it yields compound **10**. The formation of compounds **5c** and **10** from **13** are rare examples of the facile activation, at room temperature, of one of the C-H bonds of a coordinated methyl group by an adjacent metal. Although a similar process occurred in the formation of compound **2** from $[Ir_2(CO)_3(dppm)_2]$ (**1**), the methyl complex was not observed in that case (vide supra).

Although the reaction of compound **13** with ethylene gives **11**, which is the same product obtained in the reaction of this gas with **2**, the route from **13** yields **11** as a pure product in less than 1 h, while the route from the tricarbonyl yields a mixture of compounds **11** and **2** (vide supra) even after 24 h. This is consistent with the fact that the reaction with **13** involves the substitution of a weakly coordinating triflate ligand, while that with compound **2** involves the substitution of a strongly bound CO ligand.

Reaction of compound **13** with SO_2 yields $[Ir_2(CO)_2(\mu\text{-}CH_3)(\mu\text{-}SO_2)\text{-}(dppm)_2][CF_3SO_3]$ (**14**). On the basis of preliminary NMR data obtained for compound **14**, and which are discussed below, the structure shown in Scheme 3.5 is proposed. At room temperature, the ^1H NMR spectrum shows the methyl resonance as a broad signal at δ -2.15, and the methylene proton resonances as multiplets at δ 4.50 and 3.94. The high-field shift of the methyl resonance suggests the presence of an agostic C-H-Ir interaction involving the methyl group.[41] Apparently a rapid exchange between the three methyl hydrogen nuclei renders them equivalent. At -40 °C the broad methyl

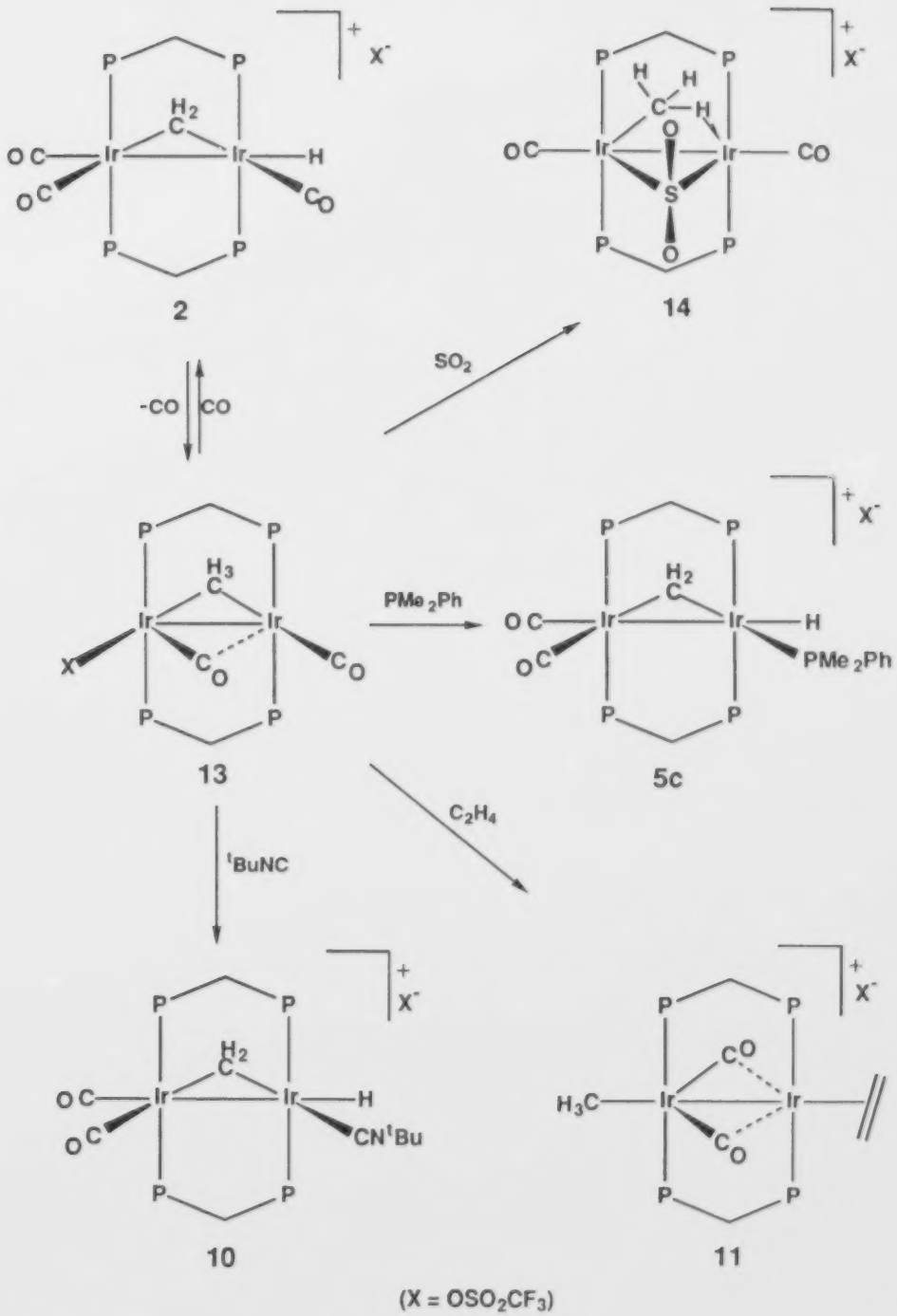

Scheme 3.5.

resonance widens considerably such that it spans a range of about 1.5 ppm in the ^1H NMR spectrum, while at -80 °C it blends into the baseline. The methylene resonances which remain reasonably well resolved at -40 °C broaden slightly at -80 °C. The $^{31}P\{^1H\}$ NMR spectrum at room temperature shows a singlet at δ -1.0, indicating that the four phosphorus nuclei are equivalent, presumably due to facile transfer of the methyl group from one metal to the other (presumably this exchange, together with that of the three methyl protons, accounts for the broadness of the methyl resonance in the ^1H NMR spectrum). At -40 °C the $^{31}P\{^1H\}$ spectrum still shows a singlet, at δ -1.6, while at -80 °C this signal broadens into a single, featureless resonance, centered at -1.9. Presumably the differences observed in the nature of the NMR signals at different temperatures result from slowing down of the methyl transfer between the two metals as the temperature is lowered. The $^{13}C\{^1H\}$ NMR spectrum at room temperature[44] shows a single CO resonance as a triplet at δ 170.8, indicating that the carbonyl carbon nuclei are equivalent. A full spectroscopic characterization of **14** is in progress, and efforts are being made to obtain crystals of this compound for an X-ray structure determination.

These transformations from terminal methyl, to symmetrically bridged methyl to asymmetrically bridged methyl, to C-H activation products, are among the most important results obtained in this study. Most of the binuclear compounds reported, which have a bridging methyl group, have it in an unsymmetrically bridging orientation, being terminally-bound to one metal center and engaging in an agostic interaction with the other,[41] a similar coordination mode to that in **14**. Furthermore, the successful syntheses of the two methyl-bridged complexes, **13** and **14**, fulfill one of the goals of this study, which was to prepare such methyl-bridged complexes.

(d) Hydrides and Reductive Elimination of Methane. Lastly, reactions of compound **2** with CF_3SO_3H, HCl and H_2 were carried out, in order to establish pathways for possible binuclear reductive elimination processes. The reaction of **2** with CF_3SO_3H results in methane loss to give $[Ir_2(CO)_3(OSO_2CF_3)(dppm)_2][CF_3SO_3]$ (**15**). The ^1H NMR spectrum of compound **15** shows only multiplets due to the dppm methylene protons at δ 5.40 and 5.35, apart from signals due to the phenyl group protons. The $^{13}C\{^1H\}$ NMR spectrum shows a multiplet at δ 168.9 and two broad resonances at δ 168.7 and 165.0, indicating the presence of three CO ligands, and this together with the CO stretches at 2023, 2004 and 1964 cm^{-1} in the IR spectrum, indicates that all the carbonyl ligands are terminally bound. The IR spectrum also shows stretches at 1323, 1272, 1260 and 1161 cm^{-1}, due to the triflate groups, suggesting that one of them is coordinated to one of the Ir centers (the stretch at 1323 cm^{-1} is typical of a coordinated triflate[39]). This is confirmed by conductivity measurements on compound **15**, in nitromethane, which show that it is a 1:1 electrolyte (Λ (10^{-3}M) = 107.6 $\Omega^{-1}cm^2mol^{-1}$).[45]

This reaction of compound **2** with CF_3SO_3H, contrasts with that of $[RhIr(CH_3)(CO)_3(dppm)_2][CF_3SO_3]$, as described in Chapter 2, which gives a stable methyl hydride product,[1] and can be rationalized by considering the site of protonation in both instances. The difference between the reactive intermediate in reactions with **2**, compound **3** (as explained later, under conclusions), and $[RhIr(CH_3)(CO)_3(dppm)_2][CF_3SO_3]$, is the position of the methyl ligand. In the 'RhIr' compound, this ligand is remote from the most likely sites of protonation (the Rh-Ir bond or the d_{z^2} orbital on Rh), while the same ligand in the diiridium compound is adjacent to these sites. Thus protonation of compound **2** could easily give rise to a cis arrangement of the methyl and hydride ligands, leading to reductive elimination of methane (as

shown in Scheme 3.6), while protonation of $[RhIr(CH_3)(CO)_3(dppm)_2]$-$[CF_3SO_3]$ results in a trans orientation of the hydrido and methyl ligands.[23] As discussed in Chapter 2, hydride rearrangement in this 'RhIr' compound is not facile, hence a cis arrangement, as required for reductive elimination, does not occur.

In a related reaction to that with CF_3SO_3H, compound **2** reacts with 1 equiv of HCl, eliminating methane, to give the known complex, $[Ir_2(CO)_2(\mu$-$CO)(\mu$-$Cl)(dppm)_2]^+$ (**16**).[46] Again this contrasts with the 'RhIr' system in which the stable hydrido-methyl product, $[RhIr(CH_3)(CO)_2(\mu$-$H)(\mu$-$Cl)$-$(dppm)_2][CF_3SO_3]$,[23] was obtained, and these results again appear to be consistent with the sites of protonation proposed above for the diiridium and 'RhIr' systems.

Compound **2** behaves in a similar way to $[RhIr(CH_3)(CO)_3(dppm)_2]$-$[CF_3SO_3]$ in its reaction with H_2,[23] resulting in CO and methane loss to give the known trihydride species, $[Ir_2(H)(CO)_2(\mu$-$H)_2(dppm)_2]^+$ (**20**),[2] the diiridium analogue of the 'RhIr' product.[23] However in contrast to the 'RhIr' product, compound **20** reacts further with H_2 to give $[Ir_2(H)_4(CO)_2(\mu$-$H)(dppm)_2][CF_3SO_3]$ (**21**), which is isolated under a stream of H_2. The $^{31}P\{^1H\}$ NMR spectrum of compound **21** shows a singlet resonance (δ -6.5 at -80 °C), due to four chemically equivalent phosphorus nuclei. The hydride region of the ^1H NMR spectrum of compound **21**, over a series of temperatures, is shown in Figure 3.6. At -80 °C it shows three broad resonances at δ -10.72, -12.90 and -16.31 with intensity ratios of 2:2:1. As the temperature is raised, the two relatively high-field resonances broaden significantly; at 25 °C the signal due to the single hydrogen blends into the baseline. Apparently the extreme broadening of the hydride resonances at -40 °C and 25 °C is due to fluxional processes occurring in compound **21** at these temperatures, but the

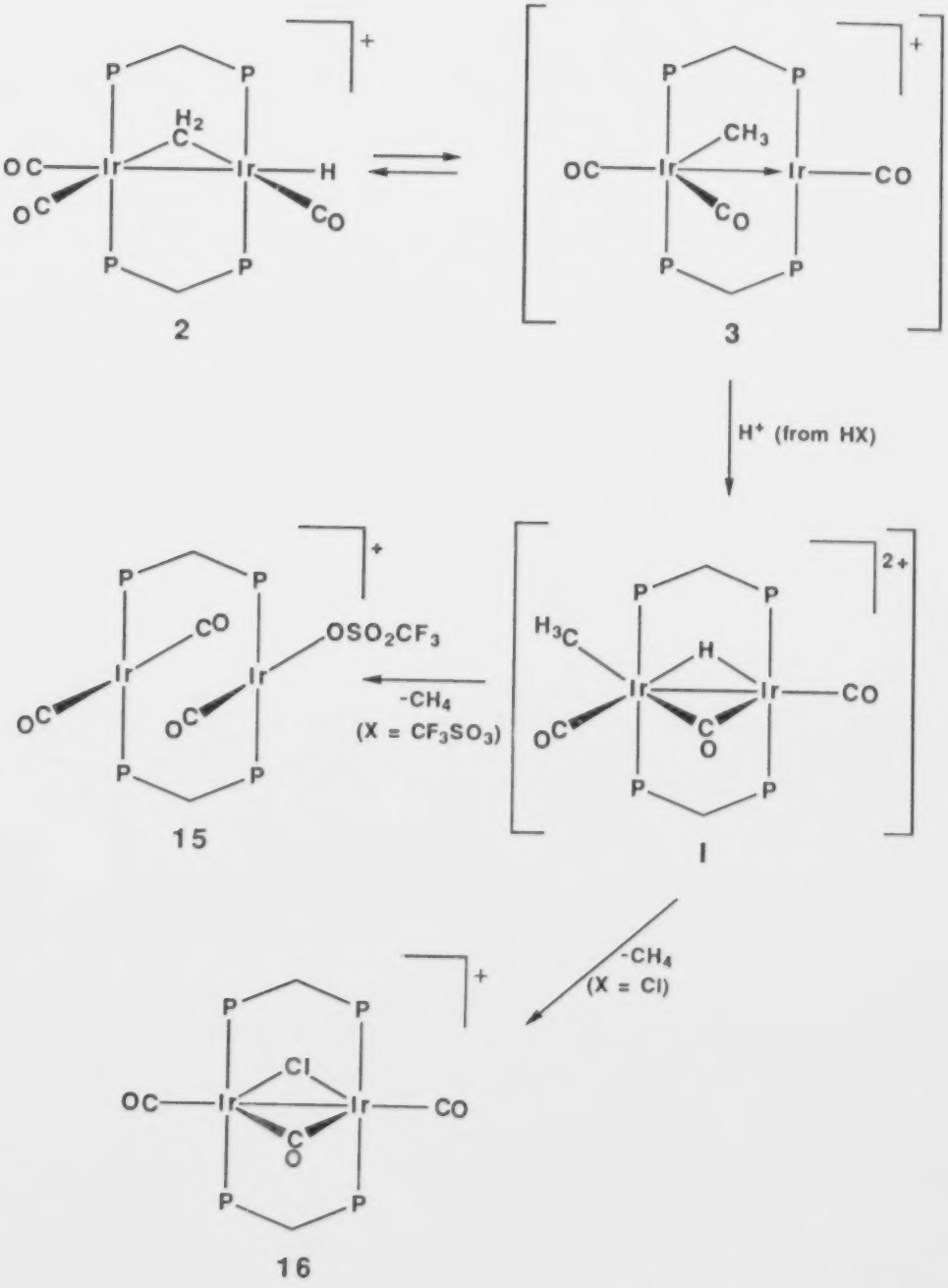

Scheme 3.6

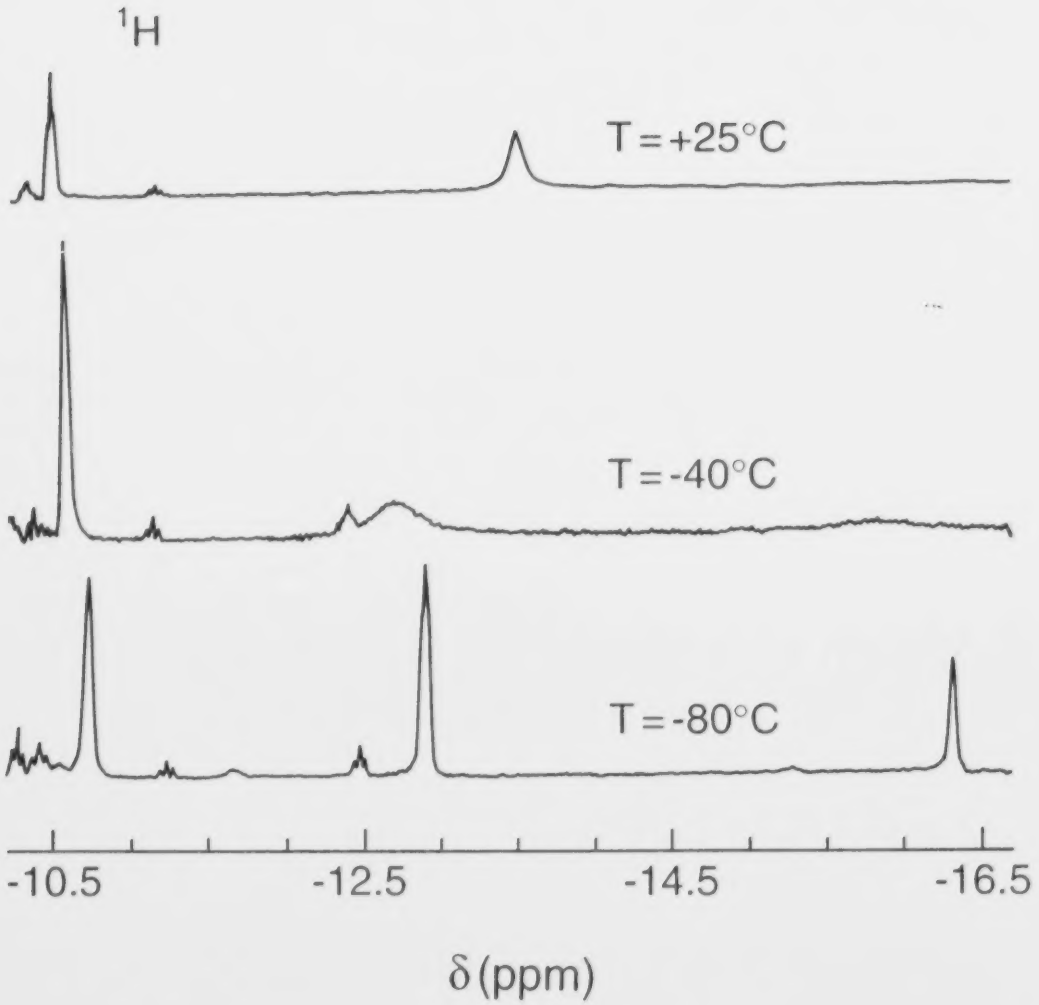

Figure 3.6. Hydride region of the ^{1}H NMR spectra of compound **21** at temperatures between -80 °C and 25 °C.

nature of these processes is not certain, considering that at 25 °C it results in four equivalent dppm methylene protons, which give rise to a single resonance at δ 4.78 (at -80 and -40 °C the ^1H NMR spectrum shows two methylene resonances).

Compound **21** has very similar spectroscopic parameters to those of the previously reported complex, $[Ir_2(H)_4(CO)_2(\mu\text{-}Cl)(dppm)_2][BF_4]$,[4] except that the bridging hydride in **21** is replaced by a bridging chloride ligand in the latter compound, and a similar structure to that proposed for the chloro compound is proposed for compound **21** (see Scheme 3.7). This compound was previously erroneously proposed to be a tetrahydride complex,[2] presumably because the fifth hydride resonance was not visible at the temperature of the NMR experiment.

In contrast to the reaction of H_2 with $[RhIr(CH_3)(CO)_3(dppm)_2][CF_3SO_3]$,[23] in which only the final product was observed, it was possible to characterize a number of solution intermediates in the reaction with compound **2**, depending on the experimental conditions. When H_2 gas is passed through a solution of compound **2** in CD_2Cl_2, in an NMR tube, and the NMR spectra of the mixture are obtained immediately, the major product obtained is $[Ir_2(H)_3(CO)_3(dppm)_2][CF_3SO_3]$ (**19**), together with compound **21** and small amounts of compound **20**, and the known species, $[Ir_2(CO)_2(\mu\text{-}H)(\mu\text{-}CO)(dppm)_2]^+$ (**18**).[8] Quenching the reaction by immersing the NMR tube in a dry-ice/acetone mixture, immediately after adding the gas, and until the NMR spectra are obtained, leads to the observation of $[Ir_2(H)_2(CH_3)(CO)_3(dppm)_2][CF_3SO_3]$ (**17**), together with compound **19** and small amounts of compounds **20**, **21** and **18**. A typical ratio of the compounds observed in this case is 29 : 16 : 2 : 2 : 1 for compound **19** : **17**: **20** : **21** : **18**, respectively. After standing at room temperature for about 5 min, there is a

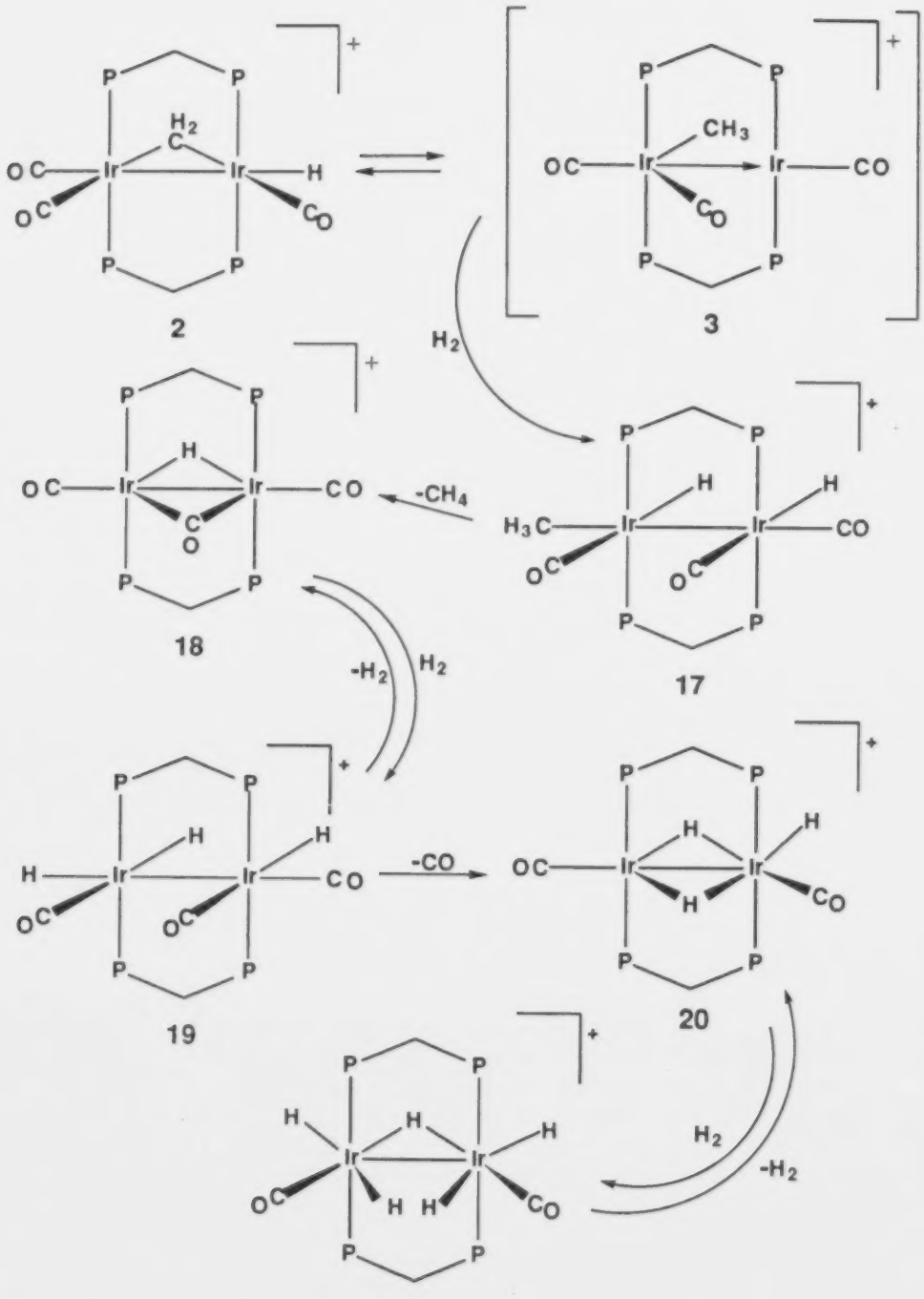

Scheme 3.7

observed in this case is 29 : 16 : 2 : 2 : 1 for compound **19** : **17**: **20** : **21** : **18**, respectively. After standing at room temperature for about 5 min, there is a substantial increase in the proportion of compound **19**, with an accompanying decrease in that of **17** in the reaction mixture. Furthermore, after standing for about 2 h at room temperature, compound **17** disappears and there is a substantial increase in the proportions of compounds **20** and **21**, accompanied by a slight decrease in those of **18** and **19**. Other experiments showed that the reaction does not occur at temperatures slightly below room temperature, and earlier work had shown that the reaction of compound **18** with H_2 gave compound **20**.[2]

The ^1H NMR spectrum of compound **17** shows the methyl resonance as a triplet at δ -0.42 together with two hydride resonances that appear as triplets at δ -9.43 and -10.81. Selective ^{31}P-decoupling experiments indicate that the methyl group is bound to the same metal as one of the hydrides, while the second hydride ligand is bound to the other metal. The $^{13}C\{^1H\}$ NMR spectrum shows two broad singlets at δ 181.3 and 157.0 with intensity ratios of 2:1, indicating that there are three carbonyl ligands in **17** (it appears that the chemical shifts of two of the CO ligands are coincidentally equivalent). All these NMR data are consistent with the structure of **17** shown in Scheme 3.7.

The ^1H NMR spectrum of compound **19** shows three triplets of equal intensity at δ -10.25, -10.40, and -12.48 in the hydride region, and selective ^{31}P-decoupling experiments show that two of the hydrides are bound to one Ir center while the third one is bound to the other Ir. The $^{13}C\{^1H\}$ NMR spectrum shows three broad singlets at δ 180.4, 179.6 and 155.2, indicating the presence of three terminal CO ligands in **19** (the chemical shifts are not sufficiently low-field for bridging carbonyl groups).

On the basis of the intermediates characterized, and all the observations made in these reactions with H_2, the reaction sequence shown in Scheme 3.7 is proposed. Apparently there is oxidative addition of H_2 to the unsaturated Ir center in compound **3** (as explained later under conclusions), with subsequent hydride migration to yield compound **17**. The latter compound loses methane, undergoing rearrangement of the ligands to give **18**, which oxidatively adds another molecule of H_2 to give **19**. Compound **19** loses CO to give **20** which forms compound **21** in the presence of H_2, while **21** loses H_2 under vacuum to give **20**.

Conclusions

Electrophilic attack of the homobinuclear complex $[Ir_2(CO)_3(dppm)_2]$ by CH_3^+ does not yield the expected methyl complex, analogous to $[RhIr(CH_3)(CO)_3(dppm)_2][CF_3SO_3]$. Instead the complex, $[Ir_2(H)(CO)_3(\mu\text{-}CH_2)(dppm)_2][CF_3SO_3]$ (**2**), the rare result of C-H activation of the methyl group by an adjacent metal, is obtained. This C-H activation process is reversible and is unusually facile.

All the reactions of compound **2** can be grouped into the following categories:

- incorporation of the new ligand, accompanied by migratory insertion of the hydride ligand onto the CH_2 ligand to give a terminal CH_3 ligand (reactions with CO and SO_2);
- CO loss accompanied by migratory insertion of the hydride ligand onto the CH_2 ligand (reaction with Me_3NO);
- substitution of one CO by the new ligand accompanied by migratory insertion of the hydride ligand onto the CH_2 ligand

(reactions with ethylene and 1,2-propadiene);

- substitution of one CO by the new ligand but with retention of the methylene hydride structure (reactions with phosphines, $P(OPh)_3$ and ^tBuNC);
- oxidative addition of (reaction with HCl and H_2) or electrophilic attack by (reaction with CF_3SO_3H) the reagent, accompanied by migratory insertion of the hydride ligand onto the CH_2 ligand with methane loss, and with or without CO loss.

In spite of these reactivity differences, it is suggested that all the reactions of **2** proceed through the initial formation of the methyl intermediate, $[Ir_2(CH_3)(CO)_3(dppm)_2][CF_3SO_3]$ (**3**) (having a coordinatively unsaturated Ir center), followed by attack and incorporation, or oxidative addition, of the incoming ligand or reagent at the coordinatively unsaturated metal center (apart from the protonation reactions that do not need a coordinatively unsaturated metal center as explained earlier). The resulting product then undergoes one of the following processes: (i) ligand rearrangement accompanied by either the coordination of a second ligand (e.g. reaction with CO), CO loss (e.g. reaction with ethylene), or methane loss (and the coordination of the anion as in the reactions with HCl and CF_3SO_3H), (ii) CO loss accompanied by C-H activation of the methyl group to give a methylene-hydride complex (reactions with phosphines and ^tBuNC), or (iii) in the case of the reaction with H_2, ligand rearrangement accompanied by methane and CO loss, as well as the oxidative addition of two additional molecules of H_2. Only the reaction of compound **2** (as well as **8**) with CO results in migratory insertion of a methyl group to a CO ligand.

The subsequent C-H activation that occurs in reactions with phosphines, triphenylphosphite and ^tBuNC, after attack of the reagents on

the coordinatively unsaturated metal center in **3**, and the accompanying CO loss, are consistent with the fact that on coordination, these ligands have weaker π-accepting properties than CO, giving rise to increased electron density at the metal centers (compared to that in **3**), and thereby favor oxidative addition (C-H activation in this case) to these centers. In this light C_2H_4 appears to be a better π-acceptor than CO, in its reaction with **2**, giving a stable methyl product as opposed to a hydrido-methylene product.

Although the reactions of **2** and those of the mixed-metal analogue, $[RhIr(CH_3)(CO)_3(dppm)_2][CF_3SO_3]$,[23] show many similarities, there are some notable differences. Some of these differences are consistent with known differences in Rh and Ir chemistry, such as the strong preference of Rh for a square planar Rh(I) orientation, the greater electron richness of Ir, the greater tendency of Rh alkyls to undergo insertion, and the fact that Ir forms stronger M-C and M-H bonds than Rh. However, other differences remain unexplained. For example, it is not clear why compound **2** and the 'RhIr' analogue react with C_2H_4 to give products that have the methyl group on the saturated metal in one case but on the unsaturated metal in the other.

Apparently the formation of stronger M-C and M-H bonds by Ir, compared to Rh, allows the characterization of intermediates in the reaction of **2** with H_2, on the basis of which a reaction pathway was proposed. No intermediates could be characterized in a similar reaction with $[RhIr(CH_3)(CO)_3(dppm)_2][CF_3SO_3]$,[23] in which the Rh-H and Rh-C bonds are weaker and more labile. Although both metals are involved in the migratory insertion of the hydride ligand onto the CH_2 ligand in **2** to give the intermediate complex, **3**, as well as in some of the other steps of the reaction sequence, the structure of $[Ir_2(H)_2(CH_3)(CO)_3(dppm)_2][CF_3SO_3]$ (**17**) suggests that the reductive elimination of methane from this compound takes place

from one metal center. However, whether the reductive elimination of H_2 from $[Ir_2(H)_4(CO)_2(\mu\text{-}H)(dppm)_2][CF_3SO_3]$ (**21**) to give $[Ir_2(H)(CO)_2(\mu\text{-}H)_2(dppm)]^+$ (**20**) takes place from one metal center or not cannot be unequivocally established on the basis of the structures of these two compounds.

The transformation of compound **3** to $[Ir_2(CO)_2(\mu\text{-}CH_3)(OSO_2CF_3)(dppm)_2]$ (**13**), and the transformation of the latter compound to $[Ir_2(H)(CO)_2(PMe_2Ph)(\mu\text{-}CH_2)(dppm)_2][CF_3SO_3]$ (**5c**) (or $[Ir_2(H)(CO)_2(^tBuNC)(\mu\text{-}CH_2)(dppm)_2][CF_3SO_3]$ (**10**)), represent a very rare case of a terminal methyl-to-bridging methyl-to-methylene-hydride transformation, while that from **3** to **13**, and **13** to $[Ir_2(CO)_2(\mu\text{-}CH_3)(\mu\text{-}SO_2)(dppm)_2][CF_3SO_3]$ (**14**) represents an interesting case of a terminal methyl-to-symmetrically bridging methyl-to agostic methyl sequence (assuming that **3** is a terminal methyl complex). These observations confirm our initial belief that such transformations should be possible by fine-tuning the electron-density at the metals, by means of varying the ancillary ligands. Furthermore, the formation of the symmetrically bridging methyl complex, **13**, is a very important result, since, as mentioned earlier, such compounds are very rare. Also, the successful syntheses of compounds **13** and **14**, fulfill one of the goals of this study, which was to prepare such methyl-bridged complexes.

References and Footnotes

1. Antwi-Nsiah, F.; Cowie, M. *Organometallics* **1992**, *11*, 3157.
2. McDonald, R.; Sutherland, B. R.; Cowie, M. *Inorg. Chem.* **1987**, *26*, 3333.
3. McDonald, R.; Cowie, M. *Inorg. Chem.* **1990**, *29*, 1564.
4. Vaartstra, B. A.; Cowie, M. *Inorg. Chem.* **1989**, *28*, 3138.
5. (a) Kubiak, C. P.; Woodcock, C.; Eisenberg, R. *Inorg.Chem.* **1982**, *21*, 2119.
   (b) Kubiak, C. P.; Eisenberg, R. *J. Am. Chem. Soc.* **1980**, *102*, 3637.
6. (a) Vaartstra, B. A. Ph.D. Thesis, University of Alberta, 1989, Chapter 6.
   (b) Vaartstra, B. A.; Cowie, M. *Organometallics* **1990**, *9*, 1594.
7. Sutherland, B. R.; Cowie, M. *Organometallics* **1985**, *4*, 1801.
8. Sutherland, B. R.; Cowie, M. *Organometallics* **1985**, *4*, 1637.
9. See also: Crabtree, R. H.; Felkin, H.; Morris, G. E.; King, T. J.; Richards, J. A. *J. Organomet. Chem.* **1976**, *113*, C7.
10. Microanalysis was not done since **5b** is always contaminated with *ca.* 20% starting material, **2**.
11. Microanalyses carried out on compound **10** consistently yielded low percentages C and H, because it is very air sensitive. The color of the compound changes from green to brown in the time time taken to carry out the analysis.
12. Bodenhausen, G.; Freeman, R.; Morris, G. A. *J. Magn. Reson.* **1976**, *23*, 171.
13. (a) Herrmann, W. A. *Adv. Organomet. Chem.* **1982**, *20*, 159.
    (b) Puddephatt, R. J. *Polyhedron* **1988**, *7*, 767.
14. (a) Calvert, R. B., Shapley, J. R. *J. Am. Chem. Soc.* **1977**, *99*, 5225.
    (b) Chetcuti, M. J.; Grant, B. E. *Organometallics* **1990**, *9*, 1345.
15. All NMR signals have the appropriate ratios of intensity.

16. Compound **3** could have either a terminally bound or a bridging methyl ligand.

17. Schmidt, G. F.; Muetterties, E. L.; Beno, M. A.; Williams, J. M. *Proc. Natl. Acad. Sci. USA* **1981**, *78*, 1318.

18. Jacobsen, E. N.; Goldberg, K. I.; Bergman, R. G. *J. Am. Chem. Soc.* **1988**, *110*, 3706.

19. Dr. R. E. D. McClung is acknowledged for carrying out these simulations.

20. Muhandiram, D. R.; McClung, R. E. D. *J. Magn. Reson.* **1987**, *71*, 187.

21. Kegley, S. E.; Pinhas, A. R. *Problems and Solutions in Organometallic Chemistry;* University Science books: Mill Valley, CA, 1986, p 25.

22. Error limits are based on the standard deviations of the calculated slope and intercept of a least-square fit to the Eyring plot.

23. See Chapter 2 of this thesis and ref 1.

24. (a) Pearson, R. G. *Chem. Rev.* **1985**, *85*, 41. (b) Collman, J. P.; Hegedus, L. S.; Norton, J. R.; Finke, R. G. *Principles and Applications of Organotransition Metal Chemistry;* University Science Books: Mill Valley, CA, 1987, pp 82, 148 and 371, and references therein.

25. See, for example: (a) McDonald, R.; Cowie, M. *Organometallics* **1990**, *9*, 2468 and ref 3.

26. NMR signals for products that are obtained as mixtures are taken from the spectra of the mixtures.

27. See, for example: (a) Flood, T. C.; Bitler, S. P. *J. Am. Chem. Soc.* **1984**, *106*, 6076. (b) Watson, P. L. *J. Am. Chem. Soc.* **1982**, *104*, 337. (c) Evitt, E. R.; Bergman, R. G. *J. Am. Chem. Soc.* **1979**, *101*, 3973.

28. (a) Summer, C. E., Jr.; Riley, P. E.; Davis, R. E.; Pettit, R. *J. Am. Chem. Soc.* **1980**, *102*, 1752. (b) Motyl, K. M.; Norton, J. R.; Schauer, C. K.; Anderson,

O. P. *J. Am. Chem. Soc.* **1982**, *104*, 7325.

29. Hostetler, M. J.; Bergman, R. G. *J. Am. Chem. Soc.* **1990**, *112*, 8621.
30. (a) Mils, S. L.; Mils, D. L.; Bau, R.; Flood, T. C. *J. Am. Chem. Soc.* **1978**, *100*, 7278. (b) Attig, T. G.; Teller, R. G.; Wu, S. -M.; Bau, R.; Wojcicki, A. *J. Am. Chem. Soc.* **1979**, *101*, 619. (c) Wojcicki, A. *Adv. Organomet. Chem.* **1974**, *12*, 31. (d) Wojcicki, A. *Acc. Chem. Res.* **1971**, *4*, 344.
31. Oke, O.; Cowie, M. unpublished work.
32. McDonald, R. Ph.D. Thesis, University of Alberta, 1991, Chapter 2.
33. See, for example: (a) Uson, R.; Fornies, J.; Espinet, P.; Fortuno, C. *J. Chem. Soc., Dalton Trans.* **1986**, 1849. (b) Cowie, M.; Dickson, R. S.; Hames B. W. *Organometallics* **1984**, *3*, 1879. (c) Kubas, G. J. *Inorg. Chem.* **1979**, *18*, 182. (d) Dwight, S. K.; Cowie, M. *Inorg. Chim. Acta* **1978**, *31*, L407. (e) Mingos, D. M. P. *Transition Met. Chem.* **1978**, *3*, 1. (f) Benner, L. S.; Olmstead, M. M.; Hope, H.; Balch, A. L. *J. Organomet. Chem.* **1978**, *153*, C81. (g) Angoletta, M.; Malatesta, L.; Caglio, G. *J. Chem. Soc., Dalton Trans.* **1977**, 2131. (h) Angoletta, M.; Bellon, P. L.; Manassero, M.; Sansoni, M. *J. Organomet. Chem.* **1974**, *81*, C40. (i) Churchill, M. R.; Krishan, L. K. *Inorg. Chem.* **1973**, *12*, 1650. (j) Churchill, M. R.; DeBoer, B. G.; Kalra, K. L. *Inorg. Chem.* **1973**, *12*, 1646. (k) Churchill, M. R.; DeBoer, B. G.; Kalra, K. L.; Reich-Rohrwig, P.; Wojcicki, A. *J. Chem. Soc., Chem. Commun.* **1972**, 981.
34. Lukehart, C. *Fundamental Transition Metal Organometallic Chemistry;* Brooks/Cole Publishing Company: Belmont, CA, 1985, p 77.
35. See, for example: (a) Xiao, J.; Cowie, M. *Organometallics* **1993**, *12*, 463. (b) Antonelli, D. M.; Cowie, M. *Organometallics* **1991**, *10*, 2550. (c) Hilts, R. W.; Franchuk, R. A.; Cowie, M. *Organometallics* **1991**, *10*, 1297.
36. Huheey, J. E.; Keiter, E. A.; Keiter, R. L. *Inorganic Chemistry: Principles of*

Structure and Reactivity, 4th ed.; Harpercollins College Publishers: New York, 1993.

37. Fanizzi, F. P.; Maresca, L.; Natile, G.; Lanfranchi, M.; Tiripicchio, A.; Pacchioni, G. *J. Chem. Soc., Chem. Commun.* **1992**, 333.
38. Chacon, S. T.; Chisholm, M. H.; Folting, K.; Huffman, J. C.; Hampden-Smith, M. J.*Organometallics* **1991**, *10*, 3722.
39. (a) Lawrence, G. A. *Chem. Rev.* **1986**, *86*, 17. (b) Schweibert, K. E.; Stryker,J. M. *Organometallics* **1993**, *12*, 600. (c) Stang, P. J.; Huang, Y.; Arif, A. M. *Organometallics* **1992**, *11*, 231. (d) Buzinkai, J. F.; Schrock, R. R. *Inorg. Chem.* **1989**, 28, 2837.
40. Torkelson, J.; Cowie, M. unpublished work.
41. Brookhart, M.; Green, M. L. H. *J. Organomet. Chem.* **1983**, 250, 395.
42. Calvert, R. B., Shapley, J. R. *J. Am. Chem. Soc.* **1978**, *100*, 7726.
43. Reinking, M. K.; Fanwick, P. E.; Kubiak, C. P. *Angew. Chem. Int. Ed. Eng.* **1989**, *28*, 1377.
44. The $^{13}C\{^1H\}$ NMR spectra for compound **14** at -40 and -80 °C each show a single resonance for the two CO ligands although the signal is very broad.
45. Geary, W. J. *Coord. Chem. Rev.* **1971**, *7*, 81.
46. Sutherland, B. R.; Cowie, M. *Inorg. Chem.* **1984**, *23*, 2324.

Chapter 4

The Reactions of $[Ir_2(H)(CO)_3(\mu\text{-}CH_2)(dppm)_2[CF_3SO_3]$ and $[RhIr(CH_3)(CO)_3(dppm)_2][CF_3SO_3]$ with Alkynes.

Introduction

The simple alkyne molecule can display a wealth of chemistry in its reactivity with transition metal complexes. Not only can the molecule bind in the η^2 fashion, in which it can function as either a 2 or 4 electron donor, but it can also undergo a variety of transformations, yielding acetylide[1] or vinylidene[2] ligands, as well as products of alkyne condensation with other substrates,[3] CO insertion into the M-C (coordinated alkyne) bonds[3a,4] or alkyne coupling.[3a,4d,5] Binuclear complexes add an additional variety to the chemistry of alkyne molecules since in addition to the above chemistry at either one of the metal centers, the involvement of a bridging mode is now possible, in which the alkyne orients itself either parallel or perpendicular to the metal-metal axis. Furthermore, in cases where the transition metal complex is an alkyl or hydrido complex, there is the added possibility of insertion of the alkyne into the M-C (alkyl)[6] or M-H bond,[7] giving vinyl products. Also, alkyne insertion into other M-heteroatom bonds have been observed in certain instances.[8]

In Chapters 2 and 3, the reactivities of the complexes, $[RhIr(CH_3)(CO)_3(dppm)_2][CF_3SO_3]$ (**1**) and $[Ir_2(H)(CO)_3(\mu\text{-}CH_2)(dppm)_2][CF_3SO_3]$ (**2**) with a variety of small molecules were reported. Since the possibility of insertion of unsaturated hydrocarbons into M-C (alkyl) bonds, leading to the formation of C-C bonds, was of interest to this research group, the reactions of compounds

1 and **2** with ethylene, 1,2-propadiene (allene) and a number of alkynes were undertaken. Furthermore, the products formed in the reactions of these two compounds with alkynes was of interest, in light of the variety of products that can be obtained in reactions with these unsaturated hydrocarbons. The results of the reactions with ethylene and allene were discussed in the two previous chapters, in which it was shown that no insertion products were formed. In this chapter the results of the reactions with alkynes are reported.

Experimental Section

General experimental conditions were as described in Chapter 2. Acetylene gas was obtained from Matheson, while ^{13}C-labelled acetylene was purchased from Cambridge Isotopes. Dimethyl acetylenedicarboxylate (DMAD) and phenylacetylene were purchased from Aldrich, and the compounds, $[RhIr(CH_3)(CO)_3(dppm)_2][CF_3SO_3]$(**1**) and $[Ir_2(H)(CO)_3(\mu\text{-}CH_2)\text{-}(dppm)_2][CF_3SO_3]$ (**2**), were prepared as reported in Chapters 2. and 3 Spectroscopic parameters for the compounds prepared are found in Tables 4.1 and 4.2.

Preparation of Compounds. (a) $[Ir_2(CH_3)(CO)_3(\mu\text{-}C{=}CH_2)(dppm)_2]\text{-}[CF_3SO_3]$ (4). The compound, $[Ir_2(H)(CO)_3(\mu\text{-}CH_2)(dppm)_2][CF_3SO_3]$ (**2**) (60 mg, 0.043 mmol) was dissolved in 7 mL of CH_2Cl_2 in a round-bottomed flask. The solution was then cooled to -78 °C, by immersing the flask in a dry-ice/acetone bath. Acetylene was then passed through the solution for 1 min, after which the mixture was stirred under a static atmosphere of the gas for 30 min at -78 °C, and then warmed to room temperature . After stirring the solution for 2 h at this temperature, during which time the color changed

Table 4.1 $^{31}P\{^1H\}$ and ^1H NMR Spectroscopic Data[a]

Compound	$\delta(^{31}P\{^1H\})^b$	$\delta(^1H)^{c,e}$
$[Ir_2(CH_3)(CO)_3(\mu\text{-}C_2H_2)((dppm)_2][CF_3SO_3]$ **(3)**	11.4 (m), -19.9 (m)	10.25 (m, 1H), 9.15(m, 1H), 4.20 (m, 2H), 3.18 (m, 2H), -0.14 (b, 3H)
$[Ir_2(CH_3)(CO)_3(\mu\text{-}C{=}CH_2)(dppm)_2][CF_3SO_3]$ **(4)**	-1.0 (m), -6.5 (m)	6.40 (s, 1H), 5.72 (s, 1H), 3.90 (m, 2H), 2.93 (m, 2H), -0.55 (t, 3H)
$[Ir_2(H)(CH_3)(CO)_3(\mu\text{-}\eta^1{:}\eta^2\text{-}C{\equiv}CH)(dppm)_2][CF_3SO_3]$ **(5)**	-13.1 (m), -26.8 (m)	8.06 (b, 1H), 4.67 (m, 2H), 4.03 (m, 2H), -0.40 (t, 3H), -9.83 (m, 1H)
$[Ir_2(CH_3)(CO)_2(PMe_3)(\mu\text{-}C{=}CH_2)(dppm)_2][CF_3SO_3]$ **(6)**[d]	-12.6 (m), -19.3 (m), -76.9 (b)	6.49 (b, 2H), 6.10 (d, b, 2H), $^4J_{P\text{-}H}$ = 9.0 Hz), 0.01 (t, 3H)

Table 4.1 (continued)

Compound	$\delta(^{31}P\{^1H\})^b$	$\delta(^1H)^{c,e}$
$[Ir_2(CH_3)(CO)_3(\mu\text{-}PhC_2H)(dppm)_2][CF_3SO_3]$ (7)	13.8 (m), -21.6 (m)	9.51 (m, 1H), 4.08 (m, 2H), 3.08 (m, 2H), 0.02 (b, 3H)
$[Ir_2(CH_3)(CO)_3(\mu\text{-}C{=}CPh(H))(dppm)_2][CF_3SO_3]$ (8)	-2.6 (m), -8.0 (m)	3.91 (m, 2H), 2.70 (m, 2H), -0.58 (t, 3H)
$[RhIr(CH_3)(CO)_3(\mu\text{-}C_2H_2)(dppm)_2][CF_3SO_3]$ (9)	22.1 (dm, $^1J_{Rh\text{-}P}$ = 151.1 Hz), -0.3 (m)	9.12 (dt, $^2J_{Rh\text{-}H}$ = 6.4 Hz, 1H), 7.63 (m, 2H), 4.35 (m, 2H), 2.83 (m, 2H), -1.00 (t, 3H)
$[RhIr(CH_3)(CO)_3(HC{=}C(H)P(Ph_2)CH_2PPh_2)(dppm)_2]$-$[CF_3SO_3]$ (10)	29.9 (m), 18.1 (ddd, $^1J_{Rh\text{-}P}$ = 152 Hz), -11.7 (m), -22.6 (m)	8.58 (t, 1H), 5.60 (dm, $^3J_{P\text{-}H}$ = 40.0 Hz, 1H), 4.12 (m, 1H), 3.95 (m, 1H), 3.72 (m, 1H), 2.88 (m, 1H), 0.46 (t, 3H)
$[RhIr(\mu\text{-}\eta^1{:}\eta^2\text{-}C{\equiv}CPh)(CO)_3(dppm)_2][CF_3SO_3]$ (11)^d	26.6 (dm, $^1J_{Rh\text{-}P}$ = 94.2 Hz), -6.0 (m)	3.82 (m, 2H), 3.32 (m, 2H)

Table 4.1 (continued)

Compound	$\delta(^{31}P\{^1H\})^b$	$\delta(^1H)^{c,e}$
$[RhIr(C{\equiv}CPh)_2(CO)_2(\mu\text{-}H)(dppm)_2][CF_3SO_3]$ **(12)**	24.1 (dm, $^1J_{Rh\text{-}P}$ = 106.1 Hz), -22.7 (m)	4.12 (m, 2H), 3.49 (m, 2H), -8.70 (dm, $^1J_{Rh\text{-}H}$ = 13.0 Hz, 1H)
$[RhIr(H)(CH_3)(CO)_3(\mu\text{-}\eta^1{:}\eta^2\text{-}C{\equiv}CPh)(dppm)_2][CF_3SO_3]$ **(13)**	24.2 (dm, $^1J_{Rh\text{-}P}$ = 102.7 Hz), -13.6 (m)	4.00 (m, 2H), 3.22 (m, 2H), 0.33 (t, 3H), -8.87 (t, 1H)
$[RhIr(CH_3)(CO)_3(C{=}CPh(H))(dppm)_2][CF_3SO_3]$ **(14)**[d]	20.1 (dm, $^1J_{Rh\text{-}P}$ = 123.3 Hz), -18.2 (m)	8.53 (t, 1H), 4.10 (m, 2H), 3.33 (m, 2H), 0.27 (b, 3H)
$[RhIr(RC{=}C(CH_3)R)(CO)_3(dppm)_2][CF_3SO_3]$ **(15)**[d] (R = CO_2Me)	16.8 (dm, $^1J_{Rh\text{-}P}$ = 119.9 Hz), -19.4 (m)	4.35 (m, 2H), 3.65(m, 2H), 3.33 (s, 3H, OCH_3), 2.22 (s, 3H, OCH_3), 0.81 (s, 3H, CH_3)
$[Ir_2(RC{=}C(CH_3)R)(CO)_3(dppm)_2][CF_3SO_3]$ **(16)**[d] (R = CO_2Me)	7.5 (m), -21.8 (m)	4.43 (m, 2H), 3.60 (m, 2H), 3.27 (s, 3H, OCH_3), 2.23 (s, 3H, OCH_3), 0.68 (s, 3H, CH_3)

Table 4.1 (continued)

Compound	$\delta(^{31}P\{^1H\})^b$	$\delta(^1H)^{c,e}$
$[Ir_2(CH_3)(CO)_3(\mu\text{-DMAD})(dppm)_2][CF_3SO_3]$ **(17)**	-10.7 (m), -28.9 (m)	4.78 (m, 2H), 4.25 (m, 2H), 3.45 (s, 3H, OCH_3), 2.13 (s, 3H, OCH_3), -0.52 (t, 3H, CH_3)

[a] Abbreviations used: s = singlet, d = doublet, t = triplet, m = multiplet, dt = doublet of triplets, dm = doublet of multiplets, b = broad, ddd = doublet of doublets of doublets. [b] Vs 85% H_3PO_4, -40 °C in CD_2Cl_2 unless otherwise stated. [c] Vs TMS, -40 °C in CD_2Cl_2 solvent unless otherwise stated. [d] NMR data at 25 °C. [e] Resonances for dppm phenyl group protons appear as multiplets in the range δ 6.90 - 8.10 for all compounds.

Table 4.2 Infrared and $^{13}C\{^1H\}$ NMR Spectroscopic Data

Compound	IR[b,c], cm^{-1}	$\delta(^{13}C\{^1H\})$[e]
$[Ir_2(CH_3)(CO)_3(\mu\text{-}C_2H_2)(dppm)_2][CF_3SO_3]$ (3)	2007 (s), 1970 (vs), 1911 (b), 1632 (med)[h]	198.7 (b, CO), 194.4 (t, CO), 181.3 (b, CO), 160.7 (dm, $^1J_{C\text{-}C}$ = 50.8 Hz), 147.1 (dm)
$[Ir_2(CH_3)(CO)_3(\mu\text{-}C{=}CH_2)(dppm)_2][CF_3SO_3]$ (4)	2004 (s), 1964 (vs), 1790 (s)	198.4 (dm, $^1J_{C_\alpha\text{-}C_\beta}$ = 67.0 Hz), 181.2 (b, CO), 175.1 (t, CO), 172.3 (t, CO), 123.5 (d, C_β)
$[Ir_2(H)(CH_3)(CO)_3(\mu\text{-}\eta^1{:}\eta^2\text{-}C{\equiv}CH)(dppm)_2][CF_3SO_3]$ (5)	-	181.8 (b, CO), 179.1 (b, CO), 154.7 (t, CO), 127.2 (dm, $\underline{C}{\equiv}CH$, $^1J_{C\text{-}C}$ = 55.3 Hz, $^2J_{P\text{-}C}$ = 13.6 Hz), 102.4 (dm, $C{\equiv}\underline{C}H$, $^2J_{P\text{-}C}$ = 11.2 Hz)
$[Ir_2(CH_3)(CO)_2(PMe_3)(\mu\text{-}C{=}CH_2)(dppm)_2][CF_3SO_3]$ (6)[d]	2010 (s), 1971 (vs)	184.3 (t, 1C), 183.8 (dt, $^2J_{P\text{-}C}$ = 15.0 Hz)
$[Ir_2(CH_3)(CO)_3(\mu\text{-}PhC_2H)(dppm)_2][CF_3SO_3]$ (7)	2011 (vs), 1970 (vs), 1785 (w), 1640 (s)[h]	198.7 (b, 1C), 191.5 (t, 1C), 182.9 (b, 1C)

Table 4.2 (continued)

Compound	IR[b,c], cm^{-1}	$\delta(^{13}C\{^1H\})$[e]
$[Ir_2(CH_3)(CO)_3(\mu\text{-}C{=}CPh(H))(dppm)_2][CF_3SO_3]$ (8)	1960 (vs), 1920 (sh), 1780 (s), 1655 (s)[h]	182.9 (b, 1C), 179.6 (t, 1C), 168.0 (t, 1C)
$[RhIr(CH_3)(CO)_3(\mu\text{-}C_2H_2)(dppm)_2][CF_3SO_3]$ (9)	-	210.2 (dt, $^1J_{Rh\text{-}C}$ = 19.0 Hz, CO), 191.0 (dt, $^1J_{Rh\text{-}C}$ = 55.3 Hz, CO), 172.8 (t, CO), 162.9 (dm, $^1J_{Rh\text{-}C}$ = 20.6 Hz), 147.0 (dm, $^1J_{C\text{-}C}$ = 53.0 Hz)
$[RhIr(CH_3)(CO)_3(HC{=}C(H)P(Ph_2)CH_2PPh_2)(dppm)_2]$-$[CF_3SO_3]$ (10)[d]	2056 (s), 2017 (vs), 1975 (s)	191.1 (dm, $^1J_{Rh\text{-}C}$ = 45.1 Hz, CO), 186.4 (dm, $^1J_{Rh\text{-}C}$ = 63.9 Hz, CO), 171.5 (m, CO), 42.1 (dm, $^1J_{Rh\text{-}C}$ = 8.4 Hz, $^1J_{C\text{-}C}$ = 36.5, C=<u>C</u>P) 33.1 (dm, $^1J_{Rh\text{-}C}$ = 11.8 Hz, Rh-<u>C</u>=C)
$[RhIr(\mu\text{-}\eta^1{:}\eta^2\text{-}C{\equiv}CPh)(CO)_3(dppm)_2][CF_3SO_3]$ (11)[f]	2000 (sh), 1955 (s), 1825 (m)	196.0 (dm, $^1J_{Rh\text{-}C}$ = 22.1 Hz, 1C), 194.6 (dt, $^1J_{Rh\text{-}C}$ = 80.3 Hz, 1C), 181.7 (t, 1C)

Table 4.2 (continued)

Compound	IR[b,c], cm^{-1}	$\delta(^{13}C\{^1H\})$[e]
$[RhIr(C{\equiv}CPh)_2(CO)_2(\mu\text{-}H)(dppm)_2][CF_3SO_3]$ (**12**)	2134 (w), 2090(s),[i] 2015 (med), 1958 (vs)	191.1 (dt, $^1J_{Rh\text{-}C}$ = 82.5 Hz), 162.7 (t, 1C)
$[RhIr(H)(CH_3)(CO)_3(\mu\text{-}\eta^1{:}\eta^2\text{-}C{\equiv}CPh)(dppm)_2]$-$[CF_3SO_3]$ (**13**)	-	193.1 (b, 1C), 192.8 (dt, $^1J_{Rh\text{-}C}$ = 80.5 Hz, 2C),
$[RhIr(CH_3)(CO)_3(C{=}CPh(H))(dppm)_2][CF_3SO_3]$ (**14**)[f]	-	200.6 (dm, $^1J_{Rh\text{-}C}$ = 5.0 Hz, 1C), 193.8 (dt, $^1J_{Rh\text{-}C}$ = 54.3 Hz, 1C), 180.8 (b, 1C)
$[RhIr(RC{=}C(CH_3)R)(CO)_3(dppm)_2][CF_3SO_3]$ (**15**)[f] (R = CO_2Me)	2022 (s), 1995 (sh), 1720 (sh), 1698 (b),[g] 1641 (med)[h]	197.9 (dm, $^1J_{Rh\text{-}C}$ = 4.0 Hz, 1C), 194.4 (dt, $^1J_{Rh\text{-}C}$ = 55.3 Hz, 1C), 176.8 (t, 1C)
$[Ir_2(RC{=}C(CH_3)R)(CO)_3(dppm)_2][CF_3SO_3]$ (**16**)[f] (R = CO_2Me)	2015 (vs), 1998 (sh), 1717 (sh), 1695 (b),[g] 1642 (med)[h]	194.7 (b, 1C), 192.0 (t, 1C), 179.5 (t, 1C)

Table 4.2 (continued)

Compound	IR[b,c], cm^{-1}	$\delta(^{13}C\{^1H\})$[e]
$[Ir_2(CH_3)(CO)_3(\mu\text{-DMAD})(dppm)_2][CF_3SO_3]$ (17)	2029 (s), 2001 (vs), 1982 (vs), 1690 (b),[g] 1635 (med)[h]	182.2 (t, 1C), 175.9 (t, 1C), 152.5 (t, 1C)

[a] Abbreviations used: med = medium, s = strong, vs = very strong, d = doublet, t = triplet, m = multiplet, dt = doublet of triplets, dm = doublet of multiplets, b = broad. [b] Nujol mull on KBr disk unless otherwise stated. [c] Values are ν(CO). [d] IR in CH_2Cl_2. [e] Vs TMS, -40 °C in CD_2Cl_2 solvent unless otherwise stated. [f] NMR data at 25 °C. [g] ν(CO) of DMAD. [h] ν(C=C). [i] ν(C≡C).

from orange to yellow, the solvent was removed under vacuum, and the solid was recrystallized from CH_2Cl_2/Et_2O yielding a yellow product in 84% yield. Anal. Calcd for $Ir_2SP_4F_3O_4C_{59}H_{49}$: C, 47.96; H, 3.46. Found: C, 47.76; H, 3.36.

(b) $[Ir_2(H)(CH_3)(CO)_3(\mu\text{-}\eta^1\text{:}\eta^2\text{-}C{\equiv}CH)(dppm)_2][CF_3SO_3]$ (5). Excess acetylene was added, by means of a gas-tight syringe, to a solution of compound **2** (30 mg, 0.021 mmol) in 0.6mL of CD_2Cl_2 at -78 °C, in an NMR tube capped with a rubber septum. NMR spectra obtained at -80 °C or -40 °C showed the presence of compound **5** (**5** was not isolated as a solid).

(c) $[Ir_2(CH_3)(CO)_3(\mu\text{-}PhC_2H)(dppm)_2][CF_3SO_3]$ (7). Compound **2** (60 mg, 0.043 mmol) was dissolved in 10 mL of CH_2Cl_2. After cooling the solution to -78 °C, 1 equiv (4.7 μL, 0.043 mmol) of phenylacetylene was added. The orange mixture was stirred for 1 h at that temperature. It was then warmed to room temperature, and stirred for another 1 h, during which time the color slowly changed to brown. The solvent was then removed under vacuum, and the residue was recrystallized from CH_2Cl_2/Et_2O, giving a brown product (76% yield). Anal. Calcd for $Ir_2SP_4F_3O_6C_{63}H_{53}$: C, 50.32; H, 3.55. Found: C, 49.52; H, 3.36.

(d) $[RhIr(CH_3)(CO)_3(\mu\text{-}C_2H_2)(dppm)_2][CF_3SO_3]$ (9). Compound **1** (30 mg, 0.023 mmol) was dissolved in 0.6 mL of CD_2Cl_2, in an NMR tube covered with a rubber septum, and then cooled to -78 °C. Excess acetylene was then added to the solution by means of a gas-tight syringe. Warming the sample to -40 °C yielded compound **9**, which was characterized by its NMR spectra (compound **9** was not isolated as a solid).

(e) [RhIr(CH_3)(CO)$_3$(dppm)(HC=C(H)P(Ph_2)CH_2PPh_2)][CF_3SO_3] (10). Acetylene was passed through a solution of compound **1** (60 mg, 0.046 mmol) in 10 mL of CH_2Cl_2, which had been cooled to -78 °C, for 1 min. The solution was then stirred under a static atmosphere of the gas, at this temperature for about 10 min and then warmed to room temperature. To obtain NMR spectra, the reaction was carried out in CD_2Cl_2 solution under the same conditions, and the spectra were obtained after keeping the solution at room temperature for about 5 min. Attempts to precipitate the product as a solid resulted in several decomposition products.

(f) [RhIr(μ-η^1:η^2-C≡CPh)(CO)$_3$(dppm)$_2$][CF_3SO_3] (11). To a solution of compound **1** (60 mg, 0.046 mmol) in 10 mL CH_2Cl_2, was added 1 equiv (5.0 μL, 0.046 mmol) of phenylacetylene. The mixture was stirred for 2 h, under a slow stream of argon, during which time the color changed from orange to red. The solvent volume was then reduced to about 5 mL, and the red solid was precipitated and washed with ether. The solid was collected and dried under a stream of argon. After recrystallizing from CH_2Cl_2/Et_2O, the product was dried again under an argon stream and then under vacuum (75% yield). Anal. Calcd for $IrRhSP_4F_3O_6C_{62}H_{49}$: C, 53.36; H, 3.53. Found: C, 52.12; H, 3.61.

(g) [RhIr(C≡CPh)$_2$(CO)$_2$(μ-H)(dppm)$_2$][CF_3SO_3] (12). The procedure for preparing compound **12** was the same as that described for compound **11**, except that an excess (*ca.* 3 equiv) instead of 1 equiv of phenylacetylene was used, and the solution color changed from orange to yellow then to orange again. The orange product is obtained in 70% yield. Anal. Calcd for

$IrRhClSP_4F_3O_5C_{69.5}H_{56}$: C, 55.10; H, 3.72; Cl, 2.34. Found: C, 54.38; H, 3.70; Cl, 2.00.

(h) $[RhIr(RC=C(CH_3)R)(CO)_3(dppm)_2][CF_3SO_3]$ (R = CO_2Me) (15). Compound **1** (60 mg, 0.046 mmol) was dissolved in 5 mL of CH_2Cl_2, and 1 equiv (5.6 μL, 0.046 mmol) of DMAD was added. The solution was then stirred for 1 h, after which time the solvent was removed under vacuum. The residue was then recrystallized from CH_2Cl_2/Et_2O, giving a yellow product (75% yield). Anal. Calcd for $IrRhSP_4F_3O_{10}C_{61}H_{53}$: C, 50.38; H, 3.67. Found C, 49.42; H, 3.44.

Reaction of Compound 2 with Acetylene at Room Temperature. The procedure was the same as that used for the preparation of compound **4**, as stated above, except that the entire reaction was carried out at room temperature, for 1 h in this case, and it yielded a mixture of compound **4** and $[Ir_2(CH_3)(CO)_3(\mu\text{-}C_2H_2)(dppm)_2][CF_3SO_3]$ (**3**) as products.

Reaction of Compound 2 with Phenylacetylene at Room Temperature. The procedure was the same as that used for the preparation of compound **7**, as stated above, except that the entire reaction was carried out at room temperature, for 1 h in this case, and it yielded a mixture of compound **7** and $[Ir_2(CH_3)(CO)_3(\mu\text{-}C{=}CPh(H))(dppm)_2][CF_3SO_3]$ (**8**) as products.

Reaction of Compound 2 with DMAD. The procedure was the same as that for the preparation of compound **15**, except that compound **2** was used instead of compound **1**, and the mixture was stirred for 2 h instead of 1 h. A

mixture of the compounds, $[Ir_2(RC{=}C(CH_3)R)(CO)_3(dppm)_2][CF_3SO_3]$ (R = CO_2Me) (**16**) and $[Ir_2(CH_3)(CO)_3(\mu\text{-DMAD})(dppm)_2][CF_3SO_3]$ (**17**), was obtained as the product in this case, as shown by its NMR spectra. The reaction was repeated using a similar procedure to that employed for the preparation of compound **7**, except that DMAD was used in this case instead of phenylacetylene and the color of the solution changed from orange to yellow. This reaction yielded the same products as those obtained from the reaction carried out at room temperature.

Reaction of Compound 4 with PMe_3. To a solution of compound **4** (60 mg, 0.042 mmol) dissolved in 5 mL of THF, was added a solution of 1 equiv of PMe_3 (42.0 μL of a 1 M solution in THF) in 5 mL of THF. The solution was then stirred for 2 h, during which time its color changed to lighter yellow. The solvent was then removed under vacuum, and the yellow solid was recrystallized from CH_2Cl_2/Et_2O. The NMR spectra showed that the product was the CO-substituted compound, $[Ir_2(CH_3)(CO)_2(PMe_3)(\mu\text{-}C{=}CH_2)(dppm)_2][CF_3SO_3]$ (**6**).

Experiment to Characterize Intermediates in the Reaction of Compound 1 with Excess Phenylacetylene. Compound **1** (30 mg, 0.023 mmol) was dissolved in 0.6 mL of CD_2Cl_2 in an NMR tube, capped with a rubber septum, and cooled to -78 °C. Phenylacetylene (7.5 μL, 0.069 mmol) was then added, and NMR spectra of the reaction mixture were then obtained at temperatures ranging from -80°C to +25°C, starting from the lowest temperature. The spectra at subsequent temperatures were obtained by warming the probe to the desired temperature, with the sample in place, and allowing the sample to stand for 20 min before recording the spectra. The

procedure was the same in the experiment with 1 equiv of phenylacetylene, except that 1 equiv instead of 3 equiv of the reagent was added in that case.

X-ray Data Collection. Orange crystals of $[RhIr(C{\equiv}CPh)_2(CO)_2(\mu\text{-}H)(dppm)_2][CF_3SO_3]\cdot 2CH_2Cl_2$ (**12**) were obtained by slow diffusion of ether into a concentrated CH_2Cl_2 solution of the compound. Several suitable crystals were mounted and flame sealed in glass capillaries under solvent vapor to minimise decomposition or deterioration due to solvent loss. Data were collected on an Enraf-Nonius CAD4 diffractometer using graphite-monochromated Mo Kα radiation. Unit cell parameters were obtained from a least-squares refinement of the setting angles of 25 reflections in the range $20.0° \leq 2\theta \leq 24.0°$. The monoclinic diffraction symmetry and the systematic absences (*h0l*, *l*=odd; *0k0*, *k*=odd) were consistent with the space group $P2_1/c$.

Intensity data were collected at 22°C using the $\theta/2\theta$ scan technique to a maximum $2\theta = 50.0°$, collecting reflections with indices of the form $+h +k \pm l$. Backgrounds were scanned for 25% of the peak width on either side of the peak scan. Three reflections were chosen as intensity standards, being remeasured at 120-min intervals of X-ray exposure time. There was no significant systematic decrease in the intensities of these standards thus no decomposition correction was applied. A total of 12976 unique reflections were measured and processed in the usual way, using a value of 0.04 for p[9] to downweight intense reflections; of these 8365 were considered to be observed ($F_o^2 \geq 3\sigma(F_o^2)$) and were used in subsequent calculations. Absorption corrections were applied to the data using the method of Walker and Stuart.[10,11] See Table 4.3 for crystal data and more information on X-ray data collection.

Table 4.3. Crystallographic Data for $[RhIr(C{\equiv}CPh)_2(CO)_2(\mu\text{-}H)(dppm)_2][CF_3SO_3]\cdot 2CH_2Cl_2$ (**12**)

formula	$C_{71}H_{59}Cl_4F_3IrO_5P_4RhS$
formula weight	1642.14
crystal shape	monoclinic prism
crystal dimensions, mm	0.39 x 0.47 x 0.62
space group	$P2_1/c$ (No. 14)
temperature, °C	22
radiation (λ, Å)	graphite-monochromated Mo Kα (0.71069)
unit cell parameters	
a, Å	17.821(3)
b, Å	24.780(5)
c, Å	17.892(3)
β, deg	117.56(1)
V, Å^3	7004(2)
Z	4
ρ(calcd), g cm^{-3}	1.557
linear absorption coefficient (μ), cm^{-1}	24.497
range of transmission factors	0.8837 - 1.0952
detector aperture, mm	(3.00 + tan θ) wide x 4.00 high
take-off angle, deg	3.0
maximum 2θ, deg	50.0
crystal-detector distance, mm	173

Table 4.3. (continued)

scan type	$\theta/2\theta$
scan rate, deg/min	between 1.43 and 6.71
scan width, deg	0.60 + 0.347 tan θ
total unique reflections	12976 ($+h +k \pm l$)
total observations (NO)	8365 ($Fo^2 \geq 3\sigma(Fo^2)$)
final no. params. varied (NV)	575
error in obs. of unit weight (GOF)[a]	2.544
R[b]	0.064
R_w[c]	0.083

[a] $\mathrm{GOF} = \left[\sum\omega(|F_o| - |F_c|)^2 / (\mathrm{NO} - \mathrm{NV})\right]^{1/2}$ where $w = 4F_o^2 / \sigma^2(F_o^2)$.

[b] $R = \sum ||F_o| - |F_c|| / \sum |F_o|$. [c] $R_w = \left[\sum\omega(|F_o| - |F_c|)^2 / \sum\omega F_o^2\right]^{1/2}$.

Structure Solution and Refinement. The structure was solved in the space group $P2_1/c$ using standard Patterson and Fourier techniques. Full matrix least-squares refinements proceeded so as to minimize the function $\sum w(|F_o| - |F_c|)^2$, where $w = 4F_o^2 / \sigma^2(F_o^2)$. All non-hydrogen atoms were ultimately located. In addition, two molecules of CH_2Cl_2 per formula unit of complex were also located. Atomic scattering factors [12,13] and anomalous dispersion terms[14] were taken from the usual tabulations. Hydrogen atoms with the exception of the methylene chloride hydrogens were included as fixed contributions but not refined. Their idealized positions were calculated from the geometries about the attached carbon atoms, using a C-H bond length of 0.95 Å, and they were assigned thermal parameters 20% greater than the equivalent isotropic B's of their attached C atoms.

The final model, with 575 parameters refined, converged to values of R = 0.064 and Rw = 0.083. In the final difference Fourier map the 10 highest residuals (1.7 - 1.2 e/Å^3) were found in the vicinity of the metal atoms, phenyl rings and solvent molecules. A typical carbon atom in an earlier synthesis had an electron density of *ca.* 5.0 e/Å^3. The positional and isotropic thermal parameters of the non-hydrogen atoms are given in Table 4.4.

Results

The reaction of $[Ir_2(H)(CO)_3(\mu\text{-}CH_2)(dppm)_2][CF_3SO_3]$ (**2**) with acetylene at ambient temperature, gives a mixture of the alkyne- and vinylidene-bridged products, $[Ir_2(CH_3)(CO)_3(\mu\text{-}C_2H_2)(dppm)_2][CF_3SO_3]$ (**3**) and $[Ir_2(CH_3)(CO)_3(\mu\text{-}C{=}CH_2)(dppm)_2][CF_3SO_3]$ (**4**), respectively, in a typical ratio of about 1.7:1. The ^1H NMR spectrum[15] of compound **3** shows the

Table 4.4. Positional and Thermal Parameters for the Atoms of $[RhIr(C{\equiv}CPh)_2(CO)_2(\mu\text{-}H)(dppm)_2][CF_3SO_3]\cdot 2CH_2Cl_2$ (**12**)[a]

Atom	*x*	*y*	*z*	*B*, Å^2[b]
Ir	0.24240(2)	0.15084(2)	0.26946(2)	2.59(1)*
Rh	0.25265(5)	0.24799(4)	0.37922(5)	2.72(2)*
S[c]	0.2939(2)	0.7391(2)	0.5487(2)	5.8(1)*
Cl(1)[d]	0.2859(5)	0.5108(3)	0.5222(5)	17.5(4)*
Cl(2)[d]	0.292(1)	0.5753(8)	0.3825(8)	20.2(8)*
Cl(2)'[e]	0.232(1)	0.5500(8)	0.372(1)	16.6(9)*
Cl(3)[d]	0.2605(6)	0.6007(6)	0.177(1)	30.5(7)*
Cl(4)[d]	0.2737(7)	0.5712(5)	0.0332(7)	32.1(6)*
P(1)	0.0983(2)	0.1483(1)	0.2297(2)	3.01(8)*
P(2)	0.1071(2)	0.2550(1)	0.3192(2)	2.97(8)*
P(3)	0.3900(2)	0.1508(1)	0.3387(2)	2.70(7)*
P(4)	0.3966(2)	0.2575(1)	0.4269(2)	2.83(8)*
F(1)[c]	0.1583(7)	0.6980(7)	0.4338(9)	15.4(7)*
F(2)[c]	0.2441(8)	0.7250(8)	0.3887(6)	17.9(8)*
F(3)[c]	0.1704(8)	0.7809(6)	0.4228(8)	16.6(7)*
O(1)	0.2204(6)	0.1164(4)	0.0946(5)	6.2(3)*
O(4)	0.2728(6)	0.2845(4)	0.5454(5)	6.2(3)*
O(101)[c]	0.2534(6)	0.7535(6)	0.5968(7)	10.1(5)*
O(102)[c]	0.3535(6)	0.7769(5)	0.5482(7)	8.8(4)*
O(103)[c]	0.3288(8)	0.6851(5)	0.5651(8)	10.1(5)*
C(1)	0.2273(7)	0.1331(5)	0.1573(8)	4.1(4)*
C(2)	0.2420(6)	0.0690(4)	0.2826(6)	3.0(3)*
C(3)	0.2376(6)	0.0214(4)	0.2758(6)	3.1(3)*
C(4)	0.2631(7)	0.2701(5)	0.4781(7)	3.8(3)
C(5)	0.2417(6)	0.2323(4)	0.2520(5)	2.9(3)*
C(6)	0.2450(6)	0.2809(5)	0.2429(6)	3.6(3)*
C(7)	0.0557(6)	0.2165(5)	0.2210(6)	2.8(3)*
C(8)	0.4330(6)	0.2182(4)	0.3632(6)	2.7(3)*
C(11)	0.0347(6)	0.1195(5)	0.1263(6)	3.1(2)
C(12)	0.0152(8)	0.1495(6)	0.0528(8)	4.9(3)

(contd.)

C(13)	-0.0364(9)	0.1280(7)	-0.0255(9)	6.5(4)
C(14)	-0.0625(8)	0.0769(6)	-0.0334(8)	5.4(3)
C(15)	-0.0456(9)	0.0474(6)	0.0346(9)	6.1(4)
C(16)	0.0066(8)	0.0685(6)	0.1163(8)	5.1(3)
C(21)	0.0646(7)	0.1128(5)	0.2986(7)	3.5(2)
C(22)	-0.0186(7)	0.1116(5)	0.2778(7)	4.5(3)
C(23)	-0.0459(9)	0.0833(7)	0.3281(9)	6.5(4)
C(24)	0.0101(9)	0.0574(6)	0.3955(9)	6.1(4)
C(25)	0.0908(8)	0.0574(6)	0.4187(8)	5.8(3)
C(26)	0.1209(7)	0.0855(5)	0.3684(7)	4.3(3)
C(31)	0.0725(7)	0.3242(5)	0.2875(7)	3.6(2)
C(32)	0.0265(8)	0.3416(6)	0.2060(8)	5.2(3)
C(33)	0.0050(9)	0.3951(7)	0.1851(9)	6.6(4)
C(34)	0.032(1)	0.4306(7)	0.251(1)	7.1(4)
C(35)	0.0756(8)	0.4165(6)	0.3304(9)	5.9(3)
C(36)	0.0936(8)	0.3624(6)	0.3492(8)	5.1(3)
C(41)	0.0517(6)	0.2344(5)	0.3769(6)	3.3(2)
C(42)	-0.0319(7)	0.2480(5)	0.3506(7)	4.5(3)
C(43)	-0.0747(8)	0.2304(6)	0.3932(8)	5.2(3)
C(44)	-0.0338(8)	0.2024(6)	0.4651(8)	5.5(3)
C(45)	0.0469(8)	0.1888(6)	0.4948(8)	5.2(3)
C(46)	0.0894(7)	0.2052(5)	0.4501(7)	3.8(2)
C(51)	0.4424(6)	0.1150(4)	0.4390(6)	3.0(2)
C(52)	0.4005(7)	0.0831(5)	0.4689(7)	3.7(2)
C(53)	0.4447(7)	0.0566(6)	0.5459(8)	4.7(3)
C(54)	0.5278(8)	0.0637(6)	0.5914(9)	5.9(3)
C(55)	0.5730(8)	0.0943(6)	0.5630(8)	5.4(3)
C(56)	0.5270(7)	0.1193(5)	0.4855(7)	3.9(3)
C(61)	0.4393(6)	0.1218(4)	0.2790(6)	2.9(2)
C(62)	0.467(1)	0.1509(7)	0.232(1)	7.1(4)
C(63)	0.499(1)	0.1256(8)	0.185(1)	8.3(5)
C(64)	0.509(1)	0.0735(7)	0.188(1)	7.4(4)
C(65)	0.482(1)	0.0440(7)	0.231(1)	7.4(4)
C(66)	0.4491(8)	0.0676(6)	0.2783(8)	5.5(3)
C(71)	0.4657(7)	0.2398(5)	0.5362(6)	3.5(2)

(contd.)

C(72)	0.4387(7)	0.2067(5)	0.5811(7)	3.9(3)
C(73)	0.4891(9)	0.1943(6)	0.6652(8)	5.7(3)
C(74)	0.5669(9)	0.2148(6)	0.7032(9)	6.0(4)
C(75)	0.5983(8)	0.2454(6)	0.6639(8)	5.6(3)
C(76)	0.5480(8)	0.2589(5)	0.5784(7)	4.7(3)
C(81)	0.4276(7)	0.3257(5)	0.4203(7)	3.5(2)
C(82)	0.4771(8)	0.3396(6)	0.3845(8)	5.0(3)
C(83)	0.502(1)	0.3936(7)	0.3807(9)	7.1(4)
C(84)	0.472(1)	0.4309(7)	0.410(1)	7.8(5)
C(85)	0.4194(9)	0.4208(7)	0.4443(9)	6.8(4)
C(86)	0.3996(8)	0.3671(6)	0.4498(8)	5.3(3)
C(91)	0.2321(6)	-0.0361(4)	0.2632(7)	3.5(3)*
C(92)	0.2663(9)	-0.0616(5)	0.2173(8)	6.1(5)*
C(93)	0.261(1)	-0.1156(7)	0.206(1)	8.7(6)*
C(94)	0.222(1)	-0.1451(6)	0.241(1)	9.7(8)*
C(95)	0.188(1)	-0.1225(6)	0.279(1)	9.3(8)*
C(96)	0.1955(9)	-0.0689(6)	0.293(1)	6.2(5)*
C(101)	0.2554(6)	0.3365(4)	0.2181(6)	2.7(3)*
C(102)	0.2811(8)	0.3414(5)	0.1565(8)	5.2(4)*
C(103)	0.291(1)	0.3895(7)	0.1279(8)	7.3(5)*
C(104)	0.273(1)	0.4336(6)	0.162(1)	8.7(6)*
C(105)	0.247(1)	0.4296(5)	0.220(1)	8.4(6)*
C(106)	0.2389(9)	0.3807(6)	0.2482(9)	7.4(5)*
C(110)[c]	0.218(1)	0.7345(9)	0.440(1)	11.5(8)*
C(111)[d]	0.260(2)	0.5695(9)	0.463(1)	14.8(8)*
C(112)[d]	0.175(1)	0.5789(8)	0.044(1)	10.1(9)*

[a]Numbers in parentheses are estimated standard deviations in the least significant digits in this and all subsequent tables. [b]Starred B values are for atoms refined anisotropically. Displacement parameters for the anisotropically refined atoms are given in the form of the equivalent isotropic Gaussian diplacement parameter defined as: $4/3[a^2\beta_{11} + b^2\beta_{22} + c^2\beta_{33} + ab(\cos\gamma)\beta_{12} + ac(\cos\beta)\beta_{13} + bc(\cos\alpha)\beta_{23}]$. [c] $CF_3SO_3^-$ anion. [d] solvent atoms. [e] this atom has 50% occupancy and is related to the unprimed atom (50% occupancy) by a rotational disorder.

methyl resonance as a broad signal at δ -0.14, and the proton resonances of the coordinated acetylene as multiplets at δ 10.25 and 9.15.[16] The $^{13}C\{^1H\}$ NMR spectrum of a ^{13}CO-enriched sample, shows broad resonances at δ 198.7 and 181.3, and a triplet at δ 194.4, and the IR spectrum[17] shows CO stretches at 2007, 1970 and 1911 cm^{-1}, suggesting the presence of three terminally bound CO ligands. Also in the IR spectrum, the peak at 1632 cm^{-1} is assigned to the C≡C stretch of the coordinated acetylene. This is within the range of 1530 - 1642 cm^{-1} observed in closely related dppm-bridged binuclear complexes in which the alkyne bridges the two metals parallel to the metal-metal axis,[18] and contrasts with the lower values of 1425 cm^{-1} reported for $[Rh_2(CO)_2(\mu\text{-}\eta^2\text{:}\eta^2\text{-}PhC_2H)(dppm)_2]$ and $[Rh_2(CO)_2(\mu\text{-}\eta^2\text{:}\eta^2\text{-}Ph_2C_2)(dppm)_2]$, in which the alkyne bridges the metals perpendicular to the metal-metal bond.[19] The $^{13}C\{^1H\}$ NMR spectrum of compound **3**, prepared by using acetylene which was ^{13}C-enriched at both positions, shows two doublets of mutiplets at δ 160.7 and 147.1 ($^1J_{C\text{-}C}$ = 50.8 Hz) due to the two carbon nuclei of the coordinated acetylene. These chemical shifts are close to those in related systems, in which the alkyne bridges two metals parallel to the metal-metal axis,[20] suggesting such a bridging mode of the acetylene in compound **3**. $^{13}C\{^{31}P\}\{^1H\}$ NMR experiments show that the alkyne resonances are actually doublets of triplets of triplets due to coupling to two sets of phosphorus nuclei and to the adjacent ^{13}C nucleus ($^2J_{P\text{-}C}$ = 11.2 Hz, $^3J_{P\text{-}C}$ = 5.0 Hz, and $^2J_{P\text{-}C}$ = 11.0 Hz, respectively[21]). Each carbon nucleus shows a larger coupling to the phosphorus atoms on one metal than to those on the other. The ^1H NMR spectrum of this sample shows the proton resonances of the bridging acetylene as two doublets of multiplets ($^1J_{C\text{-}H}$ ≈ 160 Hz for each of the protons). In a sample of compound **3** in which all the carbon nuclei of the bridging acetylene and CO ligands were ^{13}C-enriched, each of the resonances

at δ 194.4 and 181.3, shows strong coupling (21.0 Hz) to one of the carbon nuclei of the coordinated acetylene, suggesting a trans arrangement of the carbon atoms of the acetylene and two of the CO ligands.[20a] All the NMR data are consistent with the structure of compound **3** shown in Scheme 4.1.[22]

The ^{1}H NMR spectrum of compound **4** shows the methyl resonance as a triplet at δ -0.55 and the vinylidene proton resonances as singlets at δ 6.40 and 5.72. The $^{13}C\{^{1}H\}$ NMR spectrum of a ^{13}CO-enriched sample, shows a broad resonance at δ 181.2 and triplets at δ 175.1 and 172.3, indicating the presence of three CO ligands in compound **4**. Although none of these resonances is at low enough field to unequivocally indicate the presence of a symmetrically bridging carbonyl ligand, the CO stretch at 1790 cm^{-1} in the IR spectrum suggests the presence of a semibridging carbonyl ligand in compound **4**, presumably that giving rise to the broad resonance at δ 181.2. However, since this resonance is broad and the ^{31}P resonances for **4** are quite close, as shown in Table 4.1, $^{13}C\{^{31}P\}\{^{1}H\}$ NMR experiments (using the ^{13}CO-enriched sample) do not give much information about the semibridging interaction. The $^{13}C\{^{1}H\}$ NMR spectrum of **4**, prepared using ^{13}C-enriched acetylene, shows a doublet of quintets at δ 198.4 and a doublet at δ 123.5 ($^{1}J_{C\text{-}C}$ = 67.0 Hz), due to the α and β carbon atoms of the bridging vinylidene ligand. In the ^{1}H NMR spectrum of this sample, the vinylidene proton resonances appear as doublets ($^{1}J_{C\text{-}H}$ = 160 Hz for each of the protons).

Although the carbon resonance at δ 198.4 is unusually high field for a vinylidene α carbon, it is very close to that of another vinylidene compound, $[Ir_2I_2(CO)_2(\mu\text{-}C{=}CH_2)(dppm)_2]$, that was previously characterised by an X-ray structure determination in this research group (δ 194.3).[20a] In addition, the bridging vinylidene formulation for **4**, as shown in Scheme 4.1, is

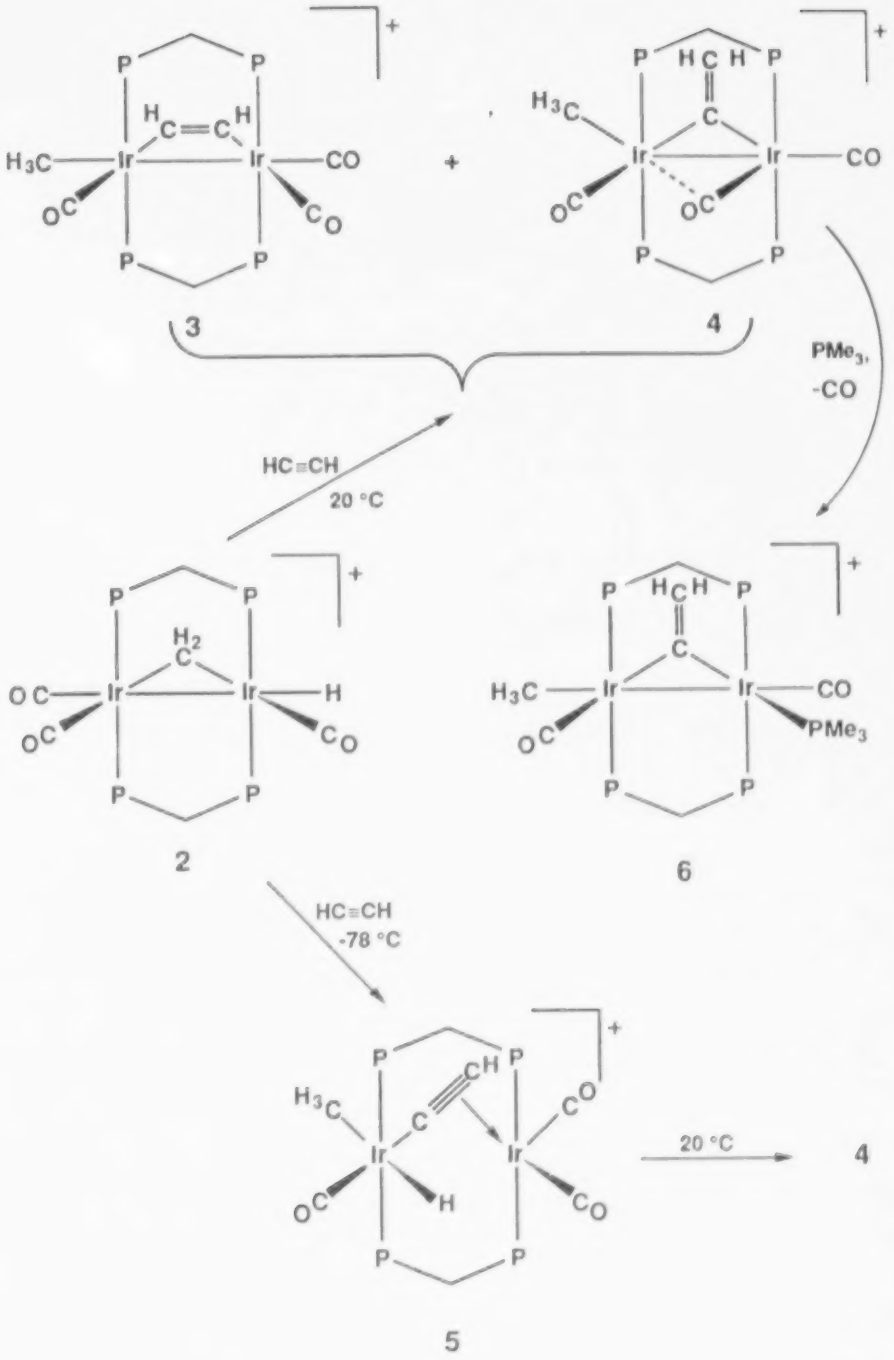

Scheme 4.1.

substantiated by $^{13}C\{^{31}P\}\{^{1}H\}$ experiments (using the sample prepared with ^{13}C-enriched acetylene) which indicate that the α carbon shows essentially equal coupling to all four phosphorus nuclei, whereas the β carbon shows no phosphorus coupling. In this experiment, decoupling either phosphorus resonance leads to the collapse of the signal at δ 198.4 into a doublet of triplets, while it collapses into a doublet on ^{31}P broadband decoupling. The signal at δ 123.5 remains as a doublet in all these decoupling experiments as expected. In samples which are ^{13}C-enriched at both the carbonyl and vinylidene carbon atoms, the carbonyl resonance at δ 175.1 shows strong coupling (23.3 Hz) to the vinylidene α carbon nucleus, while the carbonyl resonance at δ 172.3 shows weaker coupling (13.0 Hz) to the same vinylidene carbon nucleus. This suggests a trans arrangement of the vinylidene α carbon and one of the terminal CO ligands, and an orientation with respect to the other terminal CO ligand which deviates significantly from trans.[20a] $^{13}C\{^{31}P\}\{^{1}H\}$ and $^{1}H\{^{31}P\}$ NMR experiments show that the CO ligand that is trans to the vinylidene α carbon is bound to the same metal as the methyl group, while the carbonyl group that shows a weaker coupling to the α carbon is bound to the other metal together with the third CO ligand.

When compound **2** is reacted with acetylene at -78 °C, a hydrido-acetylide intermediate complex, $[Ir_2(H)(CH_3)(CO)_3(\mu\text{-}\eta^1\text{:}\eta^2\text{-}C{\equiv}CH)(dppm)_2]$-$[CF_3SO_3]$(**5**), is observed, which is converted quantitatively to the vinylidene product, compound **4**, on warming to room temperature. The ^{1}H NMR spectrum of compound **5** shows the acetylide proton resonance as a broad signal at δ 8.06, the methyl resonance as a triplet at δ -0.40, and the hydride resonance as a multiplet at δ -9.83. Selective ^{31}P decoupling experiments show that the methyl group and the hydride are terminally bound to the same metal. The $^{13}C\{^{1}H\}$ NMR spectrum of a ^{13}CO-enriched sample, shows broad

resonances at δ 181.7 and 179.1, as well as a triplet at δ 154.7, suggesting the presence of three terminal CO ligands. The $^{13}C\{^1H\}$ NMR spectrum of a sample prepared using $^{13}C_2H_2$, shows two doublets of multiplets at δ 127.1 and 102.4 ($^1J_{C\text{-}C}$ = 55.3 Hz), which are assigned to the acetylide β and α carbons, respectively. These resonances are in a similar range to those of other acetylides.[1a,7a,23] $^{13}C\{^1H\}\{^{31}P\}$ NMR experiments show that these resonances for the acetylide carbon nuclei in **5** are actually doublets of triplets of triplets, indicating that both nuclei couple to the phosphorus nuclei bound to both metals. However the α carbon nucleus shows stronger coupling to the phosphorus nuclei which are bound to the Ir bearing the methyl ligand than to the other set, while the β carbon nucleus shows the opposite effect (that is it shows stronger coupling to the phosphorus nuclei bound to the Ir that does not bear the methyl ligand). This suggests that the acetylide ligand adopts a $\sigma,\pi-$ mode of coordination. Since the α carbon is σ-bound to one of the metals, it is expected to show stronger coupling to the phosphorus nuclei bound to this metal than any of the P-C couplings displayed by the β carbon. Therefore, the assignment of the ^{13}C resonances to the α and β carbon atoms is based on the fact that the higher of the two P-C couplings displayed by the resonance at δ 127.2 ($^2J_{P\text{-}C}$ = 13.6 Hz) is greater than the corresponding value displayed by the resonance at δ 102.4 ($^2J_{P\text{-}C}$ = 11.2 Hz). The proposed $\sigma,\pi-$ coordination mode is consistent with the magnitude of the C-C coupling which is close to that of the coordinated alkyne in compound **3** and other related compounds.[20a] The ^1H NMR spectrum of this sample shows the acetylide proton resonance as a broad doublet ($^1J_{C\text{-}H} \approx$ 160 Hz). A trans orientation of the methyl and hydride ligands is proposed as the factor inhibiting methane loss in compound **5**.

Attempts to induce C-C coupling of the vinylidene and methyl group in compound **4**, by reacting with PMe_3, only resulted in the CO substitution product, $[Ir_2(CH_3)(CO)_2(PMe_3)(\mu\text{-}C{=}CH_2)(dppm)_2][CF_3SO_3]$ (**6**). The spectroscopic data for compound **6**, shown in Tables 4,1 and 4.2, are consistent with the assigned structure, shown in Scheme 4.1.

The reaction of compound **2** with phenylacetylene, again gives a mixture of the two products, $[Ir_2(CH_3)(CO)_3(\mu\text{-}PhC_2H)(dppm)_2][CF_3SO_3]$ (**7**) and $[Ir_2(CH_3)(CO)_3(\mu\text{-}C{=}CPh(H))(dppm)_2][CF_3SO_3]$ (**8**), analogous to the reaction with acetylene. Typical ratios of the two compounds obtained are 3:1 with 1 equiv, and 2:1 with excess (*ca.* 3 equiv) of phenylacetylene. The assignment of the structures of **7** and **8** (see Scheme 4.2) is based partly on their very similar NMR spectroscopic properties to those of **3** and **4**, respectively.

The ^1H NMR spectrum of compound **7** shows the proton resonance of the coordinated alkyne as a multiplet at δ 9.51, and the methyl resonance as a broad signal at δ 0.02. The $^{13}C\{^1H\}$ NMR spectrum[24] shows two broad resonances at δ 198.7 and 182.9, as well as a triplet at δ 191.5, and the IR spectrum shows CO stretches at 2011, 1970 and 1785 cm^{-1}, indicating that there are two terminal and one semibridging CO ligands in compound **7** (for a similar reason to that given for **4**). The peak at 1640 cm^{-1} in the IR spectrum, which is assigned to the C≡C stretch of the coordinated phenylacetylene, is consistent with the bridging mode (parallel to the metal-metal axis) assigned to the alkyne in **7**.[18] The orientation of the alkyne, in terms of which metal the phenyl substituent is closer to, is arbitrarily assigned since this could not be determined from the NMR spectra, and NOE (Nuclear Overhauser Effect)[25a] experiments did not yield any information on this orientation.

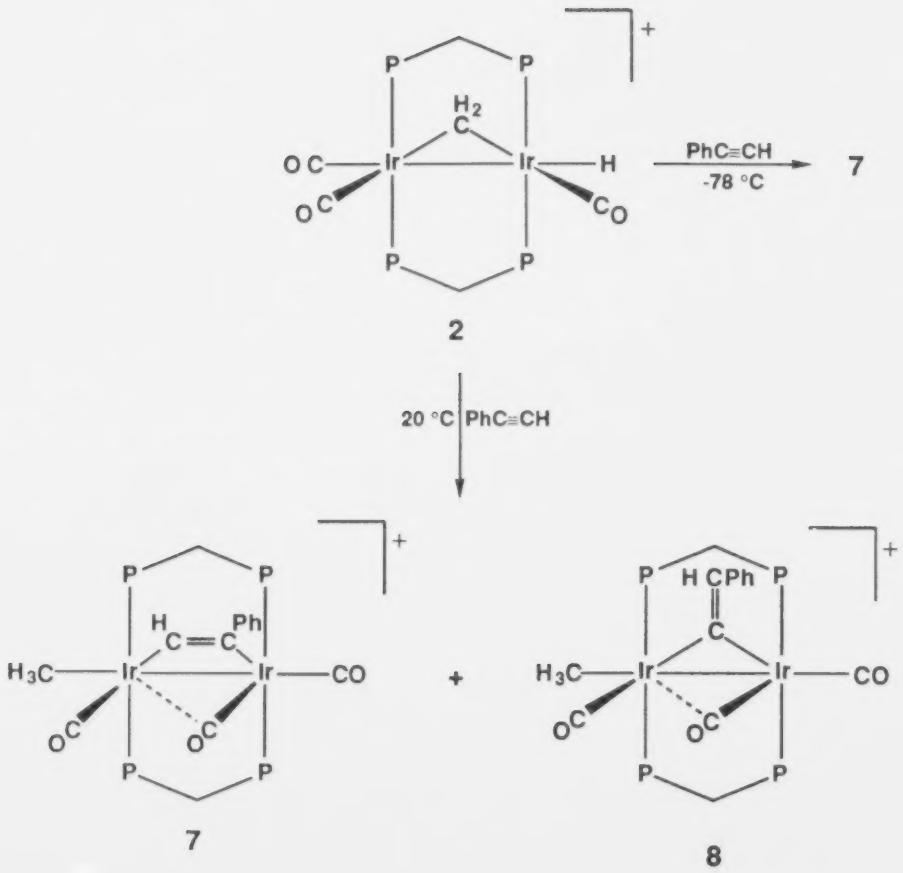

Scheme 4.2.

The ^{1}H NMR spectrum of compound **8**, shows the methyl resonance as a triplet at δ -0.58 but does not show the vinylidene proton resonance, which is presumably obscured by the phenyl resonances. The $^{13}C\{^{1}H\}$ NMR spectrum shows a broad resonance at δ 182.9 and two triplets at δ 179.6 and 168.0, while the IR spectrum shows CO stretches at 1960, 1920 and 1780 cm^{-1}, indicating the presence of two terminally bound CO ligands, and a third one that is in a semibridging position, in compound **8**. Also the IR spectrum of **8** shows a peak at 1655 cm^{-1} which is assigned to the C=C stretch of the vinylidene. The orientation of the vinylidene ligand, such that its proton is closer to the metal to which the methyl group is bound, is proposed for **8** on steric grounds.

In contrast to the chemistry of compound **2** with acetylene, the reaction with phenylacetylene at -78 °C followed by warming to room temperature, does not yield the phenylvinylidene product, **8**. Instead the alkyne bridged product, **7**, is obtained. When this low temperature reaction with phenylacetylene is monitored by NMR, no intermediate product is observed. Instead compound **7** is observed even at -78 °C.

The closely related mixed-metal species, $[RhIr(CH_3)(CO)_3(dppm)_2][CF_3SO_3]$ (**1**), also reacts with acetylene, but in this case the reaction proceeds very differently from that involving **2**, yielding instead, $[RhIr(CH_3)(CO)_3(dppm)(HC{=}C(H)P(Ph_2)CH_2PPh_2)][CF_3SO_3]$ (**10**), the unusual product of formal insertion of acetylene into one of the Rh-P bonds of **2**. The ^{31}P NMR spectrum of compound **10** shows a pattern diagnostic of an ABCDX spin system in which only one of the phosphorus nuclei shows strong coupling to Rh, consistent with a direct Rh-P bond. The spectrum displays a multiplet at δ 29.9 (showing a maximum coupling of about 9.0 Hz), a doublet of doublets of doublets at δ 18.1 for the Rh-bound P nucleus ($^{1}J_{Rh\text{-}P}$ = 152.0 Hz, $^{2}J_{P\text{-}P}$ =

48.0 Hz), and two doublets of doublets at δ -11.7 ($^2J_{P-P}$ = 406.0 Hz, $^2J_{P-P}$ = 9.3 Hz) and -22.6 ($^2J_{P-P}$ = 406.0 Hz, $^2J_{P-P}$ = 48.0 Hz). The last two resonances are due to the phosphorus nuclei bound to Ir, and the large coupling between them shows that they maintain a trans orientation with respect to each other.[26]

The ^1H NMR spectrum of compound **10** shows one of the proton resonances of the inserted acetylene as an apparent triplet at δ 8.58 ($^3J_{H-H} \approx {}^2J_{P-H} \approx$ 6.5 Hz), and the other as a doublet of multiplets at δ 5.60 ($^3J_{P-H} \approx$ 40.0 Hz). These resonances are assigned to H^1 and H^2, respectively (see Scheme 4.3 for the numbering scheme of the proton and carbon atoms). The magnitude of the P-H coupling displayed by the latter resonance suggests that the unsaturated ligand in **10** has a Z configuration, as shown in Scheme 4.3. The methyl resonance appears as a triplet at δ 0.46, while the four dppm protons, which are all inequivalent, give rise to multiplets at δ 4.12, 3.95, 3.72 and 2.88. The $^{13}C\{^1H\}$ NMR spectrum of a ^{13}CO-enriched sample of compound **10**, shows two doublets of multiplets at δ 191.1 ($^1J_{Rh-C}$ = 45.1 Hz) and 186.4 ($^1J_{Rh-C}$ = 63.9 Hz), and a multiplet at δ 171.5. Although the Rh-C coupling constant for the low-field resonance is a little low for a CO ligand that is terminally bound to Rh, the IR spectrum of compound **10** shows stretches at 2056, 2020 and 1975 cm^{-1}, none of which is in the typical range for symmetrically bridging or semibridging CO ligands. The possibility that this coupling of 45.1 Hz was due to carbon-carbon coupling between two CO ligands, as was proposed for $[RhIrI(CO)_2(\mu\text{-}CO)(\mu\text{-}DMAD)(dppm)_2][BF_4]$,[18a] was rejected, since neither of the other two CO resonances show coupling of this magnitude. It appears that the carbon nucleus showing coupling of 45.1 Hz to Rh, interacts weakly with Ir, resulting in the decreased coupling to Rh. Selective and broadband ^{31}P decoupling experiments show that the

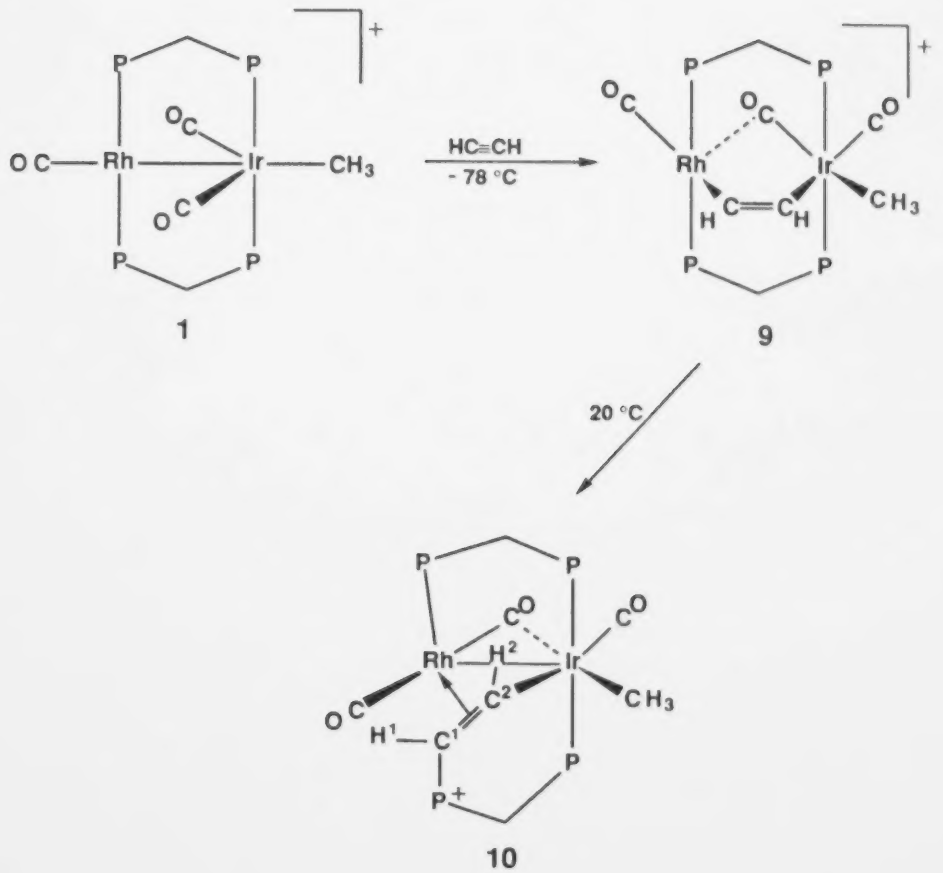

Scheme 4.3.

carbon nucleus of each CO ligand couples weakly to all four phosphorus nuclei. It is unusual in these systems for COs which are terminally bound to one metal, to couple to the phosphorus nuclei bound to another metal. In compound **10**, the coupling of the CO ligands to the phosphorus nuclei which are bound to the adjacent metal may be due to an increased interaction between the two metals as a result of the interaction of the C=C double bond of the inserted acetylene with Rh (vide infra).

The $^{13}C\{^1H\}$ NMR spectrum of **10**, prepared using ^{13}C-enriched acetylene, shows a doublet of multiplets at δ 42.1 ($^2J_{Rh-C}$ = 8.4 Hz) and a doublet of doublets of multiplets at δ 33.1 ($^1J_{P-C}$ = 76.0 Hz, $^1J_{C-C}$ = 36.5 Hz, $^1J_{Rh-C}$ = 11.8 Hz,). The latter resonance is assigned to C^1, the carbon atom of the inserted acetylene that is directly bound to one of the phosphorus atoms, because it shows a large P-C coupling, while the former resonance is assigned to C^2. These ^{13}C NMR chemical shift values for C^1 and C^2 are close to those of the coordinated olefins in $[Rh(C_2H_4)Cl(P(p\text{-tolyl})_3)_2]$ (δ 44.6),[27] $[Rh(acac)(C_2H_4)_2]$ (acac = acetyl acetonate; δ 39.6),[28] $[Pt(C_2H_4)(PPh_3)_2]$ (δ 36.3),[28] and $[Pt(C_2H_4)_2(PMePh_2)]$ (δ 36.3, 42.0),[29] while the Rh-C coupling constants (for both C^1 and C^2) compare well with values in the range of 10-16 Hz, observed for the olefinic carbon nuclei in related Rh-olefin complexes.[27,29,30] In the $^{31}P\{^1H\}$ NMR spectrum of this sample, the resonance at δ 29.9 shows an additional coupling of 76.0 Hz, which is consistent with it being directly bound to C^1. Also the ^1H NMR spectrum of this sample, shows the resonances for H^1 and H^2 as a doublet of triplets ($^1J_{C-H}$ = 131 Hz) and a doublet of doublets of multiplets ($^1J_{C-H} \approx$ 148 Hz), respectively. These C-H coupling constants are lower than those expected for sp^2 hybridized carbon atoms[25,31] and suggest a change in hybridization of the carbon atoms of the inserted acetylene in compound **10** toward sp^3. Moreover, the C-C coupling

constant ($^1J_{C-C}$ = 36.5 Hz) is significantly lower than that expected for carbon atoms linked by a C=C double bond, such as those of the coordinated alkynes (resulting in dimetalated olefins) in compounds **3** and **9** (vide infra), and is close to that of ethane (34.6 Hz).[25b] On the basis of these observations, it is proposed that there is interaction of the C=C bond of the inserted acetylene with the Rh metal, as shown, hence reducing the C=C bond order. Although compound **10** is similar, in some respects, to the zwitterionic species, $[CpRhOs(CO)_3(\mu\text{-}CO)(\mu\text{-}\eta^1\text{:}\eta^2\text{-}CH{=}C(H)(PMe_3))]$,[32] the ^{13}C NMR chemical shifts of the α and β carbons (that bound to both metals and that bound only to Rh, respectively) are δ 104.8 and 44.2, respectively (cf. δ 42.1 and 33.1 for compound **10**). It is not clear why there is such a large difference between the chemical shifts of the α carbon for the 'RhOs' compound on one hand, and **10** on the other.

In spite of the fact that all the NMR data are consistent with the structure proposed for compound **10**, as shown in Scheme 4.3, such an unusual structure cannot be unambigously established without an X-ray structure determination. Unfortunately suitable single crystals of compound **10** could not be obtained, owing to decomposition. Moreover, it slowly decomposes in solution at room temperature after about 1 h. In fact the reaction of compound **1** with acetylene has to be started at a lower temperature and warmed to room temperature, since starting at room temperature results in several decomposition products.

Although the final product in the reaction of acetylene with compound **1** is vastly different from those obtained in the reaction with compound **2**, the reaction of compound **1** proceeds through an analogous alkyne-bridged intermediate, $[RhIr(CH_3)(CO)_3(\mu\text{-}C_2H_2)(dppm)_2][CF_3SO_3]$ (**9**). Compound **9**,

which is observed in solution at -78 °C, is converted to compound **10** on warming to room temperature.

The ^{1}H NMR spectrum of compound **9** shows the proton resonances of the coordinated acetylene as a doublet of triplets at δ 9.12 ($^{2}J_{Rh-H}$ = 6.4 Hz), and a multiplet at δ 7.63, and the methyl resonance as a triplet at δ -1.00. The $^{13}C\{^{1}H\}$ NMR spectrum of a sample prepared with $^{13}C_2H_2$, shows the carbon resonances of the coordinated acetylene as two doublets of multiplets at δ 162.9 ($^{1}J_{Rh-C}$ = 20.6 Hz, $^{1}J_{C-C}$ = 53.0 Hz) and 147.0. Selective ^{31}P decoupling experiments indicate that each carbon nucleus shows larger coupling to the phosphorus nuclei bound to one metal than those bound to the other. The chemical shifts of the carbon nuclei of the coordinated acetylene in compound **9** are very close to those of compound **3** (δ 160.7 and 147.1). This observation, together with the fact that only one of the carbon nuclei of the coordinated acetylene in **9** shows coupling to Rh, is consistent with the assignment of an acetylene ligand bridging the two metals in **9**. The ^{1}H NMR spectrum of this sample shows the proton resonances of the coordinated acetylene as a doublet of doublets of triplets and a doublet of multiplets ($^{1}J_{C-H} \approx 152$ Hz for each of the protons). The $^{13}C\{^{1}H\}$ NMR spectrum of a ^{13}CO-enriched sample of compound **9**, shows a doublet of multiplets at δ 210.2 ($^{1}J_{Rh-C}$ = 19.0 Hz), a doublet of triplets at δ 191.0 ($^{1}J_{Rh-C}$ = 55.3 Hz), and a triplet at δ 172.8, indicating the presence of one semibridging carbonyl ligand (inferred from the Rh-C coupling of 19 Hz[33]) and a terminally bound carbonyl ligand each on Rh and Ir. All the NMR data are consistent with the structure of **9** shown in Scheme 4.3. The transformation of **9** to **10** can be seen as resulting from dissociation of one Rh-bound end of a diphosphine, followed by nucleophilic attack by this phosphorus at the Rh end of the bridged alkyne.

The reaction of compound **1** with phenylacetylene, differs again from any of the previous reactions of compounds **1** or **2** with acetylene or of **2** with phenylacetylene. At room temperature, compound **1** reacts with 1 equiv of phenylacetylene to give the monoacetylide product, $[RhIr(CO)_3(\mu\text{-}\eta^1{:}\eta^2\text{-}C{\equiv}CPh)(dppm)_2][CF_3SO_3]$ (**11**), accompanied by methane loss, whereas with excess phenylacetylene it gives the diacetylide product, $[RhIr(C{\equiv}CPh)_2(CO)_2(\mu\text{-}H)(dppm)_2][CF_3SO_3]$ (**12**), with the evolution of methane and CO (see Scheme 4.4).

The ^1H NMR spectrum of compound **11** shows only dppm methylene proton resonances as multiplets at δ 3.82 and 3.32, apart from the phenyl proton and solvent resonances, which is consistent with the loss of methane at some stage in the formation of this compound. The $^{13}C\{^1H\}$ NMR spectrum shows a doublet of multiplets at δ 196.0 ($^1J_{Rh\text{-}C}$ = 22.0 Hz), a doublet of triplets at δ 194.6 ($^1J_{Rh\text{-}C}$ = 80.2 Hz), and a triplet at δ 181.7, indicating the presence of a semibridging CO ligand and a terminally bound CO ligand on Rh (as shown by the coupling constants, $^1J_{Rh\text{-}C}$ = 22.0 and 80.2 Hz, respectively), as well as a terminally bound CO ligand on Ir. The peak at 1825 cm^{-1} in the IR spectrum is consistent with the presence of a semibridging CO ligand. The IR spectrum also shows peaks at 2000 and 1955 cm^{-1}, arising from the two terminally bound CO ligands. The presence of the acetylide ligand is inferred from the disappearance of the methyl group of **1**, and the formation of **12** upon reaction with an additional equivalent of phenylacetylene (the acetylide stretch cannot be unambigously assigned in the IR spectrum of compound **11**).

The ^1H NMR spectrum of compound **12** shows the hydride resonance as a doublet of multiplets at δ -8.70. Selective and broadband ^{31}P-decoupling

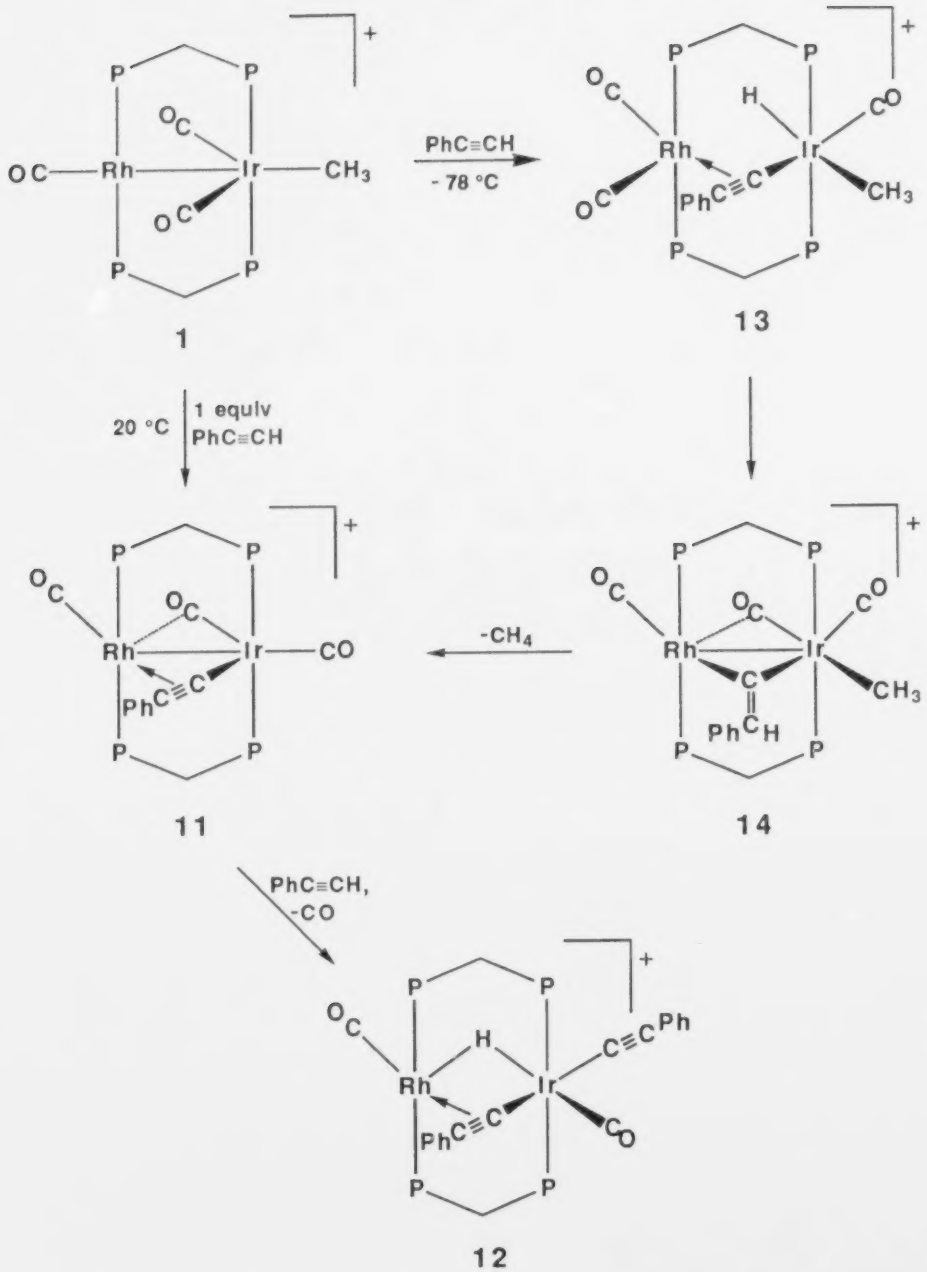

Scheme 4.4.

experiments show that this signal is actually a doublet of triplets of triplets ($^1J_{Rh-H}$ = 12.7 Hz, $^2J_{P(Ir)-H}$ = 12.0 Hz, $^2J_{P(Rh)-H}$ = 3.3 Hz). The magnitude of these two P-H coupling constants show that the hydride ligand couples more strongly to the Ir-bound phosphorus nuclei than to those bound to Rh. This observation, together with the relatively small Rh-H coupling constant,[34] indicates that the hydride ligand interacts more strongly with Ir than with Rh. The $^{13}C\{^1H\}$ NMR spectrum shows a doublet of triplets at δ 191.1 ($^1J_{Rh-C}$ = 82.5 Hz) and a triplet at δ 162.7, indicating the presence of a terminal CO ligand each on Rh and Ir. The IR spectrum shows CO stretches at 2015 and 1958 cm^{-1} as well as stretches at 2134 and 2090 cm^{-1}, assigned to the C≡C stretches of the two acetylide ligands. Although the NMR data do not unambigously establish the structure of compound **12**, the structure shown in Scheme 4.4 was established by an X-ray structure determination.

Figure 4.1 shows a perspective view of the cation of compound **12**, with the dppm ligands bridging the metal nuclei in a typical manner. Relevant bond lengths and angles are given in Tables 4.5 and 4.6. While both molecules of CH_2Cl_2 of crystallization are disordered, the triflate anion is well behaved. The diphosphine groups are oriented approximately trans to each other about the metal centers (P(1)-Ir-P(3) = 167.53(6)° and P(2)-Rh-P(4) = 168.61(7)°) and are both cis to the other atoms coordinated to the metal nuclei. The geometry about Rh is tetragonal pyramid (with an agostic Rh←H-Ir as the apical site), if the interaction between this metal and the acetylide C≡C bond is considered as occupying one of the basal coordination sites, while the CO and the two dppm phosphines occupy the other sites. About the Ir the geometry is approximately octahedral. The hydrogen atom attached to the metals was not refined but was fixed in the position obtained from the Fourier

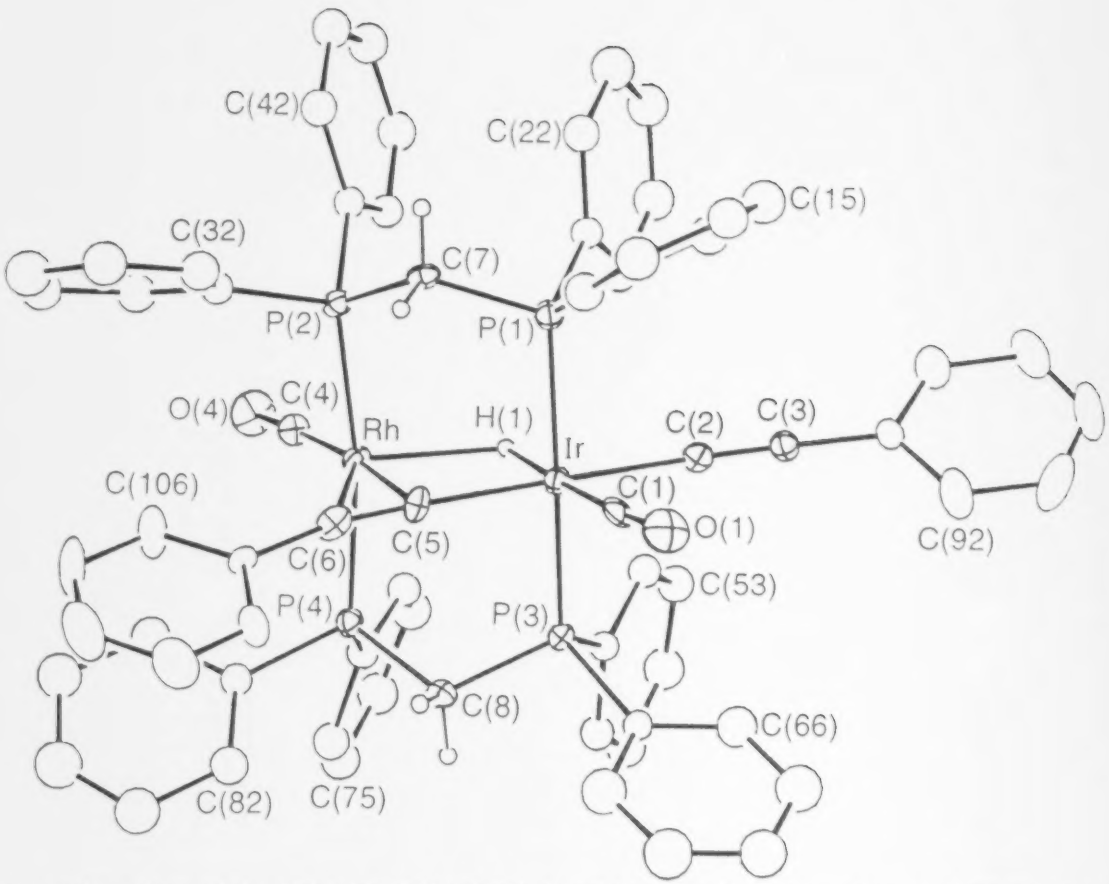

Figure 4.1. A perspective view of the $[RhIr(C{\equiv}CPh)_2(CO)_2(\mu\text{-}H)(dppm)_2]^+$ cation, showing the numbering scheme. Thermal ellipsoids are shown at the 20% level except for the hydride and methylene hydrogens, which are shown artificially small and the phenyl hydrogens, which are omitted.

Table 4.5. Selected Distances in (Å) in $[RhIr(C{\equiv}CPh)_2(CO)_2(\mu\text{-}H)(dppm)_2]\text{-}[CF_3SO_3]\cdot 2CH_2Cl_2$ (**12**)

(a) Bonded

Ir-P(1)	2.326 (2)	P(2)-C(31)	1.822 (8)
Ir-P(3)	2.332 (2)	P(2)-C(41)	1.801 (8)
Ir-C(1)	1.95 (1)	P(3)-C(8)	1.805 (7)
Ir-C(2)	2.042 (7)	P(3)-C(51)	1.824 (7)
Ir-C(5)	2.041 (8)	P(3)-C(61)	1.815 (8)
Ir-H(1)	1.6887(4)	P(4)-C(8)	1.831 (7)
Rh-P(2)	2.310 (2)	P(4)-C(71)	1.818 (8)
Rh-P(4)	2.310 (2)	P(4)-C(81)	1.801 (8)
Rh-C(4)	1.778 (8)	O(1)-C(1)	1.15 (1)
Rh-C(5)	2.228 (6)	O(4)-C(4)	1.190 (9)
Rh-C(6)	2.515(7)	C(2)-C(3)	1.185(9)
Rh-H(1)	2.0673(7)	C(3)-C(91)	1.44 (1)
P(1)-C(7)	1.830 (7)	C(5)-C(6)	1.22 (1)
P(1)-C(11)	1.811 (7)	C(6)-C(101)	1.49 (1)
P(1)-C(21)	1.827(8)		
P(2)-C(7)	1.829 (7)		

(b) Non-bonded

Ir-Rh	3.0582(8)	P(3)-P(4)	3.053(3)
P(1)-P(2)	3.056(3)		

Table 4.6. Selected Angles (deg) in $[RhIr(C{\equiv}CPh)_2(CO)_2(\mu\text{-}H)(dppm)_2][CF_3SO_3]\cdot 2CH_2Cl_2$ (**12**)

P(1)-Ir-P(3)	167.53(6)	Rh-P(2)-C(31)	111.1(3)
P(1)-Ir-C(1)	94.1(2)	Rh-P(2)-C(41)	120.5(2)
P(1)-Ir-C(2)	86.9(2)	C(7)-P(2)-C(31)	104.1(3)
P(1)-Ir-C(5)	93.0(2)	C(7)-P(2)-C(41)	103.9(3)
P(1)-Ir-H(1)	83.35(5)	C(31)-P(2)-C(41)	104.4(4)
P(3)-Ir-C(1)	97.5(2)	Ir-P(3)-C(8)	112.1(2)
P(3)-Ir-C(2)	90.1(2)	Ir-P(3)-C(51)	117.4(2)
P(3)-Ir-C(5)	90.4(2)	Ir-P(3)-C(61)	114.9(2)
P(3)-Ir-H(1)	84.89(5)	C(8)-P(3)-C(51)	104.1(3)
C(1)-Ir-C(2)	83.6(3)	C(8)-P(3)-C(61)	104.0(3)
C(1)-Ir-C(5)	94.4(3)	C(51)-P(3)-C(61)	102.7(3)
C(1)-Ir-H(1)	177.4(2)	Rh-P(4)-C(8)	111.7(2)
C(2)-Ir-C(5)	178.0(3)	Rh-P(4)-C(71)	117.2(3)
C(2)-Ir-H(1)	95.4(2)	Rh-P(4)-C(81)	113.2(3)
C(5)-Ir-H(1)	86.692)	C(8)-P(4)-C(71)	106.5(3)
P(2)-Rh-P(4)	168.61(7)	C(8)-P(4)-C(81)	104.5(3)
P(2)-Rh-C(4)	91.0(2)	C(71)-P(4)-C(81)	102.7(3)
P(2)-Rh-C(5)	89.4(2)	Ir-C(1)-O(1)	171.7(8)
P(4)-Rh-C(4)	90.8(3)	Ir-C(2)-C(3)	168.7(7)
P(4)-Rh-C(5)	87.3(2)	C(2)-C(3)-C(91)	176.9(9)
C(4)-Rh-C(5)	172.1(3)	Rh-C(4)-O(4)	178.0(7)
Ir-P(1)-C(7)	110.9(2)	Ir-C(5)-Rh	91.4(3)
Ir-P(1)-C(11)	113.8(3)	Ir-C(5)-C(6)	177.2(7)
Ir-P(1)-C(21)	117.9(2)	Rh-C(5)-C(6)	88.7(5)
C(7)-P(1)-C(11)	103.8(3)	C(5)-C(6)-C(101)	167.4(7)
C(7)-P(1)-C(21)	104.4(3)	P(1)-C(7)-P(2)	113.3(4)
C(11)-P(1)-C(21)	104.7(3)	P(3)-C(8)-P(4)	114.2(4)
Rh-P(2)-C(7)	111.3(2)		

map, therefore no significance should be attached to the derived Rh-H and Ir-H distances. The Ir-C(1) distance (1.95(1) Å) which is opposite to H(1) is significantly longer than the Rh-C(4) distance (1.778(8) Å), consistent with the high trans influence of a hydride ligand. The carbonyl geometries are normal for such terminally bound groups. The Rh-Ir distance of 3.0582(8) Å is almost exactly equal to intraligand P-P separations (P(1)-P(2) = 3.056(3)Å, P(3)-P(4) = 3.053(3) Å), suggesting that there is no significant mutual attraction of the metals, and indicating the absence of any substantial interaction between Rh and Ir. Instead the Ir-H(1) bond is viewed as functioning as an agostic bond to Rh, giving this metal an 18-electron configuration. The Rh-Ir distance is very close to that in $[RhIr(H)_2(CO)_2(\mu\text{-}Cl)(dppm)_2][BF_4]$ (3.0651(5) Å), which also does not have a formal metal-metal bond.[34] Both of the acetylides are sigma bound to Ir, with Ir-C(2) and Ir-C(5) bond lengths of 2.042(7) and 2.041(8) Å, respectively. One of the acetylide ligands is directed away from Rh, while the other one which is trans to the first one (C(2)-Ir-C(5) = 178.0(3)°), is in close proximity to Rh. This orientation of the two acetylides is similar to that found in $[Pt_2(C{\equiv}CPh)(\mu\text{-}\eta^1{:}\eta^2\text{-}C{\equiv}CPh)(\mu\text{-}SiMe_2)(PR_3)_2]$ (R = cyclo-C_6H_{11}).[35] The bending of the phenyl group of the acetylide ligand that is directed toward Rh, away from this metal (C(5)-C(6)-C(101) = 167.4(7)°), the closeness of the carbon atoms of this acetylide to Rh (Rh-C(5) = 2.228(6) Å, Rh-C(6) = 2.515(7) Å), suggest that there is a π interaction between Rh and the C(5)-C(6) acetylide bond. This π interaction is supported by the significant difference between the two acetylide C≡C stretches in the IR spectrum of compound **12** (2134 cm^{-1} and 2090 cm^{-1}). However, the small difference in the C≡C distances of the two acetylide ligands (C(2)-C(3) = 1.185(9) Å, C(5)-C(6) = 1.22(1) Å) indicates that the π interaction of the latter is weak. A similar bending of the phenyl group of one of the acetylide ligands was observed in

$[Pt_2(C{\equiv}CPh)_2(\mu\text{-}\eta^1{:}\eta^2\text{-}C{\equiv}CPh)(dppm)_2][ClO_4]$.[36] There is a slight bending of the Ir-C(2)-C(3) moiety (Ir-C(2)-C(3) = 168.7(7)°), while the Ir-C(5)-C(6) moiety is almost linear (Ir-C(5)-C(6) = 177.2(7)°). Bending of the same magnitude was observed in the acetylide ligands of, $[Rh_2(CO)_2(\mu\text{-}\eta^1{:}\eta^2\text{-}C{\equiv}C^tBu)$-$(dppm)_2][ClO_4]$[37] and $[Mn_2(\mu\text{-}H)(\mu\text{-}\eta^1{:}\eta^2\text{-}C{\equiv}CPh)(CO)_6(\mu\text{-}dppm)]$.[7a]

When the reaction of compound **1** with phenylacetylene is started at -78 °C, and monitored by NMR, while gradually warming the reaction mixture, a number of intermediates is observed. At -78 °C the NMR spectra of the reaction mixture, using 1 equiv of phenyacetylene, show the presence of **1** as the major compound, together with the compound, $[RhIr(CH_3)(H)(CO)_3(\mu\text{-}\eta^1{:}\eta^2\text{-}C{\equiv}CPh)(dppm)_2][CF_3SO_3]$ (**13**), and a small amount of another species, $[RhIr(CH_3)(CO)_3(\mu\text{-}C{=}C(H)Ph)(dppm)_2][CF_3SO_3]$ (**14**) (vide infra). As the temperature is gradually increased, the proportions of compounds **13** and **14** increase steadily, while that of **1** decreases. At -20 °C, compound **11**, the acetylide product, begins to form. As the temperature is increased further the proportions of both **1** and **13** decrease while those of **14** and **11** increase. At +25 °C the NMR spectra show the presence of only compounds **14** and **11**. Using excess reagent, the NMR spectra show a faster reaction than using 1 equiv such that by the time the temperature reaches 0 °C, compound **1** is depleted, and compound **11** begins to form. At +20 °C compound **12**, the diacetylide hydride product, begins to form while none of **13** is left.

The ^1H NMR spectrum of compound **13**, shows the hydride resonance as a triplet at δ -8.87, and the methyl resonance as a triplet at δ 0.33. Selective ^{31}P-decoupling experiments show that both the methyl and the hydride ligands are bound to Ir, since they couple only to the phosphorus nuclei bound to this metal. The $^{13}C\{^1H\}$ NMR spectrum shows a doublet of triplets

at δ 192.8 ($^1J_{Rh-C}$ = 80.5 Hz) and a broad resonance at δ 193.1, with intensity ratios of 2:1, indicating that there are two CO ligands terminally bound to Rh and one terminally bound to Ir in compound **13**. It appears that the chemical shifts of the two CO ligands bound to Rh are coincidentally equivalent. The presence of the acetylide ligand in this compound, is inferred from the presence of the hydride ligand. A trans orientation of the hydride and methyl ligands is proposed as the factor inhibiting methane loss in **13**, since it is converted to compound **14**, as the temperature is raised. The proposed μ-η^1:η^2- bonding mode of the acetylide in **11** and **13** is based on the fact that this bonding mode is adopted in several related compounds[7a,35,36,37,38] (also see compound **5**).

The next species observed, **14**, is proposed to be a phenylvinylidene complex. The ^{1}H NMR spectrum of compound **14** shows the vinylidene proton resonance as a triplet at δ 8.53. It also shows a broad resonance at δ 0.27 due to the methyl group protons. Selective ^{31}P decoupling experiments show that the methyl group is still bound to Ir. They also show that the vinylidene proton couples to the phosphorus nuclei bound to Ir. Coupling of the vinylidene protons to the dppm phosphorus nuclei is usually not observed in these compounds, so it is not clear why such coupling to only the phosphorus nuclei bound to one of the metals occurs in **14**. While the vinylidene protons in $[Pd_2Cl_2(\mu\text{-}C{=}CH_2)(dppm)_2]$[39] show coupling to the phosphorus nuclei, they couple equally with all the four phosphorus nuclei, in contrast to what is observed in compound **14**. Although the formulation of a vinylidene that is terminally bound to Rh and donates its π electrons to Ir could account for the coupling observed in **14**, such a formulation is inconsistent with electron counting. The $^{13}C\{^1H\}$ NMR spectrum of **14** shows a doublet of multiplets at δ 200.6 ($^1J_{Rh-C}$ = 5.0 Hz), a doublet of triplets at

δ 193.7 ($^1J_{Rh-C}$ = 54.3 Hz), and a broad resonance at δ 180.8, indicating the presence of a CO ligand on Ir that interacts very weakly with Rh (inferred from the small Rh-C coupling of 5 Hz), as well as a terminally bound CO ligand each on Rh and Ir. The assigned orientation of the vinylidene ligand in **14**, such that the proton of this ligand is closer to Ir, is based on the observed coupling between this proton and the Ir-bound phosphorus nuclei, and the fact that the compound is subsequently transformed to **11** via methane elimination, suggesting that the proton is close to Ir, such that its transfer to this metal can lead to elimination of methane. It is not clear, however, what involvement **14** has in this reductive elimination.

Although compounds **1** and **2** react quite differently with the non-activated alkynes, PhC≡CH and HC≡CH, their reactions with the activated alkyne, DMAD, yield similar products, $[MIr(RC{=}C(CH_3)R)(CO)_3(dppm)_2][CF_3SO_3]$ (R = CO_2Me; M = Rh (**15**), Ir (**16**)), in which the alkyne has apparently inserted into the M-C (alkyl) bonds of the precursor complexes (as shown in Schemes 4.5 and 4.6).

The ^1H NMR spectrum of the 'RhIr' compound (**15**) shows the dppm methylene proton resonances as multiplets at δ 4.35 and 3.65. It also shows three singlets at δ 3.33, 2.22, and 0.81, which are assigned to the two DMAD methyl groups and the methyl group that has undergone migratory insertion. The shifting of the methyl resonance from a triplet at δ -0.08 in compound **1** to a singlet at lower field (δ 0.81) in compound **15**, is consistent with the formal insertion of the DMAD into the M-CH_3 bond. The $^{13}C\{^1H\}$ NMR spectrum shows two doublets of triplets at δ 197.9 ($^1J_{Rh-C}$ = 4.0 Hz) and 194.4 ($^1J_{Rh-C}$ = 55.3 Hz), and a triplet at δ 176.8, indicating that there is one semibridging CO ligand, showing a very weak interaction with Rh, as well as a terminally bound CO ligand each on Rh and Ir in compound **15**. The IR spectrum of

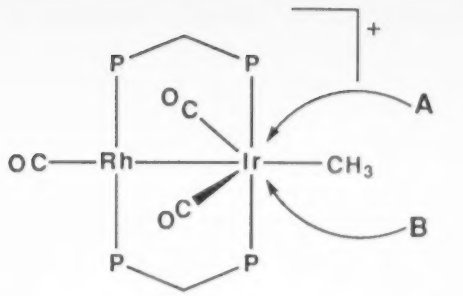

1

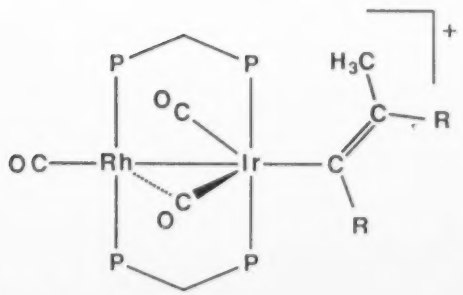

15

Scheme 4.5.

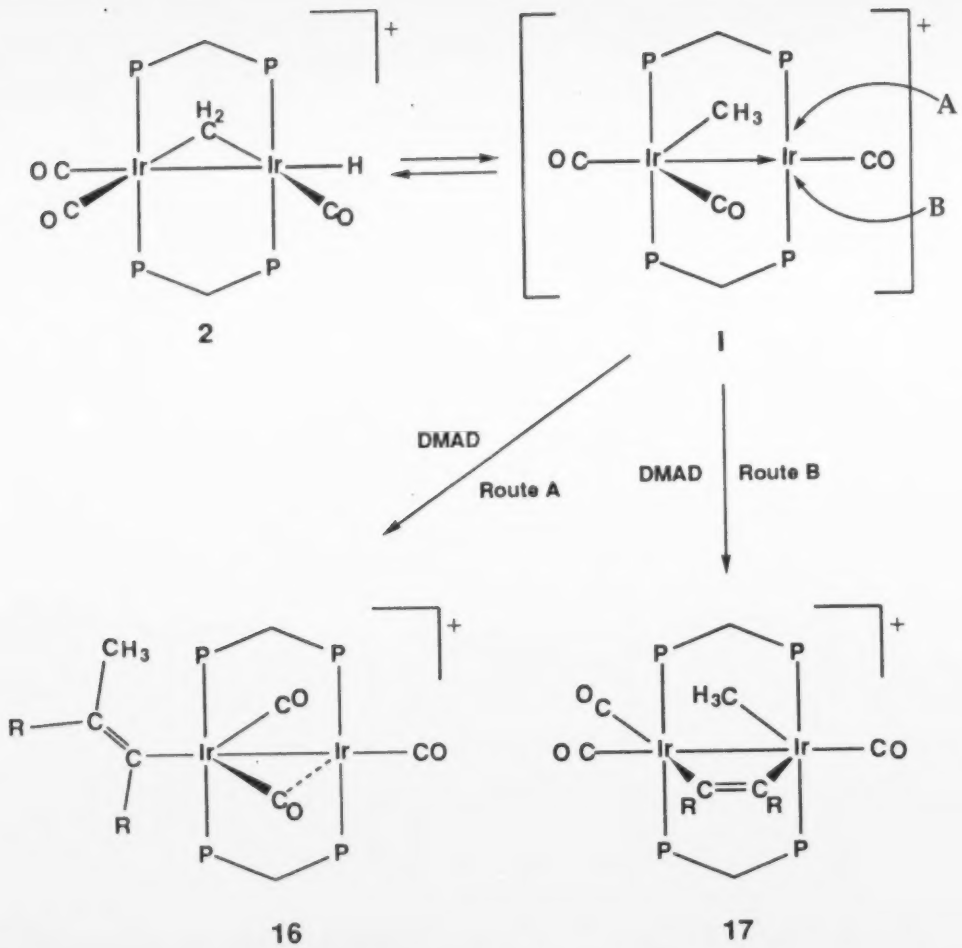

Scheme 4.6.

compound **15** shows a peak at 1720 cm^{-1}, which is consistent with the presence of a semibridging CO ligand, as well as peaks at 2022 and 1995 cm^{-1}, due to the terminal CO ligands. In addition to these stretches, the IR spectrum of **15** also shows bands at 1698 cm^{-1}, due to the CO stretch of the inserted DMAD, and at 1641 cm^{-1}, assigned to the C=C stretch of the same ligand.

The ^{1}H NMR spectrum of the diiridium compound (**16**) shows two multiplets at δ 4.43 and 3.60, representing the dppm methylene proton resonances, as well as three singlets at δ 3.27, 2.23 and 0.68, which are assigned to the two methyl groups of the inserted DMAD and the methyl group coordinated to the DMAD as a result of the insertion. The $^{13}C\{^{1}H\}$ NMR spectrum shows a broad resonance at δ 194.7 and two triplets at δ 192.0 and 179.5, while the IR spectrum shows stretches at 2015, 1998 and 1717 cm^{-1}, indicating the presence of two terminally bound and one semibridging CO ligand in compound **16**. The identification of one CO as semibridging is based on the low CO stretch in the IR spectrum and the ^{13}C chemical shift in the NMR spectrum which is not unlike those of the terminal groups. Analogies with compound **15** also support this assignment. The CO stretch of the inserted DMAD ligand appears at 1695 cm^{-1} in the IR spectrum, while the band at 1642 cm^{-1} in this spectrum is assigned to the C=C stretch of the same ligand. The similarities in the spectroscopic data for **15** and **16** support the assignment of similar structures to both compounds.

In addition to compound **16**, the reaction of **2** with DMAD also gives $[Ir_2(CH_3)(CO)_3(\mu\text{-DMAD})(dppm)_2][CF_3SO_3]$ (**17**). A typical ratio of compound **16** to compound **17**, formed in this reaction is 2:1. However, when the reaction is started at -78°C and warmed to room temperature, both products are still obtained but in the reverse ratios. The ^{1}H NMR spectrum of

compound **17** shows the dppm methylene proton resonances as multiplets at δ 4.87 and 4.26, the methyl resonances of the coordinated DMAD as singlets at δ 3.53 and 2.23, and the metal bound methyl resonance as a triplet at δ -0.40. The $^{13}C\{^1H\}$ NMR spectrum shows triplets at δ 182.8, 175.9 and 152.5, and the IR spectrum shows CO stretches at 2029, 2001 and 1982 cm^{-1}, indicating the presence of three terminal CO ligands in compound **17**. The IR spectrum also shows the CO stretch of the coordinated DMAD at 1690 cm^{-1}, and the band at 1635 cm^{-1} in this spectrum is assigned to the C≡C stretch of the same ligand. All the NMR data are consistent with the structure of **17** shown in Scheme 4.6.

Discussion

The results reported in the previous section demonstrate that the compounds, $[RhIr(CH_3)(CO)_3(dppm)_2][CF_3SO_3]$ (**1**) and $[Ir_2(H)(CO)_3(\mu\text{-}CH_2)\text{-}(dppm)_2][CF_3SO_3]$ (**2**) show some similarities in their reactions with alkynes (example with DMAD), but also show some substantial differences. Apparently subtle electronic, and probably steric, differences in compounds **1** and **2** as well as in the alkynes employed give rise to very different products in these reactions. In certain cases the final products obtained even depend on the reaction temperature, since it appears that some reactions proceed via two competing pathways, one of which is more favored at one temperature than the other.

Apparently in the reactions of compound **2** with acetylene and phenylacetylene, the interaction of the acetylenic C≡C and the C-H bond(s) with the metal centers is competitive. The interaction with the C-H bonds is the predominant one at -78 °C in the reaction with acetylene, resulting in the

formation of the hydrido acetylide product, $[Ir_2(H)(CH_3)(CO)_3(\mu\text{-}\eta^1{:}\eta^2\text{-}C{\equiv}CH)(dppm)_2][CF_3SO_3]$(**5**), by the activation of one of these bonds. Compound **5** is then converted, at room temperature, to $[Ir_2(CH_3)(CO)_3(\mu\text{-}C{=}CH_2)(dppm)_2][CF_3SO_3]$ (**4**), as shown in Scheme 4.1 In the case of the reaction with phenylacetylene, the interaction with the acetylenic C≡C bond is favored at the same temperature, and this results in the formation of the alkyne-bridged product, $[Ir_2(CH_3)(CO)_3(\mu\text{-}PhC_2H)(dppm)_2][CF_3SO_3]$ (**7**) (see Scheme 4.2). A similar competitive interaction was reported in the reaction of $[Rh_2(CO)_3(dppm)_2]$ with phenylacetylene, resulting in a mixture of the bridging alkyne and phenylvinylidene complexes, $[Rh_2(CO)_2(\mu\text{-}PhC_2H)(dppm)_2]$ and $[Rh_2(CO)_2(\mu\text{-}C{=}C(H)Ph)(dppm)_2]$, respectively, at higher temperatures, but giving the phenylvinylidene complex as the sole product at room temperature.[19] Another such competitive C-H bond addition and coordination of alkyne has been reported in the thermal reaction of $[Pt(H)(CH_2C(CH_3)_3)(dcpe)_2]$ (dcpe = bis(dicyclohexylphosphino)ethane) with *tert*-butyl acetylene, which yields approximately equal amounts of the hydrido-acetylide and η^2-alkyne products.[40]

It is perhaps surprising that at -78 °C, compound **2** favors the activation of the alkyne C-H bond of acetylene but not for phenylacetylene for which coordination of the C≡C bond is favored. One might expect that the reverse would be the case, since the increased acidity of the phenylacetylene should make it more prone to C-H activation. On the other hand, it is possible that this observation is due to the greater stability of the phenylacetylene-bridged product, relative to the acetylene-bridged product because of the backbonding interaction between the metal and the alkyne, which is expected to be greater in the phenylacetylene-bridged product than in its acetylene analogue.

The transformation of the acetylide hydride compound, **5**, to the vinylidene-bridged compound, **4**, presumably proceeds through migration of the hydride ligand to the β carbon atom of the acetylide via the adjacent metal, as shown below. We suggest that migration of the hydride ligand, in **5**,

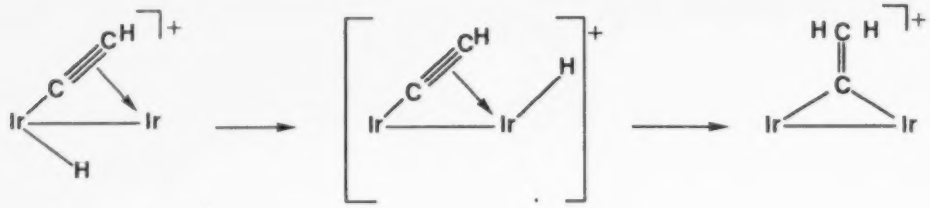

from one metal to the other can bring it into close proximity of the β carbon of the acetylide, as shown, as a result of the μ-η^1:η^2- coordination mode of the latter ligand, and this can then facilitate the subsequent metal-to-β carbon migration to give compound **4**.

Since both metals in compound **4** are coordinatively saturated, the formation of the CO substitution product $[Ir_2(CH_3)(CO)_2(PMe_3)(\mu\text{-}C{=}CH_2)(dppm)_2][CF_3SO_3]$ (**6**) could proceed via one of two pathways: (i) by dissociation of one of the CO ligands in the former complex followed by coordination of the PMe_3 ligand, (ii) or by a shift of the vinylidene ligand from the bridging position to a terminal position on the Ir bearing the methyl ligand, followed by attack of the PMe_3 at the adjacent metal and simultaneous dissociation of one CO ligand and a shift of the vinylidene ligand to the bridging position. Such a bridged-to-terminal vinylidene transformation has been observed in some closely related diiridium complexes.[20b]

The formation of $[RhIr(CH_3)(CO)_3(dppm)(HC{=}C(H)P(Ph_2)CH_2PPh_2)][CF_3SO_3]$ (**10**), from compound **1** and acetylene involves the very rare, formal insertion of the acetylene in one of the Rh-P bonds of compound **1**. A related insertion into a M-P bond involving a dppm ligand was reported in the

isomerization of $[Fe_2(CO)_5(\mu\text{-}CHCHCO)(\mu\text{-}P(Ph_2)CH_2PPh_2)]$, which is formed in the reaction of $[Fe_2(\mu\text{-}CO)(CO)_6(\mu\text{-}dppm)]$ with acetylene under UV irradiation.[41] This isomerization occurs in solution at 90 °C, to give $[Fe_2(\mu\text{-}CO)(CO)_5(\mu\text{-}C(CH_2)P(Ph_2)CH_2PPh_2)]$, in a reaction in which CCH_2 (a tautomer of acetylene) formally inserts into the Fe-P bond as shown below.

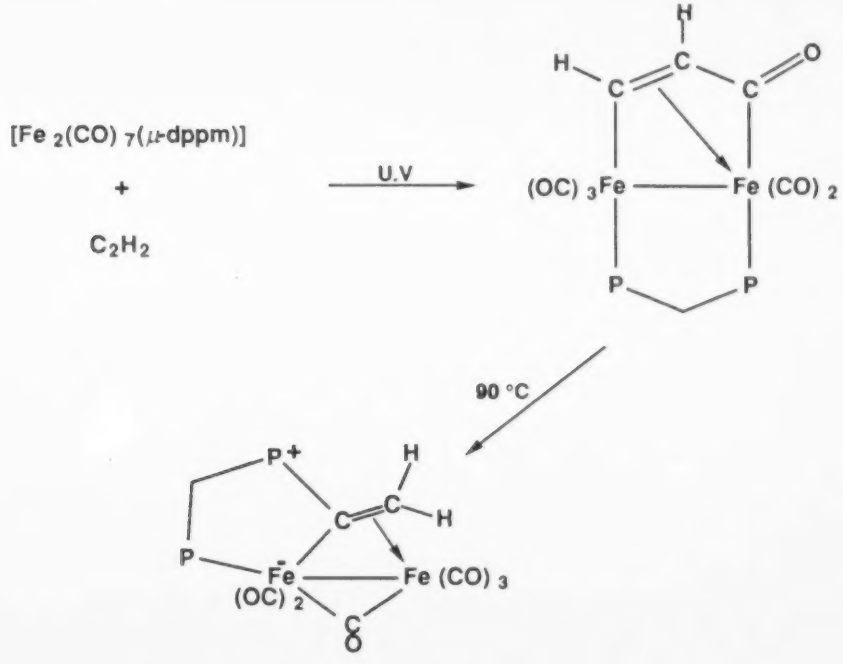

Also the $C_4H_4PPh_2$ ligand in $[Mn_2(\mu\text{-}C_4H_4PPh_2)(\mu\text{-}PPh_2)(CO)_5]$, resulting from the photolytic reaction of $[Mn_2(\mu\text{-}PPh_2)_2(CO)_8]$ with acetylene, is formally derived from a μ-PPh_2 group in the precursor, by a double insertion of acetylene into one of the M-P bonds.[42] Reactions that result in the insertion of a variety of alkynes into the Co-P bond of $[(OC)_4Ru(\mu\text{-}PPh_2)Co(CO)_3]$ have also been reported.[43] However, these examples, arising from insertion of alkynes or a vinylidene ligand into M-P bonds, required heating or photolysis, whereas compound **10** is formed at room temperature.

The conversion of $[RhIr(CH_3)(CO)_3(\mu\text{-}C_2H_2)(dppm)_2][CF_3SO_3]$ (**9**) to compound **10**, as shown in Scheme 4.3, can be seen as resulting from dissociation of one Rh-bound end of a diphosphine, followed by nucleophilic attack by this phosphorus at the Rh end of the bridged alkyne, as mentioned earlier. This is accompanied by cleavage of the Rh-C (coordinated acetylene) bond, with concomitant donation of the π electrons of the resulting unsaturated ligand to Rh. Presumably this transformation of the alkyne-bridged product, in the reaction with acetylene, occurs with compound **9** and not with **3** because the lability of a Rh-P bond is greater than that of an Ir-P bond.

On the basis of the intermediates observed, and the variations in the ratios of these compounds with temperature, in the reaction of compound **1** with phenylacetylene, the pathway shown in Scheme 4.4 is proposed. Apparently compound **1** oxidatively adds phenylacetylene to give the methyl hydrido-acetylide compound, $[RhIr(CH_3)(H)(CO)_3(\mu\text{-}\eta^1\text{:}\eta^2\text{-}C{\equiv}CPh)(dppm)_2][CF_3SO_3]$ (**13**), which isomerizes to give the phenylvinylidene methyl compound, $[RhIr(CH_3)(CO)_3(\mu\text{-}C{=}C(H)Ph)(dppm)_2][CF_3SO_3]$ (**14**). Compound **14** is then transformed to the monoacetylide compound, $[RhIr(CO)_3(\mu\text{-}\eta^1\text{:}\eta^2\text{-}C{\equiv}CPh)(dppm)_2][CF_3SO_3]$ (**11**), which in the presence of excess phenylacetylene, loses one CO ligand and oxidatively adds phenylacetylene again to give the hydrido-diacetylide product, $[RhIr(C{\equiv}CPh)_2(CO)_2(\mu\text{-}H)(dppm)_2][CF_3SO_3]$ (**12**) as the final product. While the transformation of **14** to **11** involves the reductive elimination of methane, it is not clear what function the former compound plays in this process (as mentioned earlier), although it may be that its vinylidene proton migrates to Ir before such an elimination occurs. Presumably the hydrido-methyl product

which immediately precedes methane elimination differs from **13** in having a cis arrangement of these ligands, allowing facile elimination.

It is has been shown that C-H activation of phenylacetylene occurs at -78 °C in its reaction with compound **1**, while this does not occur at the same temperature, in its reaction with **2** (although a product, compound **8**, obtained from C-H activation is formed in this reaction with **2** at 20 °C). This is surprising, considering the facile C-H activation of a coordinated methyl group that is observed in the formation of the **2** (see Chapter 3), whereas no such activation is observed in **1**. It is not clear why this occurs. The observation that compound **14** is subsequently transformed to **11** through methane elimination, whereas no such elimination occurs in the analogous diiridium phenylvinylidene compound, **8**, is possibly due to the fact that reductive elimination is more favored in Rh than in Ir compounds.

It has also been shown that both the reaction of compound **2** with acetylene and that of compound **1** with phenylacetylene, starting at -78 °C, result in hydrido-acetylide-to-vinylidene isomerizations. These involved the conversion of compound **5** to compound **4** and the conversion of compound **13** to **14** , respectively. A similar isomerization was reported in the reaction of $[Ir_2I_2(CO)(\mu\text{-}CO)(dppm)_2]$ with phenylacetylene.[20a] This reaction yielded the hydrido-acetylide complex, $[Ir_2(H)I(CO)_2(\mu\text{-}C{\equiv}CPh)(dppm)_2][I]$, at -40 °C, which isomerized at room temperature to the phenylvinylidene complex, $[Ir_2I_2(CO)_2(\mu\text{-}C{=}C(H)Ph)dppm)_2]$. Such isomerizations have also been reported in several mononuclear complexes.[44] The more unusual reverse process (ie. vinylidene-to-hydrido-acetylide) has also been reported, for example in the conversions of $[Mn_2(\mu\text{-}\eta^1{:}\eta^2\text{-}C{=}C(H)Ph)(CO)_6(\mu\text{-}dppm)]$ and

$[Mn_2(\mu\text{-}\eta^1\text{:}\eta^2\text{-}C{=}C(H)^tBu)(CO)_6(\mu\text{-}dppm)]$ to the corresponding hydrido-acetylide complexes.[7a] The isomerizations of compound **5** and compound **13**, however, appear to be irreversible.

It is proposed that all the reactions of compound **2**, proceed through the intermediate methyl complex, $[Ir_2(CH_3)(CO)_3(dppm)_2][CF_3SO_3]$ (**I**) (see Chapter 3), and it is suggested that in the reaction with DMAD, the alkyne attacks the unsaturated metal in the methyl complex at two different sites, as shown in Scheme 4.6, giving rise to the two products observed. Attack at the site cis to the methyl group leads to insertion into the M-CH_3 bond to give $[Ir_2(RC{=}C(CH_3)R)(CO)_3(dppm)_2][CF_3SO_3]$ (R = CO_2Me) (**16**), while attack at the other site gives $[Ir_2(CH_3)(CO)_3(\mu\text{-DMAD})(dppm)_2][CF_3SO_3]$ (**17**). In the case of compound **1**, on the other hand, if migration of one of the CO ligands on Ir to Rh, with concomitant attack of the DMAD at the Ir metal is presumed, as was observed in its reaction with phenylacetylene, then attack at Ir from both the front and the back of the metal-phosphorus plane will result in a cis orientation of the methyl group and the coordinated DMAD. Hence insertion is favorable in both cases and the reaction yields, $[RhIr(RC{=}C(CH_3)R)(CO)_3(dppm)_2][CF_3SO_3]$ (R = CO_2Me) (**15**), as the only product. It is not clear why the reactions of DMAD with **1** and **2** result in insertion of the alkyne into M-CH_3 bonds of the complexes (or the reactive intermediate in the case of **2**), whereas the other alkynes do not yield any insertion products.

References and Footnotes

1. (a) Werner, H.; Hohn, A.; Schulz, M. *J. Chem. Soc., Dalton Trans.* **1991**, *777*. (b) Bianchini, C.; Peruzzini, M.; Vacca, A.; Zanobini, F. *Organometallics* **1991**, *10*, 3697. (c) Holton, J.; Lappert, M. F.; Pearce, R.; Yarrow, P. I. W. *Chem. Rev.* **1983**, *83*, 135 and references therein.
2. (a) Bruce, M. I. *Chem. Rev.* **1991**, *91*, 197 and references therein. (b) Werner, H. *Angew. Chem. Int. Ed. Eng.* **1990**, *29*, 1077 and references therein.
3. (a) Shore, N. E. *Chem. Rev.* **1988**, *88*, 1081. (b) Trost, B. M.; Dyker, G.; Kulawiec, R. J. *J. Am. Chem. Soc.* **1990**, *112*, 7809.
4. (a) Dyke, A. F.; Knox, S. R.; Naish P. J.; Taylor, G. E. *J. Chem. Soc., Chem. Commun.* **1980**, 409. (b) Finnimore, S. R.; Knox, S. R.; Taylor, G. E. *J. Chem. Soc., Chem. Commun.* **1980**, 411. (c) Adams, R. D.; Chen, L.; Wu, W. *Organometallics* **1993**, *12*, 4112. (d) Adams, R. D.; Chen, G.; Chen, L.; Yin, J.*Organometallics* **1993**, *12*, 2644. (e) Adams, R. D.; Chen, G.; Chen, L.; Wu, W.; Yin, J. *J. Am. Chem. Soc.* **1991**, *113*, 9406.
5. Landon S. J.; Shulman, P. M.; Geoffroy, G. L. *J. Am. Chem. Soc.* **1985**, *107*, 6739.
6. Horton, A. D.; Orpen, A. G. *Organometallics* **1992**, *11*, 8.
7. (a) Alonso, F. J. G.; Riera, V.; Ruiz, M. A.; Tripicchio, A.; Camellini, M. T. *Organometallics* **1992**, *11*, 370. (b) Vaartstra, B. A.; Cowie, M. *Organometallics* **1990**, *9*, 1594. (c) Sutherland, B. R.; Cowie, M. *Organometallics* **1985**, *4*, 1801.
8. Yamashita, H.; Tanaka, M.; Goto, M. *Organometallics* **1993**, *12*, 988.

9. Doedens, R. J.; Ibers, J. A. *Inorg. Chem.* **1967**, *6*, 204.
10. Walker, N.; Stuart, D. *Acta Crystallogr., Sect. A: Found Crystallogr.* **1983**, *A39*, 1581.
11. Programs used were those of the Enraf-Nonius Structure Determination Package by B. A. Frenz, in addition to local programs by R. G. Ball.
12. Cromer, D. T.; Waber, J. T. *International Tables for Crystallography*; Kynoch Press: Birmingham, England, 1974; Vol. IV, Table 2.2A.
13. Stewart, R. F.; Davidson, E. R.; Simpson, W. T. *J. Chem. Phys.* **1965**, *42*, 3175.
14. Cromer, D. T.; Liberman, D. *J. Chem. Phys.* **1970**, *53*, 1891.
15. NMR signals for products that are obtained as mixtures are taken from the spectra of the mixtures.
16. All NMR signals have the appropriate ratios of intensity.
17. IR spectra are of the samples with natural abundance carbon.
18. See, for example: (a) Vaartstra, B. A.; Xiao, J.; Jenkins, J. A.; Verhagen, R.; Cowie, M. *Organometallics* **1991**, *10*, 2708. (b) Vaartstra, B. A. Ph.D. Thesis, University of Alberta, 1989. (c) Mague, J. T. *Organometallics* **1986**, *5*, 918. (d) Cowie, M.; Vasapollo, G.; Sutherland, B. R.; Ennett, J. P. *Inorg. Chem.* **1986**, *25*, 2648. (e) Sutherland, B. R.; Cowie, M. *Organometallics* **1984**, *3*, 1869. (f) Mague, J. T; Klein, C. L.; Majeste, R. J.; Stevens, E. D. *Organometallics* **1984**, *3*, 1860. (g) Cowie, M.; Dickson, R. S.; Hames B. W. *Organometallics* **1984**, *3*, 1879. (h) Puddephatt, R. J.; Thomson, M. A. *Inorg. Chem.* **1982**, *21*, 725. (i) Puddephatt, R. J.; Thomson, M. A. *Inorg. Chim. Acta* **1980**, *45*, L281.
19. (a) Berry, D. H.; Eisenberg, R. *Organometallics* **1987**, *6*, 1796. (b) Berry, D. H.; Eisenberg, R. *J. Am. Chem. Soc.* **1985**, *107*, 7181.
20. (a) Xiao, J.; Cowie, M. *Organometallics* **1993**, *12*, 463. (b) Wang, L. S.;

Cowie; M., to be submitted for publication.

21. $^{3}J_{P\text{-}C}$ for the second ^{13}C NMR signal is not well resolved.
22. Compounds such as **3**, with an alkyne bridging two metals parallel to the metal-metal axis, are sometimes referred to as dimetalated olefinic compounds in which case reference is made to the C=C stretch.
23. (a) Berenguer, J. R.; Falvello, L. R.; Lalinde, E.; Tomas, M. *Organometallics* **1993**, *12*, 6. (b) Matsuzaka, H.; Hirayama, Y.; Nishio, M.; Mizobe, Y.; Hidai, M. *Organometallics* **1993**, *12*, 36. (c) Touchard, D.; Haquette, P.; Pirio, N.; Toupet, L.; Dixneuf, P. H. *Organometallics* **1993**, *12*, 3132.
24. $^{13}C\{^{1}H\}$ NMR spectra are of ^{13}CO-enriched samples, unless otherwise stated.
25. Friebolin, H. *Basic One- and Two-Dimensional NMR Spectroscopy*; VCH Publishers: New York and Weinheim, Germany, 1991, (a) Chapter 10 (b) p 89.
26. Mague, J. T; Klein, C. L.; Majeste, R. J.; Stevens, E. D. *Organometallics* **1984**, *3*, 1860.
27. Tolman, C. A.; Meakin, P. Z.; Lindner, D. L.; Jesson, J. P. *J. Am. Chem. Soc.* **1974**, *96*, 2762.
28. Thomas, J. L. *Inorg. Chem.* **1978**, *17*, 1507 and references therein.
29. Harrison, N. C.; Murray, M.; Spencer, J. L.; Stone, F. G. A. *J. Chem. Soc., Dalton Trans.* **1978**, 1337.
30. See, for example: (a) Mann, B. E.; Taylor, B. F. *^{13}C Data for Organometallic Compounds*; Academic Press: London, 1981, p 188. (b) bodner, G. M.; Storhoff, B. N.; Doddrell, D.; Todd, L. J. *J. Chem. Soc. Chem. Commun.* **1970**, 1530. (c) Jesse, A. C.; Gijben, H. P.; Stufkens, D. J.; Vrieze, K. *Inorg. Chim. Acta* **1978**, *31*, 203. (d) Maisonnat, A.; Poilblanc, R. *Inorg. Chim. Acta* **1978**, *29*, 203.

31. Kegley, S. E.; Pinhas, A. R. *Problems and Solutions in Organometallic Chemistry;* University Science books: Mill Valley, CA, 1986, p 11.

32. Takats, J.; Washington, J.; Santarsiero, B. D., submitted for publication.

33. Antwi-Nsiah, F.; Cowie, M. *Organometallics* **1992**, *11*, 3157.

34. Vaartstra, B. A.; Cowie, M. *Inorg. Chem.* **1989**, *28*, 3138.

35. Ciriano, M.; Howard, J. A. K.; Spencer, L.; Stone, F. G. A. *J. Chem. Soc., Dalton Trans.* **1979**, 1749.

36. Yam, V. W.; Chan, L.; Lai, T. *Organometallics* **1993**, *12*, 2197.

37. Cowie, M.; Loeb, S. J. *Organometallics* **1985**, *4*, 852.

38. See for example: (a) Esteruelas, M. A.; Lahuerta, O.; Modrego, J.; Nurnberg, O.; Oro, L. A.; Rodriguez, L.; Sola, E.; Werner, H. *Organometallics* **1993**, *12*, 266. (b) McEwan, D. M.; Markham, D. P.; Pringle, P. G.; Shaw, B. L. *J. Chem. Soc., Dalton Trans.* **1986**, 1809. (c) Hutton, A.; Langrick, C. R.; McEwan, D. M.; Pringle, P. G.; Shaw, B. L. *J. Chem. Soc., Dalton Trans.* **1985**, 2121.

39. Higgins, S. J.; Shaw, B. L. *J. Chem. Soc., Chem. Commun.* **1986**, 1629.

40. Hackett, M.; Whitesides, G. M. *J. Am. Chem. Soc.* **1988**, *110*, 1449.

41. Hogarth, G.; Knox, S. A. R.; Lloyd, B. R.; Macpherson, K. A.; Morton, D. A. V.; Orpen, A. G. *J. Chem. Soc., Chem. Commun.* **1988**, 360.

42. Braga, D.; Caffyn, A. J. M.; Jennings, M. C.; Mays, M. J.; Manojlovic-Muir, L.; Raithby, P. R.; Sabatino, P.; Woulfe, K. W.; *J. Chem. Soc., Chem. Commun.* **1989**, 1401.

43. Regragui, R.; Dixneuf, P. H.; Taylor, N. J.; Carty, A. J. *Organometallics* **1990**, *9*, 2234.

44. See, for example: (a) Hohn, A.; Werner, H. *J. Organomet. Chem.* **1990**, *382*, 255. (b) Hohn, A.; Otto, H.; Dziallas, M.; Werner, H. *J. Chem. Soc., Chem. Commun.* **1987**, 852. (c) Garcia alonso, F. J.; Hohn, A.; Wolf, J.; Otto, H.;

Chapter 5

The Reactions of $[Ir_2(H)(CO)_2(\mu\text{-}H)_2(dppm)_2][BF_4]$ and Related Compounds with Alkynes and Alkenes

Introduction

The reaction of binuclear, dppm-bridged complexes with alkynes has been of longstanding interest to this research group,[1] because of the diversity of chemistry that can result in the presence of two metal centers. Some of this diversity was shown in the previous chapter in which a variety of products were obtained depending on the alkynes or on the combinations of metals. The reactions of alkynes or other unsaturated substrates with metal hydrides has been a recurring theme[1d,1g,1j] owing to the relevance of such studies in modelling binuclear catalysts in hydrogenation reactions. Earlier work[1d] had shown that $[Ir_2(H)_2(CO)_2(\mu\text{-}Cl)(dppm)_2][BF_4]$ (**I**) reacted with phenylacetylene and dimethyl acetylenedicarboxylate (DMAD) to give the compounds, $[Ir_2(RC{=}C(H)R')_2(CO)_2(\mu\text{-}Cl)(dppm)_2][BF_4]$ (R=H, R'=Ph (**IIa**) and R=R'=CO_2Me (**IIb**), respectively), in which alkyne insertion into both Ir-H bonds of the precursor had occurred. Subsequent reaction of **IIa** with H_2 gave styrene and two isomers of the tetrahydride, $[Ir_2(H)_4Cl(CO)_2(dppm)_2][BF_4]$, products of the reaction of **I** with H_2. The hydrido groups of **I** and the vinyl moities of **II** were separated by a chloro bridge in each case, so intramolecular coupling of these groups did not seem possible, and hydrogenolysis appeared to occur individually at each metal center, so some of the potential advantages of involving both metal centers in a cooperative

manner did not seem feasible. We therefore turned to chemistry of the trihydride species, $[Ir_2(H)(CO)_2(\mu\text{-}H)_2(dppm)_2][BF_4]$ (**1**).[2] The fact that two of the hydride ligands are adjacent, and there is no halide ligand separating both metals, which could possibly inhibit hydride mobility about the metal core in this compound, suggested that facile hydrogenation chemistry might be observed.

Experimental Section

General experimental conditions were as described in Chapter 2. Hexafluorobut-2-yne and tetrafluoroethylene were purchased from PCR Incorporated, while diphenylacetylene was purchased from Aldrich. $[Ir_2(CO)_3(dppm)_2]$ (**2**)[3] was prepared as previously reported, while $[Ir_2(H)(CO)_2(\mu\text{-}H)_2(dppm)_2][BF_4]$ (**1**) was prepared by a modified procedure of that reported.[2] Spectroscopic parameters for the compounds prepared are found in Tables 5.1 and 5.2.

Preparation of Compounds. (a) $[Ir_2(H)_2(CO)_2(\mu\text{-}H)(\mu\text{-DMAD})(dppm)_2][BF_4]$ (3). To the compound $[Ir_2(H)(CO)_2(\mu\text{-}H)_2(dppm)_2][BF_4]$ (**1**) (60 mg, 0.043 mmol) dissolved in 5 mL of CH_2Cl_2, was added 1 equiv (5.3 μL, 0.043 mmol) of DMAD. The solution was stirred for 3 h, after which time the volume of the solvent was reduced to about 2 mL under vacuum. The product was then precipitated, washed with Et_2O, and the resulting yellow solid collected and dried under an argon stream. After recrystallization from CH_2Cl_2/Et_2O, the product was dried again under an argon stream, and then under vacuo (60% yield). Anal. Calcd for $Ir_2P_4F_4O_6C_{58}H_{53}$: C, 48.33; H, 3.71. Found: C, 47.37; H, 3.79.

Table 5.1 $^{31}P\{^{1}H\}$ and ^{1}H NMR Spectroscopic Data[a]

Compound	IR[b,c], cm^{-1}	$\delta(^{31}P\{^{1}H\})$[e]	$\delta(^{1}H)$[f,h]
$[Ir_2(H)_2(CO)_2(\mu\text{-}H)(\mu\text{-DMAD})(dppm)_2][BF_4]$ (3)	2057 (vs), 1970 (st), 1685 (m),[i] 1575 (w)[j]	-13.7 (s)	4.72 (m, 2H), 4.44 (m, 2H), 3.15 (s, 6H), -11.30 (m, 2H), -17.81 (q, 1H)
$[Ir_2(H)_2(CO)_2(\mu\text{-}H)(\mu\text{-HFB})(dppm)_2][BF_4]$ (4)	2052 (vs), 1976 (med), 1579 (w)[j]	-14.7 (s)	4.52 (q, 4H), -11.69 (b, 2H), -17.28 (q, 1H)
$[Ir_2(H)_2(CO)_2(\mu\text{-}H)(\mu\text{-}C_2H_2)(dppm)_2][BF_4]$ (5)	-	-14.6 (s)	4.85 (m, 2H), 4.36 (m, 2H), -10.90 (m, 2H), -17.59 (q, 1H)
$[Ir_2(CO)_2(\mu\text{-}H)(\mu\text{-}Ph_2C_2)(dppm)_2][BF_4]$ (6)	1995 (vs), 1940 (sh), 1590 (w)[j]	1.5 (s)	3.27 (m, 2H), 2.55 (m, 2H), -14.08 (q, 1H)
$[Ir_2(H)(CO)_3(\mu\text{-DMAD})(dppm)_2][BF_4]$ (8)	2064 (s), 2022 (vs), 1965 (s), 1691 (s),[i] 1555 (med)[j]	-14.2 (m), -29.8 (m)	4.88 (m, 2H), 4.73 (m, 2H), 3.83 (s, 3H), 2.28 (s, 3H), -12.03 (t, $^{2}J_{P\text{-}H}$ = 16.0 Hz, 1H)

Table 5.1 (continued)

Compound	IR[b,c], cm^{-1}	$\delta(^{31}P\{^1H\})$[e]	$\delta(^1H)$[f,h]
$[Ir_2(C_2H_4)(CO)_2(\mu\text{-}H)(dppm)_2][BF_4]$ **(9)**[g]	1977 (vs)	12.3 (m), 8.0 (m)	4.25 (m, 2H), 3.68 (m, 2H), 0.90 (b, 2H), 0.62 (b, 2H), -9.93 (m, 1H)
$[Ir_2(H)_2(CO)_2(\mu\text{-}H)(\mu\text{-}C_2F_4)(dppm)_2][BF_4]$ **(10)**		-8.5 (s)	4.86 (m, 2H), 4,66 (m, 2H), -10.76 (m, 2H), -18.02 (q, 1H)

[a] Abbreviations used: med = medium, st = strong, vs = very strong, w = weak, sh = shoulder, s = singlet, t = triplet, q = quintet, m = multiplet, dm = doublet of multiplets, b = broad. [b] Nujol mull on KBr disk unless otherwise stated. [c] Values are ν(CO). [d] IR in CH_2Cl_2. [e] Vs 85% H_3PO_4, 25 °C in CD_2Cl_2 unless otherwise stated. [f] Vs TMS, 25°C in CD_2Cl_2 solvent unless otherwise stated. [g] NMR data at -80°C. [h] Resonances for dppm phenyl group protons appear as multiplets in the range δ 6.9 - 8.1 for all compounds. [i] ν(CO) of DMAD. [j] ν(C≡C).

Table 5.2 ^{19}F and $^{13}C\{^1H\}$ NMR Spectroscopic Data[a]

Compound	^{19}F[c]	$\delta(^{13}C\{^1H\})$[b]
$[Ir_2(H)_2(CO)_2(\mu\text{-}H)(\mu\text{-}HFB)(dppm)_2][BF_4]$ (4)	-54.8 (s)	
$[Ir_2(H)_2(CO)_2(\mu\text{-}H)(\mu\text{-}C_2H_2)(dppm)_2][BF_4]$ (5)		102.7 (s, $\underline{C}_2H_2$)
$[Ir_2(H)(CO)_3(\mu\text{-}DMAD)(dppm)_2][BF_4]$ (8)		176.8 (t, $^2J_{P\text{-}\underline{C}}$ = 5.4 Hz, 1C), 164.2 (dt, $^2J_{P\text{-}\underline{C}}$ = 9.0 Hz, $^3J_{C\text{-}\underline{C}}$ = 10.6 Hz, 1C), 152.5 (dt, $^2J_{P\text{-}\underline{C}}$ = 11.0 Hz, $^3J_{C\text{-}\underline{C}}$ = 10.6 Hz, 1C)
$[Ir_2(C_2H_4)(CO)_2(\mu\text{-}H)(dppm)_2][BF_4]$ (9)[d]		181.9 (b, 1C), 177.6 (t, 1C)
$[Ir_2(H)_2(CO)_2(\mu\text{-}H)(\mu\text{-}C_2F_4)(dppm)_2][BF_4]$ (10)	-73.9 (s)	

[a] Abbreviations used: s = singlet, t = triplet, b = broad, dt = doublet of triplets. [b] Vs TMS, 25 °C in CD_2Cl_2 solvent unless otherwise stated. [c] Vs $CFCl_3$, 25 °C in CD_2Cl_2 unless otherwise stated. [d] Data at -80°C.

(b) $[Ir_2(H)_2(CO)_2(\mu\text{-}H)(\mu\text{-}HFB)(dppm)_2][BF_4]$ (4). Hexafluorobut-2-yne was passed through a solution of compound **1** (60 mg, 0.043 mmol) dissolved in 5 mL of CH_2Cl_2 for 2 min. The solution was then stirred under a static atmosphere of the gas for 1 h. The product was isolated in a similar manner to that used for compound **3** (70% yield). Anal. Calcd for $Ir_2Cl_{0.5}P_4F_{10}O_2C_{56.25}H_{47.5}B$: C, 45.58; H, 3.23; Cl, 1.10. Found: C, 45.11, H; 3.07, Cl, 0.80.

(c) $[Ir_2(CO)_2(\mu\text{-}H)(\mu\text{-}Ph_2C_2)(dppm)_2][BF_4]$ (6). Compound **1** (60 mg, 0.043 mmol) was dissolved in 5 mL of CH_2Cl_2. Two equiv (15.5 mg, 0.087 mmol) of diphenylacetylene, dissolved in 2 mL of CH_2Cl_2, was then added. The mixture was stirred for 24 h, after which time the product was isolated in a similar manner to that used for compound **3**. (60% yield). Anal. Calcd for $Ir_2P_4F_4O_2C_{66}H_{55}B$: C, 53.73; H, 3.76. Found: C, 53.14; H, 3.68.

(d) $[Ir_2(H)(CO)_3(\mu\text{-}DMAD)(dppm)_2][BF_4]$ (8). Method A: One equiv (7.0 μL, 0.048 mmol) of $HBF_4{\cdot}OEt_2$ was added to a solution of $[Ir_2(CO)_3(dppm)_2]$ (**2**) (60 mg, 0.048 mmol) in 3 mL of THF, resulting in an immediate color change from orange to dark reddish-purple. One equiv (6.0 μL, 0.048 mmol) of DMAD was then added to the solution, giving rise to an immediate change in color to red. The red product was precipitated immediately with hexane, collected, and after washing with hexane, it was dried under an argon stream and then under vacuo.

Method B: 1 equiv (7.0 μL, 0.048 mmol) of $HBF_4{\cdot}OEt_2$ was added to $[Ir_2(CO)_2(\mu\text{-}\eta^2\text{:}\eta^2\text{-}DMAD)(dppm)_2]$ (**III**) (prepared from compound **2** (60 mg, 0.048 mmol) and 1 equiv of DMAD (6.0 μL, 0.048 mmol)), in 3 mL of THF. The color of the solution changed instantly to greenish-blue, to purple and

then to red. The red product was precipitated immediately with hexane. The solid was then collected and dried under argon and then under vacuo, after washing with hexane (76% yield). Anal. Calcd for $Ir_2P_4F_4O_3C_{57}H_{51}B$: C, 48.20; H, 3.50. Found: C, 48.36; H, 3.68.

(e) $[Ir_2(C_2H_4)(CO)_2(\mu\text{-}H)(dppm)_2][BF_4]$ (9). Ethylene was passed through a solution of compound **1** (60 mg, 0.043 mmol) in 6 mL of CH_2Cl_2 for 1 min. The mixture was then stirred under a static atmosphere of the gas for 4 h, during which time the color changed from orange to red. The red product was precipitated, washed with Et_2O, and dried under a stream of argon. After recrystallizing it from CH_2Cl_2/Et_2O, the it was dried again under a stream of argon and then under vacuum (70% yield). Anal. Calcd for $Ir_2P_4F_4O_2BC_{54}H_{49}$: C, 48.94; H, 3.73. Found: C, 48.04; H, 3.79

Reaction of Compound 1 with acetylene. The procedure was the same as that used for preparing compound **4**, except that acetylene was used in this case instead of hexafluorobut-2-yne, and the mixture was stirred for 24 h instead of 1 h. The reaction yielded $[Ir_2(H)_2(CO)_2(\mu\text{-}H)(\mu\text{-}C_2H_2)(dppm)_2][BF_4]$ (**5**) as the major product.

Reaction of Compound 1 with Tetrafluoroethylene. Tetrafluoroethylene was passed through a solution of compound **1** (60 mg, 0.043 mmol) in 5 mL of CH_2Cl_2 for 1 min. The solution was then stirred under a static atmosphere of the gas for 48 h. To obtain NMR spectra the reaction was carried out in CD_2Cl_2 solution. The NMR showed the presence of a mixture of compound **1** and $[Ir_2(CO)_2(\mu\text{-}H)(\mu\text{-}C_2F_4)(dppm)_2][BF_4]$ (**10**). The solid was not isolated in this reaction.

Reaction of Compound 9 with H_2. Compound **9** (30 mg, 0.024 mmol) was dissolved in 0.6 mL of CD_2Cl_2 in an NMR tube which was then capped with a rubber septum. Hydrogen was then passed through the solution for 1 min. The NMR spectra of the solution showed the presence of compound **1** and ethylene as the only products.

X-ray Data Collection. Orange crystals of $[Ir_2(C_2H_4)(CO)_2(\mu\text{-}H)(dppm)_2][BF_4]$ (**9**) were obtained by slow diffusion of ether into a concentrated CH_2Cl_2 solution of the compound. Several suitable crystals were mounted and flame sealed in glass capillaries under solvent vapor to minimise decomposition or deterioration due to solvent loss. Data were collected on an Enraf-Nonius CAD4 diffractometer using graphite-monochromated Mo Kα radiation. Unit cell parameters were obtained from a least-squares refinement of the setting angles of 25 reflections in the range $20.0° \leq 2\theta \leq 24.0°$. The monoclinic diffraction symmetry and the systematic absences (*h0l*, $h+l$=odd; *0k0*, k=odd) were consistent with the space group $P2_1/n$.

Intensity data were collected at 22°C using the $\theta/2\theta$ scan technique to a maximum $2\theta = 50.0°$, collecting reflections with indices of the form $\pm h +k +l$. Backgrounds were scanned for 25% of the peak width on either side of the peak scan. Three reflections were chosen as intensity standards, being remeasured at 120-min intervals of X-ray exposure time. There was no significant systematic decrease in the intensities of these standards thus no decomposition correction was applied. A total of 9014 unique reflections were measured and processed in the usual way, using a value of 0.04 for p^4 to downweight intense reflections; of these 6230 were

considered to be observed ($F_o^2 \geq 3\sigma(F_o^2)$) and were used in subsequent calculations. Absorption corrections were applied to the data using the method of Walker and Stuart.[5,6] See Table 5.3 for crystal data and more information on X-ray data collection.

Structure Solution and Refinement. The structure was solved in the space group $P2_1/n$ using standard Patterson and Fourier techniques. Although location of all atoms was straightforward, initial refinements resulted in unusually high thermal parameters for the atoms of the carbonyl groups and the ethylene carbon atoms. A difference Fourier calculation at this stage showed the presence of superimposed carbonyl and ethylene carbon atoms. This led to the model in which **10** is disordered in two orientations, represented as **A** and **B** in the diagram below (the dppm ligands are omitted for clarity), in an approximately 50:50 ratio (determined from the relative peak intensities of the ordered and disordered atoms). The resulting model in which the **A** and **B** orientations are superimposed is diagrammed in **C**, in which the solid lines connect atoms of one rotomer, having unprimed

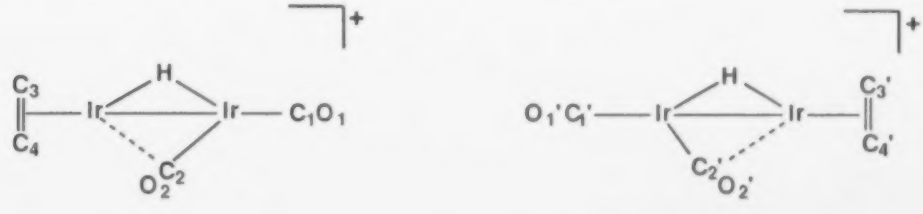

A **B**

atom labels, and the dashed lines show the other one, having primed atom labels. There is no apparent disorder involving the phosphine groups, which are well behaved. Although an alternate structure, having

Table 5.3. Crystallographic Data for $[Ir_2(C_2H_4)(CO)_2(\mu\text{-}H)(dppm)_2][BF_4]$ (**9**)

formula	$C_{54}H_{49}BF_4Ir_2O_2P_4$
formula weight	1325.1
crystal shape	monoclinic prism
crystal dimensions, mm	0.42 x 0.38 x 0.60
space group	$P2_1/n$ (nonstandard setting of $P2_1/c$, No. 14)
temperature, °C	22
radiation (λ, Å)	graphite-monochromated Mo Kα (0.71069)
unit cell parameters	
a, Å	13.687(1)
b, Å	15.459(1)
c, Å	23.813(1)
β, deg	97.87(1)
V, Å^3	4991(1)
Z	4
ρ(calcd), g cm^{-3}	1.763
linear absorption coefficient (μ), cm^{-1}	54.88
range of transmission factors	0.9099-1.1322
detector aperture, mm	(3.00 + tan θ) wide x 4.00 high
take-off angle, deg	3.0
maximum 2θ, deg	50.0
crystal-detector distance, mm	173

Table 5.3. (continued)

scan type	$\theta/2\theta$
scan rate, deg/min	between 1.43 and 6.71
scan width, deg	0.80 + 0.347 tan θ
total unique reflections	9014 ($\pm h +k +l$)
total observations (NO)	6230 ($Fo^2 \geq 3\sigma(Fo^2)$)
final no. params. varied (NV)	358
error in obs. of unit weight (GOF)[a]	1.500
R[b]	0.039
R_w[c]	0.048

[a] $\text{GOF} = [\sum w(|F_o| - |F_c|)^2 / (\text{NO} - \text{NV})]^{1/2}$ where $w = 4F_o^2 / \sigma^2(F_o^2)$.

[b] $R = \sum ||F_o| - |F_c|| / \sum |F_o|$. [c] $R_w = [\sum \omega(|F_o| - |F_c|)^2 / \sum \omega F_o^2]^{1/2}$.

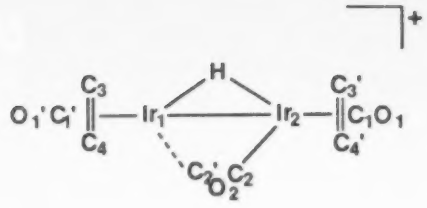

C

one CO ligand on one metal and the second one on the other metal (represented as **A'** and **B'** in the diagram below), could not be ruled out by the X-Ray study, that shown in **A** and **B** is favored for reasons that will be outlined in the discussion of the NMR spectroscopic data of compound **9**. Rotational disorder of this type is rather common in these binuclear systems.[7]

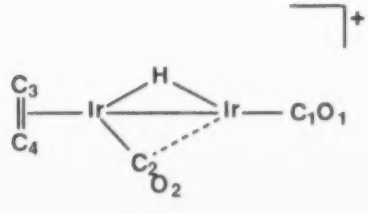

A'

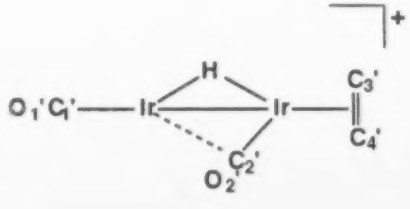

B'

All non-hydrogen atoms of the complex cation and anion as well as the hydride ligand were located. Atomic scattering factors [8,9] and anomalous dispersion terms[10] were taken from the usual tabulations. The hydride ligand was successfully refined; the other hydrogen atoms, on the other hand, were included as fixed contributions but not refined. Their idealized positions were calculated from the geometries about the attached carbon atoms, using a C-H bond length of 0.95 Å, and they were assigned

thermal parameters 20% greater than the equivalent isotropic B's of their attached C atoms.

The final model, with 358 parameters refined, converged to values of R = 0.039 and Rw = 0.048. In the final difference Fourier map the 10 highest residuals (1.37-0.94 e/Å^3) were found to be in the vicinity of the Ir, the phenyl rings, and the disordered carbonyl group atoms. A typical carbon atom in an earlier synthesis had an electron density of *ca.* 6.0 e/Å^3. The positional and isotropic thermal parameters of all refined atoms are given in Table 5.4.

Results and Discussion

The reaction of $[Ir_2(H)(CO)_2(\mu\text{-}H)_2(dppm)_2][BF_4]$ (**1**) with DMAD gives $[Ir_2(H)_2(CO)_2(\mu\text{-}H)(\mu\text{-}DMAD)(dppm)_2][BF_4]$ (**3**). Although this compound was reported previously,[11] it was obtained as one of two products from the reaction of DMAD with a mixture of **1** and $[Ir_2(H)_2(CO)_2(\mu\text{-}I)(dppm)_2][BF_4]$, and it was not fully characterized. The NMR spectroscopic data of compound **3** are the same as were previously reported, and the IR spectrum shows CO stretches at 2057 and 1970 cm^{-1}, indicating the presence of two terminal CO ligands, as well as a peak at 1685 cm^{-1}, due to the CO stretch of the coordinated DMAD. A peak at 1575 cm^{-1} in this spectrum is assigned to the C≡C stretch of the coordinated alkyne. This is within the range of 1530 - 1642 cm^{-1} observed in closely related dppm-bridged binuclear complexes in which the alkyne bridges the two metals parallel to the metal-metal axis.[1b,1h,1j,12-15] This is the alkyne coordination mode assumed in **3**.[16] In related binuclear complexes in which the alkyne bridges the two metals perpendicular to the metal-metal

Table 5.4. Positional and Thermal Parameters for the Atoms of $[Ir_2(C_2H_4)(CO)_2(\mu\text{-}H)(dppm)_2][BF_4]$ (9)[a]

Atom	*x*	*y*	*z*	*B*, Å^{2b}
Ir(1)	0.23374(2)	0.13630(2)	-0.02228(1)	2.509(7)*
Ir(2)	0.39012(2)	0.25191(2)	0.01151(1)	2.705(7)*
P(1)	0.1908(2)	0.2076(1)	-0.1073(1)	2.83(5)*
P(2)	0.3619(2)	0.3268(1)	-0.0735(1)	2.96(5)*
P(3)	0.2518(2)	0.0706(1)	0.0659(1)	2.63(5)*
P(4)	0.4171(2)	0.1949(1)	0.1024(1)	2.52(5)*
F(1)	0.4371(7)	0.0019(7)	0.7674(4)	15.3(4)*
F(2)	0.5792(7)	0.0495(9)	0.7782(5)	17.1(5)*
F(3)	0.467(1)	0.1272(7)	0.7388(5)	23.0(5)*
F(4)	0.4736(9)	0.0938(8)	0.8284(5)	16.5(5)*
O(1)	0.569(1)	0.3555(9)	0.0376(6)	5.4(3)
O(1)'	0.097(1)	0.002(1)	-0.0678(7)	6.8(4)
O(2)	0.4444(5)	0.0737(5)	-0.0437(3)	5.8(2)*
C(1)'	0.145(1)	0.054(1)	-0.0486(7)	3.0(3)
C(1)	0.494(1)	0.319(1)	0.0279(7)	3.2(3)
C(2)	0.413(1)	0.140(1)	-0.0257(8)	4.2(4)
C(2)'	0.363(1)	0.100(1)	-0.0347(7)	3.6(3)
C(3)	0.083(1)	0.085(1)	-0.0317(7)	3.7(4)
C(3)'	0.474(1)	0.362(1)	0.0468(7)	3.7(4)
C(4)'	0.545(1)	0.301(1)	0.0250(7)	3.5(4)
C(4)	0.153(2)	0.019(1)	-0.0557(9)	5.2(5)
C(5)	0.2942(6)	0.2641(5)	-0.1318(4)	3.3(2)*
C(6)	0.3753(6)	0.0830(5)	0.1048(3)	2.9(2)*
C(11)	0.1482(6)	0.1378(6)	-0.1671(3)	3.3(2)
C(12)	0.0489(7)	0.1304(6)	-0.1903(4)	4.0(2)
C(13)	0.0202(7)	0.0702(7)	-0.2315(4)	5.0(2)
C(14)	0.0878(8)	0.0192(7)	-0.2518(4)	5.3(2)
C(15)	0.1868(7)	0.0245(7)	-0.2300(4)	4.9(2)
C(16)	0.2180(7)	0.0838(6)	-0.1870(4)	4.1(2)

Table 5.4. (continued)

C(21)	0.0976(6)	0.2917(6)	-0.1072(4)	3.3(2)
C(22)	0.0629(8)	0.3353(7)	-0.1572(4)	4.9(2)
C(23)	-0.0060(8)	0.4040(8)	-0.1552(5)	5.9(3)
C(24)	-0.0330(8)	0.4268(8)	-0.1049(5)	6.2(3)
C(25)	-0.0002(8)	0.3850(7)	-0.0551(5)	5.6(2)
C(26)	0.0672(7)	0.3157(6)	-0.0573(4)	4.0(2)
C(31)	0.4704(6)	0.3573(6)	-0.1033(4)	3.4(2)
C(32)	0.5270(8)	0.2964(7)	-0.1266(5)	5.5(2)
C(33)	0.6166(9)	0.3196(9)	-0.1463(6)	7.4(3)
C(34)	0.6457(9)	0.3996(9)	-0.1411(5)	7.3(3)
C(35)	0.5983(9)	0.4625(8)	-0.1199(5)	6.6(3)
C(36)	0.5061(8)	0.4431(7)	-0.0986(5)	5.4(2)
C(41)	0.2940(6)	0.4262(6)	-0.0710(4)	3.6(2)
C(42)	0.2765(7)	0.4597(6)	-0.0205(4)	4.2(2)
C(43)	0.2265(8)	0.5386(8)	-0.0179(5)	6.0(3)
C(44)	0.1961(9)	0.5828(9)	-0.0673(5)	6.8(3)
C(45)	0.2098(9)	0.5509(8)	-0.1180(5)	6.3(3)
C(46)	0.2604(8)	0.4714(7)	-0.1207(5)	5.7(2)
C(51)	0.1687(6)	0.1094(6)	0.1131(4)	3.4(2)
C(52)	0.0937(9)	0.1656(8)	0.0937(5)	6.3(3)
C(53)	0.034(1)	0.198(1)	0.1342(6)	9.1(4)
C(54)	0.049(1)	0.172(1)	0.1875(6)	8.0(3)
C(55)	0.1175(8)	0.1166(8)	0.2060(5)	5.9(3)
C(56)	0.1804(7)	0.0841(7)	0.1690(4)	4.7(2)
C(61)	0.2337(6)	-0.0452(6)	0.0644(4)	3.7(2)
C(62)	0.2956(9)	-0.0939(9)	0.0356(5)	6.7(3)
C(63)	0.284(1)	-0.184(1)	0.0274(7)	9.6(4)
C(64)	0.205(1)	-0.2203(9)	0.0504(6)	8.0(4)
C(65)	0.147(1)	-0.1767(9)	0.0785(5)	7.4(3)
C(66)	0.1579(8)	-0.0860(8)	0.0847(5)	5.7(2)
C(71)	0.5454(6)	0.1914(5)	0.1333(3)	2.8(2)
C(72)	0.6078(8)	0.1290(7)	0.1151(4)	5.2(2)
C(73)	0.7095(9)	0.1311(8)	0.1330(5)	6.3(3)
C(74)	0.7450(9)	0.1932(8)	0.1706(5)	6.4(3)

Table 5.4. (continued)

C(75)	0.6856(8)	0.2558(7)	0.1895(5)	5.7(3)
C(76)	0.5860(7)	0.2541(6)	0.1702(4)	4.3(2)
C(81)	0.3569(6)	0.2484(6)	0.1558(3)	3.1(2)
C(82)	0.2909(7)	0.3147(6)	0.1421(4)	4.1(2)
C(83)	0.2432(8)	0.3527(7)	0.1843(5)	5.5(2)
C(84)	0.2615(8)	0.3235(8)	0.2378(5)	5.6(2)
C(85)	0.3254(7)	0.2569(7)	0.2529(4)	4.4(2)
C(86)	0.3734(7)	0.2194(6)	0.2117(4)	3.8(2)
B	0.491(1)	0.077(1)	0.7758(8)	8.5(4)
H(1)	0.250(8)	0.231(8)	0.015(5)	6(3)

[a]Numbers in parentheses are estimated standard deviations in the least significant digits in this and all subsequent tables. Primed atoms have 50% occupancy and are related to the unprimed (50% occupancy) atoms by the rotational disorder. [b]Starred B values are for atoms refined anisotropically. Displacement parameters for the anisotropically refined atoms are given in the form of the equivalent isotropic Gaussian diplacement parameter defined as:

$4/3[a^2\beta_{11} + b^2\beta_{22} + c^2\beta_{33} + ab(\cos\gamma)\beta_{12} + ac(\cos\beta)\beta_{13} + bc(\cos\alpha)\beta_{23}]$.

axis (μ-η^2:η^2- mode), the C≡C stretch usually occurs at lower frequencies. For example, a value of 1425 cm^{-1} is observed in $[Rh_2(CO)_2(\mu\text{-}\eta^2\text{:}\eta^2\text{-}PhC_2H)(dppm)_2]$ and $[Rh_2(CO)_2(\mu\text{-}\eta^2\text{:}\eta^2\text{-}Ph_2C_2)(dppm)_2]$.[17]

The reaction of compound **1** with HFB (hexafluorobut-2-yne) gives $[Ir_2(H)_2(CO)_2(\mu\text{-}H)(\mu\text{-}HFB)(dppm)_2][BF_4]$ (**4**), which is the HFB analogue of compound **3**. The spectroscopic properties of compound **4** are similar to those of compound **3**, showing a singlet at δ -14.7 in its $^{31}P\{^1H\}$ NMR spectrum, and hydride resonances at δ -11.69 (multiplet) and -17.28 (quintet), corresponding to the two terminal and one bridging hydride ligands, respectively.[18] The IR spectrum of **4** shows carbonyl stretches at 2052 and 1976 cm^{-1}, and the alkyne C≡C stretch at 1579 cm^{-1}. In the ^1H NMR spectrum of **4**, the four dppm methylene protons give rise to a quintet at δ 4.52 even at -80 °C. Although the structure proposed for **4** should have two chemically inequivalent methylene resonances, it appears that their chemical shifts are coincidentally equivalent. The ^{19}F NMR spectrum of compound **4** shows a singlet at δ -54.8, similar to that observed in related compounds.[14,15] All the NMR data are consistent with the structure of **4** shown in Scheme 5.1.

Compound **1** also reacts with acetylene to give $[Ir_2(H)_2(CO)_2(\mu\text{-}H)(\mu\text{-}C_2H_2)(dppm)_2][BF_4]$ (**5**), analogous to **3** and **4**, as shown by its very similar ^1H and $^{31}P\{^1H\}$ NMR spectroscopic parameters to those of **3** and **4**. In the ^1H NMR spectrum of **5**, the resonance for the protons of the coordinated acetylene are not observed, presumably because they are obscured by the phenyl proton resonances, as is frequently the case.[1a,17a,19] The $^{13}C\{^1H\}$ NMR spectrum of a sample of **5** obtained by use of ^{13}C-enriched acetylene shows the resonance for the coordinated acetylene as a singlet at δ 102.7.

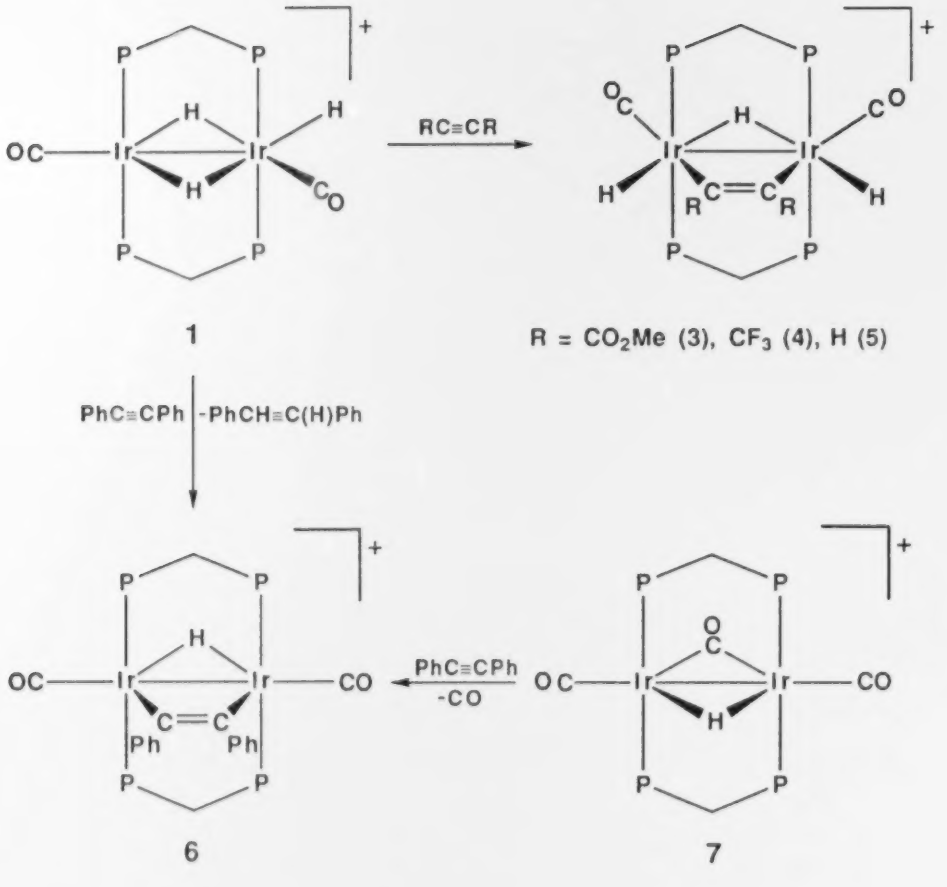

1

6

7

Scheme 5.1.

This chemical shift is close to those observed for the carbon nuclei of the coordinated alkyne in $[Ir_2(I)(CO)_2(\mu\text{-}C_2H_2)(dppm)_2][I]$.[1a] In compounds **3**, **4** and **5**, we suggest the geometry shown in Scheme 5.1, in which no two hydride ligands are cis to each other thereby inhibiting H_2 loss.

In contrast to the reactions described above, reaction of **1** with 2 equiv of diphenylacetylene results in the formation of the monohydrido compound, $[Ir_2(CO)_2(\mu\text{-}H)(\mu\text{-}Ph_2C_2)(dppm)_2][BF_4]$ (**6**). The four phosphorus nuclei of compound **6** are all equivalent, as is indicated by its $^{31}P\{^1H\}$ NMR spectrum which shows a singlet at δ 1.5. The hydride resonance appears as a quintet at δ -14.08, in the ^1H NMR spectrum, due to coupling to the four phosphorus nuclei. Two CO stretches appear at 1995 and 1940 cm^{-1}, in the IR spectrum, while a band at 1590 cm^{-1} is assigned to the C≡C stretch of the coordinated alkyne. These are consistent with the assignment of a bridging hydride ligand, two terminal CO ligands and a bridging alkyne in **6**. Compound **6** can also be obtained in the reaction of diphenylacetylene with the known compound, $[Ir_2(CO)_2(\mu\text{-}CO)(\mu\text{-}H)(dppm)_2][BF_4]$ (**7**),[3] accompanied by loss of one CO ligand.

The other product in the reaction of **1** with diphenylacetylene is *cis*-stilbene (PhCH=C(H)Ph), identified by the singlet resonance at δ 6.60 in the ^1H NMR spectrum (by comparison with an authentic sample) of the reaction mixture, when the reaction is carried out in CD_2Cl_2. The essentially quantitative formation of *cis*-stilbene, as suggested by integration of the ^1H NMR resonance, also suggests that any of the trans isomer that might have been formed must be in trace amounts. Unfortunately this cannot be confirmed by the ^1H NMR spectrum of the reaction mixture, as the resonances due to any of this isomer that might be

present will be masked by the intense signals due to the dppm and coordinated alkyne phenyl protons.

On the basis of the products obtained in the reaction of **1** with diphenylacetylene, it is proposed that it proceeds via insertion of the alkyne into one of the Ir-H bonds of **1**, followed by the coordination of another molecule of diphenylacetylene, and the elimination of *cis*-stilbene, to give the final product, **6**. However the proposed intermediate vinyl compound is not observed; even using 1 equiv of diphenylacetylene results in **6** and unreacted starting material. This reaction of **1** parallels those of $[Ru(H)_2(CO)_2(PMe_2Ph)_2]$[20] and $[Mo(\eta^5\text{-}C_5H_5)_2H_2]$[21] with the same alkyne, which resulted in the formation of *cis*-stilbene together with $[Ru(CO)_2(PhC{\equiv}CPh)(PMe_2Ph)_2]$ and $[Mo(\eta^5\text{-}C_5H_5)_2(PhC{\equiv}CPh)]$, respectively. These reactions contrast with the analogous insertion of DMAD into an Ir-H bond in $[Ir_2(H)_2(Cl)_2(CO)_2(dppm)_2]$,[1g] which did not lead to alkyne hydrogenation, presumably because the hydride and resulting vinyl moiety did not have the cis arrangement required for reductive elimination.

Compound **1** reacts with phenylacetylene to give styrene and several unidentified products. Although the number of metal-containing products has hampered their characterization, the formation of substantial amounts of styrene indicates that there is hydrogenation of the alkyne at some stage of the reaction, presumably via a similar pathway to that proposed for the reaction of **1** with diphenylacetylene. Compound **1** also reacts with 2-butyne to give mixtures of several products.

In an attempt to obtain the DMAD analogue of the alkyne-bridged, monohydrido compound **6**, the previously characterized compound, $[Ir_2(CO)_2(\mu\text{-}\eta^2{:}\eta^2\text{-DMAD})(dppm)_2]$ (**III**),[1i] was reacted with $HBF_4{\cdot}OEt_2$. This

however did not give the desired compound, but gave instead the compound, $[Ir_2(H)(CO)_3(\mu\text{-DMAD})(dppm)_2][BF_4]$ (**8**), as shown in Scheme 5.2, having one more CO ligand than the analogue of compound **6**, together with some unidentified products. These unidentified products are presumably decomposition products which are the source of the extra CO ligand. A pure sample of **8** was obtained when the compound, $[Ir_2(CO)_3(dppm)_2]$ (**2**) was reacted first with 1 equiv of $HBF_4{\cdot}OEt_2$, then with 1 equiv of DMAD before precipitating the product. The successful simulation of the 161.99 MHz $^{31}P\{^1H\}$ spectrum of **8** as that arising from an AA'BB' spin system, indicates mutually trans phosphorus atoms at each Ir center ($^2J_{P_A\text{-}P_{A'}}$ = 280 Hz, $^2J_{P_A\text{-}P_B} = {}^2J_{P_{A'}\text{-}P_{B'}}$ = 47 Hz, $^2J_{P_A\text{-}P_{B'}} = {}^2J_{P_{A'}\text{-}P_B}$ = 12 Hz and $^2J_{P_B\text{-}P_{B'}}$ = 300 Hz). These calculated P-P coupling constants are comparable to those determined for similar dppm-bridged alkyne complexes with mutually trans phosphines.[13] Since it has been observed that with dppm-bridged binuclear transition-metal complexes, bridging of the two metals by an alkyne in a $\mu\text{-}\eta^2{:}\eta^2$- fashion is accompanied by a cis orientation of the dppm phosphines,[1i,17] it is apparent that in compound **8** the DMAD now bridges the two metals parallel to the metal-metal bond. The frequency of the C≡C stretch of the coordinated alkyne in the IR spectrum (1555 cm^{-1}) is consistent with the assigned parallel coordination mode of DMAD in **8**.

The ^1H NMR spectrum of **8** shows the DMAD methyl resonances as two singlets at δ 3.83 and 2.28, while the hydride resonance appears as a triplet, due to coupling to two phosphorus nuclei, at δ -12.03 ($^2J_{P\text{-}H}$ = 16.0 Hz), showing that it is terminally bound to one of the metals. Selective ^{31}P-decoupling experiments confirm the terminal coordination mode of the hydride, as decoupling one phosphorus resonance leads to the collapse

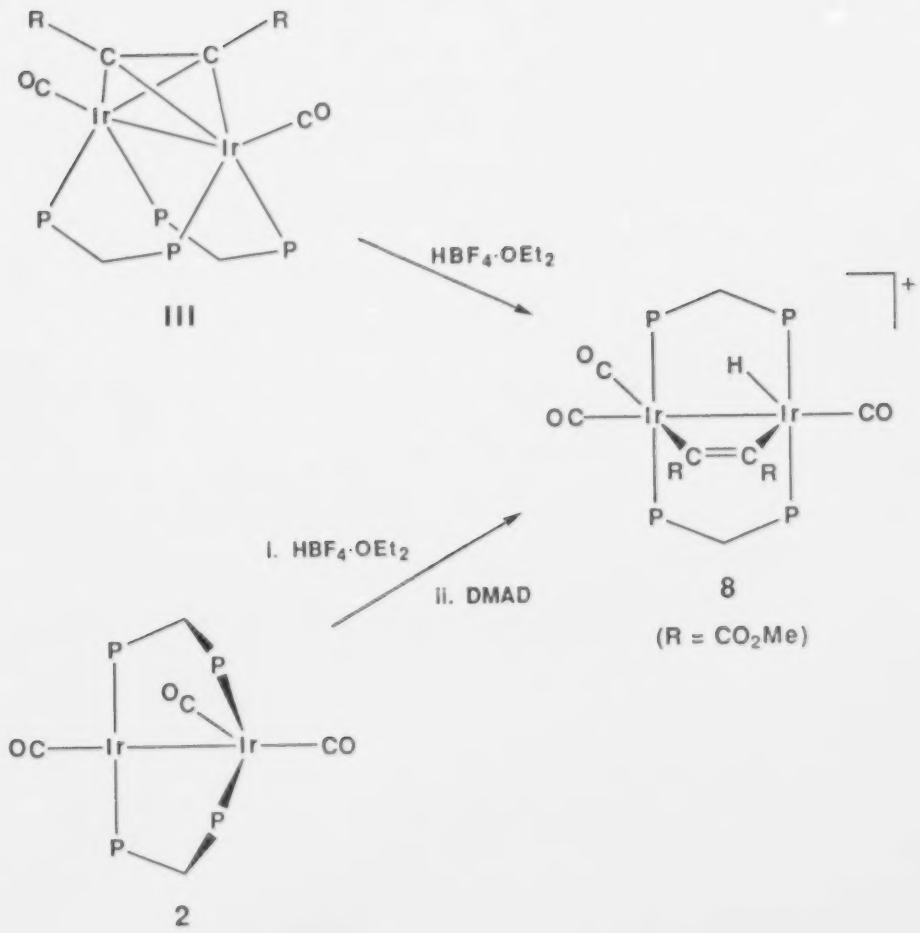
R
C
C
R
OC
Ir
Ir
CO
P
P
P
P
P
III
HBF4·OEt2
+
P
P
OC
H
OC
Ir
Ir
CO
R
C
C
R
P
P
8
(R = CO2Me)
i. HBF4·OEt2
ii. DMAD
P
P
OC
OC
Ir
Ir
CO
P
P
2

Scheme 5.2.

of the triplet to a singlet, while it remains unchanged on decoupling the other resonance. The IR spectrum shows CO stretches at 2064, 2022, 1965 and 1691 cm^{-1} (the IR stretch of lowest frequency is due to the CO of the DMAD ligand), while the $^{13}C\{^1H\}$ NMR spectrum shows a triplet at δ 176.8, and two doublets of triplets at δ 164.2 and 152.5, indicating the presence of three terminally bound CO ligands in **8**. $^{13}C\{^{31}P\}\{^1H\}$ and $^1H\{^{31}P\}$ NMR experiments show that the resonances at δ 176.8 and 152.2 are due to CO ligands that are bound to the same Ir metal while the resonance at δ 164.2 is due to a CO ligand that is bound to the second metal together with the hydride ligand. The assigned structure of compound **8**, with an approximately colinear orientation of two of the CO ligands and the Ir-Ir bond as shown in Scheme 5.2, is based on the observation that these two CO ligands (δ 164.2 and 152.5) show coupling to each other ($^3J_{C\text{-}C}$ = 10.6 Hz), whereas the CO ligands on the same metal do not show any coupling to each other. A similar orientation was proposed for the CO ligands in $[RhIr(CO)_2(\mu\text{-}I)(\mu\text{-}DMAD)(dppm)_2][BF_4]$,[1b] and for two of these ligands in $[RhIrCl(CO)_3(\mu\text{-}DMAD)(dppm)_2][ClO_4]$,[12] based on similar observations of coupling of the carbon nuclei of these ligands in their $^{13}C\{^1H\}$ NMR spectra. The change of the coordination mode of the alkyne from perpendicular to parallel to the metal-metal axis, in going from **III** to **8**, is not unexpected, in view of the fact that the former bridging mode is apparently not known in cationic binuclear dppm-bridged complexes of Rh or Ir.

As discussed above, whereas the reaction of compound **1** with diphenylacetylene and phenylacetylene result in the hydrogenation of the alkyne, no hydrogenation was observed with DMAD, acetylene and HFB. Even refluxing compound **3** in THF for several hours did not result in

insertion of the alkyne into an Ir-H bond of **1**; a required initial step in hydrogenation of the alkyne. It is possible that, in the case of the activated alkynes (DMAD and HFB), the strength of the resulting M-C bonds on coordination, as a result of the high electron withdrawing ability of the substituents, precludes any further transformation, in contrast to the unactivated alkynes in which these bonds are weaker. Furthermore, the activated alkynes have a greater tendency to bridge two metals, since they are stronger π acceptors, compared to the unactivated ones, and this could be a contributing factor to the observed trend in these reactions. In this respect acetylene appears to be an exception since this unactivated alkyne is not hydrogenated in the presence of **1**. It is not clear why this reactivity parallels that of DMAD and HFB, while being different from that of phenylacetylene and diphenylacetylene.

The reactions of compound **1** with alkynes are in contrast to those involving the related compound, $[Ir_2(H)_2(CO)_2(\mu\text{-}Cl)(dppm)_2][BF_4]$ (**I**) with DMAD and PhC≡CH in which insertion into both Ir-H bonds occurred to give stable vinyl compounds.[1d] Apparently in the case of compound **1** the presence of two adjacent hydride ligands gives rise to a cis arrangement of the vinyl group and one of the hydride ligands in the proposed intermediate (in cases where there is alkyne hydrogenation), such that elimination of the hydrogenated alkyne is more favorable than the insertion of another alkyne molecule. It is not clear, however, why the reaction of DMAD with the chloro compound, **I**, results in insertion, whereas that with the trihydride, **1**, yields an alkyne-bridged trihydride product.

Alkenes are another class of unsaturated hydrocarbons that can behave in a similar manner to alkynes as ligands, although the latter

compounds are usually more reactive owing to their higher degree of unsaturation. In light of the different reactivity patterns exhibited by compound **1** with activated alkynes on one hand, and unactivated alkynes on the other, it was of interest to see how these reactions compared with those of an activated and an unactivated alkene. Thus reactions of compound **1** with ethylene and tetrafluoroethylene were undertaken.

The reaction of compound **1** with ethylene gives the rare hydrido ethylene compound, $[Ir_2(C_2H_4)(CO)_2(\mu\text{-}H)(dppm)_2][BF_4]$ (**9**), as shown in Scheme 5.3. Ethylene rotation in **9** is consistent with the observation at -40 °C of one broad resonance at δ 0.94 for the four ethylene protons, and two broad resonances at δ 4.25 and 3.80, due to the dppm methylene protons, in the ^1H NMR spectrum. The hydride resonance appears as a broad signal at δ -10.03 in this spectrum. At -80 °C the resonance due to the ethylene protons separates into two broad signals at δ 0.90 and 0.62, while the hydride resonance appears as a pseudo quintet at δ -9.93, as a result of coupling to the four phosphorus nuclei, indicating that the hydride ligand bridges the two metals. The $^{13}C\{^1H\}$ NMR spectrum at -80 °C shows a broad resonance at δ 181.9 and a triplet at δ 177.6, suggesting the presence of two terminally bound CO ligands in compound **9**. However, selective ^{31}P-decoupling NMR experiments could not be carried out to confirm to which metals these ligands were coordinated since the phosphorus resonances are too close (the semibridging interaction shown in Scheme 5.3 for one of the CO ligands in compound **9**, is based on the solid state structure, determined by X-ray methods, as discussed later).

We suggest that the formation of compound **9** follows a similar pathway to that proposed for compound **6**, proceeding via the insertion of ethylene into one of the Ir-H bonds of compound **1**, followed by reductive

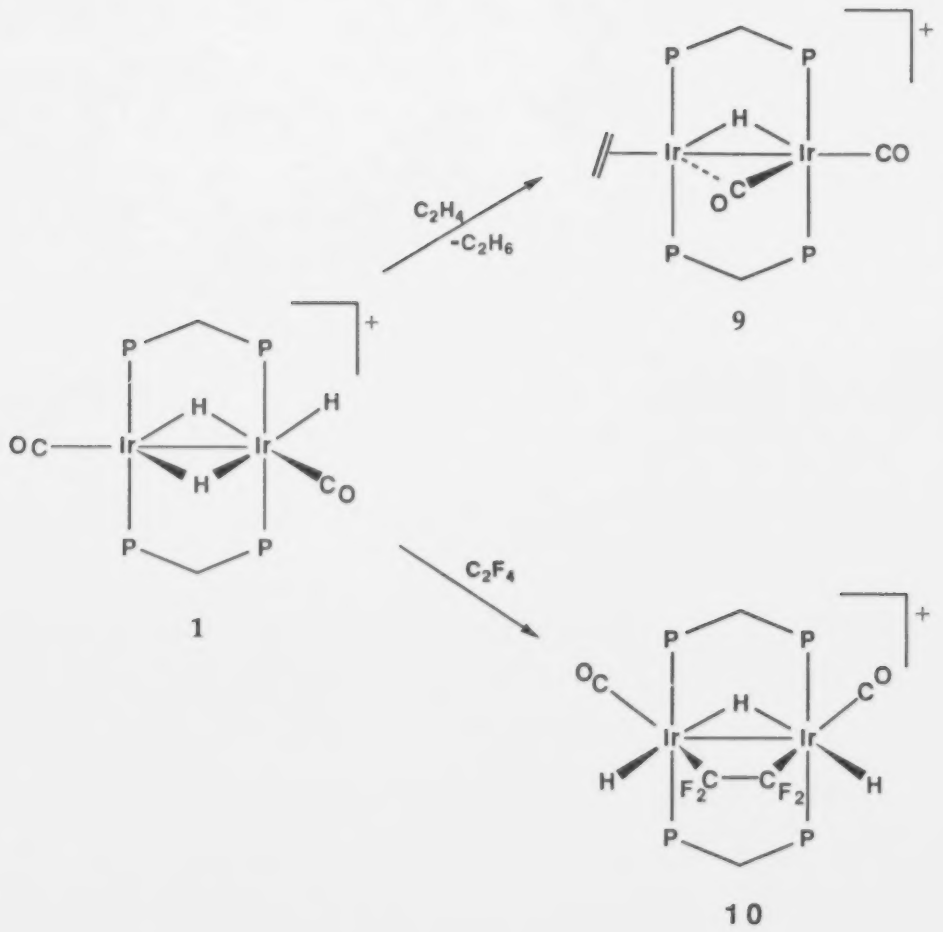
P
P
H
Ir
Ir
CO
OC
C_2H_4
$-C_2H_6$
9
OC
H
H
Ir
Ir
CO
H
1
C_2F_4
OC
CO
H
Ir
Ir
H
F_2C
CF_2
H
10

Scheme 5.3.

elimination of ethane and coordination of another molecule of ethylene. Evidence for the presence of ethane is given by the singlet that appears at δ 0.85 in the ^1H NMR spectrum of the reaction mixture. However, the proposed intermediate ethyl complex is not observed.

At room temperature the ^1H NMR spectrum of **9** shows a single very broad resonance for the four dppm methylene protons, and all the ethylene protons also give rise to one very broad resonance. Also the $^{13}C\{^1H\}$ NMR spectrum at this temperature shows a broad featureless resonance centered at δ 179.2. It is proposed that this is a result of tunnelling[23] of the hydride ligand between the metals (as shown below; the dppm ligands have been omitted for clarity) in concert with the

A

rotation of the ethylene ligand about the metal-olefin axis. Although all the ethylene protons would be equivalent as a result of this tunnelling, even in the absence of rotation of the ethylene ligand, such a rotation is suggested at this temperature since it is unlikely that it occurs at -40 °C and not at room temperature. The observed averaging of the methylene ^1H resonances and the ^{13}CO resonances argues in favor of the ligand arrangement shown above, since a structure having a CO on each metal would not equilibrate the methylene protons by the hydride tunnelling described. However, a more complex fluxional process, as shown in

Scheme 5.4, in which carbonyl transfer from one metal to the other occurs along with hydride tunnelling, cannot be ruled out.

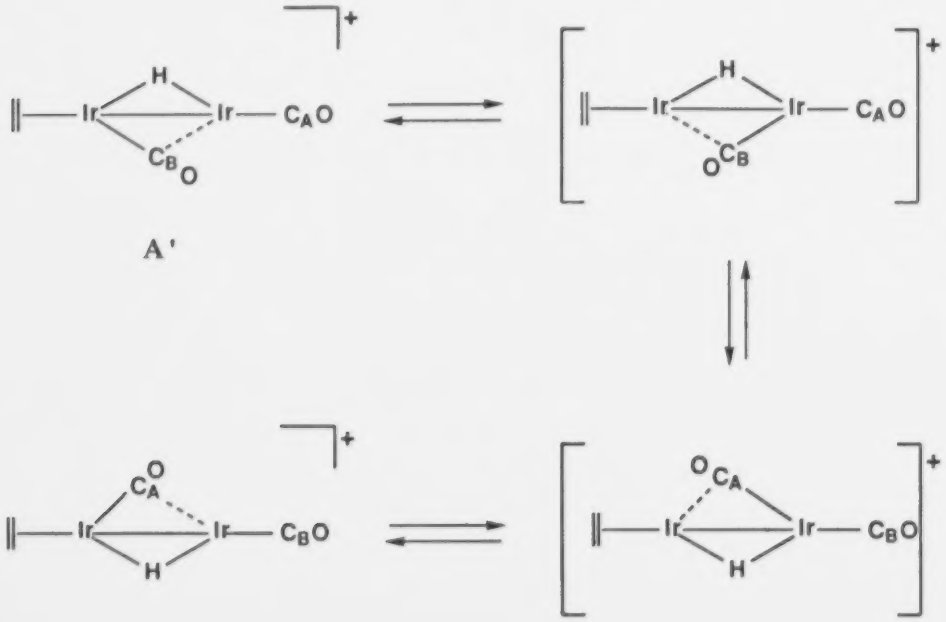

Scheme 5.4.

At -40 °C, the $^{31}P\{^{1}H\}$ NMR spectrum of compound **9** shows a very broad unresolved resonance at δ 6.8 and a multiplet at δ 12.1, while at -80 °C both resonances appear as multiplets typical of that given by an AA'BB' spin system (see Figure 5.1). It appears that the broadness of one of the ^{31}P resonances at -40 °C is due to a fluxional process that is restricted to one metal, but which is different from that due to ethylene rotation. However, the nature of this fluxional process is not clear.

Ethylene adducts of dppm-bridged binuclear complexes of Ir are

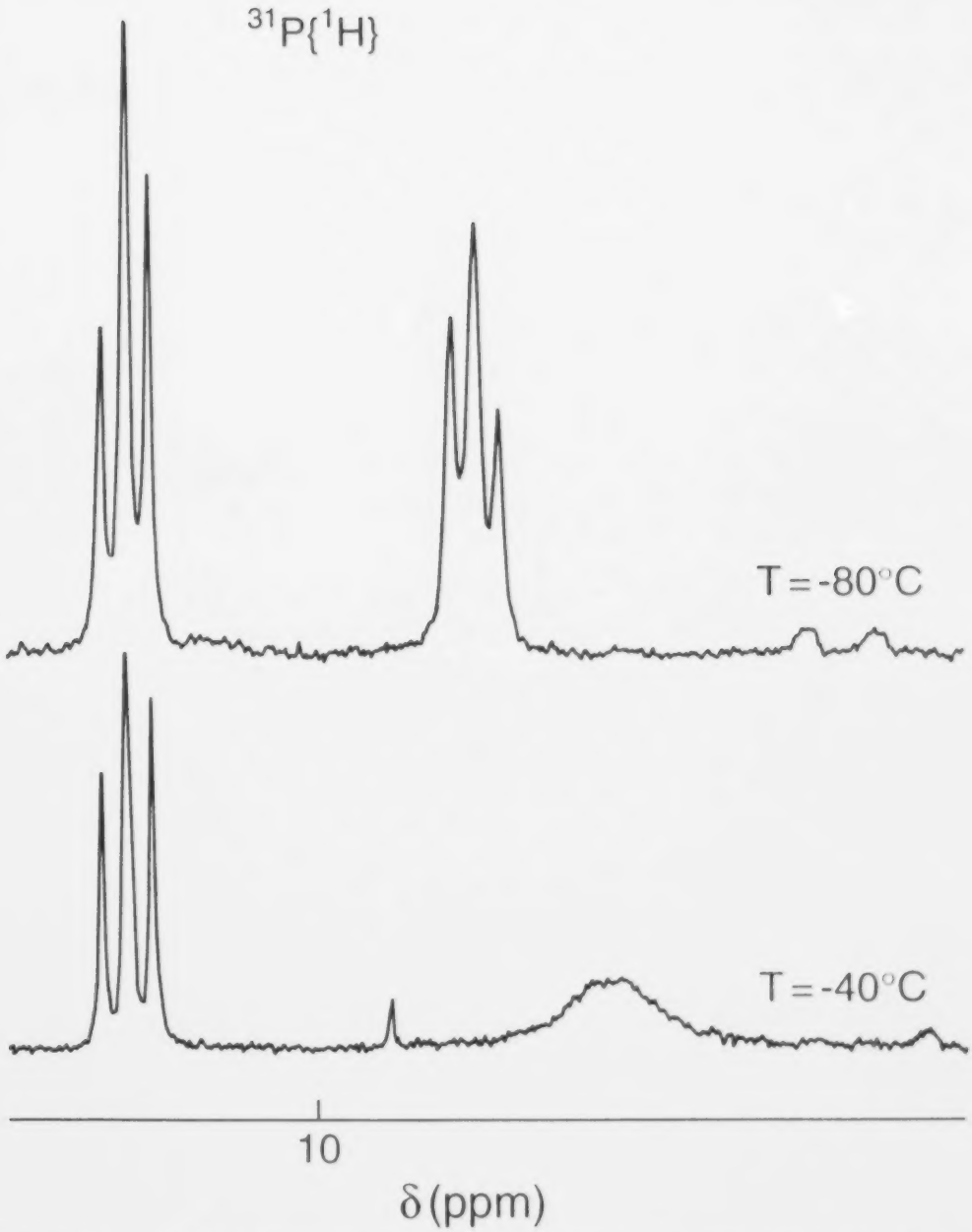

Figure 5.1. $^{31}P\{^{1}H\}$ NMR spectrum of compound **9** at -40 °C and -80 °C.

extremely rare. To our knowledge the complexes, $[MIr(CH_3)(CO)_2(C_2H_4)$-$(dppm)_2][CF_3SO_3]$ (M = Rh, Ir)[24,25] and $[Ir_2(C_2H_4)(CO)(\mu\text{-}CO)(\mu\text{-}I)(dppm)_2][X]$ (X = I, BF_4)[1b] are the only other examples.

Since no other A-frame olefin complexes had been structurally characterized, an X-ray structure determination of **9** was undertaken. Unfortunately due to the 50:50 disorder of the CO and ethylene ligands (vide supra), the position of one of the CO ligands (bound to the same metal as C_2H_4 or as the other CO) could not be unambiguously established. Nevertheless the binding mode of the ethylene is clear, and its location adjacent to the bridged hydride ligand is also unequivocal. The perspective view of the cation of **9**, shown in Figure 5.2, reflects the probable structure based on NMR studies. In Tables 5.5 and 5.6 the parameters involving both disordered molecules are shown, with the atoms of one rotomer being primed.

Owing to the disorder, there will be some uncertainty in the metal-ligand parameters; nevertheless most parameters are well determined. The complex has the bridging dppm ligands in a normal trans arrangement about the metal centers (P(1)-Ir(1)-P(3) = 170.87(6)° and P(2)-Ir(2)-P(4) = 172.32(7)), and in a cis orientation to the other atoms coordinated to the metal nuclei. The Ir(1)-Ir(2) distance of 2.8199(4) Å corresponds to a normal single bond,[1a,1b,1e,1g,2,13] and is substantially shorter than the intraligand P-P separations (P(1)-P(2) = 3.002(3), P(3)-P(4) = 3.004(3)), indicating substantial attraction of the adjacent metal centers. The geometry about each metal is different, since one metal has both carbonyls attached whereas the other has the ethylene ligand coordinated. For Ir(2), the geometry is reminiscent of a trigonal bipyramid, having both carbonyls and the hydride ligand in the equatorial plane, and axial

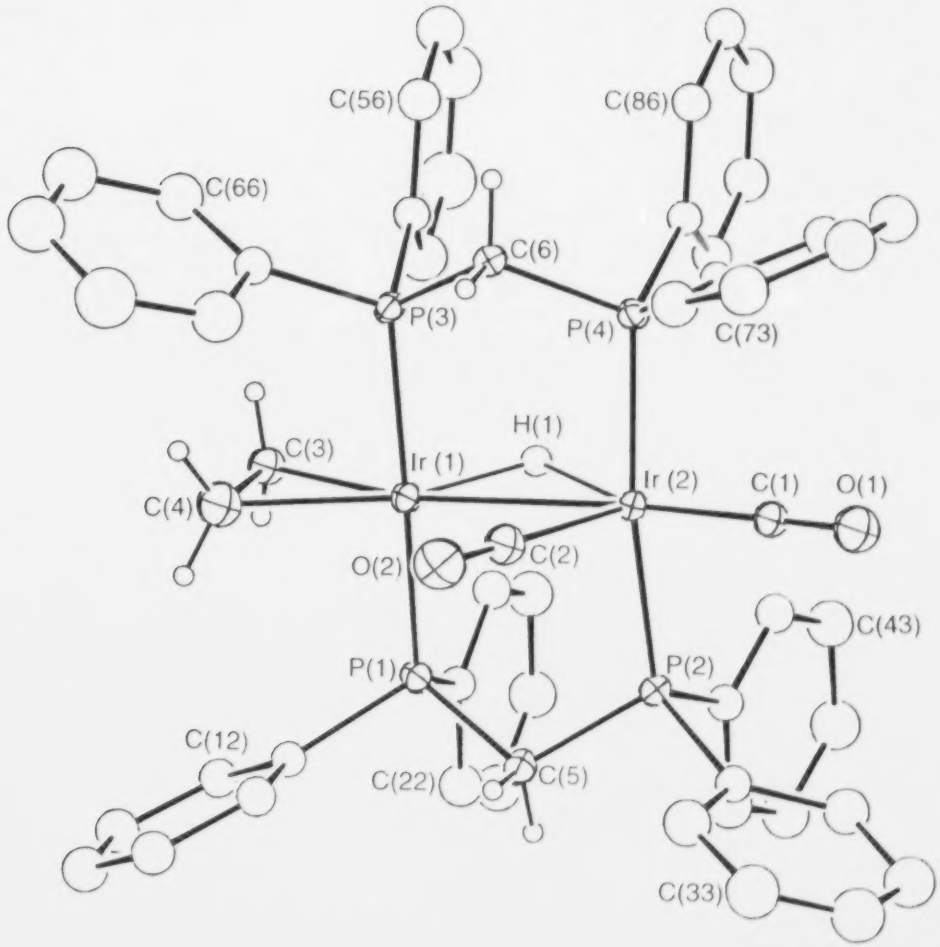

Figure 5.2. A perspective view of the $[Ir_2(C_2H_4)(CO)_2(\mu\text{-}H)(dppm)_2]^+$ cation, showing the numbering scheme. Thermal ellipsoids are shown at the 20% level except for the hydride, methylene and ethylene hydrogens, which are shown artificially small and the phenyl hydrogens, which are omitted.

Table 5.5. Selected Distances in (Å) in $[Ir_2(C_2H_4)(CO)_2(\mu\text{-}H)(dppm)_2][BF_4]$ (9)[a]

(a) Bonded

Ir(1)-H(1)	1.7(1)	P(1)-C(11)	1.818(7)
Ir(2)-H(1)	2.0(1)	P(1)-C(21)	1.821(7)
Ir(1)-Ir(2)	2.8199(4)	P(2)-C(5)	1.836(7)
Ir(1)-P(1)	2.310(2)	P(2)-C(31)	1.795(7)
Ir(1)-P(3)	2.315(2)	P(2)-C(41)	1.801(8)
Ir(1)-C(1)'	1.81(2)	P(3)-C(6)	1.822(7)
Ir(1)-C(2)	2.47(2)	P(3)-C(51)	1.808(7)
Ir(1)-C(2)'	1.91(2)	P(3)-C(61)	1.807(8)
Ir(1)-C(3)	2.20(2)	P(4)-C(6)	1.824(7)
Ir(1)-C(4)	2.22(3)	P(4)-C(71)	1.810(7)
Ir(2)-P(2)	2.318(2)	P(4)-C(81)	1.809(7)
Ir(2)-P(4)	2.319(2)	O(1)-C(1)	1.16(2)
Ir(2)-C(1)	1.76(2)	O(1)'-C(1)'	1.10(2)
Ir(2)-C(2)	1.99(2)	O(2)-C(2)	1.21(2)
Ir(2)-C(2)'	2.60(2)	O(2)-C(2)'	1.24(2)
Ir(2)-C(3)'	2.16(2)	C(2)-C(2)'	0.93(2)
Ir(2)-C(4)'	2.23(2)	C(3)-C(4)	1.56(3)
P(1)-C(5)	1.825(7)	C(3)'-C(4)'	1.51(2)

(b) Non-bonded

P(1)-P(2)	3.002(3)	C(2)-C(2)'	0.93(2)
P(3)-P(4)	3.004(3)		

[a]Primed atoms have 50% occupancy and are related to the unprimed (50% occupancy) atoms by the rotational disorder.

Table 5.6. Selected Angles (deg) in $[Ir_2(C_2H_4)(CO)_2(\mu\text{-}H)(dppm)_2][BF_4]$ (**9**)[a]

(a) Bond Angles

Ir(2)-Ir(1)-P(1)	92.27(5)	Ir(1)-P(1)-C(11)	114.7(2)
Ir(2)-Ir(1)-P(3)	92.09(5)	Ir(1)-P(1)-C(21)	115.7(2)
Ir(2)-Ir(1)-C(1)'	172.3(6)	C(5)-P(1)-C(11)	102.4(3)
Ir(2)-Ir(1)-C(2)'	63.3(5)	C(5)-P(1)-C(21)	103.5(3)
Ir(2)-Ir(1)-C(3)	157.7(4)	C(11)-P(1)-C(21)	106.0(3)
Ir(2)-Ir(1)-C(4)	160.7(6)	Ir(2)-P(2)-C(5)	113.8(2)
P(1)-Ir(1)-P(3)	170.87(6)	Ir(2)-P(2)-C(31)	115.4(2)
P(1)-Ir(1)-C(1)'	87.4(5)	Ir(2)-P(2)-C(41)	115.0(2)
P(1)-Ir(1)-C(2)'	97.7(4)	C(5)-P(2)-C(31)	101.5(3)
P(1)-Ir(1)-C(3)	87.7(4)	C(5)-P(2)-C(41)	105.4(3)
P(1)-Ir(1)-C(4)	91.3(6)	C(31)-P(2)-C(41)	104.3(3)
P(3)-Ir(1)-C(1)'	89.3(5)	Ir(1)-P(3)-C(6)	113.0(2)
P(3)-Ir(1)-C(2)'	91.5(4)	Ir(1)-P(3)-C(51)	114.8(2)
P(3)-Ir(1)-C(3)	85.2(4)	Ir(1)-P(3)-C(61)	114.8(3)
P(3)-Ir(1)-C(4)	87.2(6)	C(6)-P(3)-C(51)	105.5(3)
C(2)'-Ir(1)-C(3)	138.8(6)	C(6)-P(3)-C(61)	103.3(3)
C(2)'-Ir(1)-C(4)	97.4(8)	C(51)-P(3)-C(61)	104.2(4)
Ir(1)-Ir(2)-P(2)	92.18(5)	Ir(2)-P(4)-C(6)	112.3(2)
Ir(1)-Ir(2)-P(4)	92.47(4)	Ir(2)-P(4)-C(71)	114.4(2)
Ir(1)-Ir(2)-C(1)	174.3(6)	C(6)-P(4)-C(71)	104.5(3)
Ir(1)-Ir(2)-C(2)	58.8(5)	Ir(2)-P(4)-C(81)	116.9(2)
Ir(1)-Ir(2)-C(3)'	162.3(4)	C(6)-P(4)-C(81)	103.7(3)
Ir(1)-Ir(2)-C(4)'	157.6(4)	C(71)-P(4)-C(81)	103.7(3)
P(2)-Ir(2)-P(4)	172.32(7)	Ir(1)-C(1)'-O(1)'	174(2)
P(2)-Ir(2)-C(1)	86.2(5)	Ir(2)-C(1)-O(1)	173(2)
P(2)-Ir(2)-C(2)	93.6(5)	Ir(1)-C(2)-O(2)	113(1)
P(2)-Ir(2)-C(3)'	87.7(4)	Ir(1)-C(2)'-O(2)	178(1)
P(2)-Ir(2)-C(4)'	89.9(4)	Ir(2)-C(2)-O(2)	168(1)

Table 5.6. (continued)

P(4)-Ir(2)-C(1)	89.7(5)	Ir(2)-C(2)'-O(2)	107(1)
P(4)-Ir(2)-C(2)	94.1(5)	Ir(1)-C(3)-C(4)	70(1)
P(4)-Ir(2)-C(3)'	86.0(4)	Ir(2)-C(3)'-C(4)'	73(1)
P(4)-Ir(2)-C(4)'	88.1(4)	Ir(2)-C(4)'-C(3)'	67(1)
C(1)-Ir(2)-C(2)	115.8(8)	Ir(1)-C(4)-C(3)	68(1)
C(2)-Ir(2)-C(3)'	138.9(6)	P(1)-C(5)-P(2)	110.1(4)
C(2)-Ir(2)-C(4)'	98.8(7)	P(3)-C(6)-P(4)	110.9(4)
Ir(1)-P(1)-C(5)	113.1(2)		

(b) Torsion Angles

C(3)-Ir(1)-Ir(2)-P(4)	81.78(1.22)	P(1)-Ir(1)-Ir(2)-C(3)'	86.80(1.53)
C(4)-Ir(1)-Ir(2)-P(2)	97.77(1.62)	P(3)-Ir(1)-Ir(2)-C(4)'	90.36(1.16)

[a]Labelling as in footnote of Table 5.5.

phosphine groups, giving this metal an 18-electron count. Ir(1) has a geometry best described as square planar, in which the ethylene occupies one site and the Ir(2)-H bond, which can be viewed as forming an agostic bond to Ir(1) occupies the opposite site, with the remaining positions occupied by the mutually trans phosphorus atoms. Donation of the Ir(2)-H electron pair to the cationic Ir(1) center gives this metal the 16-electron configuration that is typical for a d^8, square planar complex. The Ir(2)-C(2) distance of 1.99(2) Å (1.91(2) Å)[26] is normal for an Ir-CO bond, while the Ir(1)-C(2) distance of 2.47(2) Å (2.60(2) Å) suggests the presence of a weak semibridging interaction. However the presence of a single CO stretch at 1977 cm^{-1} in the IR spectrum of **9** suggests that any such interaction between one of the CO ligands and the adjacent metal must be very weak. Although the deviation of the Ir(2)-C(2)-O(2) angle from linearity should give an indication of the strength of the Ir(1)-C(2) interaction, the poorly defined position of O(2), owing to the disorder, casts some doubt on this angle at C(2). The other CO ligand is essentially linear, as indicated by the Ir(2)-C(1)-O(1) angle of 173(2)°(174(2)°), and the Ir(2)-C(1) and C(1)-O(1) bond distances of 1.76(2) Å (1.81(2) Å), and 1.16(2) Å (1.10(2) Å), respectively, are normal for a terminally bound carbonyl ligand. The hydride ligand bridges the two metals in an approximately symmetrical manner, with Ir(1)-H(1) = 1.7(1) Å and Ir(2)-H(1) = 2.0(1) Å. Owing to the disorder, any assymmetry in the Ir-H distances cannot be significant but must result from the refinement model. The ethylene ligand is coordinated to Ir(1) almost perpendicular to the metal-phosphorus plane with torsion angles of C(3)-Ir(1)-Ir(2)-P(4) = 82(1)° (87(2)°) and C(4)-Ir(1)-Ir(2)-P(2) = 98(2)° (90(1)°). The C(3)-C(4) distance of 1.56(3) Å (1.51(2) Å) is approximately equal to that of a C-C single bond, and is close

to the C-C distance of the coordinated ethylene ligand in $[PtCl_2(C_2H_4)(NC_7H_{10})]$ (1.494(21) Å).[27] The Ir(1)-C(3) and Ir(1)-C(4) distances of 2.20(2) Å (2.16(2) Å) and 2.22(3) Å (2.23(2) Å), respectively, are within the expected range for Ir-C single bonds.

The orientation of the ligands in **9**, such that the coordinated ethylene is adjacent to the hydride ligand, suggests that it should be possible to induce insertion of the unsaturated ligand into an Ir-H bond to give a vinyl compound. However, ethylene loss is also a possibility, in reactions of compound **9**. In fact compound **9** reacts with H_2, losing ethylene to give compound **1**. The signal at δ 5.33 in the ^1H NMR spectrum of the reaction mixture indicates the presence of free ethylene.

The observation that compound **1** reacts with ethylene to give ethane and **9**, and that the former complex can be regenerated by reacting **9** with H_2, suggests that compound **1** is a potential catalyst for the hydrogenation of ethylene. However no catalytic studies on **1** have been undertaken.

It was anticipated that compound **9** could be obtained from the reaction of $[Ir_2(CO)_2(\mu\text{-}CO)(\mu\text{-}H)(dppm)_2][BF_4]$ (**7**) with ethylene, since $[Ir_2(CO)_2(\mu\text{-}H)(\mu\text{-}Ph_2C_2)(dppm)_2][BF_4]$ (**6**) is obtained from the reaction of **7** with diphenylacetylene, and in light of the similar pathways proposed for the formation of **6** and **9** from **1**. However **7** does not react with ethylene.

The reaction of compound **1** with tetrafluoroethylene gives a mixture of the compound, $[Ir_2(H)_2(CO)_2(\mu\text{-}H)(\mu\text{-}C_2F_4)(dppm)_2][BF_4]$ (**10**) together with starting material, in a typical ratio of 1:1. The $^{31}P\{^1H\}$ NMR spectrum of compound **10** shows a singlet at δ -8.5, indicating that all the phosphorus nuclei are equivalent. The high-field region of the ^1H NMR spectrum shows a multiplet at δ -10.76, due to the two terminal hydrides,

and a quintet (due to coupling to the four phosphorus nuclei) at δ -18.02, while the ^{19}F spectrum shows a broad resonance at δ -73.9 due to the C_2F_4 ligand (the intensity of this signal relative to that of the BF_4 anion indicates that the former signal is due to four fluorine atoms). All of these NMR data are consistent with the tetrafluoroethylene ligand bridging the two Ir centers in **10**. Binuclear complexes with bridging tetrafluoroethylene ligands are known, and include $[Fe_2(CO)_6(\mu\text{-}SMe)_2(\mu\text{-}C_2F_4)]$,[28] $[Pt_2(1,5\text{-}C_8H_{12})_2(\mu\text{-}C_2F_4)_2]$ and $[Pd_2(1,5\text{-}C_8H_{12})_2(\mu\text{-}C_2F_4)]$,[29] which are obtained by reacting tetrafluoroethylene with $[Fe(CO)_3(\mu\text{-}SMe)]_2$, $[Pt(1,5\text{-}C_8H_{12})_2]$ and $[Pd(1,5\text{-}C_8H_{12})_2]$, respectively. However, to our knowledge no binuclear dppm-bridged complexes of Ir with bridging tetrafluoroethylene ligands have been reported.

The reactions of compound **1** with ethylene and tetrafluoroethylene, once again, follow the trend observed in its reactions with alkynes, in which the unactivated unsaturated substrates undergo hydrogenation while the activated ones merely coordinate to the metal complex. The extremely slow reaction of **1** with tetrafluoroethylene, compared to that with ethylene, and the fact that the former gas does not give complete conversion of **1** to **10** is presumably steric, resulting from unfavorable interactions between the fluorine substituents and the phenyl groups of the dppm ligands.

Summary

The reactions of $[Ir_2(H)(CO)_2(\mu\text{-}H)_2(dppm)_2][BF_4]$ (**1**) with the alkynes, RC≡CR (R= CO_2Me, CF_3, and H), as well as with tetrafluoroethylene, do not result in hydrogenation of the unsaturated substrate. Instead they give

the compounds, $[Ir_2(H)_2(CO)_2(\mu\text{-}H)(\mu\text{-}L)(dppm)_2][BF_4]$ (L = DMAD (**3**), HFB (**4**), C_2H_2 (**5**), C_2F_4 (**10**)). In contrast to these reactions, that of **1** with diphenylacetylene gives $[Ir_2(CO)_2(\mu\text{-}H)(\mu\text{-}PhC{\equiv}CPh)(dppm)_2][BF_4]$ (**6**) and *cis*-stilbene, while that with ethylene gives $[Ir_2(C_2H_4)(CO)_2(\mu\text{-}H)(dppm)_2][BF_4]$ (**9**) and ethane. Compound **1** also reacts with phenylacetylene to give styrene. It has been shown that with the exception of acetylene, the substrates that are hydrogenated in their reaction with **1** are unactivated, having no strongly electron withdrawing substituents, while the activated substrates react with **1** by simply coordinating to it. As discussed earlier, this is possibly due to the strong Ir-C bonds formed by the activated substrates on coordination to **1**, which precludes any further transformation, as well as the greater tendancy for the activated alkynes to bridge the metals.

The hydrogenation of ethylene observed in its reaction with compound **1**, and the regeneration of **1** on reacting **9** with H_2, suggest that former complex is a potential catalyst for the hydrogenation of ethylene.

In a related reaction, the protonation of $[Ir_2(CO)_2(\mu\text{-}\eta^2{:}\eta^2\text{-}DMAD)(dppm)_2]$ (**III**) gives rise to a change of the coordination mode of the alkyne from perpendicular to parallel to the metal-metal axis, yielding $[Ir_2(H)(CO)_3(\mu\text{-}DMAD)(dppm)_2][BF_4]$ (**8**).

References and Footnotes

1. See, for example: (a) Xiao, J.; Cowie, M. *Organometallics* **1993**, *12*, 463. (b) Vaartstra, B. A.; Xiao, J.; Jenkins, J. A.; Verhagen, R.; Cowie, M. *Organometallics* **1991**, *10*, 2708. (c) Antonelli, D. M.; Cowie, M. *Inorg. Chem.* **1990**, *29*, 4039. (d) Vaartstra, B. A.; Cowie, M. *Organometallics* **1990**, *9*, 1594. (e) Vaartstra, B. A.; Cowie, M. *Organometallics* **1989**, *8*, 2388. (f) Cowie, M.;Vasapollo, G.; Sutherland, B. R.; Ennett, J. P. *Inorg.* **1986**, *25*, 2648. (g) Sutherland, B. R.; Cowie, M. *Organometallics* **1985**, *4*, 1801. (h) Sutherland, B. R.; Cowie, M. *Organometallics* **1984**, *3*, 1869. (i) McDonald, R. Ph.D. Thesis, University of Alberta, 1991, Chapter 5. (j) Vaartstra, B. A. Ph.D. Thesis, University of Alberta, 1989.
2. McDonald, R.; Sutherland, B. R.; Cowie, M. *Inorg. Chem.* **1987**, *26*, 3333.
3. Sutherland, B. R.; Cowie, M. *Organometallics* **1985**, *4*, 1637.
4. Doedens, R. J.; Ibers, J. A. *Inorg. Chem.* **1967**, *6*, 204.
5. Walker, N.; Stuart, D. *Acta Crystallogr., Sect. A: Found Crystallogr.* **1983**, *A39*, 1581.
6. Programs used were those of the Enraf-Nonius Structure Determination Package by B. A. Frenz, in addition to local programs by R. G. Ball.
7. See, for example: (a) Antonelli, D. M.; Cowie, M. *Organometallics* **1991**, *10*, 2173. (b) Chapter 2 of this thesis.
8. Cromer, D. T.; Waber, J. T. *International Tables for Crystallography*; Kynoch Press: Birmingham, England, 1974; Vol. IV, Table 2.2A.

9. Stewart, R. F.; Davidson, E. R.; Simpson, W. T. *J. Chem. Phys.* **1965**, *42*, 3175.

10. Cromer, D. T.; Liberman, D. *J. Chem. Phys.* **1970**, *53*, 1891.

11. See Chapter 6 of ref 1j.

12. Mague, J. T. *Organometallics* **1986**, *5*, 918.

13. Mague, J. T; Klein, C. L.; Majeste, R. J.; Stevens, E. D. *Organometallics* **1984**, *3*, 1860.

14. Cowie, M.; Dickson, R. S.; Hames B. W. *Organometallics* **1984**, *3*, 1879.

15. (a) Puddephatt, R. J.; Thomson, M. A. *Inorg. Chem.* **1982**, *21*, 725. (b) Puddephatt, R. J.; Thomson, M. A. *Inorg. Chim. Acta* **1980**, *45*, L281.

16. Such binuclear complexes, with an alkyne bridging two metals parallel to the metal-metal axis, are sometimes referred to as dimetalated olefinic compounds in which case reference is made to the C=C stretch of the olefin instead of the C≡C stretch of the coordinated alkyne.

17. (a) Berry, D. H.; Eisenberg, R. *Organometallics* **1987**, *6*, 1796. (b) Berry, D. H.; Eisenberg, R. *J. Am. Chem. Soc.* **1985**, *107*, 7181.

18. All NMR signals have the appropriate ratios of intensity.

19. See Chapter 4 of this thesis.

20. Bray, J. M.; Mawby, R. J. *J. Chem. Soc., Dalton Trans.* **1989**, 589.

21. Nakamura, A.; Otsuka, S. *J. Am. Chem. Soc.* **1972**, *94*, 1886.

23. See, for example: (a) Antonelli, D. M.; Cowie, M. *Organometallics* **1990**, *9*, 1818. (b) Antonelli, D. M.; Cowie, M. *Organometallics* **1991**, *10*, 2550. (c) McDonald, R.; Cowie, M. *Inorg. Chem.* **1990**, *29*, 1564. (d) Elliot, D. J.; Ferguson, G.; Holah, D. G.; Hughes, A. N.; Jennings, M. C.; Magnuson, V. R.; Potter, D.; Puddephatt, R. J. *Organometallics*

1986, *5*, 918.

24. See Chapters 2 and 3 of this thesis.
25. Antwi-Nsiah, F.; Cowie, M. *Organometallics* **1992**, *11*, 3157.
26. The parameter quoted in parenthesis throughout this discussion, is for the second rotomer of the disordered structure. Therefore, the two equivalent bonds involving Ir and C(2) are Ir(2)-C(2) and Ir(1)-C(2)'. See the description of the disorder given in the Structure Solution and Refinement Section.
27. Caruso, F.; Spagna, R.; Zambonelli, L. *Inorg. Chim. Acta* **1979**, *32*, L23.
28. Bonnet, J. J.; Mathieu, R.; Poilblanc, R.; Ibers, J. A. *J. Am. Chem. Soc.* **1979**, *101*, 7487.
29. Green, M.; Laguna, A.; Spencer, J. L.; Stone, F. G. A. *J. Chem. Soc., Dalton Trans.* **1977**, 1010.

Chapter 6

Conclusions

The first objective of this thesis project was to synthesize alkyl derivatives of the binuclear 'RhIr' complex, $[RhIr(CO)_3(dppm)_2]$ and its homonuclear diiridium analogue, $[Ir_2(CO)_3(dppm)_2]$. In light of the results of protonation reactions of these two binuclear compounds,[1,2] it was anticipated that their reactions with the electrophile CH_3^+ (in the form of methyl triflate) might yield the CH_3-bridged analogues of the hydrido-bridged species, which were of interest because of their relevance to C-H activation by an adjacent metal. The second step, after these alkyl complexes had been synthesized, was to investigate their reactivity with small molecules, such as CO, H_2 and alkynes, in order to obtain information on their potential utility as models for studies of some of the transformations involving metal alkyl complexes in catalysis. It was expected that the 'RhIr' complex could combine certain attractive properties of each metal (such as the catalytic activity of Rh complexes and the stability of Ir complexes) to give certain unique reactivity patterns, compared to its diiridium analogue and related mononuclear complexes. Reactions that were of particular interest included insertion reactions (of CO, SO_2, unsaturated organic substrates, etc.), leading to the formation of C-C or C-heteroatom bonds. We were also interested in the potential for two-metal involvement in binuclear reductive elimination, and in the possibilities of C-H activation of the coordinated alkyl group by the

adjacent metal. Furthermore, it was of interest to determine how the reactivities of the 'RhIr' and 'Ir_2' systems compared with each other, in the expectation that their comparison could shed some light on the roles of the two metals in the reactions involving binuclear complexes.

Several 'RhIr' and diiridium alkyl complexes, which display considerable diversity in their chemistry, have been prepared in this study. The initial complexes prepared were $[RhIr(CH_3)(CO)_3(dppm)_2][CF_3SO_3]$ (**1**) and $[Ir_2(H)(CO)_3(\mu\text{-}CH_2)(dppm)_2][CF_3SO_3]$ (**2**), from the reactions of methyl triflate with $[RhIr(CO)_3(dppm)_2]$ and $[Ir_2(CO)_3(dppm)_2]$, respectively, and these proved useful as precursors to a variety of related alkyl species.

Compound **1** differs from a number of Rh-containing binuclear alkyl complexes that have been synthesized in this research group,[3] having its alkyl group bound to the coordinatively saturated metal, while in several other closely related complexes, such as $[RhOs(CH_3)(CO)_3(dppm)_2]$[3a] and $[RhRe(CH_3)(CO)_4(dppm)_2][CF_3SO_3]$,[3b] the alkyl groups were invariably bound to the coordinatively unsaturated group 9 metal. It is particularly noteworthy that the 'RhOs' analogue is isoelectronic to the 'RhIr' species, **1**, yet still differs in the location of the alkyl group. Even more puzzling was the migration of the methyl group from Ir to Rh, upon reaction of **1** with C_2H_4 or SO_2. In the ethylene adduct, substitution of CO by ethylene has yielded a product rather analogous to the 'RhOs-methyl' complex. Although the alkylation of $[RhIr(CO)_3(dppm)_2]$ did not yield the targetted methyl-bridged species, such species are presumably involved as intermediates in the reactions in which methyl migration from Ir to Rh occurs.

In the case of the diiridium system, alkylation of $[Ir_2(CO)_3(dppm)_2]$ also did not yield a methyl-bridged product, but resulted instead in compound **2**, as mentioned above, in which one of the C-H bonds of a

coordinated methyl group has been activated by the adjacent metal towards oxidative addition. However, such an activation presumably occurs via an intermediate methyl species, $[Ir_2(CH_3)(CO)_3(dppm)_2][CF_3SO_3]$ (**3**), in which the methyl group either bridges both metals or is terminal. Although this methyl species, **3**, is not observed directly, its involvement in subsequent chemistry is implicated by the NMR study which has shown its involvement in the scrambling of the μ-CH_2 hydrogens and the hydride ligand of **2**. It is probably this methyl species which is involved in the subsequent chemistry of **2**, since it has a coordinatively unsaturated Ir center, which is not available in the methylene-hydride complex, permitting attack by various substrates. The realization of our goal of obtaining a methyl-bridged species resulted from the abstraction of a CO ligand from compound **2**, using anhydrous Me_3NO to yield $[Ir_2(CO)_2(\mu\text{-}CH_3)(OSO_2CF_3)(dppm)_2]$ (**4**). The addition of some small molecules, such as CO, phosphines and isocyanides, reverses the migratory insertion step, leading to C-H activation and the formation of the appropriate methylene-bridged hydride complexes, $[Ir_2(H)(CO)_2(L)(\mu\text{-}CH_2)(dppm)_2]^+$, while reaction with other reagents (eg C_2H_4) yield compounds containing terminal methyl groups. However, in a surprising result, reaction of **4** with SO_2 yields another methyl-bridged complex, $[Ir_2(CO)_2(\mu\text{-}CH_3)(\mu\text{-}SO_2)(dppm)_2][CF_3SO_3]$ (**5**), in which now the methyl ligand is asymmetrically bridging the metals, being σ-bound to one metal while engaging in an agostic C-H-Ir interaction to the other.[4] These transformations from terminal methyl, to symmetrically-bridged methyl, to asymmetrically-bridged methyl, to C-H activation products are among the most important results obtained in this study. Most of the binuclear compounds reported, which have a bridging methyl group, have it in an asymmetrically bridging orientation, being terminally-bound to one metal center while engaging in an agostic interaction

with the other (a similar coordination mode to that in the methyl-bridged SO_2 complex, **5**, mentioned earlier).[4] Furthermore, the successful synthesis of the two methyl-bridged complexes, **4** and **5**, fulfills one of the goals of this study, which was to prepare such methyl-bridged complexes. It is evident from the variety of coordination modes of the methyl group in the alkyl complexes obtained in this study, some of which are mentioned above, that in these binuclear systems, terminal methyl, symmetrically-bridged methyl, agostic methyl or methylene-bridged complexes can be obtained if certain ideal electronic conditions are created by use of the appropriate combinations of metals and ancillary ligands.

Secondly, this study was successful in achieving C-C bond formation, resulting from migratory insertion of the methyl group, in some of our complexes, onto a few substrate molecules. The migratory insertion involving coordinated CO groups yields a number of acyl species, and the related insertion involving an isocyanide ligand yields an iminoacyl species. The insertion of DMAD into the M-CH_3 bonds in compounds **1** and **3** (the reactive species in reactions of **2**), also occurs yielding the respective vinyl compounds. An unusual example in which C-heteroatom (C-P in this case) bond formation resulted unexpectedly, occurred from the formal insertion of acetylene into a Rh-P (dppm) bond in compound **1**. Details of these reactions are given later in this discussion (vide infra).

This study reinforces conclusions drawn from previous studies that despite the obvious similarities between Rh and Ir, some of their different properties result in some significant differences in the chemistries of binuclear 'RhIr' complexes, on one hand, and the analogous diiridium complexes, on the other.[1,2,5] Such differences in the properties of the metals include the greater basicity of Ir and the greater strengths of Ir-C and Ir-H bonds[6]

compared to those of Rh, as well as the preference by Rh of a 16-electron configuration with a square-planar coordination geometry[1,5c] and the greater tendency of Rh alkyls to undergo migratory insertion reactions compared to their Ir counterparts (resulting from the cited greater strength of Ir-C bonds compared to those of Rh).[6]

The greater basicity of Ir, which enables it to bind more carbonyl groups[7] is clearly seen in the reaction of the compound **2** with CO, which yields first, a tetracarbonyl complex $[Ir_2(CH_3)(CO)_4(dppm)_2][CF_3SO_3]$ (**6**), which reacts further with CO to yield the acyl species $[Ir_2(CH_3CO)(CO)_4(dppm)_2][CF_3SO_3]$ (**7**). Compound **1**, on the other hand, yields an acyl species, $[RhIr(CH_3CO)(CO)_3(dppm)_2][CF_3SO_3]$ (**8**), on reacting with only one equiv of CO. A similar behavior is seen in the reactions with SO_2, in which **1** yields an acyl species $[RhIr(CH_3CO)(CO)_2(\mu\text{-}SO_2)(dppm)_2][CF_3SO_3]$ (**9**), as the final product, whereas compound **2** requires the addition of CO to the initial SO_2 adduct, $[Ir_2(CH_3)(CO)_3(\mu\text{-}SO_2)(dppm)_2][CF_3SO_3]$ (**10**), to yield an acyl species $[Ir_2(CH_3CO)(CO)_3(\mu\text{-}SO_2)(dppm)_2][CF_3SO_3]$ (**11**).

Secondly, the greater strengths of Ir-H and Ir-C bonds, compared to those of Rh, which result in greater stability of Ir complexes is displayed in the characterization of a hydrido-alkyl intermediate, and several polyhydrido species, in the reaction of **2** with H_2, whereas no intermediates could be characterized in similar reactions of compound **1**. The pathway proposed for the reaction of the diiridium complex with H_2, based on the products observed , suggests that although both metals are involved in many of the transformations that occur in the reaction, the reductive elimination of methane, and that of H_2, takes place at one metal center.

Another example of the differences observed in the chemistries of the diiridium and 'RhIr' complexes in this study is seen in the C-H activation of

the coordinated methyl group that is observed in the formation of compound **2**, whereas no such activation is observed in compound **1**. This observation is possibly due to the coordinatively unsaturated metal center in the diiridium complex (the intermediate methyl complex, **3**, in this case), being more electron-rich (and thus favoring oxidative addition) than that in the 'RhIr' complex. Presumably this also accounts for the C-H activation of acetylene in its reaction with **2** to yield $[Ir_2(H)(CH_3)(CO)_3(\mu\text{-}\eta^1\text{:}\eta^2\text{-}C{\equiv}CH)(dppm)_2]$-$[CF_3SO_3]$ (**12**) as the initial product observed at low temperature (whereas in its reaction with **1**, under similar conditions, the initial product is the alkyne-bridged complex, $[RhIr(CH_3)(CO)_3(\mu\text{-}C_2H_2)(dppm)_2][CF_3SO_3]$ (**13**)).

Lastly, the strong tendency of Rh to adopt a 16-electron configuration with a square planar geometry is exhibited in the structures of several of the 'RhIr' complexes that have been characterized in this study.

While the reactivity differences between **1** and **2**, in several of their reactions, can be rationalized, there are some that cannot be explained. For example it is not clear why their reactions with ethylene yield the products, $[MIr(CH_3)(CO)_2(C_2H_4)(dppm)_2][CF_3SO_3]$ (M = Rh (**14**), Ir (**15**)), having the methyl group on the coordinatively unsaturated metal in the 'RhIr' case but on the coordinatively saturated metal in the diiridium case. Also the observation of C-H activation of the alkyne by compound **1**, in reactions with phenylacetylene, as mentioned above, while **2** (having a reactive species, **3**, with a more electron-rich coordinatively unsaturated metal), yields the alkyne bridged species, $[Ir_2(CH_3)(CO)_3(\mu\text{-}PhC_2H)(dppm)_2][CF_3SO_3]$ (**16**), as the sole product with the same reagent under similar conditions cannot be explained. It is also noteworthy that the opposite is true in their reactions with acetylene itself. Another puzzling difference in the reactivities of **1** and **2** is that displayed in their reactions with ^{t}BuNC. The reaction with **1** results in

migratory insertion of the methyl ligand onto the coordinated carbon atom of the isocyanide, with concomitant coordination of the nitrogen to Rh and CO loss to yield the iminoacyl-bridged complex, $[RhIr(CO)_2(\mu\text{-}C(CH_3)=N^tBu)(dppm)_2][CF_3SO_3]$ (**17**), whereas that with **2** leads to CO substitution accompanied by C-H activation of the methyl group (in the reactive intermediate, **3**) to yield $[Ir_2(H)(CO)_2(\mu\text{-}CH_2)(^tBuNC)(dppm)_2][CF_3SO_3]$ (**18**). The fact that the methyl group is bound to an Ir center in both **1** and **3**, makes it difficult to rationalize this difference in reactivity. However, it is possible that the 'RhIr' reaction proceeds via an intermediate which has the methyl and ^{t}BuNC groups both on Rh, which would explain the more facile migratory insertion.

In addition to these differences, the 'RhIr' and diiridium complexes also display some similarities. For example, both **1** and **2** react with DMAD to yield $[MIr(RC=C(CH_3)R)(CO)_2(dppm)_2][CF_3SO_3]$ (R = CO_2Me; M = Rh (**19**) and Ir (**20**), respectively), which are products of alkyne insertion into M-C(alkyl) bonds, while the reactions of both of them with phosphines and phosphites result in CO substitution. Also their reactions with hydrogen yield the known trihydrides $[MIr(H)(CO)_2(\mu\text{-}H)_2(dppm)_2]^+$ (M = Rh (**21**), Ir (**22**)),[1,5e] as the final products, through liberation of methane and CO.

Another important observation that was made in this study is the metal-metal cooperativity displayed by the two metals in several of the binuclear complexes. These are seen in the many ligand migrations that occur between the two metal centers and in the changes in coordination modes from terminal to bridging and vice versa. Examples include, the transfer of the methyl group from Ir to Rh, exhibited in the reactions of **1** with SO_2 and ethylene, the transfer of a hydride between the two Ir centers and the movement of a CO ligand from a terminal to a bridging position, that are

observed in the reaction of **2** with H_2. Other examples include the activation of a C-H bond of a coordinated methyl group to give the methylene hydride complex, **2**, and the migratory insertion of the hydride ligand in this complex onto the CH_2 group to generate methyl complexes such as **4** and the proposed reactive intermediate, **3**. Such cooperativity is also displayed clearly in the C-H activation processes that occur in the reactions of **4** with PMe_2Ph and ^tBuNC, to yield $[Ir_2(H)(CO)_2(\mu\text{-}CH_2)(PMe_2Ph)(dppm)_2][CF_3SO_3]$ (**23**) and **18**, respectively. This last process is one of the key results of this study.

The structures of the hydrido-acetylides, $[Ir_2(H)(CH_3)(CO)_3(\mu\text{-}\eta^1\text{:}\eta^2\text{-}C{\equiv}CH)(dppm)_2][CF_3SO_3]$ (**12**) and $[RhIr(H)(CH_3)(CO)_3(\mu\text{-}\eta^1\text{:}\eta^2\text{-}C{\equiv}CPh)(dppm)_2][CF_3SO_3]$ (**24**), and those of the vinylidene complexes, $[Ir_2(CH_3)(CO)_3(\mu\text{-}C{=}CH_2)(dppm)_2][CF_3SO_3]$ (**25**) and $[RhIr(CH_3)(CO)_3(\mu\text{-}C{=}C(H)Ph)(dppm)_2][CF_3SO_3]$ (**26**), respectively, to which they are subsequently transformed, suggest a probable pathway for the hydrido-acetylide-to-vinylidene transformations involved. Evidently this isomerization proceeds through the migration of the hydride ligand to the β-carbon of the acetylide ligand. Presuming that, in the case of these two 'RhIr' and diiridium hydrido-acetylide compounds, the hydride migration proceeds via the adjacent metal, it was suggested in Chapter 4 that such a migration could bring this ligand into close proximity of the acetylide ligand, as a result of the $\mu\text{-}\eta^1\text{:}\eta^2$-coordination mode of the latter ligand, and that this could then facilitate the subsequent metal-to-β-carbon migration to yield the vinylidene compounds. It can be seen, therefore, that the hydrido-acetylide to vinylidene isomerizations constitute one of the transformations in which metal-metal cooperativity is displayed by certain compounds in this study.

Apparently the greater reactivity of the 'RhIr' and diiridium alkyl complexes, observed in this study, compared to those of the 'RhRe' and

'IrRe'[3b] complexes, is partly due to the greater involvement of both metals in the complexes in this study, in their reactions, whereas in those of the Re complexes the chemistry occured primarily at one metal (the group 9 metal).

Although dppm ligands usually play a 'spectator' role in reactions of complexes containing them, neither attacking nor being attacked by other ligands or substrates,[8] one of the very rare cases of their direct involvement in reactions is displayed in the transformation of $[RhIr(CH_3)(CO)_3(\mu\text{-}C_2H_2)(dppm)_2][CF_3SO_3]$ (**13**), which is the initial product characterized in the low temperature reaction of **1** with acetylene (as mentioned earlier), to $[RhIr(CH_3)(CO)_3(HC{=}C(H)P(Ph)_2CH_2PPh_2)(dppm)][CF_3SO_3]$ (**27**). This transformation, which constitutes a formal insertion of acetylene into a Rh-P(dppm) bond, presumably results from dissociation of one end of a diphosphine, followed by attack of this phosphorus on the alkyne carbon that is bound to Ir, with simultaneous dissociation of the carbon from Ir and coordination of the π-bond of the formally inserted acetylene to Ir.

This study has clearly shown that binuclear diiridium and 'RhIr' alkyl complexes can be readily prepared, and that they undergo many of the transformations involving alkyl complexes, which occur in catalysis, such as migratory insertions of the alkyl group, reductive elimination of alkanes, oxidative addition of hydrogen, ligand association and dissociation, C-H activation of the alkyl group (and the reverse; migratory insertion of a hydride ligand onto an alkylidene to yield an alkyl group), and insertion of unsaturated organic substrates into M-C(alkyl) bonds. This, together with the observation that they exhibit metal-metal cooperativity, indicates that they could serve as good models for the study of these processes. One other important result of this study is the number of intermediates that have been characterized at low temperature by NMR spectroscopy. It appears that the

ability of Ir to form more stable complexes accounts in part for the stability conferred on the intermediates, such that they can be characterized. This makes these alkyl complexes all the more attractive as models for studies of catalytic processes, such as those outlined above, involving alkyl derivatives. Also, in this study, three 'RhIr' complexes, **1**, **17** and $[RhIr(C{\equiv}CPh)_2(CO)_2(\mu\text{-}H)(dppm)_2][CF_3SO_3]$ (**28**), have been characterized by X-ray crystallographic methods, adding to the only two reported dppm-bridged 'RhIr' complexes previously characterized by this method.[1,5c]

Although C-H activation of a coordinated methyl group was observed in the formation of **2**, as mentioned previously, it has not been possible to exploit this activation in this study, in the sense that the hydride ligand could neither be abstracted, replaced with a chloride, nor induced to undergo migratory insertion with any substrates. Apparently this is due to the facile interconversion between the methylene-hydride and the methyl complexes, **2** and **3**, respectively, making the latter complex the reactive species in the reactions of compound **2**. Thus it is expected that such reactivity involving the hydride ligand will be more favored in other methylene-hydride complexes obtained, such as $[Ir_2(H)(CO)_2(\mu\text{-}CH_2)(PMe_3)(dppm)_2][CF_3SO_3]$ (**29**), which have stronger σ-donor and weaker π-acceptor ligands in place of one of the CO ligands. This is because these ligands stabilize the hydrido-methylene complex and these complexes apparently do not exhibit any hydrido-methylene-to-methyl interconversion, making the hydride ligand more accessible. On this account, further reactivity studies involving these CO-substituted complexes are recommended. Furthermore studies of the reactivities of the two bridging methyl compounds, **4** and **5** are recommended. The reactions with alkynes will be especially interesting, since these will definitely yield different products from those obtained with **2**, in

light of the observation that the latter complex yields products with three CO ligands in these reactions, as shown in Chapter 4, whereas the methyl-bridged complexes have only two CO ligands and in addition one of these complexes has an SO_2 ligand in place of the third CO ligand.

The second objective of this thesis project was to extend the alkyne and alkene hydrogenation chemistry, which had been carried out with $[Ir_2(H)_2(Cl)_2(CO)_2(dppm)_2]$[5f] and $[Ir_2(H)_2(CO)_2(\mu\text{-}Cl)(dppm)_2][BF_4]$,[5f,5b] to the trihydride complex, $[Ir_2(H)(CO)_2(\mu\text{-}H)_2(dppm)_2][BF_4]$,[5a] with the anticipation that the presence of two adjacent hydride ligands in the trihydride might lead to facile hydrogenation chemistry, since on insertion of an alkyne (or alkene) into an Ir-H bond of this compound, the resulting vinyl (or alkyl) ligand could still be cis to a hydride ligand, thus enhancing the possibility of reductive elimination of the hydrogenated substrate. The reactions of the trihydride complex with alkynes and alkenes are described in Chapter 5.

The reactions of $[Ir_2(H)(CO)_2(\mu\text{-}H)_2(dppm)_2][BF_4]$ with acetylene as well as with alkynes and alkenes, having electron withdrawing substituents, such as DMAD, HFB, and tetrafluoroethylene, yield the alkyne- or alkene-bridged products, $[Ir_2(H)_2(CO)_2(\mu\text{-}H)(\mu\text{-}C_2R_2)(dppm)_2][BF_4]$ (R = CO_2Me, (**30**) CF_3 (**31**) and F_2 (**32**), respectively), while those with the unactivated alkynes, phenylacetylene and diphenylacetylene, as well as with ethylene result in the hydrogenation of the unsaturated organic substrates to yield styrene, stilbene and ethane, respectively. In contrast to the reaction with phenylacetylene, which yields several metal containing products that were difficult to characterize (in addition to the organic product), those with diphenylacetylene and ethylene yield $[Ir_2(CO)_2(\mu\text{-}C_2Ph_2)(\mu\text{-}H)(dppm)_2][BF_4]$ (**33**) and $[Ir_2(C_2H_4)(CO)_2(\mu\text{-}H)(dppm)_2][BF_4]$ (**34**), respectively, as the only metal-containing products. Apparently these monohydrido products result

from the hydrogenation of one molecule of the unsaturated organic substrate accompanied by the coordination of a second molecule. The reluctance of the activated alkynes to undergo hydrogenation is possibly due to the strength of the metal-carbon bonds they give rise to on coordination, which presumably prevents any further transformation, as well as their greater tendency to bridge the two metals, as a result of their stronger π-acceptor capability, compared to the unactivated alkynes. However it is not clear why acetylene reacts in a similar way to the activated alkynes and not the unactivated ones.

The hydrido-ethylene complex, **34**, which is one of the very few reported A-Frame complexes containing ethylene,[9] has been characterized by an X-ray structure determination in this study, and it is the first such complex, to our knowledge to be characterized by this means. Another result of the study with the trihydride complex was the observation that its reaction with ethylene is reversible, in that the hydrido-ethylene product reacts with hydrogen to regenerate the former complex, suggesting that the trihydride complex can serve as a catalyst for the hydrogenation of ethylene. In light of this observation, catalytic studies involving the trihydride complex and analogous alkenes, which might yield hydrogenation products for which turnovers would be easier to determine, were considered, but these were not carried out since the parallel study of the reactivity of the 'RhIr' and diiridium alkyl complexes proved to be particularly interesting and was pursued at the expense of the hydrogenation chemistry. Such catalytic hydrogenation studies ought to be carried out, and are also recommended.

The results of this study give an indication of the diversity of chemistry that can occur with binuclear systems, as a result of the cooperativity between the two metals that they display. It has been shown that many of the transformations that occur in the reactions carried out in this study involve

such cooperative behavior, and thus such diversity in reactivity cannot be obtained with mononuclear complexes.

References and Footnotes

1. McDonald, R.; Cowie, M. *Inorg. Chem.* **1990**, *29*, 1564.
2. Sutherland, B. R.; Cowie, M. *Organometallics* **1985**, *4*, 1637.
3. (a) Hilts, R. W.; Moro, G.; Sterenberg, B. T.; Cowie, M., manuscript in preparation. (b) Antonelli, D. M.; Cowie, M. *Organometallics* **1991**, *10*, 2550. (c) Wang, L. S.; Cowie; M., to be submitted for publication. (d) Graham, T.; Mao, T.; Van Gastel, F.; Cowie, M., unpublished work.
4. Brookhart, M.; Green, M. L. H. *J. Organomet. Chem.* **1983**, 250, 395.
5. (a) McDonald, R.; Cowie, M. *Organometallics* **1990**, *9*, 2468. (b) Vaartstra, B. A.; Cowie, M. *Organometallics* **1990**, *9*, 1594. (c) Vaartstra, B. A.; Cowie, M. *Inorg. Chem.* **1989**, *28*, 3138. (d) Vaartstra, B. A.; Cowie, M. *Organometallics* **1989**, *8*, 2388. (e) McDonald, R.; Sutherland, B. R.; Cowie, M. *Inorg. Chem.* **1987**, *26*, 3333. (f) Sutherland, B. R.; Cowie, M. *Organometallics* **1985**, *4*, 1801. (g) McDonald, R. Ph.D. Thesis, University of Alberta, 1991, Chapter 4. (h) Vaartstra, B. A. Ph.D. Thesis, University of Alberta, 1989, Chapter 6.
6. (a) Collman, J. P.; Hegedus, L. S.; Norton, J. R.; Finke, R. G. *Principles and Applications of Organotransition Metal Chemistry;* University Science Books: Mill Valley, CA, 1987; Chapter 6. (b) Pearson, R. G. *Chem. Rev.* **1985**, *85*, 41.
7. See Chapter 2 of ref 5g.
8. (a) Chaudret, B; Delavaux, B.; Poilblanc, R. *Coord. Chem. Rev.* **1988**, *86*, 191. (b) Puddephatt, R. J. *Chem. Soc. Rev.* **1983**, *12*, 99.
9. Vaartstra, B. A.; Xiao, J.; Jenkins, J. A.; Verhagen, R.; Cowie, M. *Organometallics* **1991**, *10*, 2708.

Appendix

Solvents and Drying Agents

Benzene	Sodium benzophenone ketyl
Dichloromethane	Phosphorus pentoxide
Diethyl ether	Sodium benzophenone ketyl
Hexanes	Sodium benzophenone ketyl
Methanol	Sodium metal
Nitromethane	4A Molecular sieves
Tetrahydrofuran	Sodium benzophenone ketyl
Toluene	Sodium benzophenone ketyl